

**SCIENTIFIC GROUNDS  
OF STRUCTURAL AND PRODUCTION CONCEPTS  
TO PROVIDE AIRCRAFT LIFE TIME**

2018

MINISTRY OF SCIENCE AND EDUCATION OF UKRAINE  
National Aerospace N.E. Zhukovskiy University “Kharkiv Aviation Institute”

**SCIENTIFIC GROUNDS  
OF STRUCTURAL AND PRODUCTION CONCEPTS  
TO PROVIDE AIRCRAFT LIFE TIME**

Kharkiv “KhAI” 2018

**UDC 629.7.017**  
**S40**

Подано наукові основи інтегрованого проектування високоресурсної авіаційної техніки, викладено конструктивно-технологічні рішення для забезпечення заданого ресурсу авіаційної техніки в зонах функціональних отворів, зрізних нерознімних і рознімних болтових з'єднань, клепанних з'єднань, способи затримки росту втомних тріщин у тонкостінних конструкціях, виконаних з алюмінієвих сплавів. Наведено конструктивно-технологічні методи підвищення втомної довговічності болтових з'єднань титанових елементів авіаційних конструкцій з урахуванням фретинг-корозії, викладено особливості назначення ресурсу планера транспортних літаків.

Для науковців та інженерів авіаційної промисловості, а також викладачів, студентів і аспірантів авіаційних університетів.

Composite authors: V. A. Boguslayev, A. G. Grebenikov, N. I. Moskalenko,  
A. M. Gumennyi, E. T. Vasilevskiy, A. P. Eretin,  
V. F. Sementsov, V. A. Grebenikov, O. M. Stoliarchuk

Reviewers: PhD, prof. A. K. Myalitsa,  
PhD, prof V. B. Loginov

S40 Scientific Grounds of Structural and Production Concepts to Provide Aircraft Life Time  
[Text]: V. A. Boguslaev, S. A. Bychkov, A. G. Grebenikov, N. I. Moskalenko,  
A. M. Gumennyi, E. T. Vasilevsky, A. P. Eeretin, V. F. Sementsov, V. A. Grebenikov,  
O. M. Stolyarchuk, etc. – Study Guide. Nat. Aerospace Univ. named after N.Ye. Zhukovskiy  
“KhAI”, 2019 – 268 pages.

ISBN 978-966-662-570-3

The scientific grounds of integrated design of high-performance aircraft are presented, constructive and technological solutions are given to provide a given life of aircraft in areas of functional openings, shear detachable and non-detachable bolted joints, riveted joints, ways to delay the growth of fatigue cracks in thin-walled structures made of aluminum alloys. Structural and technological methods for increasing the fatigue life of bolted joints of titanium elements of aircraft structures with allowance for fretting corrosion are presented, and the features of assigning the airframe life time of transport aircraft are described.

For scientists and engineers of the aviation industry, as well as teachers, students and post-graduates of aviation universities.

Figs 144. Tables 35. Bibliography: 87 names.

**УДК 629.7.017**

**ISBN 978-966-662-570-3**

© Коллектив авторов, 2017  
© АО «Мотор Сич», ГП «АНТОНОВ», 2017  
© Национальный аэрокосмический  
университет им. Н.Е. Жуковского  
«Харьковский авиационный институт», 2017

## CONTENTS

INTRODUCTION .....	7
<i>Chapter 1</i> PRINCIPLES OF CODES FOR PROVISION OF AIRCRAFT SERVICE LIFE .....	9
1.1. Evaluation of the fatigue strength of transport category airplanes in accordance with aviation regulations. Part 25 (airworthiness standards: transport category).....	9
1.2. Fatigue evaluation of the civil light aircrafts in accordance with Air Regulations. Part 23 (airworthiness standards for civil light aircrafts)....	12
1.3. Evaluation of the rotocraft fatigue strength in the transport category in accordance with aviation regulations. Part 29 (airworthiness standards for rotary-wing vehicles of the transport category) .....	15
1.4. Construction safety according to the strength requirements in long- term operation (MOC 25.571) .....	17
<i>Chapter 2</i> PECULIARITIES OF SELECTION OF STRUCTURAL MATERIALS FOR AIRCRAFT .....	50
2.1. Application features of aluminum alloys in the aircraft structure .....	55
2.2. Application features of titanium alloys in aircraft structures .....	57
2.3. Application features of steels in the aircraft structures .....	59
2.4. Application features of magnesium alloys in the aircraft structures .....	61
<i>Chapter 3</i> METHODOLOGY OF INTEGRATED DESIGNING OF AIRCRAFT ASSEMBLED STRUCTURES OF SCHEDULED LIFE .....	62
3.1. New concept and the scientific basis for the integrated design methodology to achievement of regulated durability of assembled thin- walled aircraft designs using computer-integrated systems CAD\CAM\CAE .....	62
3.2. Method of integrated design and getting the scheduled durability of shear bolted joints of aircraft assembled structures .....	79
3.3. New design and production concepts aimed at providing higher endurance of aircraft assembly structure shear bolted joints.....	86
3.4. Computer Aided Design Procedure to Obtain Specified Endurance of Shear Rivet Joints in Aircraft Thin-Wall Assembly Structures .....	90
3.5. New Structural-Production Concepts for Shear Riveted Joints of Aircraft Assembly Thin-Wall Structures.....	98



3.6. New structural-process procedures and techniques in delay of fatigue cracks growth favorable for service life increase of assembled structural components.....	102
3.7. Conclusions .....	106
<i>Chapter 4</i> STRUCTURAL-PROCESS METHODS AIRCRAFT TITANIUM STRUCTURAL COMPONENT BOLTED JOINTS. FATIGUE ENDURANCE UPGRADING WITH FRETTING-CORROSION TAKEN INTO ACCOUNT .....	109
4.1. Estimation-experimental method to determine effect produced by fretting-corrosion fatigue endurance of titanium structural members produced from VT6 alloy.....	109
4.2. Determination method of effect produced by structural and process data of bolted joints on parts coupling interaction characteristics.....	111
4.3. Experimental study of effect produced by structural-process parameters on fatigue endurance of structural members joints from VT6 alloy.....	114
4.4. Study of structural process method application to upgrade fatigue of bolted joints in aircraft titanium structural members with an account made for fretting corrosion .....	116
4.5. Conclusions .....	119
<i>Chapter 5</i> STRUCTURAL-PROCESS METHOD TO INCREASE FATIGUE ENDURANCE OF AIRCRAFT AIRFRAME MEMBERS DETACHABLE BOLTED JOINTS .....	121
5.1. Scientific justification of fatigue endurance increase method for structural elements of detachable bolted joints by local and barrier reduction.....	121
5.2. Local SSS and fatigue endurance characteristics study of airframe structural members test-pieces in area of detachable bolted joints .....	125
5.3. Fatigue endurance characteristics experimental studies of airframe structural members standard models in detachable bolted joints area	128
5.4. Structural-processing technique to upgrade fatigue endurance of detachable bolted joints .....	131
5.5. Conclusions .....	132

<i>Chapter 6</i> STRUCTURAL-PROCESSING TECHNIQUE TO PROVIDE AIRFRAME SERVICE LIFE IN FUNCTIONAL HOLES AREA.....	134
6.1. Scientific backgrounds of structural-processing techniques to provide airframe fatigue endurance in functional holes area.....	134
6.2. Studies to determine effect produced by local plastic strain methods on airframe structural members SSS characteristics in area of functional holes.....	140
6.3. Experimental studies to determine effect produced by methods of processing airframe structural members in area of functional holes on static strength and fatigue endurance .....	143
6.4. Conclusions .....	146
<i>Chapter 7</i> ANALYSIS IN SPECIFYING SERVICE LIFE PECULIARITIES FOR TRANSPORT CATEGORY AIRCRAFT .....	148
7.1. Detection of life time characteristics at the phase of laboratory studies	151
7.2. Assigned life time specifying at operation phase.....	158
7.3. Studies target and problems .....	163
<i>Chapter 8</i> PROCEDURE DEVELOPMENT IN REVEALING AVAILABLE LIFE CHARACTERISTICS OF TRANSPORT AIRCRAFT AIRFRAME STRUCTURE USING MARKED LOADING PROGRAM AT LABORATORY TESTS STAGE .....	164
8.1. Procedure development in marking programmable loading under conduction of laboratory survivability tests.....	164
8.2. Investigation of preliminary positive overload effect upon structural element lifetime.....	176
8.3. Development of method intended to determine damage ratio caused by cyclic loads at stage of fatigue crack propagation .....	184
8.4. Investigation of compression loads effect upon propagation rate of fatigue crack .....	188
8.5. Recommendations on account of compressive load effect when calculating equivalents between cyclic loads at the stage of fatigue crack growth .....	206
<i>Chapter 9</i> DEVELOPMENT OF METHOD TO DETERMINE FATIGUE CRACK CRITICAL LENGTH IN TESTING SINGLE STRUCTURAL SPECIMEN FOR RESIDUAL STRENGTH.....	211
9.1. Development of method to determine critical size of fatigue damage	

while testing specimens for residual strength.....	211
9.2. Test of full-scale wing structure.....	217
<i>Chapter 10</i> DEVELOPMENT OF TECHNIQUE FOR REALIZATION OF AVAILABLE LIFETIME CHARACTERISTICS IN OPERATION ACCOUNTING INDIVIDUAL LOADING .....	221
10.1. Development of technique accounting individual wing lifetime depletion.....	221
10.2. Peculiarities of establishing specified lifetime to aircraft periodically used for special applications .....	224
10.3. Peculiarities of overhaul-period renewal and prolongation of lifetime to aging aircraft.....	225
10.4. Development of method to execute aircraft training touch-and-go landings to reduce depletion of airframe structure lifetime .....	231
10.5. Development of recommendations for operating divisions on rational use of an-22 aircraft lifetime .....	241
<i>Chapter 11</i> IMPLEMENTATION OF DEVELOPED METHODS TO DETERMINE AND EMBED AVAILABLE SERVICE LIFE CHARACTERISITCS OF TRANSPORT AIRCRAFT .....	253
BIBLIOGRAPHY.....	259

## INTRODUCTION

---

Provision of a service life of aircraft designs is one of the actual problems of creating the aircrafts. When designing the specified service life and reliability of aircrafts is foreseen and provided in the production process, and achieved during operation.

Designing of modern aircrafts on the fail-safe concept is a complex scientific and technical challenge that is being addressed through the integration of scientific research of specialists representing the aviation industry and scientific centers.

Service life of aircraft is largely determined by the endurance strength of the structural members. In accordance with the standard requirements of the Aviation Rules (AP 25.571) secure service life is identified by the formula.

$$T = \frac{N}{\eta},$$

where  $N$  is the average durability;  $\eta$  – coefficient of reliability. The value  $\eta$  is selected so that the probability of fatigue failure is virtually zero within a safe (assigned) service life.

The main factors that lead to deterioration of performance characteristics or failures of parts, assemblies and units of aircraft are: fatigue, corrosion, wear, fretting corrosion, human factor. These factors largely depend on the state of the surface, its physical and chemical properties. Control over the surface properties allows to improve fatigue, tribotechnical and corrosive characteristics of aircraft structures.

The destruction of the structural members of fatigue is the result of cyclical, dynamic loading and additional factors (structural, operational, industrial, environment, material quality, coatings, producibility, monitoring the status of the structure in the course of providing its life cycle).

Experience of aircraft operation shows that it is impossible to completely eliminate corrosion of aviation materials. When designing the material of the structure, scheme of its coating, the choice of a constructive solution in view of the corrosive behaviour, time to completion of periodic inspections and routine maintenance are selected based on specific types of corrosion damage and the location of specific structural member.

Issues of wear parts of aircraft engineering mechanisms are relevant. There are the following kinds of wear: oxidative, adhesion, abrasive, erosive, fretting wear. Fretting wear is the most dangerous for aircraft units.

When proceeding to the operation of aircrafts in compliance with its technical state implemented is a new method to determine the service life. It is based on the principle of improved survivability or damage tolerance. Damage tolerance provides the structure failure safe guarantee by setting a time frame for its inspection in operation to detect any damage, to repair or replace the damaged items.

Service life that is set on principle of increased survivability is the time when a certain number of defects may be detected in a structure (like cracks of a given size), but it can be operated between maintenance checks or repairs.

When selecting the structural materials to provide the service life account must be taken of its static strength, yield, ductility, fracture toughness (resistance to cracking), fatigue, corrosion resistance, resistance to stress corrosion cracking, corrosion and mechanical fatigue, speed of the growth of fatigue cracks, wear resistance, resistance to fretting-fatigue.

Designing, manufacturing, testing and operation of durable aircrafts based on the fail-safe principle require the efforts of many scientists and engineers who are proficient in methodology of integrated design, production and engineering analysis using CAD/CAM/CAE/PLM.

The monograph presents only some results of the research performed by the authors and the recommendations of aircraft service life provision by constructive and manufacturing methods which were developed at the National Aerospace University named after N. E. Zhukovsky "Kharkiv Aviation Institute", ANTONOV Company and "Motor Sich" public joint stock company.

*Chapter 1*  
**PRINCIPLES OF CODES FOR PROVISION  
OF AIRCRAFT SERVICE LIFE**

---

1.1. EVALUATION OF THE FATIGUE STRENGTH OF TRANSPORT CATEGORY AIRPLANES IN ACCORDANCE WITH AVIATION REGULATIONS. PART 25 (AIRWORTHINESS STANDARDS: TRANSPORT CATEGORY)

**Damage-tolerance and fatigue evaluation of structure**

(a) **General.** An evaluation of the strength, detail design, and fabrication must show that catastrophic failure due to fatigue, corrosion, manufacturing defects, or accidental damage, will be avoided throughout the operational life of the airplane. This evaluation must be conducted in accordance with the provisions of paragraphs (b) and (e) of this section, except as specified in paragraph (c) of this section, for each part of the structure that could contribute to a catastrophic failure (such as wing, empennage, control surfaces and their systems, the fuselage, engine mounting, landing gear, and their related primary attachments). For turbojet powered airplanes, those parts that could contribute to a catastrophic failure must also be evaluated under paragraph (d) of this section. In addition, the following apply:

(1) Each evaluation required by this section must include:

(i) The standard loading spectra, temperatures, and humidities expected in service;

(ii) The identification of principal structural elements and detail design points, the failure of which could cause catastrophic failure of the airplane; and;

(iii) An analysis, supported by test evidence, of the principal structural elements and detail design points identified in paragraph (a)(1)(ii) of this section.

(2) The service history of airplanes of similar structural design, taking due account of differences in operating conditions and procedures, may be used in the evaluations required by this section.

(3) Based on the evaluations required by this paragraph, inspections or other procedures must be established, as necessary, to prevent catastrophic failure, and must be included in the Airworthiness Limitations Section of the Instructions for Continued Airworthiness required by §25.1529. The limitations of the validity of engineering data for the justification of the requirements for the maintenance engineering program (LOV), expressed in the amount of permissible operating time (in flight hours or the number of flights or simultaneously in both units), provided for in this paragraph, should also be included in the section "Airworthiness Limits" Instructions for maintaining airworthiness, as required by requirements 25.1529. Inspection thresholds for the following types of structure must be established based on crack growth analyses and/or tests, assuming the structure contains an initial flaw of the maximum probable size that could exist as a result of manufacturing or service-induced damage:

(i) Single load path structure;

(ii) Multiple load path “fail-safe” structure and crack arrest “fail-safe” structure, where it cannot be demonstrated that load path failure, partial failure, or crack arrest will be detected and repaired during normal maintenance, inspection, or operation of an airplane prior to failure of the remaining structure.

(4) The documentation developed in accordance with paragraph (a) (3) of this section shall be periodically updated on the basis of recording and analyzing the results of studies, tests and accumulated experience in the operation of aircraft of this type. A procedure should be defined to ensure the reliability and timeliness of such accounting.

(b) **Damage-tolerance evaluation.** The evaluation must include a determination of the probable locations and modes of damage due to fatigue, corrosion, or accidental damage. Repeated load and static analyses supported by test evidence and (if available) service experience must also be incorporated in the evaluation. Special consideration for widespread fatigue damage must be included where the design is such that this type of damage could occur. It must be demonstrated with sufficient full-scale fatigue test evidence that widespread fatigue damage will not occur within the design service goal of the airplane. The type certificate may be issued prior to completion of full-scale fatigue testing, provided the Administrator has approved a plan for completing the required tests, and the airworthiness limitations section of the instructions for continued airworthiness required by §25.1529 of this part specifies that no airplane may be operated beyond a number of cycles equal to  $\frac{1}{2}$  the number of cycles accumulated on the fatigue test article, until such testing is completed. The extent of damage for residual strength evaluation at any time within the operational life of the airplane must be consistent with the initial detectability and subsequent growth under repeated loads. The residual strength evaluation must show that the remaining structure is able to withstand loads (considered as static ultimate loads) corresponding to the following conditions:

(1) The limit symmetrical maneuvering conditions specified in §25.337 at all speeds up to  $V_C$  and in §25.345.

(2) The limit gust conditions specified in §25.341 at the specified speeds up to  $V_C$  and in §25.345.

(3) The limit rolling conditions specified in §25.349 and the limit unsymmetrical conditions specified in §§25.367 and 25.427 (a) through (c), at speeds up to  $V_C$ .

(4) The limit yaw maneuvering conditions specified in §25.351(a, b and d) at the specified speeds up to  $V_C$ .

(5) For pressurized cabins, the following conditions:

(i) The normal operating differential pressure combined with the expected external aerodynamic pressures applied simultaneously with the flight loading conditions specified in paragraphs (b) (1) through (4) of this section, if they have a significant effect;

(ii) The maximum value of normal operating differential pressure (including the expected external aerodynamic pressures during 1 g level flight) multiplied by a factor of 1.15, omitting other loads.

(6) For landing gear and parts of airframe structure that are influenced directly by the forces in the landing gear, – the limit ground loading conditions specified in §§25.473, 25.491, and 25.493.

Other combinations of loads should also be considered if they are computational for certain structural elements.

If significant changes in structural stiffness or geometry, or both, follow from a structural failure, or its partial failure, their effect on damage tolerance must be further investigated considering the requirements specified in § 25.629 (b) (2).

(c) **Fatigue (safe-life) evaluation.** Compliance with the damage-tolerance requirements of paragraph (a) (3) and (b) of this section is not required if the applicant establishes that their application for particular structure is impractical. This structure must be shown by analysis, supported by test evidence, to be able to withstand the repeated loads of variable magnitude expected during its service life without detectable cracks.

(d) **Sonic fatigue strength.** It must be shown by analysis, supported by test evidence, or by the service history of airplanes of similar structural design and sonic excitation environment, that:

(1) Sonic fatigue cracks are not probable in any part of the flight structure subject to sonic excitation.

(2) Catastrophic failure caused by sonic cracks is not probable assuming that the loads prescribed in paragraph (b) of this section are applied to all areas affected by those cracks.

(e) **Damage-tolerance (discrete source) evaluation.** The airplane must be capable of successfully completing a flight during which likely structural damage occurs as a result of:

(1) Impact with a bird (loading conditions – see 25.631).

(2) Uncontained fan blade impact.

(3) Uncontained engine failure; or

(4) Uncontained high energy rotating machinery failure.

The damaged structure must be able to withstand the static loads (considered as ultimate loads) which are reasonably expected to occur on the flight. Dynamic effects on these static loads need not be considered. Corrective action to be taken by the pilot following the incident, such as limiting maneuvers, avoiding turbulence, and reducing speed, must be considered. If significant changes in structural stiffness or geometry, or both, follow from a structural failure or partial failure, the effect on damage tolerance must be further investigated 25.629(b)(2).



1.2. FATIGUE EVALUATION OF THE CIVIL LIGHT AIRCRAFTS IN ACCORDANCE WITH AIR REGULATIONS. PART 23 (AIRWORTHINESS STANDARDS FOR CIVIL LIGHT AIRCRAFTS)

**Metallic Pressurized Cabin Structures**

For normal, utility, and acrobatic category airplanes, the strength, detail design, and fabrication of the metallic structure of the pressure cabin must be evaluated under one of the following:

(a) A fatigue strength investigation in which the structure is shown by tests, or by analysis supported by test evidence, to be able to withstand the repeated loads of variable magnitude expected in service; or

(b) A fail safe strength investigation, in which it is shown by analysis, tests, or both that catastrophic failure of the structure is not probable after fatigue failure, or obvious partial failure, of a principal structural element, and that the remaining structures are able to withstand a static ultimate load factor of 100 percent of the limit load factor at  $V_C$ , considering the combined effects of normal operating pressures, expected external aerodynamic pressures, and flight loads. These loads must be multiplied by a factor of 1.15 unless the dynamic effect of failure under static load are otherwise considered;

(c) The damage tolerance evaluation of Sec. 23.573(b).

**Airframe Metallic Structure**

(a) For normal, utility, and acrobatic category airplanes, the strength, detail design, and fabrication of those parts of the glider design that can be disastrous in case of failure must be analyzed on the basis of one of the approaches outlined below, unless it is shown that the design, the operating stress level, materials and the expected operating conditions are comparable, in terms of accumulation of fatigue, with a similar design for which there is a vast satisfactory operating experience:

(1) A fatigue strength investigation in which the structure is shown by tests, or by analysis supported by test evidence, to be able to withstand the repeated loads of variable magnitude expected in service; or

(2) A fail safe strength investigation, in which it is shown by analysis, tests, or both that catastrophic failure of the structure is not probable after fatigue failure, or obvious partial failure, of a principal structural element, and that the remaining structures are able to withstand a static ultimate load factor of 100 percent of the limit load factor, or;

(3) The damage tolerance evaluation of Sec. 23.573(b).

**Damage tolerance and fatigue evaluation of structure**

(a) **Composite airframe structure.** Composite airframe structure must be evaluated under this paragraph instead of Secs. 23.571 and 23.572. The applicant must evaluate the composite airframe structure, the failure of which would result in catastrophic loss of the airplane, in each wing (including canards, tandem wings, and winglets), empennage, their carry through and attaching structure, movable control surfaces and their attaching structure, fuselage, and pres-

sure cabin using the damage-tolerance criteria prescribed in paragraphs (a)(1) through (a)(4) of this section unless shown to be impractical. If the applicant establishes that damage-tolerance criteria is impractical for a particular structure, the structure must be evaluated in accordance with paragraphs (a)(1) and (a)(6) of this section. Where bonded joints are used, the structure must also be evaluated in accordance with paragraph (a)(5) of this section. The effects of material variability and environmental conditions on the strength and durability properties of the composite materials must be accounted for in the evaluations required by this section.

(1) It must be demonstrated by tests, or by analysis supported by tests, that the structure is capable of carrying ultimate load with damage up to the threshold of detectability considering the inspection procedures employed.

(2) The growth rate or no-growth of damage that may occur from fatigue, corrosion, manufacturing flaws or impact damage, under repeated loads expected in service, must be established by tests or analysis supported by tests.

(3) The structure must be shown by residual strength tests, or analysis supported by residual strength tests, to be able to withstand critical limit flight loads, considered as ultimate loads, with the extent of detectable damage consistent with the results of the damage tolerance evaluations. For pressurized cabins, the following loads must be withstood:

(i) Critical limit flight loads with the combined effects of normal operating pressure and expected external aerodynamic pressures;

(ii) The expected external aerodynamic pressures in 1g flight combined with a cabin differential pressure equal to 1.1 times the normal operating differential pressure without any other load.

(4) The damage growth, between initial detectability and the value selected for residual strength demonstrations, factored to obtain inspection intervals, must allow development of an inspection program suitable for application by operation and maintenance personnel.

(5) For any bonded joint, the failure of which would result in catastrophic loss of the airplane, the limit load capacity must be substantiated by one of the following methods:

(i) The maximum disbonds of each bonded joint consistent with the capability to withstand the loads in paragraph (a) (3) of this section must be determined by analysis, tests, or both. Disbonds of each bonded joint greater than this must be prevented by design features; or

(ii) Proof testing must be conducted on each production article that will apply the critical limit design load to each critical bonded joint; or

(iii) Repeatable and reliable non-destructive inspection techniques must be established that ensure the strength of each joint.

(6) If it is shown that the use is permitted for it to be carried out for any part of the structure, it must be demonstrated by performing one of the following conditions:

(i) After the fatigue damage or explicit (apparent) partial destruction of the structure of this failure is not likely and the remaining structure is able to with-

stand as the estimated load equal to 100 % of the most critical maximum operating load; or

(ii) This part of the design is able to withstand the expected in operation variable loads of different sizes. Sufficient component, subcomponent, element, or coupon tests must be done to establish the fatigue scatter factor and the environmental effects. Damage up to the threshold of detectability and ultimate load residual strength capability must be considered in the demonstration.

(b) **Metallic airframe structure.** If the applicant elects to use Section 23.571(c) or Section 23.572(a)(3), then the damage tolerance evaluation must include a determination of the probable locations and modes of damage due to fatigue, corrosion, or accidental damage. The determination must be by analysis supported by test evidence and, if available, service experience. Damage at multiple sites due to fatigue must be included where the design is such that this type of damage can be expected to occur. The evaluation must incorporate repeated load and static analyses supported by test evidence. The extent of damage for residual strength evaluation at any time within the operational life of the airplane must be consistent with the initial detectability and subsequent growth under repeated loads. The residual strength evaluation must show that the remaining structure is able to withstand critical limit flight loads, considered as ultimate, with the extent of detectable damage consistent with the results of the damage tolerance evaluations. For pressurized cabins, the following load must be withstood:

(1) The normal operating differential pressure combined with the expected external aerodynamic pressures applied simultaneously with the flight loading conditions specified in this part, and.

(2) The expected external aerodynamic pressures in 1g flight combined with a cabin differential pressure equal to 1.1 times the normal operating differential pressure without any other load.

### **Damage tolerance and fatigue analysis of aircraft metal structures of the transitional category**

For aircraft of the transitional category:

(a) **Damage tolerance of metal structures.** The evaluation of the strength, detailed design and construction of the structure should show that catastrophic failure of the structure due to fatigue, corrosion, defects or damage will be excluded during the operation of the aircraft. This evaluation shall be conducted in accordance with the requirements of 23.573, except as provided in paragraph (b) of this paragraph, for each major constructive element, the destruction of which may be catastrophic.

(b) **Assessment of fatigue (a safe resource).** The requirements set forth in paragraph (a) of this paragraph are not required if the Applicant has established that the requirements for the admissibility of damage for a given design are practically impracticable. For such a construction, it should be shown by an appropriate analysis on the basis of calculations supported by the results of fatigue resistance tests that it will be possible to avoid catastrophic failure from the effect of the variable loads expected within the established resource. At the

same time, appropriate reliability factors should be applied.

**Analysis of variable loads and order of maintaining airworthiness**

(a) Analysis carried out in accordance with the requirements of this subsection shall:

(1) Include a standard load spectrum (i.e. loads with ground-based driving regimes, ground-air-ground cycle, maneuver loads, loads from atmospheric turbulence).

(2) Consider the significant mutual influence of aerodynamic surfaces.

(3) Consider the significant impact on the loading of the structure caused by the disruption of the flow from the rotating propeller and the buffeting caused by the action of the converging vortices.

Based on the results of the analysis carried out in accordance with the requirements of 23.571, 23.572, 23.573 or 23.574, inspections and / or other measures necessary to prevent accidental or catastrophic destruction should be provided; they should be included in the "Limits on Airworthiness" sections of the airworthiness instructions developed in accordance with requirements 23.1529.

1.3.EVALUATION OF THE ROTOCRAFT FATIGUE STRENGTH IN THE TRANSPORT CATEGORY IN ACCORDANCE WITH AVIATION REGULATIONS. PART 29 (AIRWORTHINESS STANDARDS FOR ROTARY-WING VEHICLES OF THE TRANSPORT CATEGORY)

**Fatigue Evaluation of Structure**

(a) **General.** Evaluation of the strength of the basic elements, the design features of individual locations and production technology should show that their catastrophic failure can not occur due to fatigue, taking into account the influence of the external environment, characteristic / occurring defects, wear or accidental damage. It is necessary to evaluate the following parts of the structure, but not limited to them: screws, transmission from the engine to the hub screws, control systems, fuselage, moving and fixed control surfaces, fastening of engines and transmission, chassis and the main elements of their fastening.

Additionally, the following is required:

(1) Each estimate required by this paragraph shall include:

(i) the set of the main structural elements, the destruction of which can lead to a catastrophic destruction of the rotorcraft;

(ii) the measurement in load flight or stresses in the elements defined in accordance with paragraph (a) (1) (i) of this paragraph, under all critical conditions in the entire range of restrictions complying with the requirements of paragraph 29.309 (including height effect), with taking into account that overloading during maneuvering should not exceed the maximum values expected during operation; and

(iii) the load spectrum is as heavy as expected in use for loads or stresses determined in accordance with paragraph (a) (1) (ii) of this paragraph, including operation with an external load, if provided, and other operations with high re-

peatability of loading cycles.

(2) On the basis of the estimates required by this paragraph, the time limits for examinations of replacements, their combinations or other procedures necessary to avoid catastrophic destruction should be established. The timing of inspections, replacements, combinations thereof or other procedures should be included in the "Limitations of Airworthiness" section of the Continuing Airworthiness Manual in accordance with paragraph 29.1529 and A29.4 of Appendix A of this Part.

**(b) Assessment of fatigue tolerance (including the admissibility of defects)**

It should be shown by convincing tests and, if available, experience of operation, that the structure can tolerate fatigue. The assessment of the permissibility of fatigue should take into account the requirements of one of the paragraphs. (b)(1), (2) or (3) of this paragraph or a combination thereof, and also includes the identification of possible places and types of damage caused by fatigue, taking into account the influence of the environment, the characteristic defects encountered or accidental damage. Compliance with fatigue tolerance requirements should be shown. (b) (1), or (2) of this paragraph, unless the Applicant has established that such methods of proving the fatigue defect allowability are not applicable to a particular design because of limitations in geometric parameters, controllability, or design experience, safe resource in accordance with paragraph (b)(3) of this paragraph.

**(1) Estimation of a safe resource with an acceptable defect.**

It should be shown that the design in the presence of a defect is capable of withstanding repeated loads of variable magnitude without detecting defect growth at the following intervals:

- (i) the resource of the rotorcraft; or
- (ii) within the replacement period, in accordance with A29.4 of Annex A of this Part.

**(2) Assessment of the safety of damage (residual strength after defect development).** It should be shown that, after partial damage, the structure is capable of withstanding the operational stresses assumed in the design, without deterioration during the period between inspections, established in accordance with A29.4 of Annex A of this Part. Operational loads are defined in 29.301 (a):

- (i) the evaluation of the residual strength should show that the structure with the developed defect is able to withstand, without destruction, within its lifetime, the operational loads adopted in the design;
- (ii) the inspection intervals and methods of inspection necessary to detect damage should be established before the limit values for residual strength conditions are reached;
- (iii) if, after structural damage or partial fracture, significant changes in rigidity or its geometric parameters or both occur together, further studies of the defect tolerance are necessary.

**(3) Evaluation of a safe resource.** It should be shown that the structure is capable of withstanding repeated loads of variable magnitude without the ap-

pearance of detectable cracks during the following intervals:

- (i) the resource of the rotorcraft; or
- (ii) within the replacement deadlines in accordance with A29.4 of Appendix A of this Part.**

#### 1.4. CONSTRUCTION SAFETY ACCORDING TO THE STRENGTH REQUIREMENTS IN LONG-TERM OPERATION (MOC 25.571)

##### **Introduction**

This document is a guide to Conformity Assessment Techniques (hereinafter referred to as MOC) for regulatory requirements of AP 25.571.

MOC of AP 25.571 provides recommended approaches, procedures, methods, quantitative characteristics, etc., through which compliance with regulatory requirements is ensured. The words "must", "should", "necessary", "not allowed" etc. are used in the document to indicate that the following instructions will be acceptable according to the MOC.

The use of unified approaches when establishing compliance with the requirements of 25.571 is highly desirable. At the same time, one should realize that the complexity of new design solutions and new production technologies, unusual characteristics and configurations of aircraft may require changes and deviations from the approaches described in these "MOC". However, careful adherence to these methods of determining compliance should be encouraged in every possible way.

It should be taken into consideration that the MOC is based, first of all, on the long-term experience in the creation, certification and operation of domestic aircraft, that was accumulated by Industry, Operators and State Organizations (experimental design bureau, TsAGI, SRI CA, State Aviation Register), and extensively use the proven methodology of maintaining long-term safe operation of domestic civil aircraft, given in the Airworthiness Standards. At the same time, the recommendations of the MOC also largely apply foreign experience.

##### **Definitions**

**Construction safety in terms of strength requirements** – the property (feature) of the structure and the way of maintaining its durability in operation, which makes it possible to maintain the strength of the structure at the allowed level, including cases of possible unintended and non-overly long periods of reduced initial strength, caused by degradation processes and / or their combination (fatigue, corrosion, etc.), as well as accidental damage or damage from discrete sources. When making a construction, three basic principles for ensuring its safety are distinguished according to the strength requirements: damage tolerance, the safety of destruction (damage), and the safe life (length of service).

**Damage tolerance** is a property of a construction and a way of ensuring its safety in terms of strength requirements by setting the dates for the first and subsequent inspections of the construction in operation in order to detect possible damage and subsequent repair of the construction or replacement of the

damaged element before the point when a strength reduction is no more acceptable.

**Safety of destruction (damage)** is a property of a construction and a way of ensuring its safety in terms of strength requirements that supposes creating of such a construction that will have a residual strength even after a possible major damage or its main force element destruction, and despite the unrepaired condition this strength will not decrease to more than allowed extent in a period of time during which the damage (destruction) can be revealed.

**Safe life (length of service)** is a property of a construction and a way of ensuring its safety in terms of strength, which does not require special control in operation, by establishing the allowed operating time, calculated in the number of flights, landings, flight hours, operation cycles, in calendar duration (years), as well as in other units that can characterize the rate of reduction in strength due to degradation processes (fatigue, corrosion, etc.), during which the construction will not cause damage that reduces strength below an acceptable level.

**Operational durability** is a general term describing the properties of a construction and methods of ensuring its safety in terms of strength requirements, including damage tolerance and the safety of destruction (damage).

**The assigned resource (service life)** is the total operating time (the calendar operating time) of the aircraft, in terms of which the operation should be terminated irrespective of its condition. Uninterrupted operation is ensured by the timely extension of the next assigned resources (service lives) up to the decommissioning of the aircraft.

**The design lifetime (length of service)** of the construction is the time interval (in flights, flight hours, years) established during the design and / or certification, during which the required level of the construction safety is provided in terms of strength.

**The primary load-carrying structure** is a construction that takes up flight and ground loads and loads from overpressure.

**The primary structural members** are elements of the primary load-carrying structure that take up a significant part of the flight and ground loads and loads from excess pressure; its integrity is essential for maintaining the overall integrity of the aircraft structure.

**Particularly crucial structural elements** are the primary structural members of the construction that are in single-load condition, single failure (destruction, damage) of which leads to an emergency or catastrophic situation.

**Critical points of construction** – parts, elements, zones, local places of construction which operational durability determine the safety level in terms of the construction strength as a whole.

**One-track loading** is realized if the applied loads are ultimately transferred by a single element, the destruction of which leads to a loss of the construction ability to take up the applied loads.

**Multi-track loading** is realized in such a construction where after the destruction of separate element(-s), the applied loads are safely redistributed between the remaining elements of the structure.

**Extensive fatigue damage** is a fatigue damage of a construction in one or more adjacent parts where numerous cracks of such dimensions and density are present that the residual strength of the structure cannot be maintained further at an acceptable level.

**Multiple damage** is the condition of the damaged structure leading to the extensive fatigue damage characterized by the simultaneous presence of fatigue cracks in the same structural element (i.e. fatigue cracks, which in case of combining, with or without other damage, will result in reducing the residual strength below the allowed level).

**Multi-element damage** is the condition of the damaged structure resulting in extensive fatigue damage, characterized by the simultaneous presence of fatigue cracks in adjacent structural elements.

#### **General instructions:**

1. It must be ensured and confirmed that structural damages, directly leading to an emergency or catastrophic situation, are practically impossible within the limits of the established operating time (assigned resources, service lives).

Meeting this requirement, besides creating the appropriate aircraft design, should be provided by technological processes of manufacturing and repair, maintenance and compliance with established rules and operating conditions and should be confirmed by:

- The results of the corresponding calculations;
- The research of actual operating conditions, including operating loads and environmental characteristics;
- The results of flight strength tests;
- The results of laboratory and bench tests of full-scale structures, their parts and structural members;
- The experience in the operation of aircraft of this type and (or) aircraft of similar types.

2. One should make a list of critical design points, which considering ensures the completeness of the design analysis as a whole. The list of critical points can be developed (projected) at the design stage and is improved based on the results of laboratory tests and operational experience.

To clarify the list of critical points, results of construction state detailed monitoring should be analysed (using instrumental procedures) with disassembly (unriveting) of permanent joints. Such control must necessarily be made for constructions upon completion of full-scale laboratory tests on fatigue resistance and residual strength, and also if possible (and, if necessary) for individual aircraft of the park (or their parts) with a large operating time (service life).

For all critical points of construction, especially for highly crucial structural elements, in accordance with subsequent requirements and recommendations,



conditions must be established to ensure safe development of the assigned resources (service lives).

3. When designing the aircraft, the operational durability of the construction must be ensured. The exception can be those parts (elements, parts) of the construction, where the requirements of operational durability are practically impossible.

The inspection conditions should be provided and the means of construction primary members monitoring (including instrumental) during operation should be determined, especially in the zones of possible occurrence of fatigue, corrosion and accidental operational damage.

The possible slower growth of probable damage should be ensured so that the required inspection period (instrumental control) is acceptable, allowing reliable detection of the damage until the critical state.

When providing safety characteristics of structural failure, it is recommended to accept states with regulated damages as limiting states (see Appendix 1).

4. For places of construction that are critical for fatigue strength, the fatigue resistance should be provided at the design stage, taking into account the design life. It is recommended to provide an interval to the first examination according to the conditions of fatigue resistance not less than 50 % of the design life. At the same time, attention must be paid to the selection of the appropriate material, the overall strength of the structure, the maximum possible reduction in stress concentration, and the maximum increase in fatigue resistance based on the use of appropriate structural and technological measures. The production processes for the manufacture of aircraft structure elements and their assembly should ensure the stability of characteristics affecting performance and fatigue life within the limits of the established resources in the expected operating conditions. The recommended form for presenting the results of the analysis of the directive technological process parameters is given in Appendix 2.

The effectiveness of measures is checked by laboratory tests of individual structural elements (attachment fittings, joints, panels, compartments, etc.).

5. For critical points in terms of corrosion resistance, established on the basis of existing experience, effective anticorrosive protection must be provided during its design. At the same time, attention should be paid to the selection of the appropriate structural material, its sensitivity to corrosion under stress and to other types of corrosion is taken into account, and the degree of environmental aggressiveness is also considered. Particular attention should be paid to the surface of the joining elements that allow mutual movement during the loading process, as well as to those elements of the structure in which corrosion under stress may occur, where it is necessary measures ensuring the absence of significant internal residual stresses (in assembly, welding, technological procedures and other) should be provided.

6. According to the results of work, an appropriate analysis should be carried out and the possibility and conditions (measures) of working off the project resource by aircraft should be substantiated on paragraphs 3, 4 and 5. The procedure (system) of ensuring and maintaining the safety of the structure should

be developed and justified based on the conditions of durability under long-term operation on the basis of recording and analyzing the results of studies, tests and accumulated experience in the operation of aircraft of this type. For domestic aircraft operated in foreign countries, it is recommended to use the guidance of paragraph 7 of these "MOC" to gradually establish and increase the assigned resources (service lives). In other cases, for example, when selling domestic aircraft abroad or operating foreign aircraft, other procedures may be developed, providing equivalent safety, including the experience of the world aviation community.

Regardless of the type of procedure for ensuring the safety of the structure in terms of durability under long-term operation, the Applicant must demonstrate the availability and reliability of operation in such a procedure of:

- 1) a system of periodic operation documents refinement with explanation of the chosen intervals between such refinements;
- 2) systems for the collection and analysis of data on the following:
  - The nature and operating conditions and loading of the aircraft in the park (if the Applicant does not show that he used a deliberately conservative load spectrum);
  - Technical condition of operated aircraft of this type.

Justification of the project resource possibility must be included in the proof documentation for the aircraft certification.

7. The safety of the structure in terms of strength requirements during long-term operation is confirmed at the stages of development and specification of operational documentation:

- a) before the start of regular operation when establishing the initial assigned resource (service life) to the fleet of aircraft;
- b) in the course of operation, as the fleet of aircraft (or individual groups or individually separate aircraft models) is established, the previously assigned resources (service lives), successively (incrementally) increasing until the aircraft are decommissioned, on the basis of:
  - clarification of the nature and operating conditions of the aircraft fleet (individual groups or individual aircraft), including the accumulation of statistics on the parameters of flight and the frequency of center of gravity acceleration, as well as clarifying, if necessary, the loading of aircraft assemblies based on the results of special flight tests;
  - analysis of the results of additional (if necessary) laboratory tests, including structures with operating time in service;
  - analysis of all available information on the technical condition of the aircraft in operation of this type, especially the results of tests performed just before the establishment of the next assigned resource. Prior to the establishment of the next assigned resource, the condition of specifically these structures are monitored for every aircraft.

The designer includes in the operational documentation the requirements for the Operator on the procedure for providing the necessary information to en-

sure the completeness of the analysis in accordance with the requirements of this paragraph.

8. Operational safety should be monitored by operating experience of the entire fleet and, if necessary, group of main flight aircrafts.

When summarizing the operating experience, it is necessary to take into account the failures, malfunctions and structural defects found on the fleet aircraft with all forms of maintenance and repair. The operating conditions of the fleet and individual aircraft can be controlled on the basis of data processing of on-board staff means for objective control.

Aircrafts of the main group should be appointed from among the aircraft leading the rest of the fleet according to operational time, or sharply differing in terms of operation and loading. The number and group of main planes are set specifically for each type of aircraft.

On each plane of the main group in an increased volume and continuously (systematically), the conditions of its operation must be taken into account, and the loading conditions on the basis of regular airplanes and, in the case of their installation, of special means should be determined.

The control over the correctness and completeness of the analysis of the above information is also carried out in the process of certification of the Operators when they apply for aircraft and flight routes.

9. In determining the assigned resources (specification of operational documentation), the conditions for ensuring safety of flights within the established resource should be specified (clarified), namely, the following should be listed:

- elements (parts) of the design with limited life, subject to replacement;
- places of construction, subject to refinement;
- places of construction subject to control;

and the dates (periodicity) of these activities are indicated.

For the construction points under work, as well as for the construction points undergoing repair related to the detected damage, the necessary addition to the list of critical locations is formed (see para. 2).

Appendix 3 contains the recommended form of the Technical Opinion on the establishment of the assigned resource for a particular type of aircraft fleet (according to the conditions for the fatigue strength of the structure), and in Appendix 3 there is the recommended form of the Technical Opinion on the establishment of the assigned resource to a single unit or group of aircraft of a certain type (under the conditions of fatigue strength of the structure).

Appendix 4 provides the recommended form for submitting summary information on the resource characteristics of the critical points of the structure.

10. For more efficient operation, the assigned resources and intervals before and between replacements, refinements and inspections may be established not only in the number of flights, flight hours, operation cycles, but also in other units more closely related to the actual, individual for each structure (or groups of structures) by the accumulation of damage during operation. To determine the rate of such accumulation, systematically analyzed data on actual

operating conditions can be used, as well as specialized on-board devices and systems.

11. According to the results of works to ensure the safety of the structure during long-term operation and in accordance with the instructions of para. 6, appropriate clarifications and recommendations to the operational documentation shall be made in the established order.

### **Limit State According to Residual Strength Conditions**

1. The limiting state of a structure according to the conditions of residual strength is considered to be the worst state when the structure continues to meet the relevant requirements of 25.571 (b). The presence of a condition worse than the limit one is unacceptable and should be qualified as a loss of safety. When assigning the time of the first inspection or when meeting the requirements of 25.571 (c), any less damaged (including undamaged) state of the structure can be taken as a marginal safety state. If such a state is assumed to be a condition characterized by the absence of detectable damage, it should be shown that the maximum undetectable damage size does not lead to a state where the design does not meet the relevant requirements of 25.571 (b).

#### **Notes:**

a) The construction in this paragraph can be understood as a separate structural element, as well as a combination of elements that together provide the necessary strength. For a particularly crucial structural element, its damaged limit state is considered. For a set of redundant structural elements in a multi-path loading condition, limiting states characterized by secondary damage after complete destruction of individual elements can be considered.

b) Special attention should be paid to the possible multi-focal damage. In the absence of direct quantitative analysis, it is recommended (in the margin of reliability) to take the same amount of damage in each of the identical foci while determining the limiting state.

2. The limit state should be detected either visually, which is most preferable, or with the help of approved methods and tools of instrumental control; Exceptions may amount to cases specified in requirements 25.571 (c).

3. The fulfillment of requirements 25.571 (b) is usually confirmed by direct results of full-scale tests on the residual strength of the particular structure or by recounting the results of these tests to other critical points. Recalculations are carried out using approved calculation methods, supported by the results of similar tests.

Full-scale tests are tests of the structure as a whole, as well as such laboratory residual strength tests, which, under the conditions of loading and fixing, approach the test conditions of the structure as a whole.

With reliable methods for evaluating the residual strength, confirmed by the results of static tests and residual strength tests of such structures, it is possible to use the results of direct calculation using such methods. The calculations are based on the average values of the material characteristics.

4. As a main object for residual strength tests, it is recommended to use a model of a structure that has been tested for fatigue resistance. In addition to

the damage that has occurred during these tests, it is advisable to create artificial damage, including the partial or complete destruction of individual structural elements. The places and the degree of damage created during the tests are determined depending on the particular type of construction, taking into account its controllability and the reliability of means and methods of detecting damage in operation.

**Notes:**

a) In case of partial artificial damage, it is necessary to ensure a reliable imitation of conditions at the ends of cracks corresponding to their fatigue development under operating conditions. In particular, it is recommended that cracks should be grown by applying variable loads.

b) For residual strength tests, a model of a structure that has been subjected to static tests may be used.

5 Corrosion damage to structural elements can be simulated by mechanical damage. The level of equivalence or the degree of conservatism of such a replacement in terms of residual strength is established on the basis of engineering analysis, if necessary, using as the corresponding calculations, as well as test results.

**Maximum detectable damage size:**

1. For each critical point of the structure, taking into account the used methods and the means of monitoring its condition in operation and during repairs, the greatest damage should be determined, which may remain undetected (with a probability of not more than 0.05).

2. The size of such damage, taken as the maximum undetectable, is specified taking into account:

a) the results of various means and methods of monitoring in field laboratory tests related to fatigue resistance and residual strength;

b) factors that impair the basic (laboratory) characteristics of maintainability in actual operation, with the adoption of the corresponding additional reserves for the amount of maximum undetectable damage.

3. The existing experience in conducting and monitoring similar structures should be used to the fullest extent, special attention should be given to the cases and reasons for the late detection of damage.

**Allowed operating time**

**Allowed operating time of the critical point according to the fatigue resistance conditions:**

1. It should be ensured and confirmed that the emergence of the critical state of the critical point in the process of operation (within the safe resource, the permissible operating time before the first inspection and between inspections) is almost impossible. In order to reduce the likelihood of the limit state emergence, the following can be recommended:

a) To take into account the possibility of accidental initial damage in the production process – determine the size of the safe resource and operating time before the first inspection based on the duration of growth of the fatigue crack from the initial damage to its critical size. The recommended sizes of initial

manufacturing defects accepted in this kind of calculations are given in Appendix 5.

b) To take into account the possibility of accidental operational damage – accept the interval between subsequent inspections as an operating time before the first inspection.

For particularly crucial constructive elements, these recommendations are compulsory.

2. For each critical point of the structure a standard loading spectrum in operation should be determined, based on:

- A standard flight (or a set of standard flights with the relative proportion of their implementation), including towing modes, taxiing to the start, testing the engines on the ground, takeoff run, climb, cruising, descent, approach, landing run and taxiing on the parking, taking into account their duration (length) and the totality of other parameters characterizing each of these modes;

- Repeatability of loads caused by the effects of atmospheric turbulence, taking into account different flight heights and different geographic areas corresponding to the operational routes of the aircraft;

- Repeatability of maneuvering loads associated with the conditions and rules for the operation of aircraft of this type;

- Repeatability of loads during landing, engine operation and when driving on the ground (towing, taxiing, take-off run, landing run);

- Repeatability of loads with the use of wing high lift devices and various methods of braking the aircraft in air and on land, as well as using various types of automatic devices in flight:

- Repeatability of excess pressure in the pressurized cabin during normal operation and during its pressure test after repairs.

**Notes:**

a) Standard loading spectra should also take into account loads such as high-frequency loads from a slipstream or jet engine, from aerodynamic pressure pulsations, loads from uneven heating of a structure, loads from unbalance of wheels, and others, if on the basis of the conducted analysis and available experience it is established that these loads can affect the resource of the concerned design.

b) Standard loading spectra of load carrying structure movable elements (the extension-retraction system, flaps, etc.) must reflect the necessary combination of variable loads and movements in order to take into account the effect of wear and corrosion in the joints. As well as changes in the tension related to the kinematics of movement, if it is established on the basis of the conducted analysis or available experience that this influence may be significant.

3. The design critical area fatigue characteristics are determined mainly by the results of representative laboratory tests of the concerned structure, and (or) also fatigue resistance tests that according to the loading conditions and the coverage of possible critical locations, are close to the test conditions of the structure as a whole.

The test structure portliness should be brought to the attention under the conditions of stability of the characteristics of production processes affecting the durability.

As a rule, initial (undamaged and not in service) structure is subjected to the tests. It is recommended that the volume of its laboratory tests carried out with satisfactory results by the time of issue of the type certificate corresponds to at least one design service life (without the reliability coefficients specified in para. 8).

To expedite the necessary data on the fatigue resistance at the stage of crack growth, tests can be conducted on the design with artificially damages (initiators of fatigue cracks' growth) of critical areas. In this case, considerations similar to those in Note 1 to para. 4 should be taken into account.

The total volume of full-scale fatigue resistance tests must be at least three design service lives.

In order to maximize the opportunities inherent in the design and to take into account the effect on the residual durability and operational survivability of the main load-carrying components of the design under actual operating conditions, including the environment, temperature effects, flows of minor standard interventions in the design during operation, as well as other factors, which can lead to a decrease in the predicted strength characteristics, it is recommended to conduct tests of structures that have completed a significant part of the the design service life or (if any) having an operating time in excess of the value of the design service life. The objects, the order and the volumes of such tests are determined in each particular case.

4. Fatigue tests are carried out on a set of external effects and variable loads, corresponding to those on the concerned design in use. If it is not possible to carry out such complex tests, the effect of loads and (or) external influences, not applied to the structure, should be reliably estimated.

5. As a rule, the following things are subjected to fatigue tests:

- Wing, including ailerons, flaps, slats and other elements of the wing high lift devices;
- Tail unit (stabilizer, fin, elevator and rudder);
- Fuselage with pressurized cabin and transparency elements;
- Landing gear, including wheels and brakes;
- Mechanical elements of aircraft linkage,
- Engine pods,

as well as the assemblies and structural elements that ensure the mutual load-carrying docking of the specified parts and assemblies.

**Notes:**

a) Fatigue tests must also be conducted to other parts of the structure, assemblies and installations that are part of the main load-carrying structure of the design, if their destruction in flight or during movement on the ground directly threatens flight safety.

b) The design subjected to static tests, as a rule, is not allowed to fatigue tests, unless the special analysis shows the possibility and methods of using the results of such tests.

c) Tests and the establishment of assigned resources of wheels and brakes are carried out by special techniques.

6. The fatigue test program should reproduce the standard loading spectra in operation as fully as possible in all critical locations, taking into account the influence of various modes and load components, and taking into account the combination of the variable loads and the motion of the movable elements of the load-carrying structure. For each critical location of the structure, the equivalent in terms of damageability during tests and operation, with a possible difference in the equivalent value at the stage before the occurrence of fatigue damage from the value at the stage of the development of the damage, should be determined by appropriate calculation and / or test results of the design samples.

**Notes:**

a) It is recommended to include blocks of "marker loads" in the testing program in order to improve the reliability of the results of the subsequent fractographic analysis of fracture surfaces (fatigue cracks). The development of blocks of "marker loads" is carried out by a special method.

b) In the process of step-by-step establishment of increased values of the assigned resource, the values of equivalents should be specified on a special basis of experience and the data of a comparative analysis of the laboratory tests results on fatigue resistance and materials on the technical condition of the aircraft fleet.

7. The permissible operating time corresponding to the fatigue resistance characteristics obtained, as a rule, according to para. 3, is determined by dividing the total reliability factor and the average operating time of the critical location in question (according to the test results of identical designs including, possibly, according to different programs), taking into account the values of equivalents specified in para. 6. In this case, the value of the safety resource and the permissible operating time before the first inspection is determined by the average number of cycles (blocks) that the design has withstood until reaching the limit state, and the permissible operating time (interval) between inspections by the average number of cycles (blocks) at the stage of development of fatigue damage from the maximum undetectable size to the corresponding limit state.

If the states of identical critical locations of different design instances that arise and are fixed during testing do not allow to conduct their direct comparison and averaging of the required characteristics of endurance, the average operating time is determined by the results of a special analysis using methods of computational, statistical and engineering extrapolation.

8. The value of the total reliability factor  $\eta$  is defined as  $\eta = \eta_1 \eta_2 \eta_3 \eta_4 \eta_5$ . The numerical values of the coefficients included in this work are taken in accordance with the instructions given below.



8.1. The value of coefficient  $\eta_1$  taking into account the compliance level of the fatigue resistance structure of the testing program with the actual loads nature in operation, depending on the their proximity degree with appropriate justification, is taken in the range  $1 < \eta_1 < 1.5$ .

Coefficient  $\eta_1 = 1.0$  under the test program, sufficiently reflecting the totality of the loads repeated in operation both in magnitude and in the sequence of their action.

While using the calculated methods that provide a sufficiently high degree of calculation accuracy or obtain deliberately conservative estimates, used to determine the equivalents of the approbated and confirmed by experimental data, the value of the reliability factor  $\eta_1$  can be reduced up to the value  $\eta_1 = 1.0$ .

#### **Note**

In availability of test results for various programs requiring the use of different values of coefficient  $\eta_1$ , the dividing by a corresponding coefficient  $\eta_1$  is performed prior to the average of the test results.

8.2. The value of coefficient  $\eta_2$ , taking into account the degree of danger and controllability of destruction, is assumed to be equal to:

$\eta_2 = 1.0$ ; if on the assumption of tests and / or calculation it is shown that the fatigue damage not exceeding the limiting state of damage (partial destruction) of redundant structural elements under conditions of multi beam loading will be known during post-flight inspections and / or maintenance schedules of the lowest periodicity;

$\eta_2 = 1.2$ ; if such damage cannot be clearly detected during post-flight inspections and (or) the maintenance procedures for the least periodicity;

$\eta_2 = 1.5$ ; if the fatigue damage occurs in a particularly critical element, that is in a single-load condition.

8.3. Coefficient  $\eta_3$  takes into account differences from standard (average) load conditions of individual groups and / or aircraft instances due to the peculiarities of their operation, geographic conditions, length of tracks, etc. The value of the coefficient  $\eta_3$  should be determined by the results of a special analysis effect of possible variations in operating conditions on the specific critical locations loading. If such an analysis is not carried out, the value of the coefficient  $\eta_3$  is taken equal to:

$\eta_3 = 1.5$  using reliable experimental data to determine the loading corresponding to the standard (average) operating conditions;

$\eta_3 = 2.0$ , if the reliability of the experimental definition of loading is insufficiently justified or if materials, obtained on the basis of an acceptable calculation method, are used.

#### **Notes**

If the most severe operating conditions are accepted as standard conditions or if loading reliable individual record is carried out by methods and means taking into account objectively all the significant features of the operation of an aircraft of this type, the reliability factor  $\eta_3$  can be assumed equal to 1.0.

8.4. The value of coefficient  $\eta_4$ , taking into account the difference of fatigue resistance characteristics, is adopted depending on the determined resource characteristics (safety life, the moment of the first inspection, the interval between inspections) and the number of tested identical structures.

Standard measures of scatter are used (the standard deviation of the logarithm of durability is 0.15), when determining the safe resource and the moment of the first inspection for structures made of aluminum alloys. Accordingly, the coefficient  $\eta_4$  is taken from Table 1.1, taking into account the notes to this paragraph.

Table 1.1

Calculation of Coefficient  $\eta_4$ 

Sample, q-ty	1	2	3	4	5	6
$\eta_4$	5.0	4.0	3.5	3.2	3.1	3.0

The standard measures of scatter are used when determining the interval between inspections for aluminum alloy structures (the standard deviation of the logarithm of the duration of crack growth from the maximum non-detectable to critical size is 0.10). Accordingly, the coefficient  $\eta_4$  is taken from Table 1.2, taking into account the notes to this paragraph.

Table 1.2

Calculation of Coefficient  $\eta_4$ 

Sample, q-ty	1	2	3	4	5	6
$\eta_4$	3.0	2.5	2.3	2.2	2.1	2.0

**Notes:**

1. The reliability factor  $\eta_4$  increases by  $\eta_m$  times for load carrying structure made of high-tensile-strength steel (especially for welded seams) and titanium alloys. The value of  $\eta_m$  is taken to be 1.5 and can be refined in the presence of justifying experimental materials.

2. The right and left components are considered to be identical.

3. If the states characteristics of identical critical locations in different design instances recorded during testing are such that direct sharing of the obtained longevity values is not possible, their reduction to comparable values and the choice of the coefficient  $\eta_4$  in accordance with Table 1.1 and Table 1.2 is based on the special analysis results. In particular, if no damage occurred at any of the tests at the critical location in question, in determining the permissible operating time for establishing a safe resource or the moment of the first inspection, any single result or any group of results can be used provided that the reliability factor is applied in accordance with Table 1.1 and the implementation of Note 4 to this paragraph.

4. If the ratio of the corresponding maximum ( $N_{max}$ ) and minimum ( $N_{min}$ ) operating time (for a set of tested specimens) exceeds the values given in the corresponding rows of Table 1.3, the required value of the reliability factor  $\eta_4$  is determined by the formula:

$$\eta_4 = \eta_{4t}^{\frac{N_{max}/N_{min}}{(N_{max}/N_{min})_t}},$$

where  $\eta_{4t}$  is taken from Table 1.1 and 1.2, and the corresponding values  $(N_{max}/N_{min})_t$  are taken from Table 1.3.

Table 1.3

The Ratio of the Corresponding Maximum ( $N_{max}$ )  
and Minimum ( $N_{min}$ ) Operating Time

Specimen, q-ty	2	3	4	5	6	Appliance
$(N_{max}/N_{min})_t$	1.4	1.7	1.9	2.1	2.3	While determining the safe resource and the time of the first inspection
$(N_{max}/N_{min})_t$	1.25	1.40	1.55	1.65	1.75	While determining the interval between inspections

If the number of tested structures exceeds six, the value of the coefficient  $\eta_4$  and the regulated value  $(N_{max}/N_{min})$  are established on the basis of a special analysis.

8.5. The coefficient  $\eta_5$ , characterizing the degree of the influence of real operating conditions, including the environment, temperature effects, etc. for the duration of growth of fatigue cracks, is taken equal to:

$\eta_5 = 1.0$ ; if it is shown that the actual operating conditions are sufficiently reproduced in tests or are taken into account in the calculation by an acceptable method;

$\eta_5 = 1.5$  in all other cases.

9. If during the fatigue tests, a structural component is destroyed or damaged, its replacement or repair of the damaged area is carried out; it is necessary to carry out loading up to a certain acceptable number of cycles in order to study the duration of the development of damage before replacement (repair) after the detection of damage. Tests should be continued to determine the resource characteristics of other critical locations of the structure, including those formed in connection with the performance of the qualification repair, and to verify the effectiveness of this repair. At the same time, the operating time of the replaced or repaired structural element is counted from the beginning of its testing, and the rest of the construction – according to the total volume of tests.

**Note**

If the replacement or repair causes a significant change in the stress state in the components of the rest structure, these changes should be taken into ac-

count by the appropriate refinement of the values of the equivalents. If this fact is impossible or unreliable, further tests of such elements are considered to be non-qualifying.

10. In the absence of direct test results of the construction in question, the fatigue resistance characteristics can be determined by suitable computational and experimental methods based on modern concepts of fatigue and fracture mechanics and using, first and foremost, possible ways of recalculating the test results of certain critical areas of the design in question to other critical ones. These methods should be supported by available experimental materials, including the results of testing structural elements (panels, assemblies, etc.).

11. The results of the recalculation are considered as the results of direct field tests, and therefore the values of the reliability coefficients adopted with the use of the test results are fully preserved in the case of recalculation.

12. When used for critical locations for which recalculation is not possible, direct calculation methods should determine the average characteristics of fatigue resistance (including the duration of crack growth) using the mean values of the material characteristics and, subsequently, the reliability coefficients in para. 8, in the same way as it is done in the presence of direct results of laboratory tests or the results of their recalculation. To facilitate comparison with the test results, it is recommended that the calculated determination of the fatigue resistance characteristics be carried out for the loads of the full-scale test program (i.e., to obtain a calculated analogy of test results) followed by the use of equivalents.

Applied calculation methods should contain a reasonable amount of additional margin for durability, taking into account possible errors in the calculation (incomplete conformity of the stress-strain state of the critical location of the full-scale structure and tested samples, approximation of the scale factor, differences in the loading structure, etc.). The value of this margin can be taken reduced to one, if the experience of carrying out similar calculations shows that the calculation method used yields knowingly conservative estimates. In the absence of such experience or justification of the value of the additional margin accepted, its value is assumed to be equal to two.

**Note**

If the accumulated data on a large volume of experimental materials are used as initial data for the application of direct calculation methods, the values of the reliability coefficients  $\eta_4$  in Table 1.1 or Table 1.2 are assumed to be equal to their minimum values.

13. The operation of the controlled critical location for which the requirements of 25.571 (b) are fulfilled and practicable can be carried out individually up to the point of detection at the next inspection of the fatigue crack at each critical area of each individual specimen of the structure. The decision on the possibility and ways of further exploitation of this critical area of construction is made on the basis of the results of a special analysis.

However, it should be taking into account that as the operating time of overall design increases, the likelihood of simultaneous presence of fatigue

cracks in a number of critical locations in the construction, in particular, the probability of multifocal damage, increases. In this regard, in order to justify the possibility of exploitation, an analysis should be made of the rate of development of fatigue damage and the reliability of their detection in operation, taking into account the expected mutual location of their occurrence. If this analysis is not carried out or its results are unreliable, the total permissible operating time of the controlled critical area (subject to the necessary inspections within it) should not exceed (taking into account the values of equivalents) half of the total volume of its operating time obtained in laboratory tests for fatigue resistance.

A similar approach should be applied when calculating methods for estimating fatigue resistance.

### **Notes**

As a measure of additional safety from the viewpoint of occurrence of possible corrosion and/or accidental damage, it is recommended to control critical areas where the safety of operation is ensured by meeting the requirements of 25.571 (c), for example critical locations in the landing gear design.

14. If the critical area is uncontrolled (in particular, if the maximum undetectable size exceeds the size of the damage corresponding to the limiting state) or poorly controlled, inspection due to its unreliability, as a rule, is ineffective; in this case, the permissible operating time before the first inspection (or any smaller one) for this critical area is taken as a safe resource that determines the time of the replacement of the structural element or the refinement (repair) of the critical area.

### **Admissible Operating Time of Critical Area according to Conditions of Corrosion Resistance**

1. It should be ensured and confirmed that the emergence of the critical state of the critical area in terms of corrosion resistance during operation (within the permissible operating time before the first inspection and the permissible operating time between inspections) is almost unbelievable.

2. The permissible operating time according to the conditions of corrosion resistance before the first inspection and the permissible operating time between inspections is established in units of the calendar operating life (in years). In accordance with this, the terms for carrying out the necessary replacements, refinements and inspections within the assigned resource are established.

3. The mean values of the time before occurrence and duration of growth of possible corrosion damage should be determined on the basis of analysis and accumulation of data on the experience of operation of similar structures in conditions close to those considered, taking into account the available experimental materials for testing in corrosive environments of specimens and structural elements and depending on the following factors:

- The expected effectiveness of special protection and coatings of the material;
- The sensitivity of the material to stress corrosion;
- The sensitivity of the material to other types of corrosion;

- The degree of aggressiveness of the environment;
- Load characteristics.

4. The permissible operating time before the first inspection and the values of the intervals between inspections in operation are determined by estimating the average durations carried out in accordance with para. 3, taking into account the reliability of the data used. The necessary margins must be taken to account for possible deviations from the mean values. When setting permissible operating time, thorough inspections should be carried out at least as often as at the following intervals:

- External surfaces of the structure – annually;
- Internal design elements in places where moisture may accumulate – once in 2–4 years.

Mandatory inspections of internal structural elements are carried out at least once every 8–10 years.

### **Assessment of Damage Admissibility (discrete source)**

1. It is assumed that the fact of structural damage by discrete sources listed in AP 25.571(e) immediately becomes known to the crew. All possible variants of damage to the structure of the aircraft and its systems should be considered, the most unfavorable both in terms of maintaining the strength of the remaining undamaged part of the structure and the possibility of safe completion of the flight. To establish compliance with the requirements of AP 25.571(e), it should be shown with an acceptable level of confidence that:

- The remaining structure retains static strength corresponding to the maximum loads (considered as calculated) expected both at the time of the event and during the completion of the flight; or
- The aircraft is capable of safely completing the flight even in the case of insufficient strength of the remaining structure (in cases of non-localized separation of engine debris or other units with rotors having large kinetic energy). It is recommended to use the probabilistic approaches described in Appendix R25A-0 in AP 25.

2. The maximum loads taken must be determined taking into account the response of the crew at the time of the event in question. It should also be taken into account the actions of the crew, aimed at avoiding heavy loads in a situation where it is known that the aircraft may be in a damaged condition. In the absence of a more rational analysis, it is proposed to consider the following conditions of design loading:

2.1. At the time of the event:

a) Maximum normal operating overpressure (including expected external aerodynamic pressure during horizontal flight), increased by 1.1 times in combination with horizontal flight loads.

b) The aircraft in the mode of horizontal flight should remain able to withstand the loads that arise when the flight path changes from maneuver or other causes associated with the event. In this case, it is necessary to take into account possible damage to the controls and the corresponding corrective actions of the pilot.

2. After the event occurred:

a) The aircraft should withstand:

- 70 % of the maximum operational maneuvering loads in combination with the corresponding excess pressure (including also the expected external aerodynamic pressure);
- 40 % of the maximum operating speed of the gust at the speed  $V_c$  (vertical or lateral gusts) also in combination with the corresponding excess pressure (also including the expected external aerodynamic pressure). In this case, the loading of the aircraft at all flight speeds up to the maximum possible after the event has to be considered.

b) It should also be shown that the flutter does not emerge on the airplane until the speed  $V_c/M_c$  with all the structural changes caused by the event.

### Appendices

Appendix 1:

Table 1.4

#### Regulated Damages

Assembly	Type of Failure
The whole structure	Destruction one of the elements with multiple-path load transfer
Torsion box wing and fin	<p>Double-span crack of the skin (with two interstringer distances) at any place along the span with a destroyed stiffener (stringer), and specifically in the area of longitudinal joint of the panels (skin), with a destroyed re-joint stringer and a crack in both panels.</p> <p>Simultaneous complete destruction of the extreme spar cap (front or rear), a crack in the spar web up to 1/3 of its height and a crack in the skin under the destroyed cap with a length of one interstringer distance.</p> <p>Complete destruction of one from the panels.</p> <p>Complete destruction of a spar web.</p> <p>Complete destruction of one section from the profiles of the wing transverse joint.</p> <p>Complete destruction of one from the elements of the hinge subunits in flight control surfaces.</p>
Fuselage	<p>Double-span crack of the skin (with two interstringer distances) in the lateral direction of the fuselage with a destroyed stringer.</p> <p>Double-span crack of the skin (with two interstringer distances) in the longitudinal direction of the fuselage with a destroyed frame.</p> <p>A crack (simultaneously in the skin and edge strip) around the cut-outs for cleaning the landing gear legs, at the doors, luggage access doors, etc. (150 mm).</p> <p>Crack in the hermetic webs and bottoms (up to 800–1000 mm)</p>
Fuselage-to-wing joint or fuselage-to-tail joint	Complete destruction of one component from junction members

## Appendix 2:

Table 1.5

List of Parameters of Directive Production Processes for the Manufacture of Main Load-Carrying Elements of the Aircraft Design, Ensuring Stability of Their Fatigue Property

Directive Process	Standard process documentation	Process main parameters that determine the durability	Control means of basic parameters in production	Confirmation of the pre-set basic parameters
Performance of bolted-type connection with elastoplastic interference	RTM 1.4.112182 (Technical Guide) Performance of bolted-type joints with elastoplastic interference in packages of aluminum alloys	Interference 0.8–1.2%. Accuracy and roughness of the opening. Extension, mechanical deployment	Checking the formation of openings N7.100 % acceptance test of bolts. Geometry of the lead-in and smooth parts of the bolt. Type of lubricant PP95/3	Technical report of the NIAT (National Institute of Aviation Technologies) and TsAGI (Central Institute of Aerohydrodynamics) No. 1407, 1982.

**Note** This table includes the production processes used specifically to improve the fatigue response and crack resistance.

## Appendix 3:

## CONCLUSION No.

on the establishment of the (initial) assigned service life of ..... flight hours ..... flights to a glider, landing gear and mechanical components of their retraction-extension system, to the mechanical components of the control system and configuration changes, to the structural elements ensuring mutual power connection of the glider parts and assemblies, aircraft ..... according to the conditions of the design strength during long-term operation.

1. Requirements specifications No..... (agreement No. ... , statement No. ...) assign the resource of ... flight hours, ... flights before the disposal of the aircraft, which is confirmed by "Justification" No ... .. from...

Conclusion No... ..from.... for the glider, the landing gear and the mechanical components of the control system and the configuration changes of the aircraft ... ..within (beyond) established resource before the disposal sets assigned life of ... flight hours of ...flights according to the structural fatigue conditions.

2. Since before ... flight fleets... including a group of main aircrafts, has the following operating time:



Table 1.6

## Interval between Operating Time

Interval between operation time	Fleet, %	Interval between operation time	Fleet, %
Flight hours		Number of flights	

3. The main group consists of aircrafts, namely:

– aircraft (s) No. ...operated in ...Administration (Company ... ..) with the operation time of respectively of ... flight hours, ...flights, ...flight hours, ...flights, etc .

– aircraft(s) No. ...operated in ... Administration (Company ...) with operation time ... and so on.

4 The overall technical state of the aircraft ... taking into account the expected level of logistics and also organizational support of operation does not prevent the establishment of the assigned life of... flight hours, ... flights (Ref. report No. ...from ...) under the conditions mentioned in this Conclusion.

*NOTE TO THE TEXT. When establishing the initial assigned life, the second paragraph of Section 1 and Sections 2 through 4 are omitted, as a rule. A brief information about the attempted operation or operation of similar structural variations may seem more appropriate here.*

5. When establishing (initial) assigned resource for the aircraft fleet ... in general (for a group of aircraft ..., aircraft ...No ...) as the calculated operating conditions based on the results of the available statistics are accepted (Ref. materials No ...) the following main parameters characterizing the average (standard) flight in the fleet (for a group of aircraft, for aircraft No. ...) and determining the loading of critical construction parts:

- Take-off weight of the aircraft
  - Fuel weight at take-off
  - Payload
  - Endurance
  - Cruise altitude
  - Length of taxiing operation before take-off
  - The length of taxiing operation after landing
  - Cruise speed
  - Speed at retraction (of landing gear, slats, flaps)
  - Speed at extension (of landing gear, slats, flaps)
- etc.

Some less general flight parameters that determine the loading only of certain critical construction parts, as well as the used characteristics of the frequency in overloads, are shown in the Justification of the Conclusion. For other parameters it is assumed that operation is carried out within the limit of the

permissible FM value range, leading to the greatest loading of the corresponding assemblies.

6. When analyzing was considered the structural durability and survivability of the glider, the landing gear and the mechanical elements of the steering system and the configuration of the aircraft, ... critical areas, of which in addition to Conclusion No. ...from ... – ...areas, including in the construction of:

- Wing ...areas;
  - Fuselage ... areas;
  - Wing-to-the fuselage joints ... areas;
  - Tail ... areas;
  - Tail-to-the fuselage joints... areas;
  - Vertical and horizontal joints ... areas;
  - Landing gear ...areas;
  - Landing gear joints on the wing and fuselage ...areas;
  - Gear follow-up linkage... areas;
  - Controls of aircraft... areas;
  - Steering linkage of aircraft ... areas;
  - Junctural members and steering linkage with the main structure ... areas;
  - Flaps and their controls... areas;
  - Slats and their controls... areas.
  - Engine installation and installation of junctural elements with the main structure of ...areas,
- etc.

From the total number of ... critical areas, including "secondary" critical areas that have arisen in the construction as a result of maintenance development (with established operating time), as well as modifications based on the results of inspections in operation and during repairs of ... areas are determined on the basis of engineering analysis taking into account the experience of compatible structures and educated estimates of the stress-strain behavior; ... areas additionally based on the results of laboratory tests for endurance (reports No. ...). including ... areas by results of disassembling (unriveting) after endurance and residual strength test (reports No. ...); ...areas additionally based on the experience of actual operation and repairs of the aircraft fleet and their leading groups (reports No....), including ... areas by results (reports No. ...) disassembling (unriveting) of the aircraft (aircrafts) structure No. ... with the elapsed time in operation of ... flight hours, ... flights.

7. To establish the assigned life, was carried out a target inspection of the aircraft structure No. ... in an agreed volume for the purpose of a qualification (certification) justification about the sufficiency of the critical locations list (report No. ...).

*NOTE TO THE TEXT. When setting the initial assigned life, this paragraph is omitted.*

8. A definition was made in all critical areas (or an estimate in the safety factor) of their actual loading in the design operating conditions using the following materials (additional to Conclusion No. ...from ...):

- statistics of the average CG acceleration frequency under the air conditions during operation of aerodynamic prototypes... in the amount of ... flight hours (reports No. ...);
- statistics of the CG acceleration frequency under the air conditions during operation of fleet and the leading groups of aircrafts... in the amount of ... flight hours, including differentiation by individual groups and aircraft samples in the amount of ... flight hours (reports No. ....);
- the list of operating aerodromes of the flight fleet... and statistics (forecast) relative shares of different aerodromes in the process of standard operation (reports No. ...);
- information about the obstacle characteristics of the main aerodromes from the operating of the flight fleet ... (reports No. ...);
- statistics of the CG acceleration frequency in the center of gravity of the leading group and the flight fleet... .. in ground operation modes in the amount of ... take-off runs ... , landing runs and ... km of taxiing (reports No. ...);
- the results of flight and structural tests to determine the loading of the structure in air (the total amount of measurements ... flights, including ... flight hours when flying in a turbulent atmosphere) and ground (the total amount of ... takeoff operations and landings on ... aerodromes with the total amount of taxiing operations of ... km) operating modes (reports No. ...);
- results of calculation data based on time-tested methods of repeatability of the loading in air and ground operation (reports No. ...);
- results of calculations on the tested methods of loads when functioning in terrestrial and air modes of operation (reports No. ...).

9. In support of the established assigned life and the conditions of its development in operation were carried out the following steps:

- laboratory endurance tests (additional to the materials of Conclusion No. ... from ...) with the determination of the durability before the detection of fatigue damages and the characteristics from the duration of their development (reports No. ...), using the disassembling (unriveting) materials of a proven design (reports No. ....) and fractographic analysis of kinks (reports No. ...). The equivalents between the loading in laboratory tests and the actual loading in the design operating conditions (reports No. ... ..) are determined for each critical area, according to the corresponding calculation methods.

The general state of the tests is presented in Table 1.7.

Table 1.7

## State of Endurance Testing

No	Name of the structural member	Maximum number of identical tested samples with the same critical area	Maximum number of test program types	The elapsed time in the number of standard flights (taking into account the reliability factors required in accordance with the test program $\eta 1$ )		Notes
				Maximum achieved reliability over the entire considered critical areas considered	Minimum achieved reliability over the entire considered critical areas considered	
1	Wing	4	8	103856	18500	The results of permissible element tests are used
18	Junctural elements of controls and steering linkage with basic structure	6	5	53411(42800)	–	The results of calculations are used

*NOTE. If tests lack for at least one of the critical areas of any structural section, column 6 contains a dash indicating that it is compulsory to use acceptable computational methods for this structural section to determine the average durability for the unexplored critical areas;*

– laboratory residual strength tests (additional to the materials of Conclusion No. ... from ... ) if fatigue damages obtained as a result of laboratory endurance tests are available in ... critical areas of. Damages were created artificially for critical areas (reports No. ...). The general state of the tests is shown in Table 1.8.

Table 1.8

## Residual Strength Test Condition

No.	Structural member	Number of considered critical areas *	Maximum number of identical tested samples of critical areas	Maximum number of a design cases of loading	Residual strength value of the design load, %		Notes
					maximum obtained value for all critical areas	minimum value for the critical areas considered	
1	2	3	4	5	6	7	8
1	Wing	27	3	2	73%	67%	The results of permissible element tests are used
13	Engine mount	9	1	1	67%	–	The results of calculations are used

\*When establishing a resource based on the "safe resource" principle, for the remaining critical areas obvious storing of the required residual strength (for example, the absence of fatigue cracks during the endurance test) is assumed.

*NOTE. If tests lack for at least one of the critical areas of any structural section, column 7 contains a dash, indicating that it is compulsory to use acceptable computational methods to determine the residual strength of untested critical areas;*

– special research, including the analysis of the experience from monitoring the structural state in the process of laboratory tests, with account of materials of unriveting, for the choice of means and methods to monitor the technical condition of the structure in operation and during repairs that provide the necessary resolution and reliability of inspections (reports No. ...).

10. To control the equivalents between loading in laboratory tests on endurance and loading in actual operation was used a comparison between the technical condition of the critical areas in the structure and its elapsed time in the operation, expressed in operating units (flights, flight hours, etc., reports

No. ...) . with the appropriate characteristics and elapsed time, expressed in "laboratory" units (cycles, blocks, etc, reports No. ....). The application of appropriate methods in such comparison (reports No. ....) showed that for ....critical places, the educated estimates of equivalents do not conflict (are in agreement or taken into the safety margin) with the operational experience; these values of equivalents are used to analyze the results of laboratory tests and to determine the resource characteristics of such critical areas. For ... critical areas, the educated estimates of equivalents proved to be unreliable, and therefore the values of the elapsed time in laboratory tests, expressed in operational units, were corrected and coordinated with operating experience according to the corresponding methods. In the corresponding lines of Table 1.2 are indicated the clarified values of the elapsed time in the operating experience (the predicted values are given in parentheses).

*NOTE TO THE TEXT. When establishing the initial assigned life, Section 10 in the above form is omitted, as a rule, but it is highly advisable to duplicate such information on the aircraft prototypes in the Conclusion.*

11. According to the results of the conducted work, the "Justification of the Conclusion on the Establishment (Initial) Assigned Resource of ... flight hours ... of flying to the glider, landing gear and mechanical elements of the steering system and the reconfiguration of the aircraft ... was established according to the fatigue strength conditions of the structure" No. ...of ...with the main following conclusions:

(1) If the requirements of Section 4.9 of the Airworthiness Requirements (AR) (or AP25.571, or AP23.571 and AP23.572) are satisfied, the permissible elapsed time under the fatigue strength conditions of the glider structure, landing gear and mechanical elements of the steering system and the reconfiguration of the aircraft... exceeds, in general, the assigned life of... flight hours of ... flights except for ... critical areas that require special measures during operation and during repairs for safe practice of the resource.

(2) Life characteristics of these critical places are given in Table 1.9. Conclusions are the basis to form the quantitative requirements specified in the appendixes to the conclusion on the terms and procedure for the development of the assigned life.

Table 1.9

**Life Characteristics of Critical Areas of Structural Members  
that Require Activities within the Assigned Life**

No.	Critical area	Accepted elapsed time			Total reliability coefficient required by AR / Excessive durability			Note
		"Safe resource" or the beginning of inspections	Interval between inspections	Resource based on survivability	to "safe resource" or to the beginning of inspections	to the interval between inspections	to the resource in view of survivability	
1	Eye lug of the upper hinge bracket lug, 2nd flap track	2300 flights	560 flights	5700 flights	4.0/1.17	4.0/3.2	2.0/1.3	
7	Fitting joint of the main landing gear leg-to-the lower wing surface	8580 flights	Not undefined	Not undefined	4.8/1.0	–	–	Practically not inspected place

**Conclusions:**

1. Establish ...the (initial) assigned life of ... flight hours ... flights for the glider, landing gear, mechanical elements and reconfiguration of the aircraft under the following conditions:

– replacement of parts and components with a limited life in accordance with Appendix 1:

– structural modification in accordance with Appendix 2;

– structure inspections in accordance with Appendix 3.

2. Add the operational and repair documentation of the aircraft .... in accordance with para. 1 of the Conclusion.

3. If the conditions of paragraphs 1 and 2 of the Conclusions are satisfied, meeting the requirements of Section 4.9 of AP (or AP25.571 or AP23.571 and AP25.572) is provided.

Appendix to conclusion 1:

Table 1.10

List of Parts and Components with a Limited Life, subject to Periodic Replacement in the Process of Practice of the Assigned Life of \_\_\_\_ Flight Hours, \_\_\_\_ Flights

No.	Name	Life limit	Recommended form in the MRO system	Notes
3	The drawing lever of ... retraction-extension system of a nose landing gear	3200 flights	At each over-haul	A new condition in relation to the Conclusion ... from ...
8	Drawing bolt... of drawing bracket-to-rear wing spar mount	700 flights 1500 flight hours	For each F2	Conditions in relation to the Conclusion ... from ... are saved (changed)

Note. The Conditions mentioned in subparagraphs \_\_\_\_ of Appendix 1 to Conclusion \_\_\_\_ from \_\_\_\_, are canceled.

Appendix to Conclusion 2:

Table 1.11

List of Construction Areas Subject to Further Development during the Assigned Life of \_\_\_\_ flight hours, \_\_\_\_ flights

No	Area in construction	Time frames for modification process	Preferred form in MRS system	Documentation to be updated	Notes
4	Installation of the plate in the drawing hatch area... in the wall of the front spar along rib...	6700–8300 flights	Overhaul reconditioning	Bulletin No... from	New conditions regarding to Conclusion...from...



Notes of the Conditions specified in subparagraphs \_\_\_\_ of Annex 2 to Conclusion \_\_\_\_ as of \_\_\_\_, are cancelled.

Appendix to Conclusion 3:

Table 1.12

List of Construction Areas to Be Monitored during the Assigned Life Practice of \_\_\_\_ flight hours, \_\_\_\_ flights

No.	Construction area	Control method	Beginning of the control		Intervals between inspection		Documentation to be revised	Notes
			Time frames	Preferred form in MR system	Time frames	Preferred form in MR system		
2	The area of the flap in the area of attachment of the carriage along rib...	Eddy current	Maximum 4000 flights	Overhaul reconditioning	Minimum in 1000 flights	F-3	Bulletin No... from	New conditions regarding Conclusion... from
7	Lower wing lining in the area of the joint along rib...	Visual	Maximum 570 flights	F-2	Minimum in 240 flights	200 hours	Bulletin No... from	Conditions regarding to Conclusion... from... are saved

Notes of the Conditions specified in subparagraphs \_\_\_\_ of Appendix 3 to Conclusion \_\_\_\_ from \_\_\_\_, are cancelled.

Appendix 3:

#### CONCLUSION No. ....

on the conditions of an airplane practice ... board No. ... of the assigned life of ... flight hours of ... flights to airframe, landing gear and mechanical elements of extension-retraction system, mechanical elements of the control system and configuration changes, to the elements of the design ensuring mutual load-bearing coupling of parts of the airframe and assemblies, aircraft ... in terms of the structural strength during long-term operation.

1. Order of the Minister of Infrastructure No. .... from .... from ... to aircraft .... (a group of aircraft ..... of offices (AP)), including plane ..... No. .... assigns life of ..... flight hours ..... flights has been set. The basis for the assigned life was the Conclusion is a combined by the Experimental Design Office, Central Aerodynamic University and State Research Institute "Conclusion .... No. ... from about establishment of the assigned life of ..... flight hours of ..... flights to the airframe, landing gear and mechanical elements of the extension-retraction system, mechanical elements of the control system and configuration changes,

to the elements of the design ensuring mutual load-bearing coupling of parts of the airframe and assemblies, aircraft ... in terms of the structural strength during long-term operation", which is confirmed by "Justification" No. ... from ... .

The present Conclusion on the conditions of practice of the assigned life of ..... flight hours ..... for the airplane No. .... is issued on request ..... No. ... from ...

2. Airplane ..... board No. .... (issued by Manufacturer plant No....) from the beginning of operation to ..... 20..(year) was in operation .... where practiced..... flights ..... of flight hours; from ..... to ..... was operated ..... where practiced (and so on); from .... up to the present time is operated in .... The total operating time as of ..... is ... flights ..... flight hours. During the whole operation ... major repairs have been carried out on the plane, the last of which was carried out at ..... the plant in..... 20..(year) when practicing ..... flight ..... flight hours.

a) OPTION 1 (standard)

The main load-bearing structure of the the airframe, landing gear and mechanical elements of the extension-retraction system, mechanical elements of the control system and configuration changes, to the elements of the design ensuring mutual load-bearing coupling of parts of the airframe and assemblies, aircraft ... (plant No. ....) does not differ from the standard design of aircraft ....

b) OPTION 2

The main load-bearing structure of the the airframe, landing gear and mechanical elements of the extension-retraction system, mechanical elements of the control system and configuration changes, to the elements of the design ensuring mutual load-bearing coupling of parts of the airframe and assemblies, aircraft ... (plant No. ....) differs from the standard design of aircraft .... (to the extent of a detailed description of the differences).

In addition to the analysis, described in "Justification" No. ... from ... for all critical areas of the main load-bearing structure of the aircraft ..., board No. .... (plant No. ....) different from the standard design, using the available results of full-scale tests or based on the conservative method (s) for calculating the durability and/or survivability, the required life characteristics are given in Table 1.7.

3. Airplane ... board No. .... (issued by Manufacturer plant No....)

a) Within the limits of the achieved operating time, all the modifications of the main load-bearing structure of the airframe, the landing gear and mechanical elements of the system for of the extension-retraction system, mechanical elements of the control system and configuration changes, to the elements of the design ensuring mutual load-bearing coupling of parts of the airframe and assemblies are fulfilled, namely: (the enumeration of bulletins, non-fulfillment of which creates a threat to operational safety, and the deadlines of improvement fulfillment).

b) On the airplane ....., board No. .... (plant No. ....) (OPTION 2. probable) within the operating time reached, the operating and maintenance documentation does not provide for improvement of the main load-bearing structure of the airframe, landing gear and mechanical elements of the extension-retraction system, mechanical elements of the control system and configuration changes,

structural elements ensuring mutual load-bearing coupling of parts of the airframe and assemblies.

c) On the airplane ....., board No. .... (plant No. ....) (OPTION 3. probable) within the operating time reached, the operating and maintenance documentation does not provide for the following improvement of the main load-bearing structure of the airframe, landing gear and mechanical elements of the extension-retraction system, mechanical elements of the control system and configuration changes, structural elements ensuring mutual load-bearing coupling of parts of the airframe and assemblies (the enumeration of non-fulfilled bulletins; the required comments and references to documentation, which ground implemented other conditions in operational publications, are given. Those conditions ensure equivalent safety level, for example, inspections).

4. In support of setting the conditions stipulated by the given Conclusion to practice the assigned life of ..... flights, ..... flight hours by the aircraft board No... (plant No.) the following is used:

a) Data on the technical condition of the aircraft fleet..... including data on the aircraft ..... board No. .... (plant No. ....) for the entire period of its operation. During the ...flights, ... flight hours there was an accidental damage to the skin of the lower surface of the wing in the zone of ..... rib of outer wing. Repaired by ... Life characteristics of the repair zone are determined by a conservative calculation (reference to the corresponding validation). Instrumental control is provided in operation (reference to the justification of the time limits for control);

b) The results of a special study of technical condition of aircraft ..... board No. .... (plant No. ....) after practicing of ..... flights, ..... flight hours conducted under Program No. ....from....

The following fatigue and corrosion damages were found in the process of study of the aircraft technical condition (following are examples of text):

– Crack I = .... mm of the vertical cap of the lower cap of the spar II of the left inner wing in the area of the crack sample selection conducted earlier (bullet No.) (for ..... flights). The crack extends along the radial transition of the horizontal-to-vertical shelves. In operation, instrumental control is provided (reference to the justification of the time limits for control):

– Crack I = .... mm of the skin of the upper panel of the right outer wing extending from the hole near the plate installed on bull. No .... In operation, instrumental control is provided (reference to the justification of the time limits for control):

– Corrosion depth to h = .... mm on the outside of the board beam in the area of frame ... . Corrosion is selected. Paint coating is restored. The selection of corrosion does not reduce the static strength below the required strength.

A number of plates on the upper surface of the wing (... pieces) and on the tail part of the fuselage (... pieces) were also revealed; In operation, visual control of these zones is provided.

The overall technical condition of the aircraft ..... taking into account the expected logistics level does not prevent the assignment of an assigned life of ..... flying hours, ..... flights (see report No. .... from. ....) under conditions.....

NOTES TO THE TEXT. *When assigning the initial assigned life, the second paragraph of section 1 and sections 2-4, as a rule, are omitted. However, it may be expedient to make a brief statement of useful information about the experimental operation or operation of similar design modifications.*

#### Appendix 4:

#### SUMMARY

on life characteristics according to fatigue resistance conditions of the critical area of the airframe design (by the time of assignment of the assigned life of flying hours, ..... flights)

1. Designation of critical area (description, sketch).
2. The limit state (the nature of the damage in the limit state, the critical size of the damage  $l_{crit}$ ).

3. Durability before the limit state  $N_{summ}$  according to the materials of full-scale tests and/or results of recalculations and direct calculations (in the number of program cycles, blocks, etc.) for each test (recalculation, calculation) of the critical location in question.

If  $N_s$  is assumed to be durability before a state less damaged than the limit state, for example, before an undamaged state, the corresponding  $N_s$  value is marked with the ">" sign. If when determining the  $N_s$  the data on durability before the damage presumably exceeding the limit is used, for example, the results of fatigue tests under the program, not containing the maximum operational loads, the actual test results should be reliably adjusted.

4. The maximum undetectable size of damage  $l_0$  for the accepted (recommended) method of control in operation.

5. Durability of the DN between the states  $l_0$  and  $l_{crit}$  from the materials of full-scale tests (including tests of the construction with artificially applied initiators of fatigue cracks) and/or the results of recalculations and direct calculations for each test (recalculation, calculation) of the critical area in question.

6. Equivalent  $E$  (ratio of damage of the program, block cycle loads-to standard flight loads) or equivalents of  $E_1$  and  $E_2$ , if they are adopted unequal for different stages of fatigue.

7. The values of the reliability factor  $\eta_1$  required for each test (recalculation, calculation) (see MOS of AP 25.571).

8. Durability of  $T_s$  before the limit state, expressed in operational units (standard flights) to for each test (recalculation, calculation) taking into account equivalents and required reliability coefficients  $\eta_1$ .

9. Durability of DT between the states, characterized by  $l_0$  and  $l_{cr}$  damage, expressed in operating units (standard flights), for each test (recalculation, calculation) taking into account equivalents and required reliability coefficients  $\eta_1$ .

10. The average value of durability  $T_s$  for all used test results (recalculations, calculations).

11. Average value of DT durability for all used test results (recalculations, calculations).

12. The values of standard reliability factors:  $\eta_2$ ,  $\eta_3$ ,  $\eta_4$  и  $\eta = \eta_2 \eta_3 \eta_4$ , used to determine the required interval between inspections and the time of the first inspection (or, if the requirements are met AP 25.571 (c), the value of the "safe life").

13. Values of permissible operating time between inspections and up to the time of the first inspection (or until the "safe resource" is depleted).

14. The values of the assigned life characteristics (the interval between inspections, the time of the first inspection or the value of the "safe life").

15. Values of the actual reliability factors  $\eta_a$ , defined as the ratio of the values of the average durability of DT and Ts (see paras 10 and 11) to the corresponding values of the assigned life characteristics.

16. Values of excess durability  $D \eta_a$ , defined as the ratio of the values of permissible operating time (see para. 13) to the corresponding values of the assigned life characteristics. [21]

Summary data on the life characteristics of all critical areas should be combined in a single table.

Appendix 5:

### Recommended Sizes of Initial Manufacturing Defects

In one load-bearing section, a defect is considered for only one concentrator.

1. For thin sheets of thickness  $t < 2$  mm, through cracks from both sides of the hole (see Fig. 1.1).

2. For thick sheets, plates, thin plates, quarter-circle corner cracks from both sides of the hole (see Fig. 1.2).

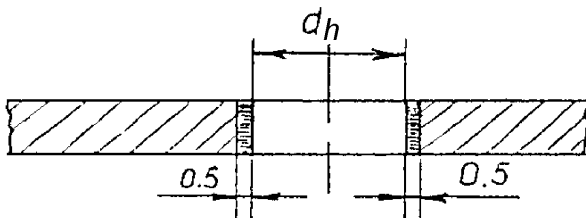


Fig. 1.1 Recommended Sizes of Initial Manufacturing Defects for Thin Sheets

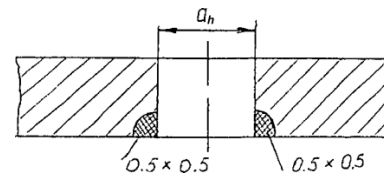


Fig. 1.2 Recommended Sizes of Initial Manufacturing Defects for thick sheets

3. For fillets surface crack (see Fig. 1.3).

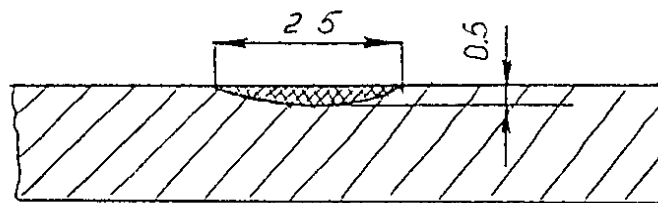


Fig. 1.3 Recommended Sizes of Initial Manufacturing Defects for Fillets Surface Crack

Note: Foreign requirements (by FAA and US Air Force) assume the presence of manufacturing defects on one side of each hole in one load-bearing section, with one "leading" defect ( $L_1 = 1.25$  mm) and the remaining associated defects ( $L_2 = 0.125$  mm) (see Fig. 1.4).

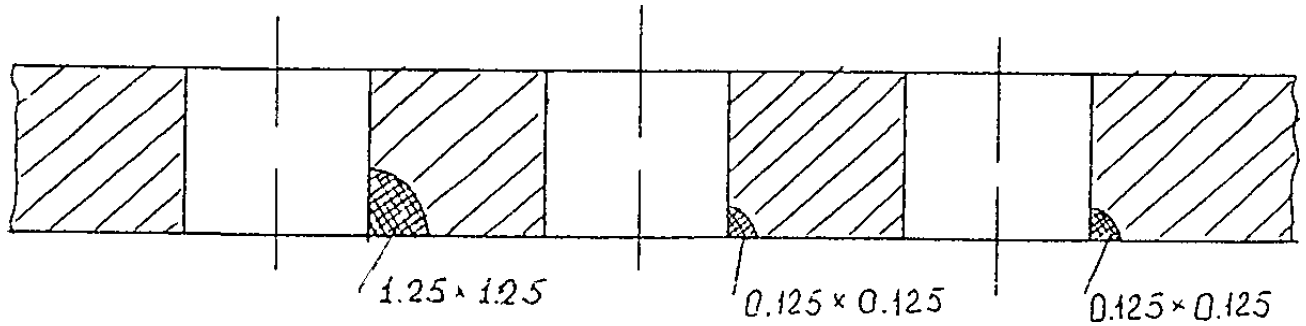


Fig. 1.4 Presence of Manufacturing Defects on One Side of Each Hole in One Load-Bearing Section

## Chapter 2

## PECULIARITIES OF SELECTION OF STRUCTURAL MATERIALS FOR AIRCRAFT

---

For many years the main structural material (65...75 %) is aluminum, or rather, its alloys. In addition to aluminum, a significant place in aviation technology is occupied by structural (medium-strength and high-strength) and corrosion-resistant steels (8...10 %), titanium alloys (1.5...3.0 %). In recent years, in aviation constructions, the share of magnesium alloys has decreased, due to their low corrosion resistance and increase in the calendar resource of aircraft, and the volume of use of titanium alloys has increased for the same reason. The volume of use of composite materials on a nonmetallic and, to a lesser extent, a metal matrix has increased quite significantly. According to the data of all aircraft building companies, the weight of composite materials is up to 20 % of the weight of the airframe, leaving behind aluminum alloys. According to Boeing, the weight of carbon-epoxy composites in the Dreamliner B787 is 50 % of the weight of the airframe, which is today a record in the use of composite materials. [15, 86, 87]

When selecting the material for a particular design of aircraft they primarily pay attention to ensuring its mechanical strength and stiffness at minimum weight, that is, to ensure the maximum weight efficiency of the material.

The *weight efficiency* of the material is evaluated by the specific strength of  $\sigma_u/d$ , the specific stiffness  $E/d$  and the specific resistance to cracking  $K_{1c}/d$ .

From the physical point of view, the concept of *specific strength* determines the length of a given material that is destroyed without load under the action of gravity of the Earth, and is measured in meters:

$$\left[ \frac{\sigma_t}{d} \right] = \left[ \frac{kg / mm^2}{kg / m^3} \right] = 10^6 m$$

Analyzing the operating conditions of aircraft parts, we can conclude that most of them work under bending loads. If, at such a load, two parts made of different materials are compared, the ratio of their masses will be:

- for strength conditions

$$\frac{m_1}{m_2} = \left( \frac{\sigma_{U2}}{\sigma_{U1}} \right)^{2/3} \cdot \frac{D_1}{D_2};$$

- for stiffness conditions

$$\frac{m_1}{m_2} = \left( \frac{E_1}{E_2} \right)^{1/2} \cdot \frac{D_1}{D_2};$$

and the ratio of the cross-sections of the elements that take up the bending loads will be:

$$\frac{\delta_2}{\delta_1} = \left( \frac{E_1}{E_2} \right)^{1/4},$$

where  $m_1$  and  $m_2$  are masses;  $D_1$  and  $D_2$  are the diameters;  $\delta_1$  and  $\delta_2$  are the

cross sections of the first and second parts, respectively.

The generalized comparative characteristics of aerospace materials (at a temperature of 20 °C) are given in Table 2.1.

Table 2.1

Comparative Characteristics of Materials Used in Aircraft Structures

Material	Density $d$ , kg/m <sup>3</sup>	Stiffening limit $\sigma_u$ , MPa	Elasticity modu- lus $E$ , HPa	Strength/w eight ratio $\sigma_u/d$ , km	Specific stiffness, $E/d$ , km
Aluminum alloys	2700	400–650	72	14.8–24.0	26500
Magnesia alloys	1800	200–340	45	11.0–18.9	25000
Titanic alloys	4500	500–1300	120	11.0–29.0	26600
Steel of average strength	7800	800–1300	210	10.3–16.7	27000
High-tensile-strength steel	7800	1300–2300	210	16.7–29.5	27000
Composite material	1400 – 2600	500–1300	35–250	40–60	25000 – 100000

From the data in Table 2.1, it can be seen that, according to the main indicators, composite materials are fundamentally superior to traditional alloys.

Taking into account that the current aircraft (including supersonic), as well as engines and rockets operate at elevated temperatures, it is often necessary to take into account the properties of materials at these temperatures. The change in the strength characteristics of the main structural materials is shown in Fig. 2.1.

A clearer representation of the effect of temperature on the properties of materials demonstrates the dependence "specific strength – temperature" (Fig. 2.2). These characteristics indicate that the temperature up to 150 °C, even low-alloy ( $\alpha+\beta$ ) titanic alloy VT6 exceeds for superior specific strength both aluminum alloys and steel. In the temperature range of 300...500 °C ( $\alpha+\beta$ ) titanic alloy has a maximum specific strength, but overalloyed high strength alloy VT22 is applied then. In accordance with this indicator, titanium alloys are more efficient than other structural materials used in aircraft building industry.



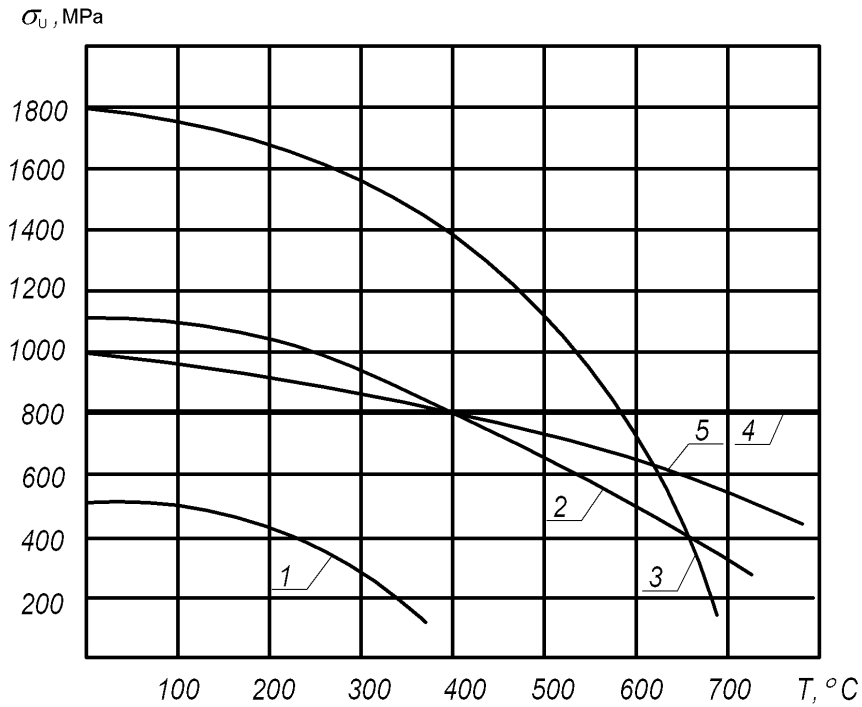


Fig. 2.1 – Main Structural Materials' Strength Characteristics ( $\sigma_u$ ) Versus Temperature (T): 1 – aluminum alloys; 2 – medium strength steel; 3 – high-strength steels; 4 – nickel superalloys; 5 – titanium alloys

$\sigma_u/d, km$

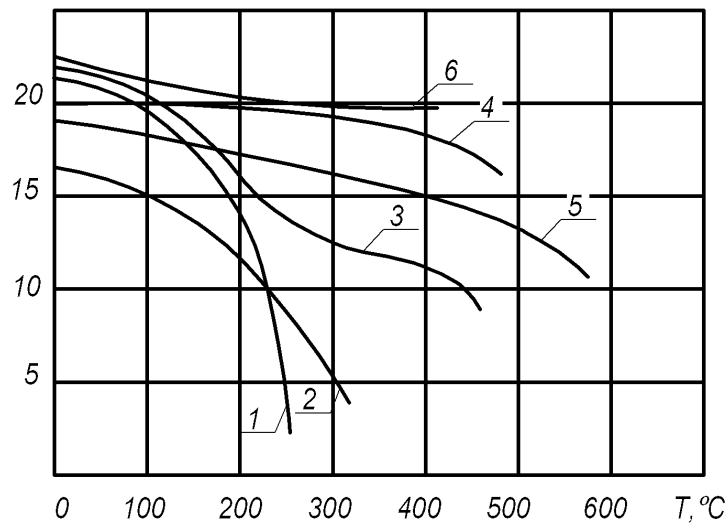


Fig. 2.2 – Specific Strength ( $\sigma_u/d$ ) of Structural Alloys Versus Temperature (T):

- 1 – aluminum alloy V95; 2 – aluminum alloy D16;  
 3 – titanium alloy VT6; 4 – alloy steel 30HGSA; 5 – corrosion-resistant steel VNS-2; 6 – titanium alloy VT22

The dependences shown in Fig. 2.2 show that starting from a certain temperature value (characteristic for each type of alloy), a sharp decrease in the strength of the material is observed, which must be taken into account when calculating the structure. In addition, for materials subjected to elevated temperatures, it is also necessary to take into account high-temperature creep, which manifests itself in changing the dimensions of the part under a constant load, which is sometimes much lower than the yield strength of the material.

In order to understand the approaches to the selection of materials for the airframe, you need to know how its primary members work. The aircraft airframe can be divided into five main members: the fuselage (which in turn is divided into the nose section, middle section and tail section), wing, tail (horizontal and vertical), landing gear and systems (aircraft control system, hydraulic system, fuel system, air system). Each of these members takes up their characteristic loads (always symmetrical), which primarily determine the selection of material for their manufacture. [15, 86, 87]

The fuselage is generally made of aluminum alloys: the skin and longitudinal framework are made of alloy D16 (duralumin), and the transverse framework is made of high-strength alloys V93, V95, 1933. The specific loads on the fuselage (except for the fuselage centre section) are low.

The wing carries all the loads both from the aircraft weight and wind weight (resulting from the airflow effect). In such conditions, the wing functions in such a way that its upper surface is in the compressed position, and the lower one is in the extended position. Therefore, the upper part of the wing is made of high-strength aluminum alloy V95, which has the maximum strength/weight ratio among all the standard aluminum alloys. The lower part of the wing is made of duralumin D16, which has higher fatigue performance. In recent years, research on the use of high-strength alloy V96Ts3 to construct the upper part of the wing has been carried out (this research is made mainly on increasing the ductility properties and fatigue life of the alloy).

The leading edges of the wing and tail, heated to prevent icing, are made of heat-resisting aluminum alloy AK4-1, and on the latest aircraft model – from alloy 1370, as more workable in comparison with alloy AK4-1.

The aircraft control surfaces (on the wing and tail) are made of high-modulus carbon composites based on the conditions of maximum hardness (minimum elastic deformation during deviation).

Tail can be made of aluminum alloys, however, the approach to selection of the material is the same as for the wing. In the new A/C, the tail is a monolithic integral structure made of carbon composites, which provides a significant weight effect. Polymer matrix composite materials are also used to produce wing and tail fillets, undercarriage bay fairings and so on.

As noted above, the main criteria for the selection of structural materials, as well as aluminum alloys, are their specific values of strength, stiffness and fatigue. Nevertheless, corrosion, which, as a rule, develops in the construction beyond the expiration of 10–20 years of A/C operation, also sets its requirements for the A/C design. A firm compromise solution is necessary to select the materials at the design stage because the corrosion damage is postponed in time from the design stage, and the strength, operation (easy servicing) and cost aspects contradict corrosion-resisting requirements. This can be justified by a standard example of the corrosion-resisting properties-to-aluminum alloys strength properties ratio, which subject material to hardening and aging (see Fig. 2.3).

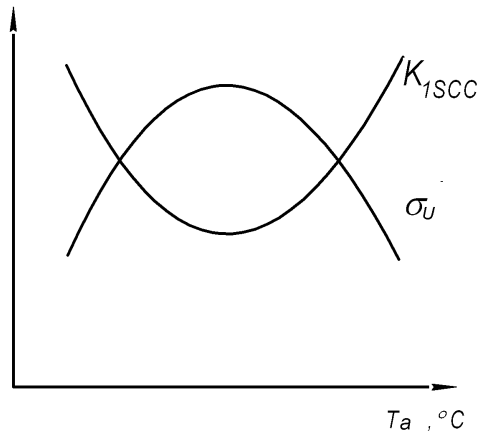


Fig. 2.3 – Ratio Between the Critical Stress of Corrosion Cracking Stress Intensity Factor ( $F_{1SCC}$ ) and Tensile Strength ( $\sigma_u$ ), Depending on the Aging Temperature ( $T_{cm}$ ) of Aluminum Alloys

As follows from Fig. 2.3, the maximum strength of the alloy corresponds to the minimum corrosion resistance, and lack of aging or over-aging of the alloy is necessary to ensure its operability, and such procedures are done, as a rule, for specific alloys (see thermal treating of aluminum alloys). As far as corrosion-resistant properties are concerned it is also necessary to take into account the electrochemical properties of the contacting materials, their type and the possibility of applying protective coatings, their operating conditions and so on while selecting the structural material.

Landing gear carries considerable dynamic loads during A/C take-off and, especially, landing. Aluminum alloys with the necessary minimum dimensions of the assembly (the landing gear struts must be retracted from the A/C bypass duct/secondary flow contours to reduce the aerodynamic drag) cannot function due to their mechanical properties. Therefore, the landing gear assemblies are made of high-strength titanium alloys (VT22) or high-strength constructional steels (30HGSN2MA, VKS170, VKS210). Moreover, the titanium alloys are preferable in new constructions also due to corrosion resistance, as mentioned above.

A/C systems perform various functions that impose their requirements on the selection of material for their construction. For example, the control wheel, control column and pedals cannot be small, as the pilot must feel control. Loads on these elements are insignificant, therefore they are traditionally made of molding magnesium alloys having a minimum specific weight and sufficient strength for these elements. Corrosion resistance for such elements is not critical. In the latest A/C models, the control wheel is made of polymers using the *Rapid Prototyping* method.

Pipelines of the A/C air system, through which hot air is transmitted (temperature of which is up to 350 °C) from the engine to the leading edges of the wing and tail, can be made of thin-walled tubes of corrosion-resistant steels or titanium alloys. Since titanium has the smallest temperature coefficient of linear expansion  $\alpha = 9 \cdot 10^{-6}$  degr.  $^{-1}$ , a low density of  $d = 4500$  kg/m $^3$  and a rather high strength  $\sigma_u = 600$  MPa (for PT-7M alloy) among other metals, it is

optimal material to manufacture long parts, operating in conditions of thermal cycles (-60...+350 °C) and attached to the "cold" frame. In this case is required a minimum number of compensators, which take up the thermal loads from the "frame", namely from the AE airframe, with the thermal extension of the pipelines, whose total length reaches hundreds of meters. The minimum thickness of the pipe web is limited by technological possibilities. The weight of titanium pipelines is less than the weight of the rest.

From the examples listed above, it can be concluded that the selection of materials for A/C parts and assemblies is determined by their design features, operating conditions, external factors, including corrosion and thermal factors, and is a creative process that equally requires knowledge of both material properties and A/C structure. [15, 86, 87]

## 2.1. APPLICATION FEATURES OF ALUMINUM ALLOYS IN THE AIRCRAFT STRUCTURE

Aluminum alloys are characterized by low density, corrosive-resistant strength, relatively high electrical and thermal conductivity; they can relatively easy take hot and cold deformation, rolling, forging, pressing, drawing, and sheet stamping. All aluminum alloys can be welded by spot welding, and special alloys – by melting and other types of welding. Aluminum alloys can be easily processed by cutting, protective decorative coatings can be applied to their surface. In the modern aviation industry, aluminum alloys are the basic material for making both the airframe (including fuselage, wing, tail fin, horizontal stabilizer) and system parts (including hydraulic system, fuel system, control systems). [15, 86, 87]

Non-alloyed aluminum (the second number "0" in the marking) is not used in the aircraft industry because of its low strength ( $\sigma_u \sim 100$  MPa). Non-alloyed aluminum is used to make containers (barrels), pipelines, and foil.

The alloys of Al-Mn and Al-Mg dopant system (the second number "4" and "5" in the marking, AMg and AMts) are used in the aviation industry almost in parallel to make unloaded welded parts, operating under aggressive conditions:

- Pipelines and hydraulic tanks of the drain lines (low-pressure lines) in the hydraulic system;
- Unloaded welded brackets in the control system.

The use of such alloys is associated with their high corrosion-resistance characteristics and almost identical to the base material strength of welded seams, which are long working in an aggressive corrosive atmosphere.

Rivets with increased plasticity and corrosion-resistance characteristics are made from AMr5П alloy.

Alloy D16 (1160, 1161, 1163) has been the basic aluminum alloy for aircraft structure for many decades. An analogue to this alloy are alloys 2024 (1160), 2324 (1163) of Al-Cu-Mg dopant system. All the main load-bearing members that determine the operational life of a passenger aircraft (in military aircraft is available less or is not available at all) are made of this alloy (and its modifications): lower wing panels (skin), stringers, fuselage sheeting,

spars, beams, frames, fin and horizontal stabilizer parts. In addition, various non-welded parts of A/C systems carrying tension and compression loads (brackets, fittings) are made of this alloy.

Alloy D16 is used in the T state – after hardening and natural aging (96 hours). Alloy D16 has a tensile strength (depending on the semi-finished product) which is equal to  $\sigma_u = 410...500$  MPa and the highest fatigue strength characteristics among aluminum alloys with a good ratio of endurance, crack toughness and resistance to fatigue crack growth, which determines its wide and almost mandatory application.

As for disadvantages of alloy D16, they include its unworthiness for welding (welded seam cracks due to the formation of  $\text{CuAl}_2$  intermetallide), insufficient corrosion resistance under stress and intercrystalline corrosion (ICC), low rate of fatigue crack growth resistance and limited temperature (80 °C) for long-term operation.

In the aircraft industry among the alloys of the dopant system alloys B65 (1165) have been used to make rivets and alloy AK4-1 (1141) to make A/C parts, operating for a long time under the conditions of heat rise up to 175 °C. The increased operating temperature of alloy AK4-1 is provided by its additional alloying of Fe and Ni and the formation of heat resistant intermetallic strengthening phases.

In subsonic airplanes the skins of leading edges, wing, fin and horizontal stabilizer are made of alloy AK4-1. They are heated by hot air to prevent icing. In new aircraft, alloy AK4-1, due to its low technological properties and low corrosion resistance, has been replaced by alloy 1370 (6013) of the Al-Mg-Si dopant system. Alloy 1370 (6013) with similar strength characteristics, has significant advantages in comparison with alloy AK4-1 in terms of corrosion resistance, weldability, plasticity.

Other alloys of this dopant system (except for alloy AK6 and AK8) are practically not used in aircraft building industry, but thanks to low price, high technological plasticity, corrosion resistance and weldability, they are widely used in other industries – construction, car and ship industry, general engineering.

Alloys AK6 (1360) and AK8 (1380) are used to make large forged parts (stampings), including to make strong brackets. In modern A/C they are replaced by more durable and corrosion-resistant alloys of the Al-Zn-Mg-Cu dopant system (alloys V93, V95, V96Ts3).

Alloy V93 (1930, 1933 – zirconium alloy) is used to produce large parts of a complex geometric shape for the internal A/C framework (frames, spars, landing gear levers, etc.) due to high static strength ( $\sigma_u$  500 MPa), corrosion resistance and burning section (up to 200 mm for alloy 1930, 80 to 150 mm for stampings of alloy 1933 after hardening in cold water). Such parts are made of massive stampings and forgings. Alloy B93 has no prototypes.

Alloy B95 (1950, 1973) is a prototype of alloy 7075 in the world classification. It is the most durable serial alloy for the aviation industry with

strength  $\sigma_u = 460 \dots 580$  MPa, depending on the semi-finished product. It is better than alloy D16 in terms of static strength and corrosion resistance, however, it has worse fatigue characteristics. Therefore, it is used to make A/C parts, which are loaded with compressing stresses during the operation, for example, the wing upper panels, horizontal stabilizers, spars, stringers (in the compressed area).

At present, attempts are made to use a stronger alloy V96Ts3 (1965) (which is a prototype of alloy 7055 in the world classification) instead of alloy V95. It has the strength limit  $\sigma_u = 600\text{--}650$  MPa (in the T12 state – hardening and three-phase aging). The implementation of this alloy is kept under by its low plasticity and fatigue life. To improve these characteristics searches are conducted towards the application of complex heat treatment modes.

Since the 60s of the last century, thanks to the work of Soviet materials scientists in the aircraft industry, the use of the lightest aluminum alloys of 1420-1470 series (analogues of alloys 8090, 2090 in the world classification) has begun. The use of these alloys had had both ups and downs for forty years. The first alloy 1420 of this dopant system had the strength characteristics identical with alloy D16, but less density by almost 10 %, elastic modulus greater by almost 14 % and good technological and corrosion properties. This made it possible to save from 10 to 15 % of the weight without re-designing of the parts. Such an alloy immediately drew the attention of the designer, and it was introduced on many aircraft types. However, after almost 15 years of operation, the parts of alloy 1420 began to get out of order along the corrosion cracking mechanism under the influence of operational solar heating. This led to the removal of the alloy from the construction of long-term operation. Further, new alloys and technological methods were developed to prevent this deficiency, however, insufficient fatigue characteristics and high price (almost 2 times more than that of alloy D16) became an obstacle for the modern application of Al-Li system alloys. Considering the intensity of work on alloys of this system in different countries, the situation may change for better in future.

Aluminum casting alloys used in A/C are represented by such grades as AL9 (AK7ch), VAL10 (AM4, 5Kd) and VAL14. They are used to make parts of a complex spatial shape with minimal surface treatment, which do not carry significant loads in operation. It gives them economic advantages in comparison with other types of semi-finished products. It is the reason of a limited number of alloy grades used in A/C structures, where preference is given to reliability factors.

Currently the highest achievement in the field of aluminum alloys for aircraft manufacturing is the development of “aluminum alloy-polymer” laminar compositions (grades: ALOR, SIAL, GLARE), which have extremely high specific characteristics of durability, but also a rather high price. [15, 86, 87]

## 2.2. APPLICATION FEATURES OF TITANIUM ALLOYS IN AIRCRAFT CONSTRUCTIONS

Titanium alloys are unique materials for many industries, including aviation industry, due to their inherent complex of physico-mechanical and chemical properties. [15, 86, 87]

In the aviation industry, there are four main areas of application of titanium alloys that coincide with their properties:

1. Dilute alloys of increased plasticity to manufacture items of complex spatial shape.
2. High-strength alloys to manufacture mission-critical high-loaded A/C assemblies and units.
3. Heat-resistant alloys to manufacture parts, mainly engine, operating at temperatures up to 600 °C.
4. Casting alloys.

The use of the first group alloys in A/C, which includes commercially pure titanium, is due to:

- High corrosion resistance of titanium (manufacturing of frames around access doors and doors where moisture accumulation is possible);
- High melting temperature and chemical resistance (manufacturing of skins, which are influenced by the flame jet from the engine, fire-blocking fire barriers);
- The minimum temperature coefficient of linear expansion among all metals (manufacturing of thin-wall pipelines of the air system).

Another direction of application of titanium alloys is based on the maximum specific strength of high-strength titanium alloys in comparison with other structural metals. In particular, for alloy VT22, the specific strength is  $\sigma_u/d \approx 27$  that is much higher than that for steels and aluminum alloys widely used in the aviation industry. Therefore, parts and assemblies made of high-strength titanium alloys are used where the maximum specific strength is required in combination with excellent corrosion-resistant properties. The characteristic assemblies are landing gears, bearing members (brackets) of the wing and fuselage, hydraulic cylinders, and so on.

The third direction of application of titanium alloys is determined by a slow decrease in their strength and plastic flow when heated to a temperature of 600 °C. Specific strength of heat-resistant alloys within this range exceeds that of superalloys.

Foundry titanium alloys have appeared relatively recently, although the first titanium alloy castings were obtained early in the development of titanium metallurgical industry.

Industrialization of shaped castings from titanium alloys has lasted for a long time by now. Difficulties in producing of shaped castings from titanium are determined by its high activity in liquid state when combined with gases, as well as with all known fire-resistant materials. Another circumstance delaying the development of titanium casting is the lack of a special foundry equipment that allows melting and casting of metal in a protective gas atmosphere or vacuum.

Currently, despite the presence of vacuum equipment with inductive or cathodic methods of melting and transforming of shaped castings into expendable shapes of graphite, wide spreading of titanium casting is prevented by its too high price, the worst set of physical and mechanical properties and less reliability as compared to deformable alloys. Therefore, cast titanium parts are used exclusively in cases where their shape does not allow manufacturing from deformable semi-finished products using mechanical method. In the latest A/C models, foundry titanium alloys are not used due to their high price and the need to have special equipment. [15, 86, 87]

Titanium alloys used in A/C are listed in Table 2.2

Table 2.2

## Application of Titanium Alloys in A/C

Alloy grade	Dopant system	Semi-finished product	Application
VT1-00	Non-alloyed	Bars, wire	Cathodes for ionic-plasma deposition of coatings, welding wire
VT1-0 (PT-1M)	Non-alloyed	Sheets, pipes, wire, bars	Pipelines parts of air system, bent brackets, foil for honeycomb fillers of composite materials, rivets
PT-7M	Ti-2Al-2,5Zr	Thin-walled pipes, sheets	Pipelines
OT4-1	Ti-2Al-1,5Mn	Sheets, bars, stamping	Frames around access doors and doors, bent and stamped brackets, pipeline elements, fire barriers, hard plates
VT6C	Ti-6Al-4V	Sheets, bars	Spiked coverings of cargo compartment floor
VT6	Ti-6Al-5V	Sheets, bars, stamping, plates	Fasteners, including threaded fasteners, control rods, welded brackets
VT16	Ti-2Al-5Mo-5V	Bars	Fasteners with rolling thread
VT3-1	Ti-6Al-2,5Mo-2Cr-Fe-Si	Bars, stamping, thick-walled pipes	Brackets, fasteners, clamp stocks
BT22	Ti-5Al-5Mo-5V-1,5Cr-Fe	Bars, plates, stamping, forgings, thick-walled tubes	Brackets, landing gear parts, including welded parts, cylinder actuators, swivel glands, threaded fasteners (large), guiding rails



### 2.3. APPLICATION FEATURES OF STEELS IN THE AIRCRAFT STRUCTURES

In the modern A/C structures the use of steel is constantly decreasing. It has the following objective reasons:

- Firstly, in order for steel to compete in terms of specific strength with modern aluminum and titanium alloys, the specific strength of which is 20 and 27, the maximum strength of the steel should be equal as follows  $\sigma_u = 2000$  MPa. Steels with such strength exist, but their use is limited due to their sensitivity to stress concentrators:

- Secondly, it has low corrosion resistance, in particular, low stress corrosion cracking stress intensity, which is especially important for A/C having a long service life.

Despite these drawbacks, steel parts account for about 10 % of the A/C airframe weight. The main advantages, on which their use is based, are a high modulus of elasticity, a relatively low price, traditions in the application of similar constructions and reliability proven during service. [15, 86, 87]

Steels in A/C structures, depending on the class, can be conditionally divided into the following types:

- Carbonic unalloyed steels, used for low-loaded parts, in particular bolts obtained by cold heading, and for parts whose manufacturing technology requires considerable plastic deformation;

- The most common constructional low- and medium-alloyed steels with medium strength. Various strength members are made of these steels. They are hardenable by heat treatment up to  $\sigma_u = 900...1400$  MPa, in particular welded and those that are subject to chemical–thermal treatment (nitriding, casehardening);

- High-strength constructional steels, which can be hardened by heat treatment up to  $\sigma_u > 1400$  MPa and that are used for manufacturing of A/C highly-loaded critical parts. They are divided into high-strength medium-alloy and martensitic-aging steels;

- The use of steels of each class depends on their physical-chemical-mechanical properties, performance, taking into account operating conditions: loads, contact with other materials, medium, presence or absence of friction, etc rust-free and heat resistant steels, used to manufacture corrosion-resistant

parts. [15, 86, 87]

#### 2.4. APPLICATION FEATURES OF MAGNESIUM ALLOYS IN THE AIRCRAFT STRUCTURES

The use of magnesium alloys in A/C structure is due to the minimum specific weight of magnesium among constructional metals at medium strength, which makes it possible to manufacture low- and medium-loaded parts with maximum weight coefficient. In addition, magnesium alloys have a high ability to absorb energy of a blow and vibrations. High specific heat storage capacity is also a positive property of magnesium. The disadvantage of magnesium alloys is their low corrosion resistance, which is the reason for their rare use in A/C of a long service life. Nevertheless, with appropriate protection, parts made of magnesium alloys can operate reliably under any weather conditions, including in contact with mineral oils, kerosene, gasoline, in alkaline environment, in contact with liquid and gaseous dehydrated oxygen and other environments non-aggressive to magnesium.

It is not recommended to use magnesium alloys in the following cases:

- Without corrosion-resistant protection of the surface which corresponds to the operating conditions;
- In seawater, in the acids environment, in their solutions and in vapors of other environments aggressive to magnesium;
- In places where accumulation of condensate is possible;
- For strength members located in places inaccessible for periodic inspection;
- For parts that are affected by air erosion during operation.

Two classes of magnesium alloys are used in A/C: deformable (MA8 and MA14 (VM65-1)) and foundry (ML5pch and ML8). [15, 86, 87]

*Chapter 3***METHODOLOGY OF INTEGRATED DESIGNING OF AIRCRAFT  
ASSEMBLED STRUCTURES OF SCHEDULED LIFE**

---

**3.1. NEW CONCEPT AND THE SCIENTIFIC BASIS FOR THE INTEGRATED DESIGN  
METHODOLOGY TO ACHIEVEMENT OF REGULATED DURABILITY OF ASSEMBLED THIN-WALLED  
AIRCRAFT DESIGNS USING COMPUTER-INTEGRATED SYSTEMS CAD\CAM\CAE**

The aviation industry is one of the leading priority directions of the Ukrainian industry development. To create a new competitive aircraft it is necessary to perform new scientific developments and create design methods, better than competitors do. The aircraft specified service life (for airplanes – 80000 to 90000 flight hours), at minimal mass expenditure, is one of the major parameters of competitiveness, the methodology of integrated design is largely used for assembled thin-walled structures of aircraft, its development is a promising scientific direction. [8, 9].

In establishing the methods of analytical and computer-aided design of aircraft assembled structures participated many Ukrainian and foreign scientists.

However, when developing these methods modern high tech computer integrated CAD/CAM/CAE were not applied. Their introduction in practice of designing required a new methodology of designing, modelling, engineering analysis and preproduction of the assembled aircraft thin-walled structures. Lack of experience in achieving the desired characteristics of structural efficiency using the CAD/CAM/CAE systems inhibits integration of experimental design methods with methods of computer modeling of the design. It does not allow to conduct high-quality integrated design of aircraft assembled structures, that can provide their life cycle [8, 9, 16].

In this regard, the development of a methodology for integrated design and computer simulation of aircraft designs is very relevant, and the creation of methods to achieve regulated service life characteristics of assembled structures and their joints with minimization of mass has great practical importance in solving flight safety issue under conditions of prolonged operation of aircraft.

The development of the information technologies made it possible to solve some problems in design of the aircraft assembly structures. An aircraft exploded view drawing that involves a great number of assembly structures is illustrated in Fig. 3.1. But because of the multifactor current task and as a result, the necessity of different specialists involvement (strength engineers, designers, process engineers, operators), the integration of their efforts to solve the problem in creation of the aircraft assembly structures was not succeeded.

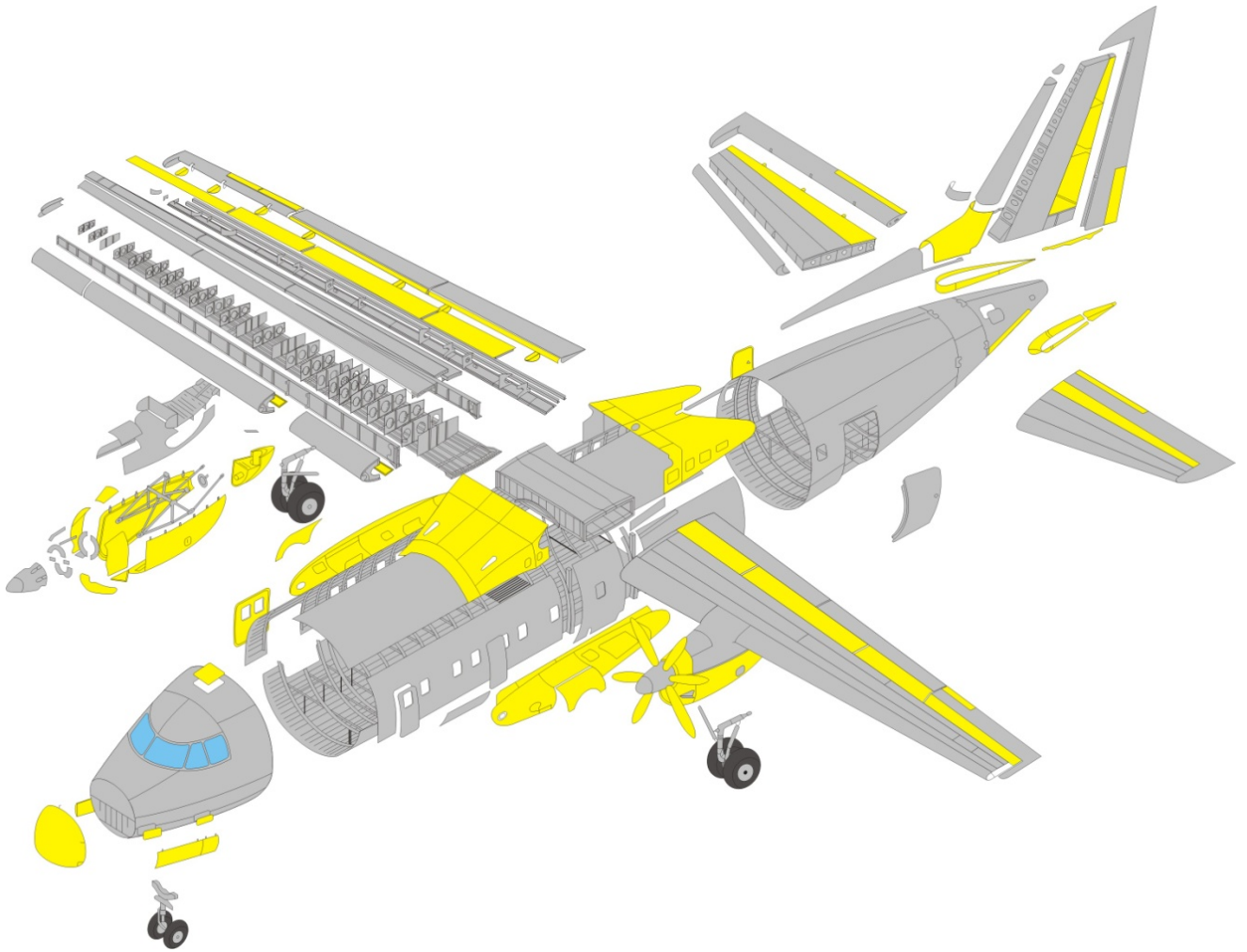


Fig. 3.1 – Aircraft Exploded View Drawing

Everything mentioned-above resulted in need for creation of a new design methodology that must involve the new methods and procedures of aircraft structure designing, preproduction, test and operation.

The new method must be an integrated method of the aircraft assembly structures designing and modelling with the aid of the CAD/CAM/CAE/PLM computer integrated system basing on the development of the three-dimensional analytical master copy of aircraft surface, its components, assembly units, new structural components, fasteners, computer-aided methods of analysis of the three-dimensional local deflected mode in joint member, new procedures in setting the fasteners with the elastoplastic radial interference followed by the experimental computing method in determination of the fatigue life characteristics of the standard joint models. This will make possible to design the assembly structure joints with the specified static strength, fatigue life, airtightness and external surface quality characteristics under minimal expenditure of mass.

It is known that the service life of the aircraft structures is determined by the

service life of its structural components to be significantly dependent on the working life of the bolted joints (Fig 3.2), being the sources of the fatigue crack initiation caused by both constructive stress concentration and the development of the fretting corrosion (Fig.3 3). Standard fatigue failure analysis and wing joints working life data obtained as a result of tests conducted in TsAGI are illustrated in Fig. 3.4 [11, 12].

It has been established that the working life of the crosswise joints is within the limits of the plate with a hole. It has been also established, that installation of bolts in the holes of the joint parts with axial and radial interference is one of the best efficient means to enhance the fatigue life of the shear bolted joints [8, 9].

Analysis of the design methods of assembled structures, taking into account fatigue (Fig. 3.5) shows that there is a need for further development of methods for predicting the effect of constructive and technological factors on durability of bolted joints to ensure their service life [11, 12].

In order to take into account the effect of the fretting corrosion along the contacting surfaces on the durability of the joint, the designed empirical relation is applied (Fig. 3.6) [11, 12].

Presently actual is a problem of development of the method for estimating the duration of highly-resourceful joints with axial and radial interference. The problem combines both the accumulated statistical material and the latest methods of engineering analysis of local stress-strain behavior in the concentrator zones, taking into account the loading history of assembly structures.

The use of computer systems CAD\CAM\CAE will allow to combine the theoretical background of designing the joints of aircraft assembly structures with the methods of engineering analysis and three-dimensional computer modeling.

The most common joints used in aircraft structure are riveted joints of thin-walled structures made of aluminum alloys.

Standard riveted joints of the airframe structural members are shown in Fig. 3.7. They are made by using blind rivets and rivets with protruding snap heads.

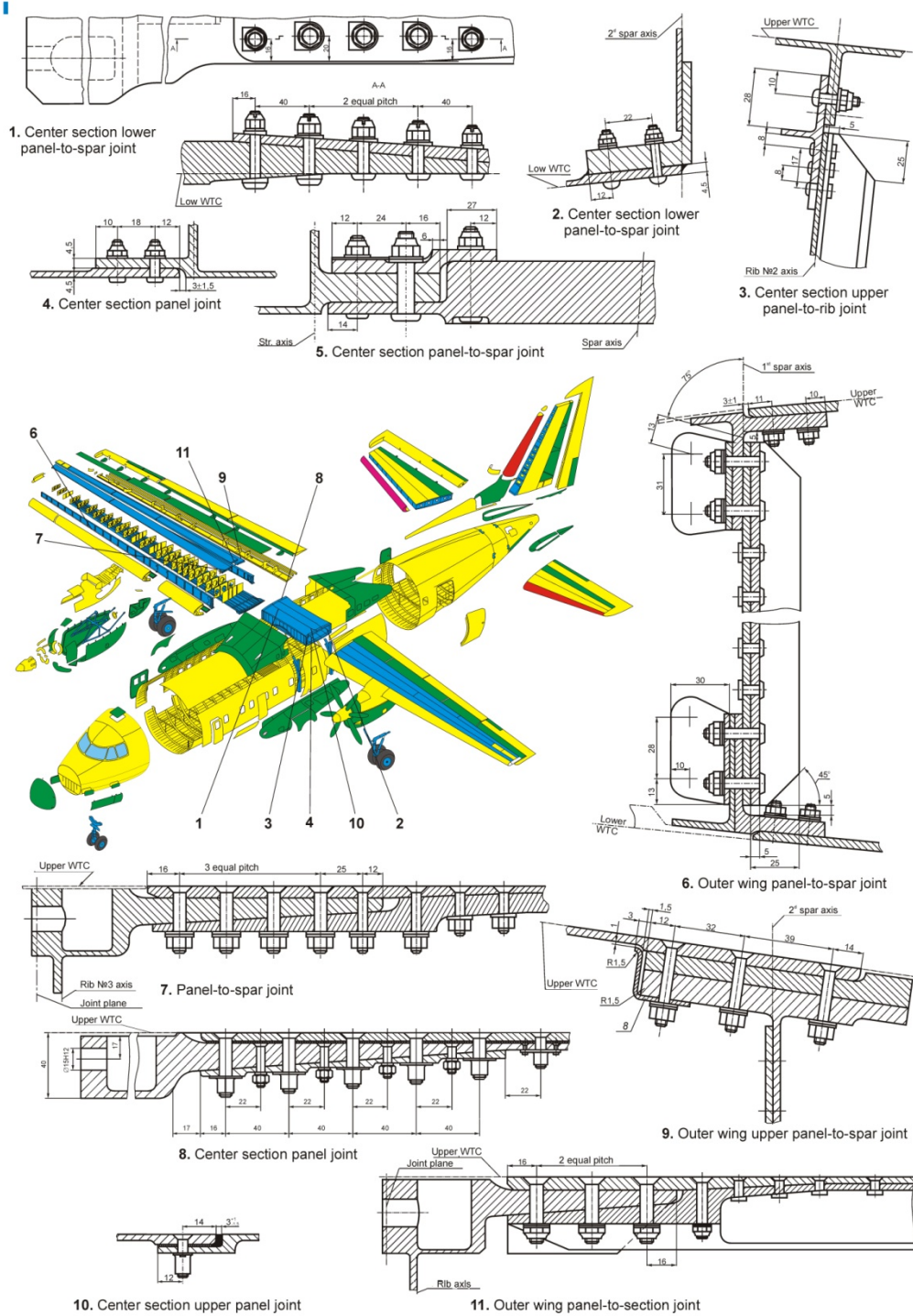
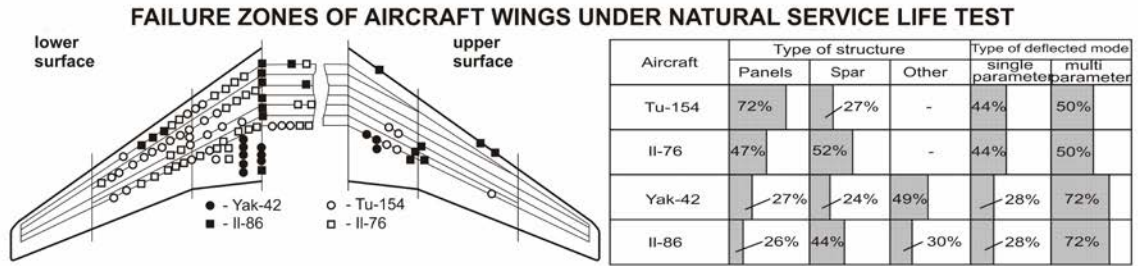
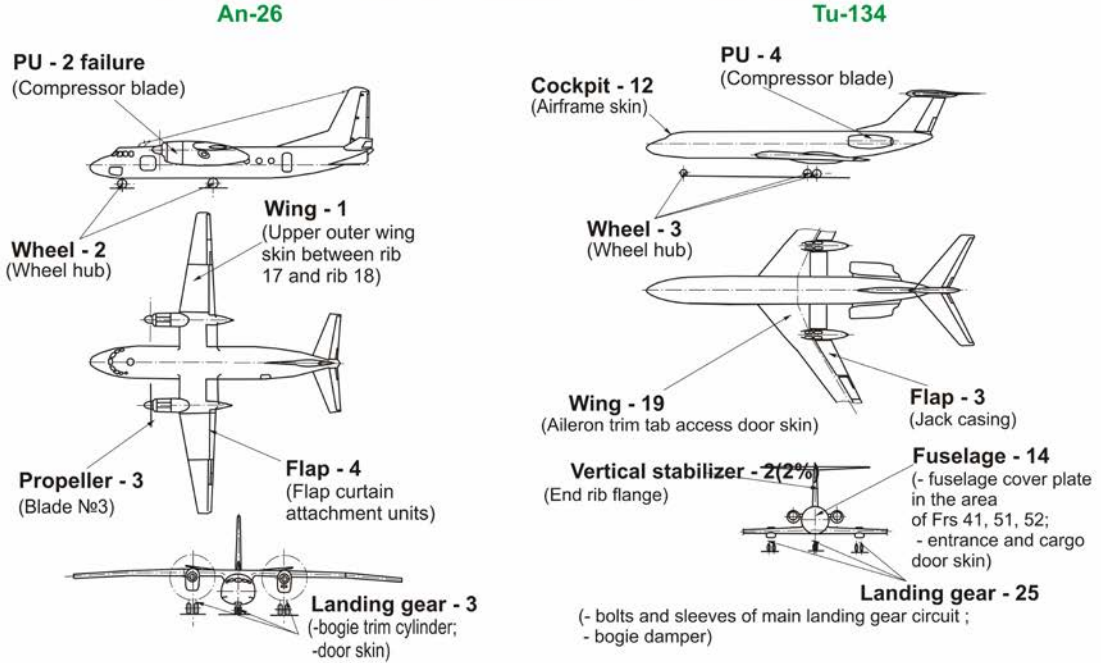


Fig. 3.2 – Aircraft Airframe. Aircraft Assembly Structures. Standard Bolted Joints





### FAILURE ZONES IN AIRCRAFT PRIMARY STRUCTURAL MEMBERS



During the period from 86.11.23 till 92.06.30 15 fatigue damage events were detected on An-26 airplanes in Kharkov Aviation Technical Base. During the period from 86.11.23 till 92.06.30 82 fatigue damage events were detected on Tu-134 airplanes in Kharkov Aviation Technical Base.

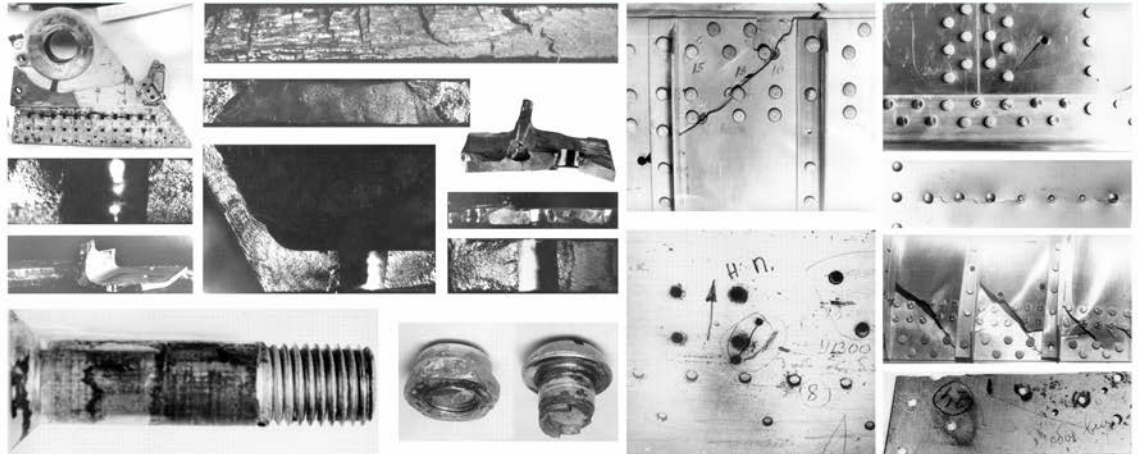
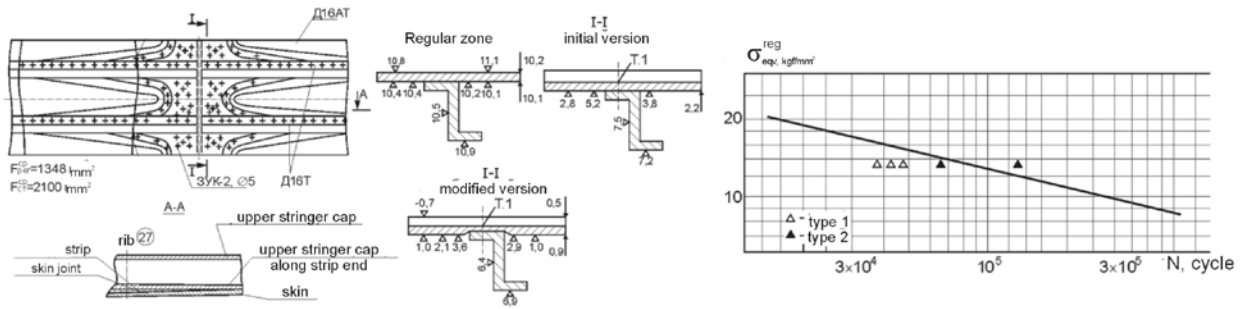
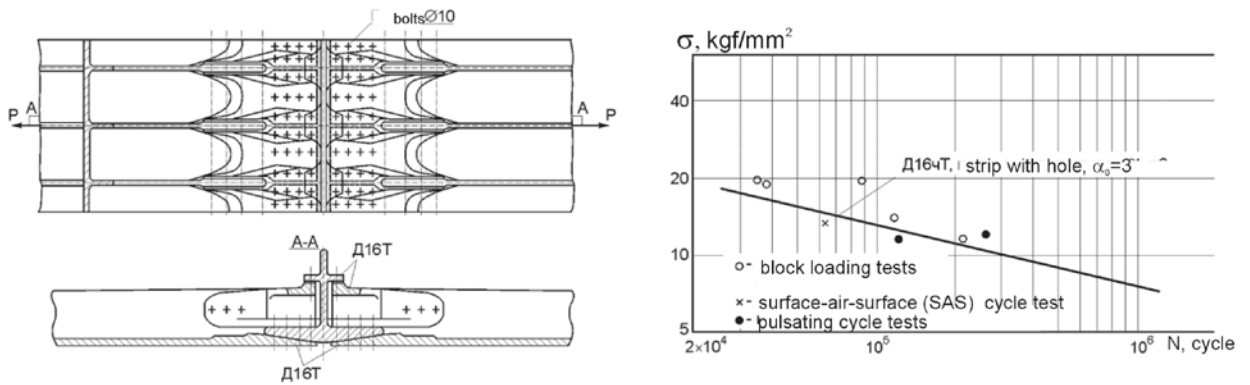


Fig. 3.3 – Aircraft Primary Structure Under Operation and Service Life Test. Fatigue Failure Zones and Patterns

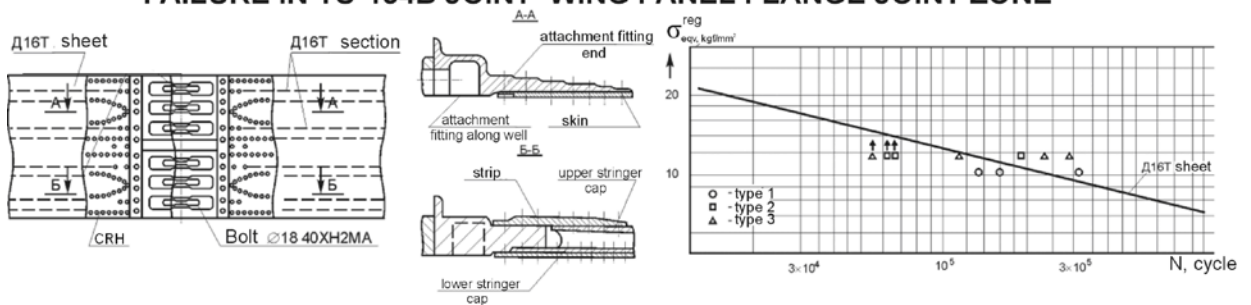
**FAILURE IN LATERAL JOINT ZONE OF TU-154 LOWER WING PANEL SKIN**



**FAILURE IN LATERAL JOINT ZONE OF II-86 LOWER WING PANEL SKIN**



**FAILURE IN TU-154B JOINT WING PANEL FLANGE JOINT ZONE**



**LIFE ESTIMATION OF IL-86 LOWER WING PANEL LONGITUDINAL JOINTS WITH REFERENCE TO PANEL TEST RESULTS**

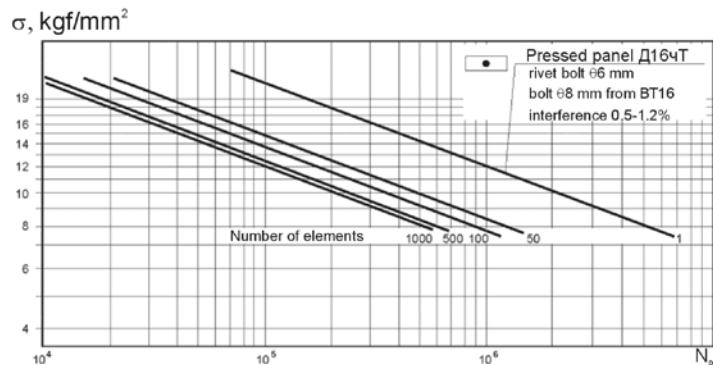
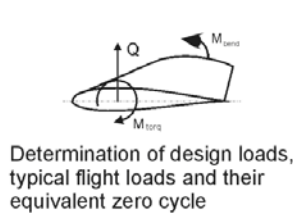
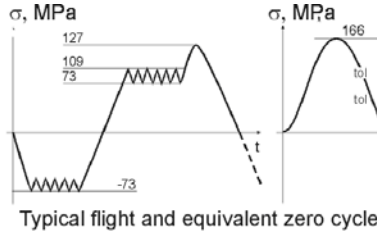


Fig. 3.4 – Standard Fatigue Failures and Service Life Analysis (by reference to TsAGI materials) Wing Joints





Determination of design loads, typical flight loads and their equivalent zero cycle



Typical flight and equivalent zero cycle

$$\sigma_{oeqv} = \begin{cases} \sqrt{2\sigma_a\sigma_{max}} & \sigma_m \geq 0; \\ \sqrt{2(\sigma_a + 0,2\sigma_m)} & \sigma_m \leq 0 \text{ and } \sigma_{max} \geq 0; \\ 0 & \sigma_{max} < 0. \end{cases}$$

$$\sigma_{oeqv} = \sqrt[4]{\sum_{i=1}^k n_i \cdot \sigma_{oi}^4}$$

Determination of the geometrical parameters provided that structural static strength is reached:

undercompression  $\sigma_{tol} \leq \sigma_{crit}$   
 under tension  $\sigma_{tol} = K_1 \sigma_{ult}$   $K_1 = 0,93$ .  
 Determination of the regular zone life at the sketch design stage from the equation of the plate endurance curve with a hole:

$$N = \frac{C}{\sigma_m^{2m}} \geq N_{given}$$

Correction of the tolerable stresses lever (2<sup>nd</sup> approximation):

$$K_2 = \sqrt[4]{\frac{N_{des}}{N_{1approx}}}; [\sigma_{calc}]_2 = [\sigma_{calc}]_1 / K_2$$

Correction of the regular zone geometrical parameters at the 2<sup>nd</sup> approximation stage. Determination of the geometrical parameters of the aircraft assembly structure joints:

$$P = \frac{\delta \cdot t}{m \cdot n} \sqrt{\sigma^2 + \tau^2} \leq P_{fract} = K_1 \sigma_B F_1;$$

$$P_{bear} = \delta \delta \sigma_{bear fract loc} \leq P_{fract}$$

$$P_{sh loc} = 2H \delta \tau_{sh fract loc} \leq P_{fract}; P_{sh} \leq \frac{\pi d^2}{4} \tau_{sh fract bolt} \cdot n_{bolt} \xi \cdot m$$

Determination of the typical joints life according to the techniques known:

$$\lg N_{pr} = \left[ \frac{\sigma_{apr}}{101,505(\sigma_{ult} - \sigma_{mpr})^{0,63}} - 0,01478 \right] \cdot 0,47619$$

$$K_a = \frac{\sigma_a}{\sigma_{an}} = K_s + [0,0394K_t(25,4 + d)\beta - K_s] \frac{(\lg N)^4}{1000 + (\lg N)^4}$$

$$K_t = 0,6 + 0,95 \frac{D}{d}; K_{eff} = g(K_t - K_s) + K_s$$

$$K_A = K_g R + K_n(1 - R); C_{Tn} = [2 + (1 - \frac{d}{D})^3] / (1 - \frac{d}{D})$$

$$\sigma_{afr} = 2,344(\sigma_{ult} - \sigma_{mfr})^{0,63} [0,64 + 43,3(\lg N)^{-2,1}] - 4,068(\lg N)^{0,918K_t} \sigma_c^{0,32} K_m$$

$$\sigma_0^*(N) = k_{bear}(N) \sigma_{bear} + k_{loc} \sigma_{loc} + k_{bnd}(N) \sigma_{bnd}$$

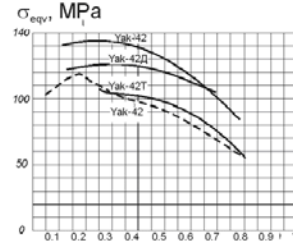
$$N = \frac{1}{W_{rd}^{\alpha} R_m}$$
 where  $R_m = R(1 - r \frac{\sigma_m}{\sigma_{ult}})$

$$(\Delta \epsilon_{plast}) N^{\alpha} = const, \quad \alpha = 0,6$$

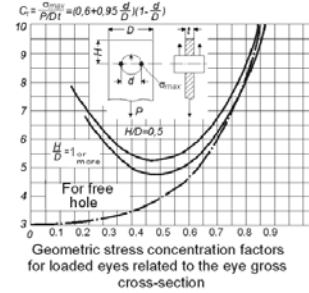
$$(\Delta \epsilon_{elast}) N^{\beta} = const, \quad \beta = 0,12$$

$$T_i = \frac{N_{bcd}}{\eta} + \frac{N_{wc}}{\eta^T} \geq T_{given}$$

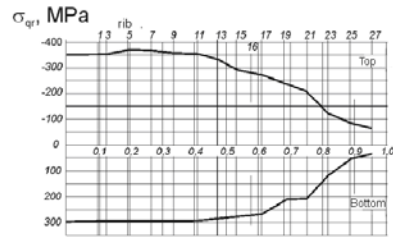
$$\eta = \eta_1 \cdot \eta_2 \cdot \eta_3 \cdot \eta_4 \cdot \eta_5 \geq 6; \quad \eta_T \geq 2$$



Equivalent stresses on the wing lower surface spanwise for different aircraft



Geometric stress concentration factors for loaded eyes related to the eye gross cross-section



Distribution of the design gross stresses on the lower and upper panels of Yak-42 aircraft wing

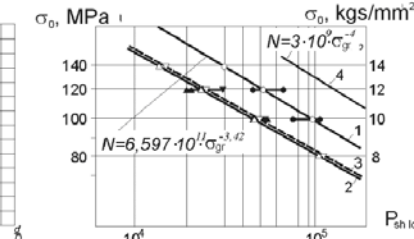
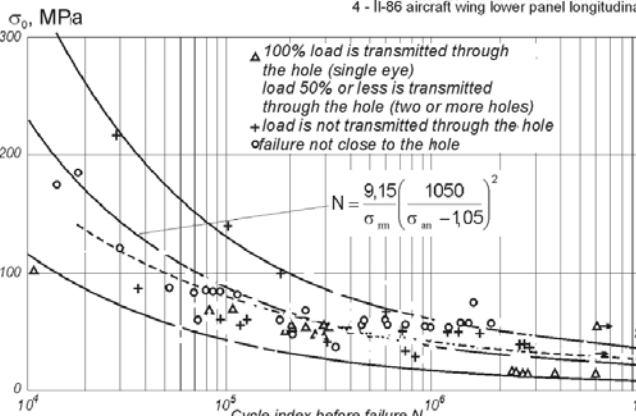
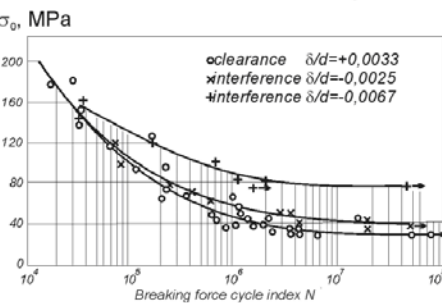


Plate endurance curve from D16-T with a hole:  
 1 - plate as-received condition with a parallel hole;  
 2 - plate as-received condition with a countersink hole;  
 3 - plate anodized in HX with a countersink hole;  
 4 - Il-86 aircraft wing lower panel longitudinal connection;

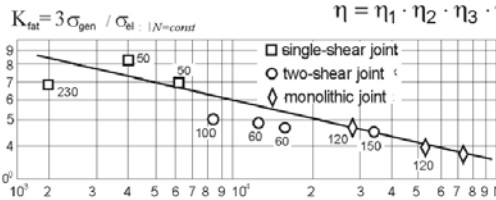


Experimental service life of typical aircraft joints made from aluminum alloys



Interference influence on the service life of the eyes from aluminum alloys

$$N_c \geq N_{reg}$$



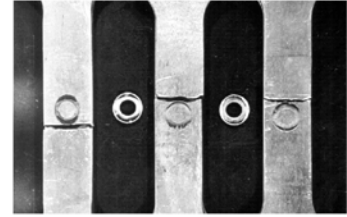
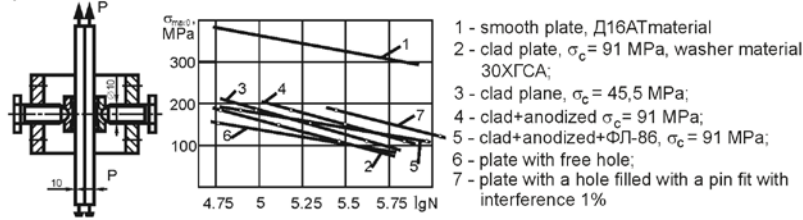
Fatigue ratio-to-service life dependence on the joint type

Influence of loading condition change on the service life:

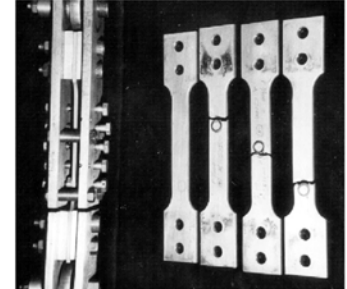
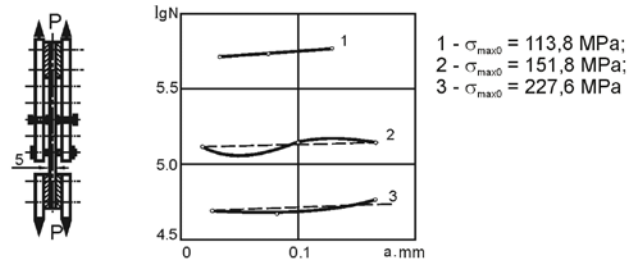
$$\frac{N'}{N''} = \frac{\sigma_{mn}''}{\sigma_{mn}'} \left( \frac{\sigma_{an}'' - 1,05}{\sigma_{an}' - 1,05} \right)^2$$

Fig. 3.5 – Analysis of Design Methods of Assembly Structures with Fatigue Taken into Account

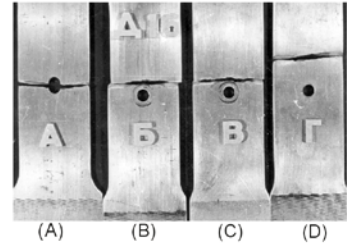
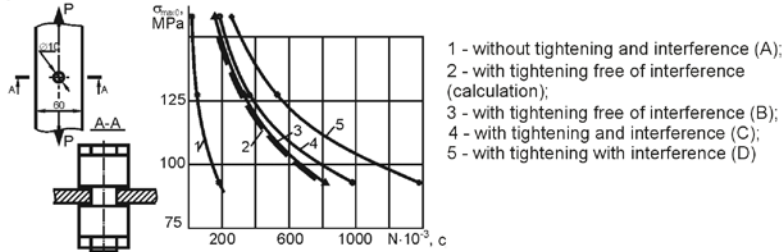
a) CONTACT PRESSURE INFLUENCE ON THE PLATE LIFE



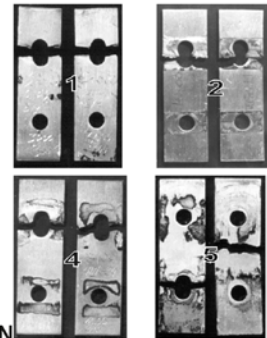
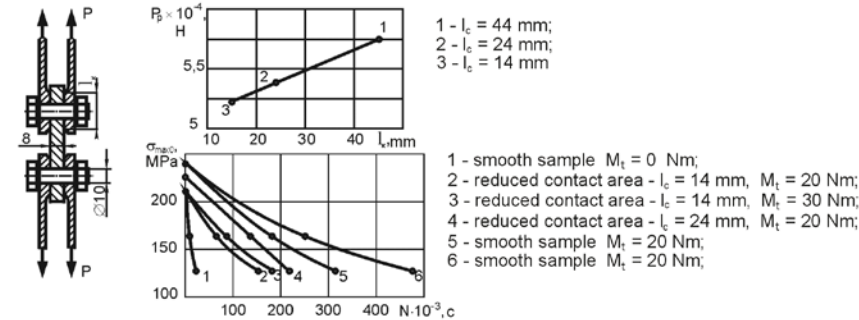
b) MICRODISPLACEMENT INFLUENCE ON FLAT PLATE LIFE



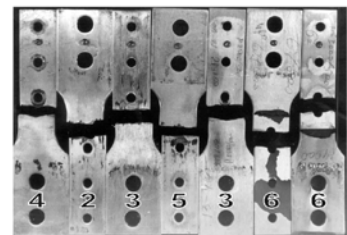
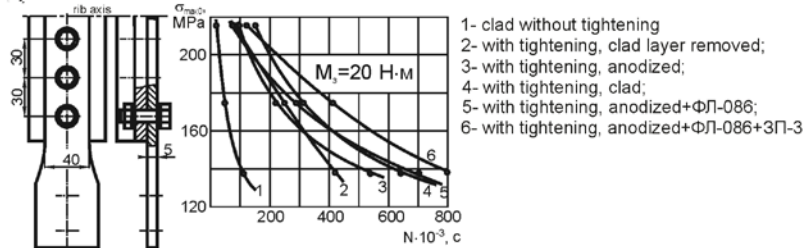
c) AXIAL AND RADIAL INTERFERENCE INFLUENCE ON THE SERVICE LIFE OF THE PLATE WITH A HOLE



d) CONTACT AREA AND TIGHTENING INFLUENCE ON THE SERVICE LIFE OF THE TWO SHEAR CONNECTION



e) COATINGS INFLUENCE ON THE SERVICE LIFE OF THE SINGLE SHEAR CONNECTION



$$\sigma_{\text{afr}} = 2.344(\sigma_{\text{ult}} - \sigma_{\text{mfr}})^{0,63} [0.64 + 43.3(\lg N)^{-2,1}] - 4.068(\lg N)^{0,918} K_{\text{cor}} \sigma_c^{0,32} K_m K_{fc}$$

Fig. 3.6 – Contact Pressure, Microdisplacement, Design-Processing Factors Influence on the Service Life of Structural Components of the Assembly Structure Bolted Joints under Fretting-Corrosion Conditions

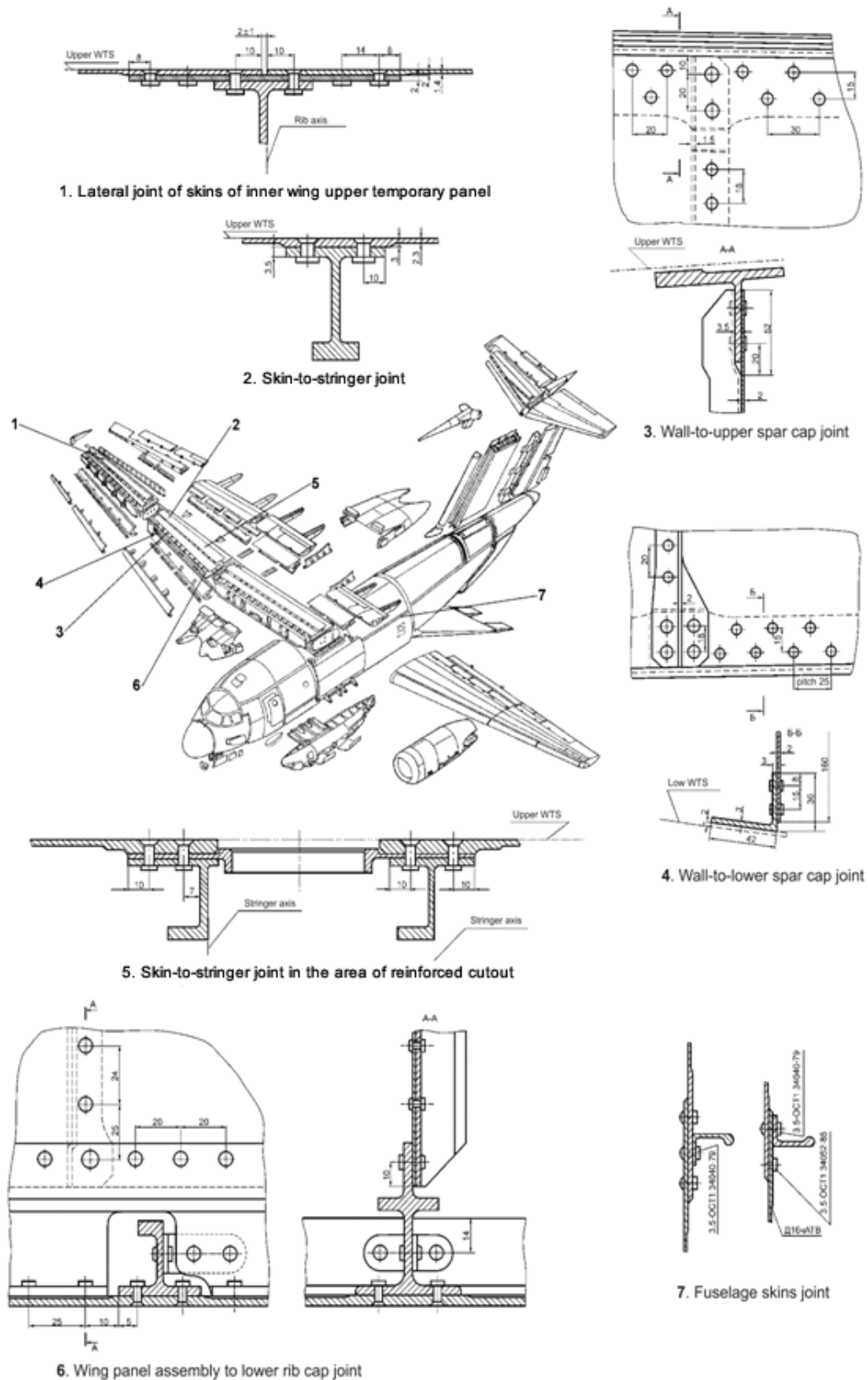


Fig. 3.7 – Aircraft Airframe Structural Components Standard Riveted Joints

In our country, in the "An" airframe design the blind riveted joints are made with using the rivets provided with a crown compensator in accordance with OST1 34052-85. The peculiarity of the joints with using these rivets is that the protrusion of the snap heads required by the external surface quality conditions can be realized only by their mechanical cleaning (milling), since the protruding part of the snap head before the riveting (size of a compensator) is much higher than the value necessary for filling the gaps in the countersink portion and to create a radial interference in the joint over the height of the rivet. In the process of cleaning, the protective anticorrosive coating is removed from the rivet snap heads and damage to it and the skin on the adjacent sections is not excluded, due to the tightening of the latter, and when using a manual mechanical tool for sanding. The results of measuring the protrusion of the rivet snap heads of 3 mm in diameter above the skin surface showed that after riveting before milling, the protrusion of the rivet heads from 0.3 to 0.71 mm is actually realized, after milling – from 0.03 to 0.27 mm. In this case, the protrusion height up to 0.1 mm is realized only in 44 % of the rivets. At the same time, the thickness of the shells' tightening in the areas of its attachment to the frames is 0.42 mm. The tightening to 0.05 mm is realized in the setting zone of 50 % rivets, the tightening from 0.051 to 0.1 mm – in the setting zone of 24 % rivets [12, 13, 15].

Thus, the development of new types of rivets, the technology of their installation, the methodology of their integrated design and modeling, methods for predicting their durability using computer integrated systems remains an urgent task.

The design of plane airframe, designed on the principle of safe damage or operated according to the technical state, must have sufficient survivability and service life in the presence of fatigue cracks of subcritical length in their elements.

$$T = \frac{N_{dbc}}{\eta} + \frac{N_s}{\eta_f},$$

Where  $N_{dbc}$  – durability before the appearance of a crack;  $N_s$  – durability from the moment of crack formation to the structure destruction;  $\eta$ ,  $\eta_f$  – reliability factors.

The durability of structures previously designed on the principle of a safe service life and being currently in operation, the information content of their fatigue tests can be significantly increased by using integrated methods for delaying the development of fatigue cracks, restoring strength and tightness.

At the beginning of its development, the plane of the fatigue crack is per-

pendicular to the middle surface of the plate, and then turns at an angle of  $\varphi = 45^\circ \dots 60^\circ$  to this surface (see Fig. 3.8). A breakaway type crack is transformed to a single and (or) double shear type. The transition from single to double shear in plates of  $\delta = 2 \dots 2.5$  mm thickness is detected for fatigue crack lengths  $2l = 80 \dots 120$  mm, and in plates of 5 mm thickness at lengths  $2 \cdot l = 20 \dots 50$  mm at the operating level of cyclic loads. At the same time, the front of the fatigue crack top in the areas of its stable growth in thin-walled air structures has a convex (elliptical or oval) shape. The change in the type of fracture in thin-walled structures is explained by the increase in the plasticity zone and, as a consequence, by the transition from the flat-deformed state to the plane-stressed state at the crack peaks as its length increases.

Experimental studies show that the direction of development of the fatigue crack of irregularity in a thin-walled structure changes significantly: holes, stiffeners, anisotropy of the sheet metal material, redistribution of stress fields as a result of crack development.

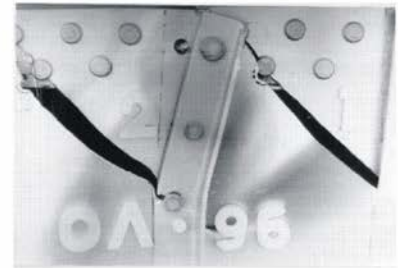
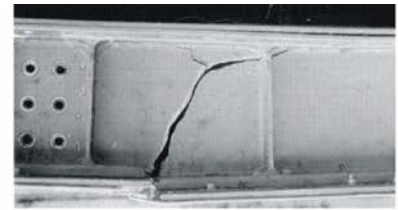
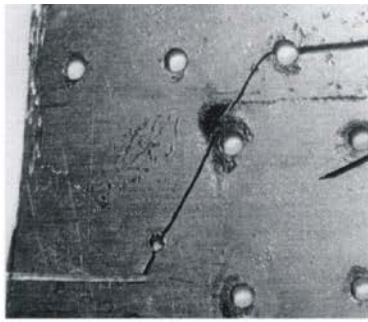
When a crack is close to the hole (or to the edge of the part), the bridge between the crack tip front and the hole wall is broken normally by a tear-off type or by a shear type.

On the basis of the revealed nature of the development of fatigue cracks and the type of fatigue failure of thin-walled structures, it is advisable to make a hole at the tip of the crack whose diameter is equal to or twice the thickness  $\delta$  of the sheet metal with a crack or more (see Fig. 3.8). The diameter can be reduced by placing the center of the hole at a distance from the top of the crack in the direction of its growth.

The contour of the hole with the center at the tip of the crack must be guaranteed to cover the entire front of its tip. Since the plane of the fatigue crack developing in a shear type makes an angle of about  $\varphi = 45^\circ$  with the midsurface of the sheet article, the nominal diameter of the hole at the crack tip must be chosen from the condition  $d_0 \geq 2\delta$ .

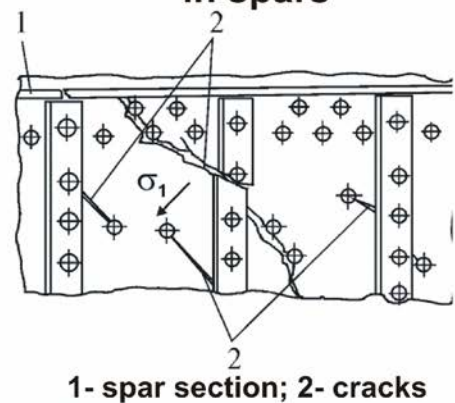
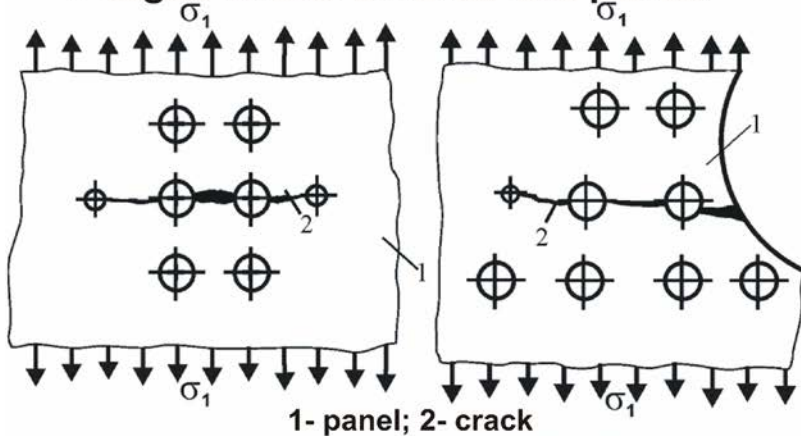
The formation of a hole of this diameter because of structural and technological limitations is not always possible and appropriate, for example, for large thickness of sheet articles. In addition, it often becomes necessary to make a hole whose center is displaced relative to the original direction of the fatigue crack propagation.



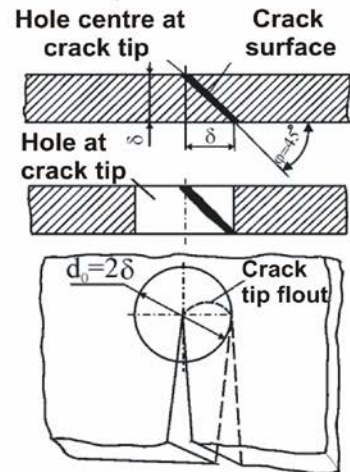
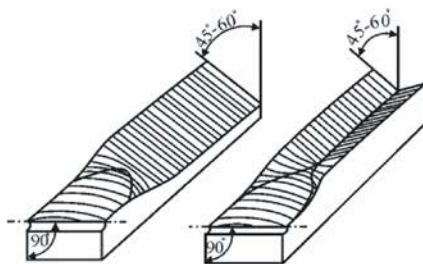


**Fatigue cracks in skins and panels**

**Fatigue cracks in spars**



**FATIGUE CRACK DEVELOPS PERPENDICULARLY TO ACTION OF MAIN TENSILE STRESSES  $\sigma_1$**



**Transformation of separated type crack to ordinary or double shear type**

**Parameters of holes made in fatigue crack tips**

**Fig. 3.8 – Nature of Fatigue Crack Development in Thin-Walled Structures of Aircraft Airframe under Operation and Life Test Conditions**

Making holes in the tops of cracks slows the crack growth, but does not stop it. The increase in residual durability with this method of crack retention with a length of 30 mm at the operational level of loads is 1.5 – 2 times compared to the residual life of the skin with a crack without drilling its ends. To ensure an assigned service life in the presence of cracks, it is necessary to develop new ways to delay their growth at the operational stage.

The analysis of previous studies in the field of design methods of aircraft assemblies of scheduled durability allows to formulate the purpose of this subsection of work and to determine the tasks, the solution of which ensures its achievement.

The purpose of this study is to ensure the scheduled durability of aircraft assemblies at all stages of the aircraft service life by developing methods for their integrated design by using the computer systems.

The state analysis of the problem of the design of aircraft assemblies with scheduled durability is carried out. The principles and methods for designing the aircraft assemblies, analytical methods for calculation of the aircraft parameters at the stage of preliminary design are analyzed, the features of automated and system design are considered.

From the analysis it follows that in the process of introducing the CAD \ CAM \ CAE computer integrated systems in designing to ensure the competitiveness of domestic aircraft, it is necessary to develop a methodology of integrated design of aircraft assemblies and their joints.

The analysis of design methods for aircraft assemblies, shear bolted and riveted joints taking into account fatigue is carried out. It is shown that in order to provide a service life for modern aircraft, it is necessary to develop methods for integrated designing and achievement of the scheduled durability of shear bolted and riveted joints, as well as to develop methods for delaying the growth of fatigue cracks to extend the service life of assembled thin-walled structures.

The integrated design method combines the methods of analytical design and computer parametric three-dimensional modeling of aircraft structure both as a whole, and its components, assembly units and parts that ensure their operability throughout the life cycle.

The primary load-carrying elements of the airframe are attached by various types of fasteners, which determine the service life of the airframe. The mass, life, aerodynamic and aesthetic characteristics of the aircraft depend on the quality of their designing and manufacturing. The previously used methods of automated design of aircraft assembled structures were based on two-dimensional models and their molding loft and did not allow to integrate them with the pre-production engineering systems and engineering analysis systems. The development and introduction of the CAD \ CAM \ CAE computer integrated systems into the production, science and learning process led to the need to create a new concept of integrated design of assembled aircraft structures (Fig. 3.9) [8, 10].

All works on the integrated design of the airplane assembled structures are performed in a single information environment of the aircraft under development. Engineering and processing databases are used.

Based on the proposed concept, the following principles of integrated design of aircraft assembled structures have been developed:

1. The principle of creating analytical standards of the aircraft assembled structures

Three-dimensional computer models of master geometry, space distribution, analytical standards of components of aircraft assembled structures are created using analytical geometry methods using the integrated CAD / CAM / CAE / PLM systems in a single information environment for aircraft life cycle support.

2. The principle of creating a master geometry of the airplane appearance

The parameters of the appearance of a new aircraft having minimum mass and the scheduled durability should satisfy the given prospective mission requirements (MR), the Aviation Rules, the concept of creating a new aircraft and be determined from the relationships:

$$\begin{aligned}
 & MR, AR \rightarrow \text{aircraft configuration} \rightarrow \\
 \rightarrow m_0 &= \frac{m_{op.i.\&eq} + m_{eq\&cntrl} + m_{pl}}{1 - \left[ \bar{m}_s(p, n_{des.ovrld}, N_{sch}, \lambda, RGP) + \bar{m}_{pp}(p, t_0, \gamma_e, R, N_e) + \bar{m}_F(p, C_f, k, L) \right]} \rightarrow \\
 \rightarrow m_{0\ min} &\rightarrow P_{opt} \rightarrow t_{opt} \rightarrow P_0 \rightarrow S_i \rightarrow \text{sections}_i \rightarrow (l_i, \lambda_i, \chi_i, \bar{c}_i, \eta_i, D_f, L_{VT}, L_{HT}) \rightarrow \\
 &\rightarrow (\bar{x}_T - \bar{x}_F) \rightarrow \text{analytical standard of aircraft surface.}
 \end{aligned}$$

3. The principle of designing regular zones of aircraft assembled structures

The design parameters and technology for the implementation of regular zones of aircraft structures should provide for carrying the design ultimate loads, the scheduled durability under the loads equivalent to the loads acting during a standard flight in the operating environment, the specified fatigue quality factor ( $K_f$ ), the given quality of the external surface, the air-tightness degree, and satisfy the following inequalities:

$$\begin{aligned}
 P_u &\geq P_d \left[ DP_{r.z.}, \sigma_{o.z} (N_{s.r.z.}) \right]; N_s \leq N_{d.r.z.} (DP_{r.z.}, \sigma_{0eq}, \sigma_d, TI) \\
 \Delta_3 &< 0 \text{ at } P = P_{op}; \Delta h \leq 0.05mm;
 \end{aligned}$$



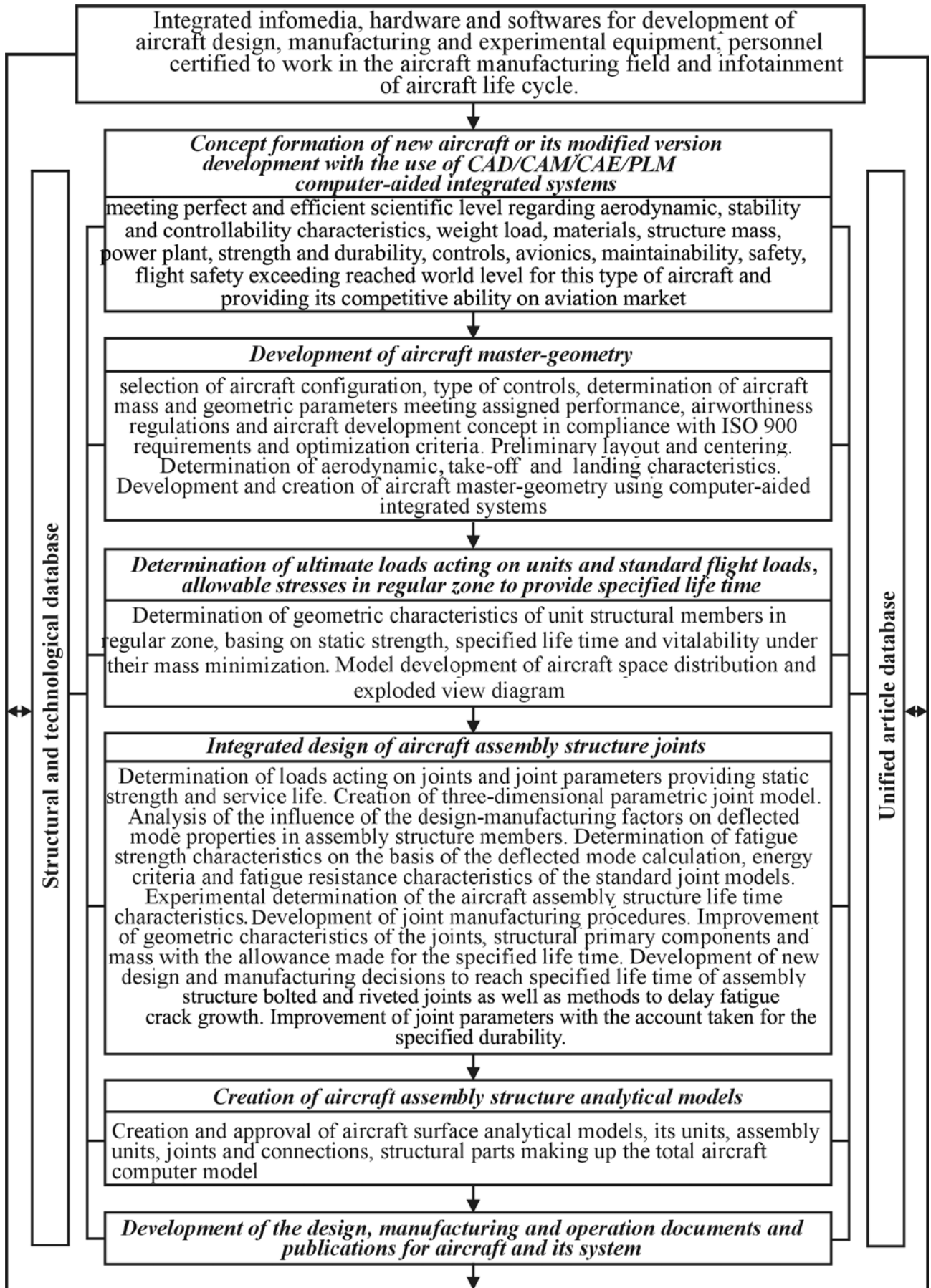


Fig. 3.9 – New Concept of Aircraft Assembly Structure Integrated Design

4. The principle of designing irregular zones of aircraft assembled structures

The design parameters and technology for the implementation of irregular zones of aircraft structures should provide for carrying the design loads in irregular zone under static loading, the scheduled durability, the given quality of the external surface, the air-tightness degree, that are equal to regular zone characteristics or exceed them, and satisfy the following inequalities:

$$P_{br} \geq P_{est}(DP_{r.z}, \sigma_{o.z}(N_{s.ir.z}));$$

$$\Delta h_{ir.z} \leq \Delta h_{r.z}; \Delta_{3ir.z} < \Delta_{3r.z};$$

$$N_s \leq \min(N_{d.ir.z}(DP_{ir.z}, (\sigma_{0eq} \cdot \varepsilon_{eq}), \sigma_d, TI));$$

$$N_{ex}(DP_{ir.z}, \sigma_0, \sigma_d, TI).$$

5. The principle of supporting and achieving survivability of assembled aircraft structures with fatigue cracks

The design parameters of safely destructible prefabricated aircraft structures should provide the ability to control critical locations, detect fatigue cracks and apply progressive ways to delay their growth, restore the bearing capacity and leak tightness of the damaged structure, and satisfy the following inequalities:

$$(N_{CGDT}/N_{d.s}) > 1; \Delta_{D,CGDT} < 0.$$

In the process of implementing these principles, scientifically based methods of integrated design of assembled joints of aircraft structures of the assigned resource, which are presented in the following sections, have been developed.

The methods for creating master geometry (Fig. 3.10), the model of the space distribution (Fig. 3.11), the parametric analytical standards of assembled units (Fig. 3.12) of aircraft structures, the geometry model of the entire product (Fig. 3.13). have been developed.

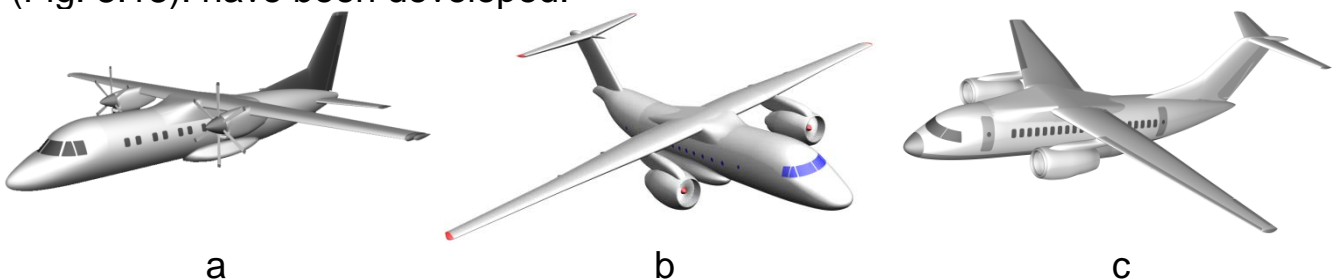


Fig. 3.10 – Aircraft Master-Geometry (Surface Model) Creative Method by the Use of CAD\CAM\CAE Siemens NX Computer-Aided Integrated Systems:  
a – An-140; b – An-74TK-300; c – An-148

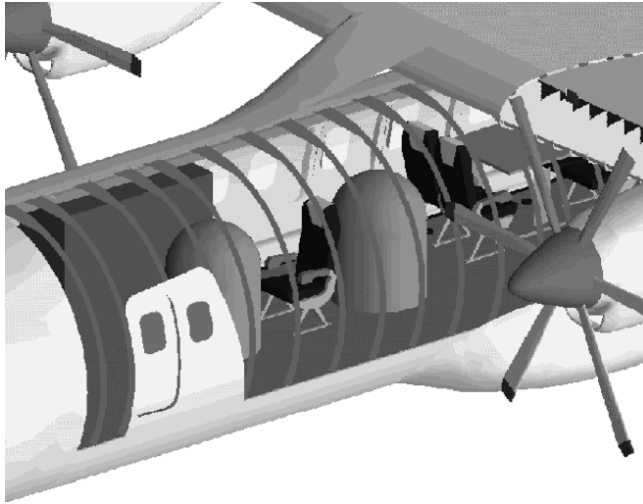


Fig. 3.11 – Segment of Space Distribution Model

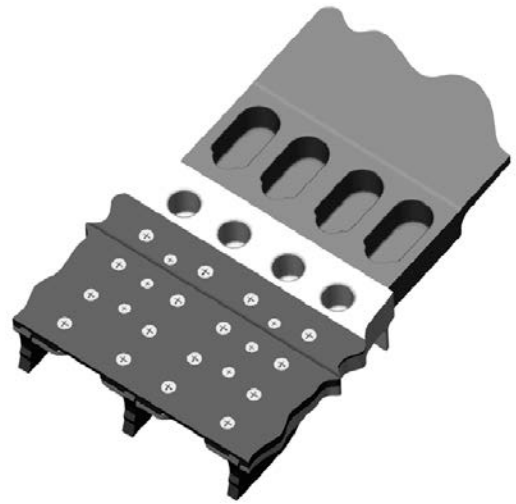


Fig. 3.12 – Joint Segment

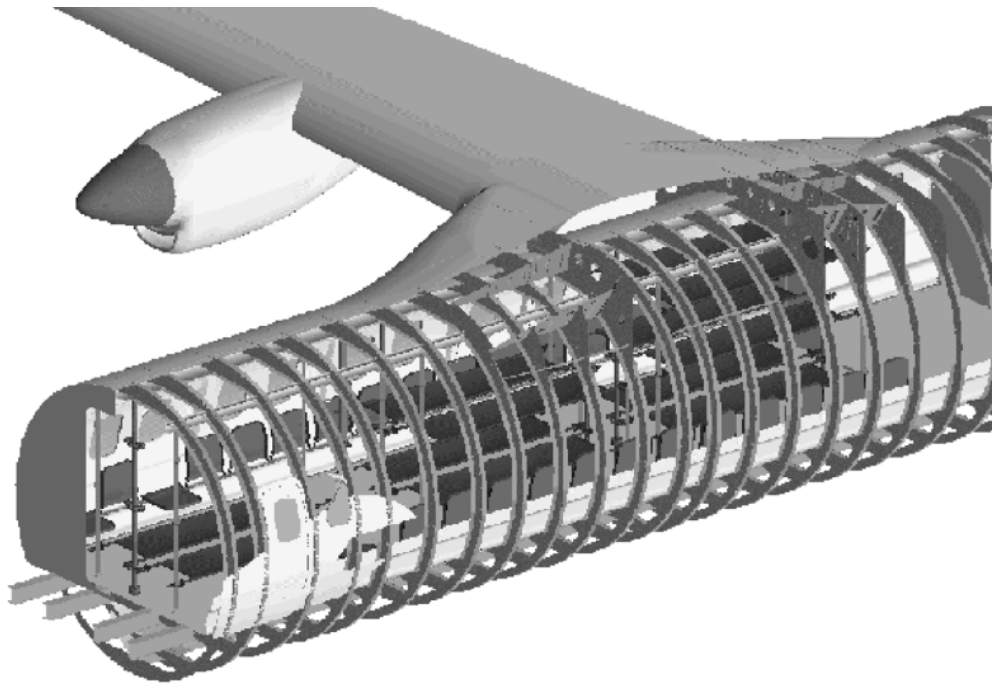


Fig 3.13 – Segment of Complete Definition Model

A method for analyzing the effect of design process parameters on the characteristics of the local strain-stress state of elements within regular zones of assembled aircraft structures has been developed using the ANSYS system, considering geometric, physical nonlinearities and contact interaction of structural members. It is tested on the example of the analysis of the local strain-stress state of the plate with a hole provided with a bolt with interference and tightness.

The characteristics of fatigue resistance of standard models of the regular

zone of assembled airplane structures have been obtained experimentally. Criteria for calculation and experimental dependences have been developed to predict the durability of regular zones of assembled structures. A method to predict the durability of zones of high-resource assembled aircraft structures based on the energy criterion, taking into account fretting corrosion and joint fabrication process has been developed.

The developed concept, principles and methods of integrated design of assembled airplane structures are the methodological basis for fabrication of airframe primary members joints with the specified characteristics of static strength, service life, air tightness and external surface quality with minimum weight of the joint.

### 3.2. METHOD OF INTEGRATED DESIGN AND GETTING THE SCHEDULED DURABILITY OF SHEAR BOLTED JOINTS OF AIRCRAFT ASSEMBLED STRUCTURES

Fig. 3.14 shows the method of integrated design and getting the scheduled durability of various bolted joints of assembled airplane structures.

The main component of the method of integrated design of shear bolted joints is the technique of integrated analysis of the effect of design process parameters on the characteristics of local strain-stress state in the elements of the shear bolted joints, taking into account physical geometric and contact nonlinearities using the ANSYS integrated analysis system (Fig. 3.15) [8, 13, 14].

The analysis technique has been tested in calculating the characteristics of local strain-stress state in the elements of standard single-row and multi-row shear joints made with elastoplastic radial interference and tightening.

The change in contact pressures (Fig. 3.16), gaps and local specific energy of deformation (Fig. 3.17) with a change in loading level has been investigated. It allows to predict the characteristics of scheduled durability in the zone of concentration of specific energy of deformation and contact pressures.

In Fig. 3.17 the numbers indicate: 1 – a plate with a hole provided with a blind bolt; 2 – double-shear single-row blind joint; 3 – double-shear three-row blind joint.

The characteristics of the fatigue resistance of standard bolted joints have been experimentally obtained. Based on them criterial dependencies for the calculation of the durability of joints have been developed (Fig. 3.18)

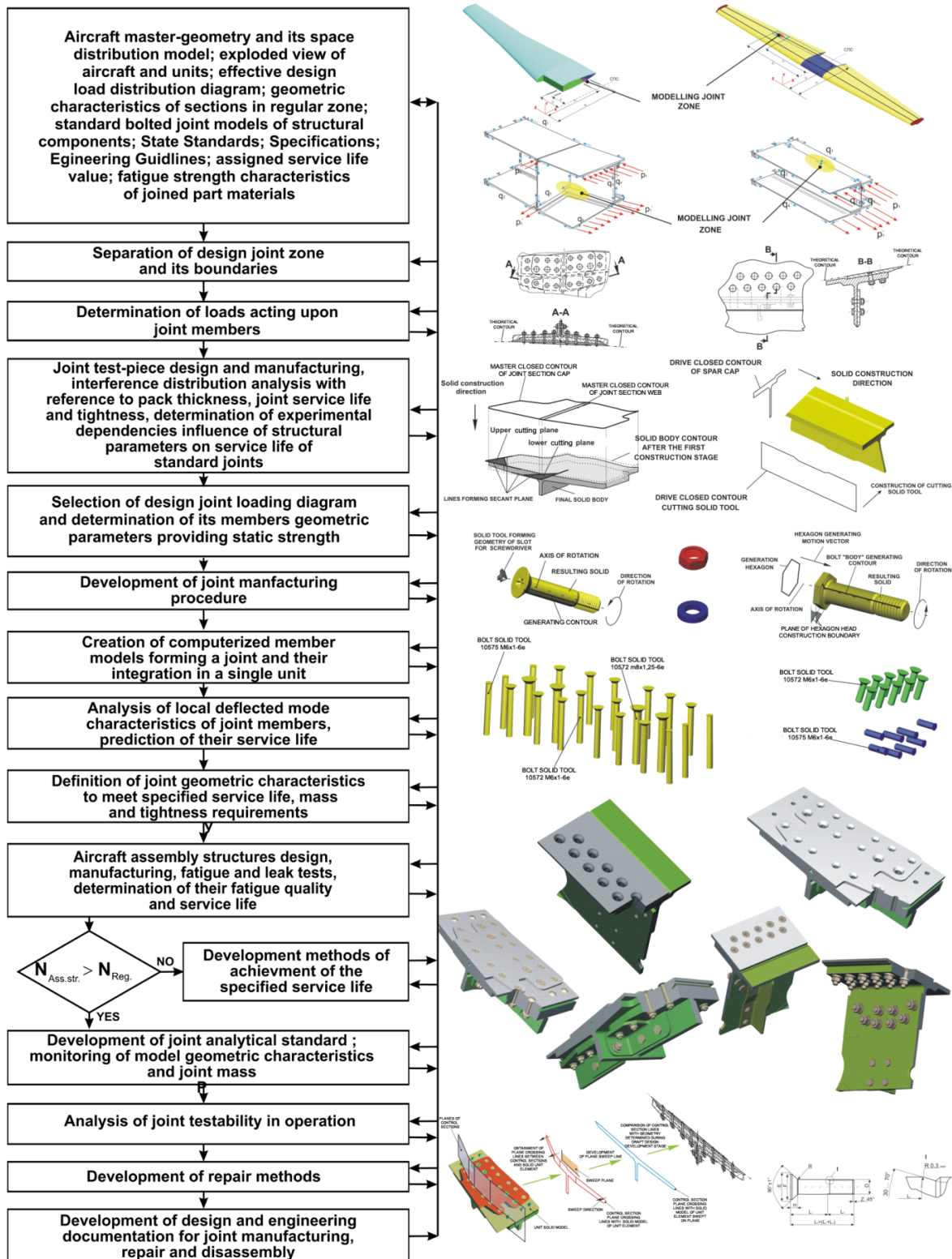


Fig. 3.14 – Method of Integrated Design, Simulation and Achievement of Regulated Durability of Shear Bolted Joints of Prefabricated Structures of Aircraft Assembled Structures



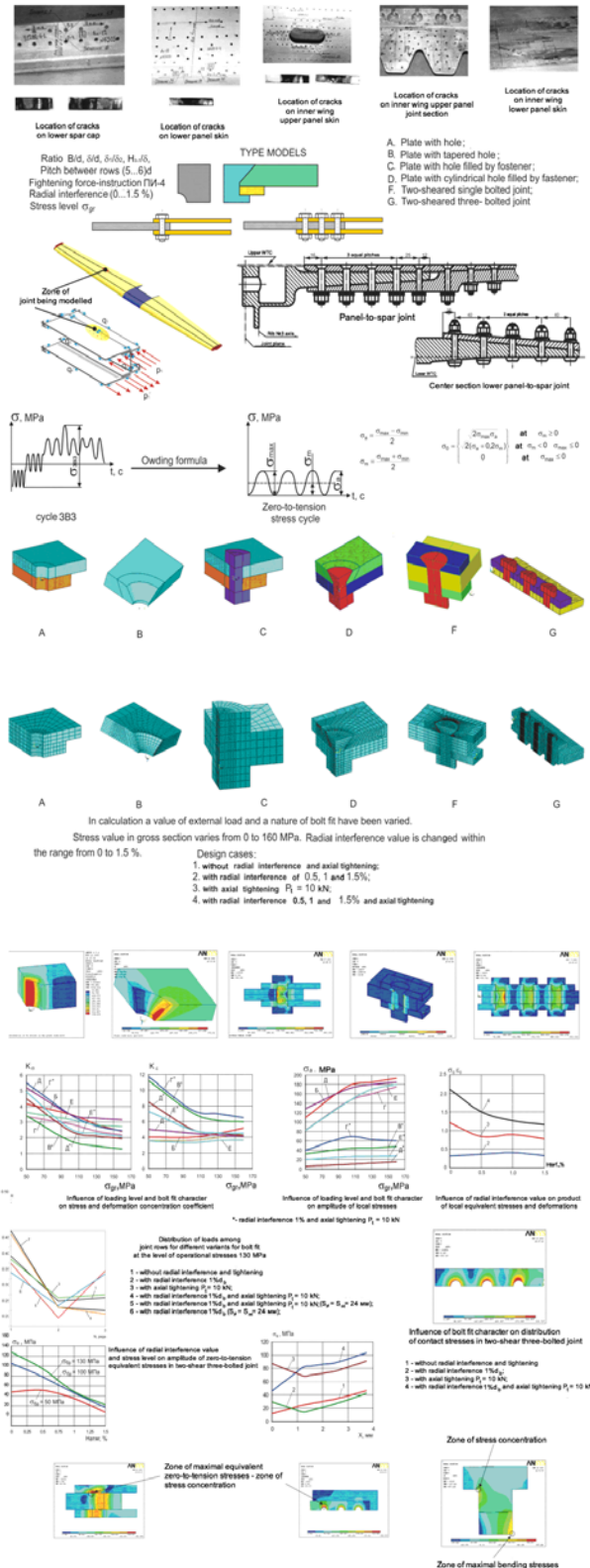
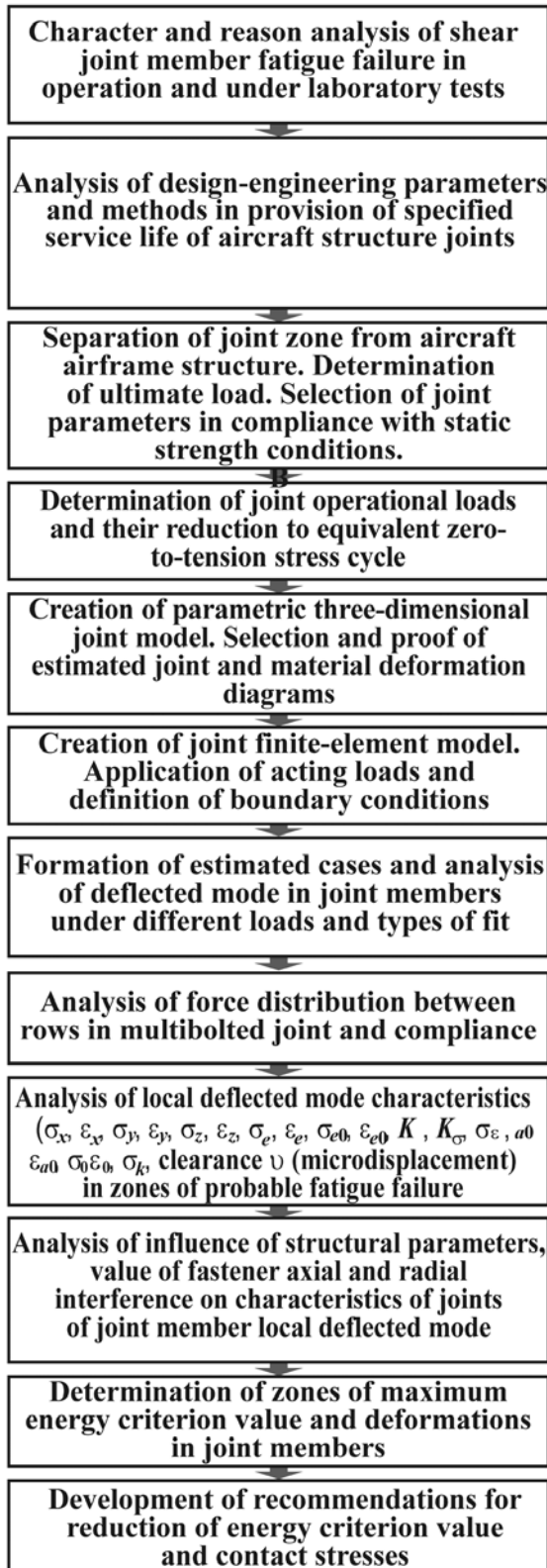


Fig. 3.15 – Computer-Aided Analysis Procedure of Influence Produced by Constructive and Technological Parameter on Local Stress-Strain State of Shear Bolted Joint Members

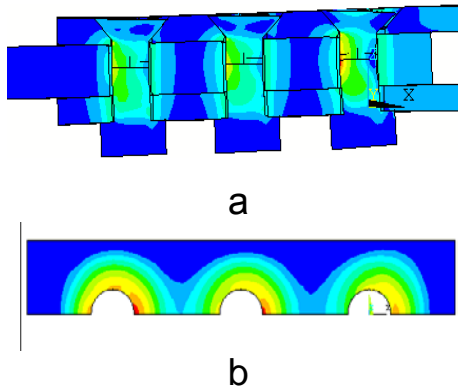


Fig. 3.16 – Nature of strain members joint (a) and coupling pressures distribution field (b) between upper overlay and plate at a level of external loading  $\sigma_p^{gr} = 48$  MPa ( $\sigma_s^{gr.e} = 100$  MPa) (displacement scale – 20:1)

$W_0$ , MPa

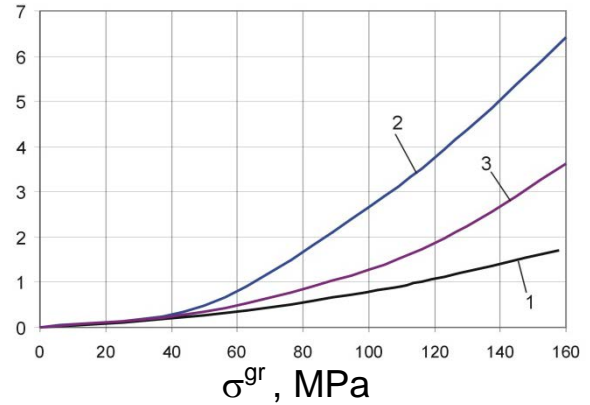


Fig. 3.17 – Loading level influence on complete specific strain energy change in area of probable fatigue failures of standard test pieces with a radial interference of 1 %  $d_b$  and axial tightening of 10 kN

Fig. 3.18 – Fatigue curves:

1 – plate with a counterformed hole, anodized

$$N\sigma^{3.58377} = 6.97894 \cdot 10^{11};$$

2 – plate with a hole filled by countersunk bolt with a radial axial interference of

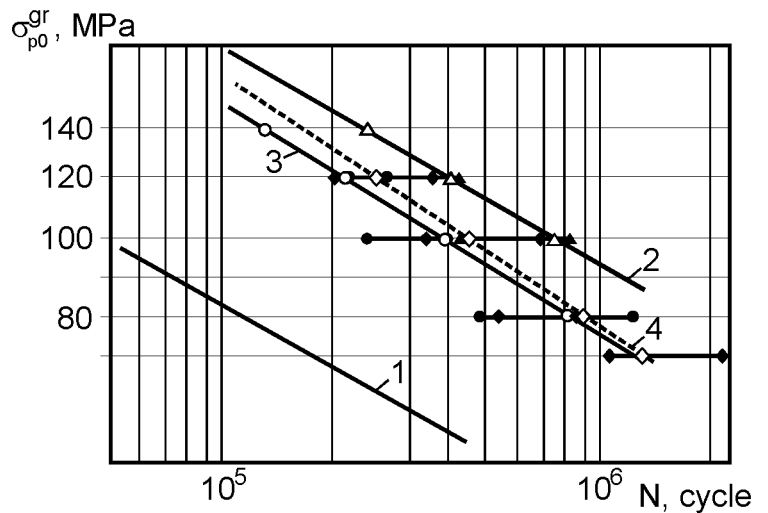
$$N\sigma^{3.07512} = 8.66973 \cdot 10^{11};$$

3 – single row double shear joint with a radial and axial interference of

$$N_f \sigma^{3.2977} = 1.48473 \cdot 10^{12};$$

4 – triple row double shear joint with a radial and axial interference of

$$N_f \cdot \sigma^{3.066} = 5.95009 \cdot 10^{11}$$



New procedure of determining load distribution between the rows in shear multi row bolted groups of assembly structures by using ANSYS system on the basis of estimated joint resilience has been developed.

Influence of radial interference on joint resilience changing has been determined as well as loading increase of utmost rows in joints with radial interference. This procedure has been validated under estimation of loads between the rows of eight rows shear bolted group (Fig. 3.19) fabricated from 30HGSA steel.

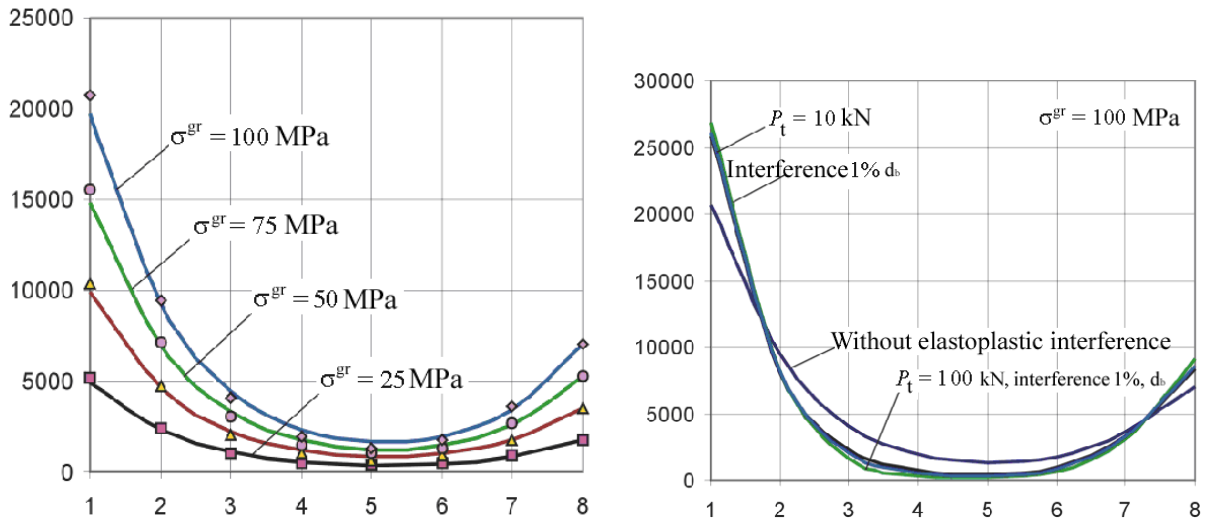


Fig. 3.19 – Effect Produced by External Loading  $\sigma_{gr}$  on Distribution of Loads as per Rows

Theoretical distribution of loads is specified by lines while points show estimation by method of final elements using COMBIN39 special element.

A new procedure has been proposed to predict effect produced by the structural and production parameters of shear countersunk bolted groups on their endurance (life time) with an account made for variations of complete specific strain energy values in areas of probable fatigue failure and intensive development of fretting corrosion:

$$N_m = \frac{C_b}{(\sigma_{b0}^{gr})^m (W_{0m}/W_{0b})^k} \quad \text{and} \quad \sigma_{af} = 2,344(\sigma_u - \sigma_{mf})^{0.63} \left[ 0.64 + 43.3(\lg N)^{-2.1} \right] - 4.068(\lg N)^{0.918K} \cdot \sigma_c^{0.32} K_m K_{NF},$$

where  $W_{0b}$ ,  $W_{0m}$  and  $k$  – is complete specific strain energy at the highest stress area close to basic hole and modified test pieces respectively and failure level factor expressed by a ratio of deformed modified test-piece state in compare with basic one;  $\sigma_c$  – coupling stresses in fretting-corrosion area, MPa;  $K_C$  – factor accounting an effect produced by the coatings on stress amplitude values decrease under specified endurance;  $K_m$  – a factor accounting a change of coupling type;  $K_{NF}$  – a factor accounting type of bolt fit.

Validation procedure under estimation of endurance (life time) and its variation for standard bolted joints:

- 1) plate with a counter bore hole filled by a countersunk bolt 5015A at a radial interference of 1 % and axial tightening of 10kN;
- 2) two-shear single row countersunk bolted joint with 5015A bolts placed at a radial interference of 1 %  $d_b$  and axial tightening of 10kN;



3) two-shear three row countersunk bolted joint with 5015A bolts set with a radial interference of 1 %  $d_b$  and axial tightening of 10kN.

Estimation and fatigue test results are shown in Fig. 3.20. Desired agreement between estimated and experimental data has been stated.

Creation procedure of computerized models of aircraft assembly structure bolted joints has been developed by the use of Siemens NX system enabling to provide parametric modelling of joints during computed-aided design of joints (Fig. 3.21).

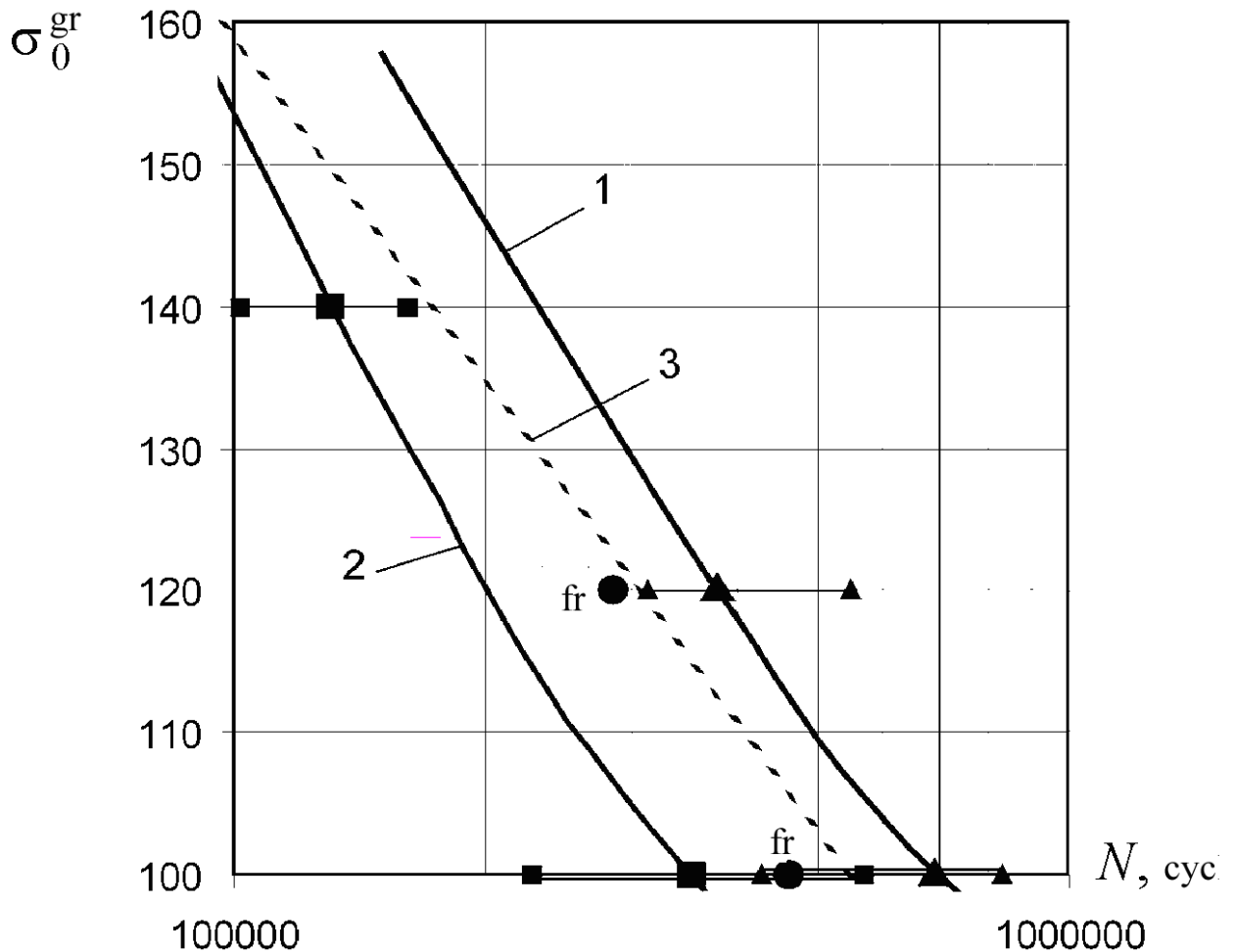


Fig. 3.20 – Fatigue Curves of Standard Test Pieces Plotted According to Test Results and by Means of Estimation. Spread of test results and fretting corrosion failure points is depicted

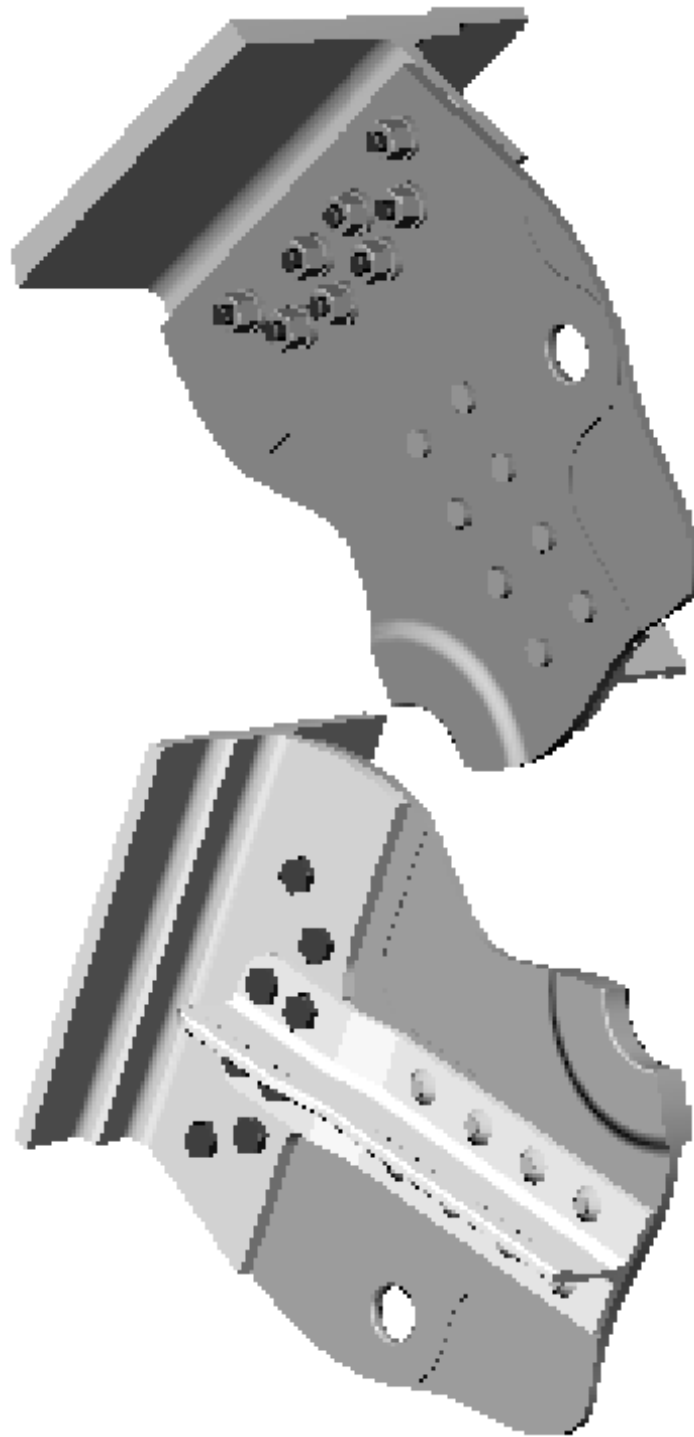


Fig. 3.21 – Analytical Bolted Joint Model of Spar Web, Cap And Stiffener

So, bolted joint structural properties and their production procedure providing specified level of static strength desired endurance and proofness under minimal joints weight and fatigue properties exceeding pre-achieved level have been determined as a result of computer-aided designing and modelling of aircraft assembly structure joints using CAD/CAM/CAE/PLM systems.

### 3.3. NEW DESIGN AND PRODUCTION CONCEPTS AIMED AT PROVIDING HIGHER ENDURANCE OF AIRCRAFT ASSEMBLY STRUCTURE SHEAR BOLTED JOINTS

New design and production concepts aimed at providing higher endurance of different aircraft assembly structure bolted joints are presented in Fig. 3.22.

Positive effect produced by local interference in transitional zones of counter bored holes for bolt setting has been used. Feasibility of in application of countersunk bolts with three-coned head (Fig. 3.23) providing desired interference along the total pack thickness [18, 13, 14] has been studied.

Local interference application efficiency of countersunk bolts with three-coned head has been investigated during fatigue tests of countersunk shear joint test pieces (Figs 3.24, 3.25) [8, 13, 14, 15].

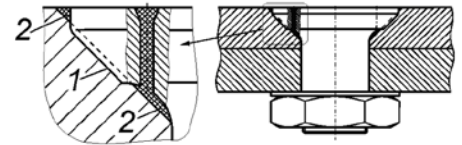
Fretting corrosion prevention technique by applying BK-9 adhesive agent at joint surface alongside with the use of local interference has been studied. Efficiency of adhesive layer has been proved by fatigue tests of single and multi-bolted shear joints (Fig. 3.26).

It has been found that a combined application of modified bolts with any interference and an adhesive layer on surface joint provide endurance increase at 8.6 times in compare with the endurance of the similar test pieces assembled without application of adhesive agent in countersunk bolts 5015A with a radial interference of 1 %  $d_b$ .

In addition, this chapter describes the ways of increasing fatigue endurance of bolted joints by the use of unloading lightening holes of smaller diameter located ahead and behind axial hole along the load line acting on the joint. It has been proved that availability of lightning holes provides stress concentration decrease at the edge of hole bolted and bolt loading level and correspondingly hole webs in sheet due to joint compliance increase resulting in increasing joint endurance 1.8–1.9 times.

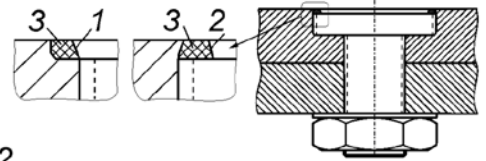
Conic surface of a countersunk insert bolt head is produced as an annular collar 1, with annular grooves 2 at the head butt and under the head near the bolt body being filled with sealant.

A.c. 649894



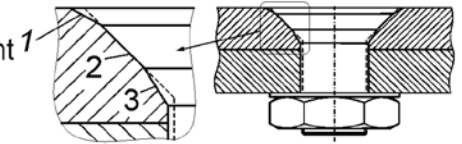
The countersunk insert bolt head and socket for it are cylindrical; near-butts portion of an insert head has side conic annular collar 1 or offset 2; surface annular groove 3 filled with sealant

A.c. 627252

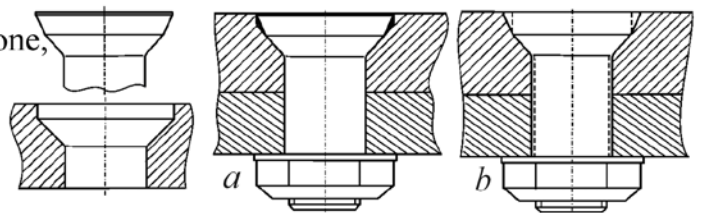


The countersunk insert bolt head is triple-cone, the angle of the first cone is less than the countersinking angle of a hole in a joint component, the angle of the second cone equals it the angle of the third cone is more than it.

A.c. 781422

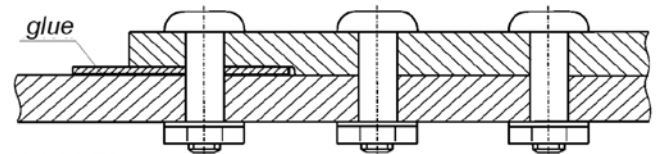


The countersunk insert bolt head is double-cone, countersinking is cylindrical-conic, joints: *a* - detachable with sealant in the annular hollow, *b* - one-piece with radial interference along the body and insert head.



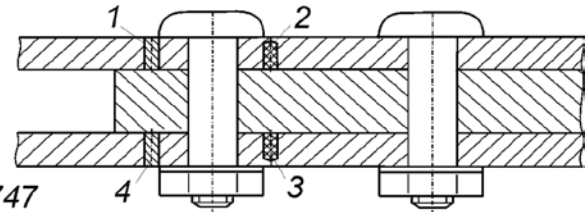
The strip is glued to the joint part in the area of the first row of fasteners. The strength of the strip material is equal or more than that of the part material.

A.c. 1203252



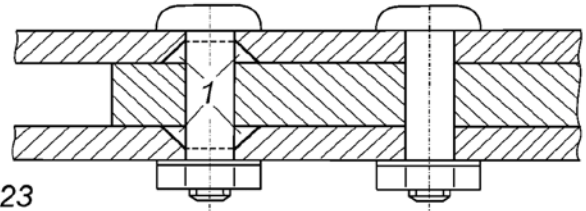
In the joint parts in front of and behind the first row of holes for fasteners, the through holes 1 and blind holes 2 are made. These holes are filled with sealant 3 or with pins 4 installed with radial interference.

A.c. 1303747



The holes in strips for the first row of fasteners are produced with conic cavities 1 located on the side of joint strips contact surface.

A.c. 1754923



The loading of parts with static load, which corresponds to operating load, and which is unloaded after the formation of a hole and placing of fasteners in that hole with radial interference.

A.c. 1388176

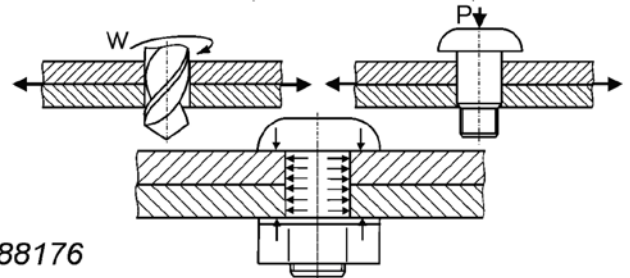


Fig. 3.22 – New Design and Production Concepts Aimed at Cyclic Endurance and Proofness Increase of Shear Bolted Joints Used in Aircraft Structural Components

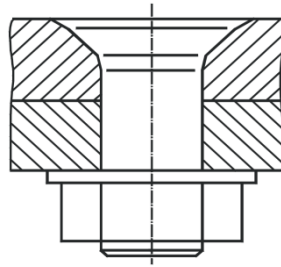


Fig. 3.23 – Countersunk Bolt with Three-Coned Hole

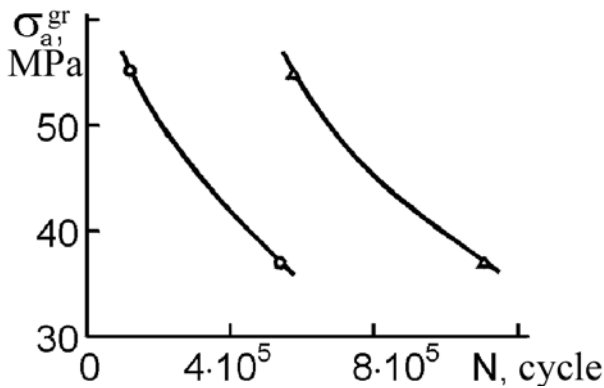
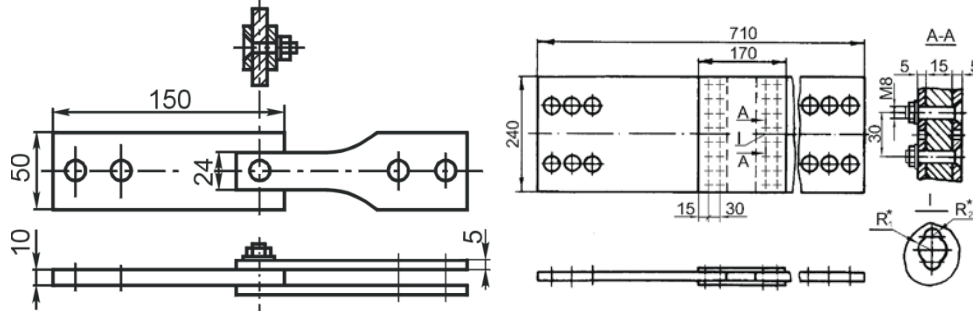


Fig. 3.24 – Effect produced by setting bolts with three-coned head on endurance of single bolted joints: 1 – 5015A; 2 – bolts with three-coned head

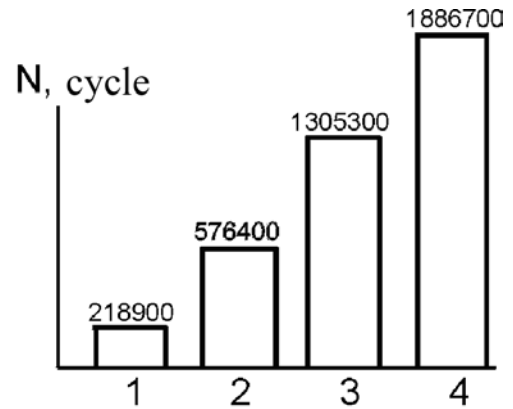


Fig. 3.25 – Effect produced by setting bolts with three-coned head on endurance of multi-bolted joints: 1 – 5015A bolts; 2 – bolts with three-coned head; 3 – 5015A bolt + adhesive agent; 4 – bolts with three-coned head + adhesive

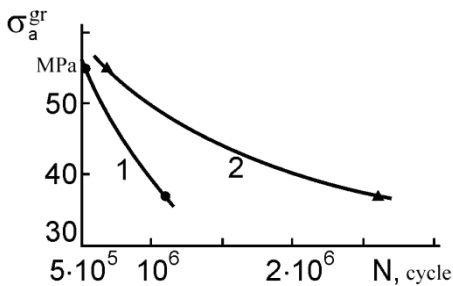


Fig. 3.26 – Adhesive Layer Efficiency in Single-Bolted Countersunk Joints

Endurance increasing technique has been developed for multi-row joints by setting unloading liners (Fig. 3.27) [13; 14; 16]. Analysis of fatigue test results has been shown that application of unloading liners leads to higher cyclic endurance of test-pieces by its increase at 1.6–2.1 times.

Ways of increasing endurance of assembly panels-to-joint section have been validated.

Analysis of fatigue test results demonstrates that techniques have been developed to increase cyclic endurance of assembly stringer panels-to-jointing section joint points at 1.6–3.8 times.

Effect produced by application of polymer fillers on the endurance of single shear bolted tapered joints has been discussed.

Fatigue tests have demonstrated that the polymer fillers are quite satisfactory means and proved production ability of shear tapered joints operating under cyclic loads.

Everything mentioned above results in decreased of fretting corrosion intensity and in increase of test-piece endurance approximately at 1.8–3.6 times.

A new technique has been experimentally studied in this section resulting increase of single shear joints endurance on the rigid section by means of local overlays thickening in the area of utmost row (Fig. 3.28) [13, 14, 16].

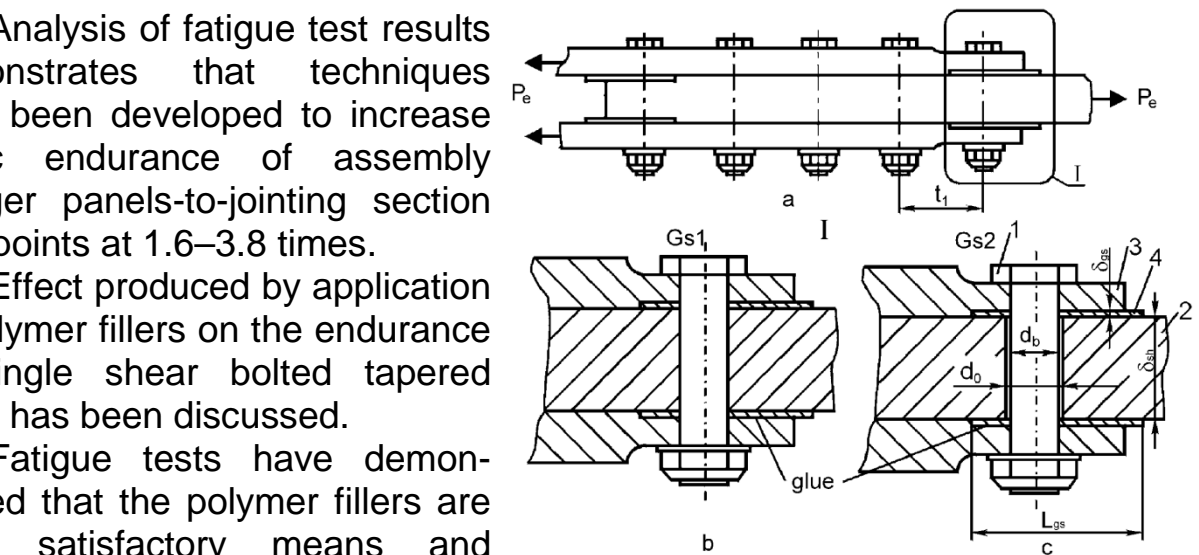


Fig. 3.27 – Unloading Liners View in Multi-Row Joints

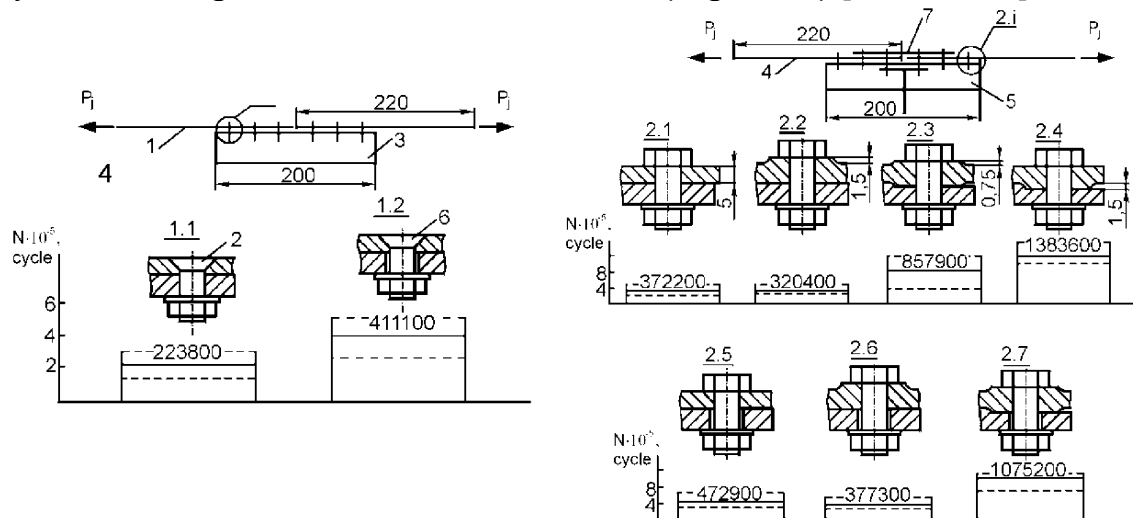


Fig. 3.28 – Rigid Section. Joint Test Pieces: 1 – D16AT15 steel plate; 2 – bolt 5015-8-25; 3, 5 – section D16T-Pr315-7; 4 – plate D16T; 6 – bolt with three-cones countersunk head; 7 – splice plate

It has been found that the fatigue endurance of single shear bolted joints in parts fabricated from D16AT15 sheet with utmost rows having unloading elements to be higher in compare with fatigue endurance free of unloading elements at 1.9–3.7 times.

### 3.4. COMPUTER AIDED DESIGN PROCEDURE TO OBTAIN SPECIFIED ENDURANCE OF SHEAR RIVET JOINTS IN AIRCRAFT THIN-WALL ASSEMBLY STRUCTURES

Riveted joints properties are determined on the base of the estimation and experimental methods aimed at the study of their strength, local strain and stress state fatigue resistance, production ability, new design and manufacturing concepts as a results of computer-aided designing and property modeling with the help of computer-aided systems. Also, design and production documentation is under development to create joins, their test and repair during service life [13, 14].

Method of computer-aided design to achieve specified endurance of shear riveted joints (Fig. 3.29) comprises several procedures:

1. Skin riveted joints design procedure at the phase of draft design makes it possible to select feasible properties of the joins with specified endurance at its minimum weight [6].

This procedure covers selection of joins materials with high weight efficiency as well as selection and optimization of join properties and conditions ensuring static strength and join endurance.

Optimization of join properties is performed to meet minimum mass (weight) criteria. According to optimization procedure areas with minimum weight are determined and subdivided into several fields. Minimum weight values are determined in the center of each field and an optimum variant is selected by means of comparison. Selection of optimization numerical method can be explained by the fact that weight minimum and limitations are nonlinear functions of design data while the design data are discretely changeable values. Estimation of feasible joins properties is conducted according to block diagram shown in Fig. 3.30.

2. Procedure of three dimensional and computer aided modeling for standard riveted joints of aircraft assembly structures.

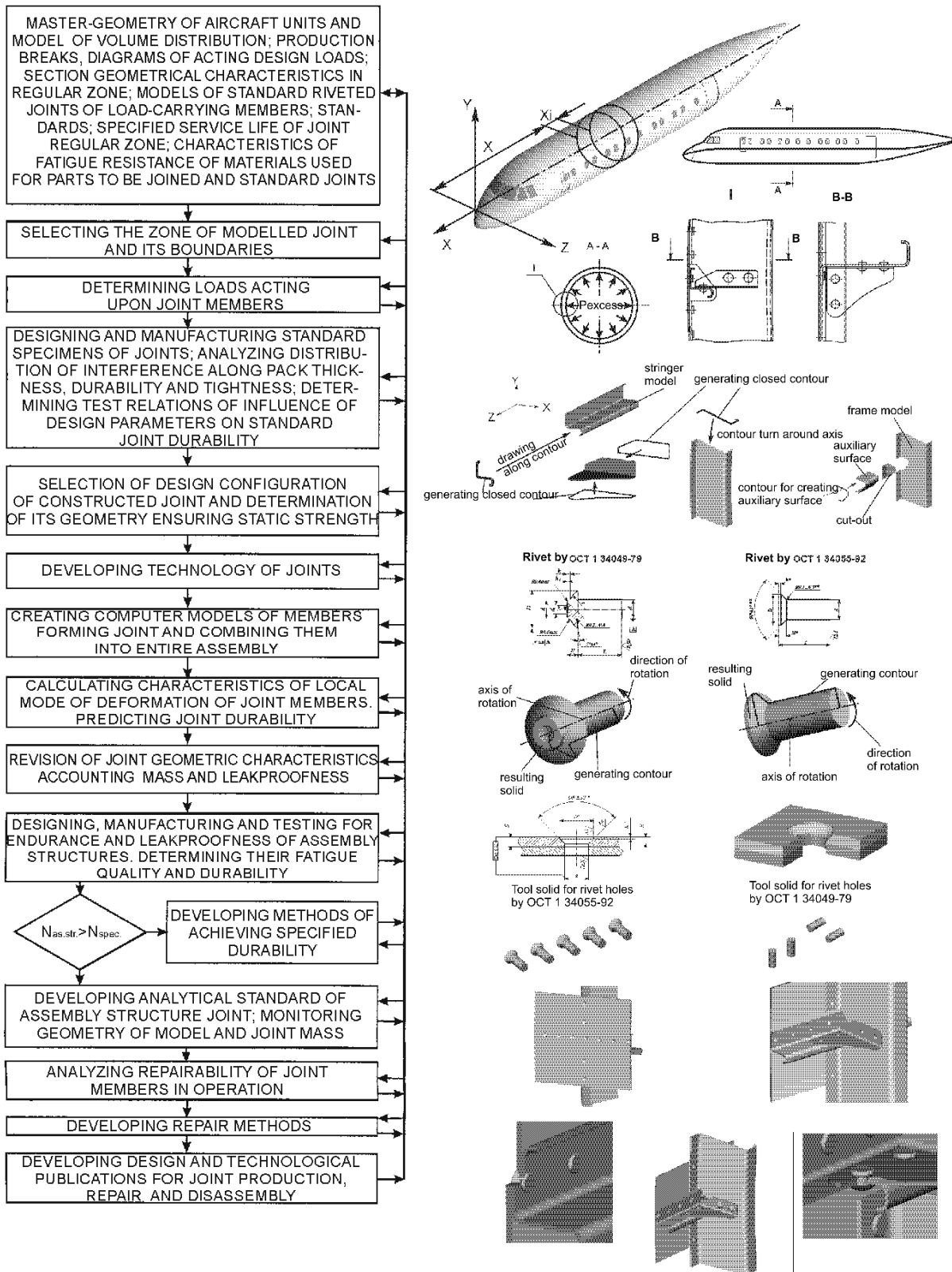
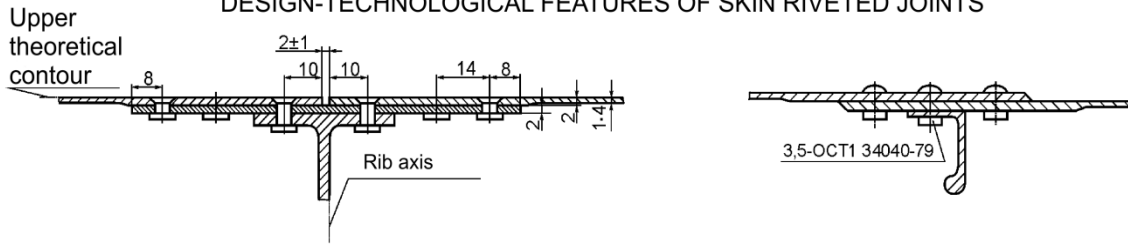


Fig. 3.29 – Computer Aided Designing and Modeling Procedure for Standard Riveted Joints of Aircraft Assembly Structures



DESIGN-TECHNOLOGICAL FEATURES OF SKIN RIVETED JOINTS



SELECTION OF PARAMETERS OF JOINTS HAVING MINIMAL MASS

Target function

$$M = M_P + M_{Fast} - M_{Hole}$$

$$M = (S_1 + S_2)[4d + (n-1)b_1] \cdot l \cdot \rho_{skin} + n \cdot \frac{l}{b} (S_1 + S_2 + 2.4d) \frac{\pi d^2}{4} \rho_{rivet} - n \cdot \frac{l}{b} (S_1 + S_2) \frac{\pi d^2}{4} \rho_{skin}$$

$l$  - joint length       $b$  - rivet pitch in row

Constraints

$$\frac{\pi d^2}{4} \tau_{shear}^3 \cdot n \geq S_p \cdot b \cdot \sigma_p;$$

$$n \cdot S_1 \cdot d \cdot \sigma_{bear} \geq S_p \cdot b \cdot \sigma_p;$$

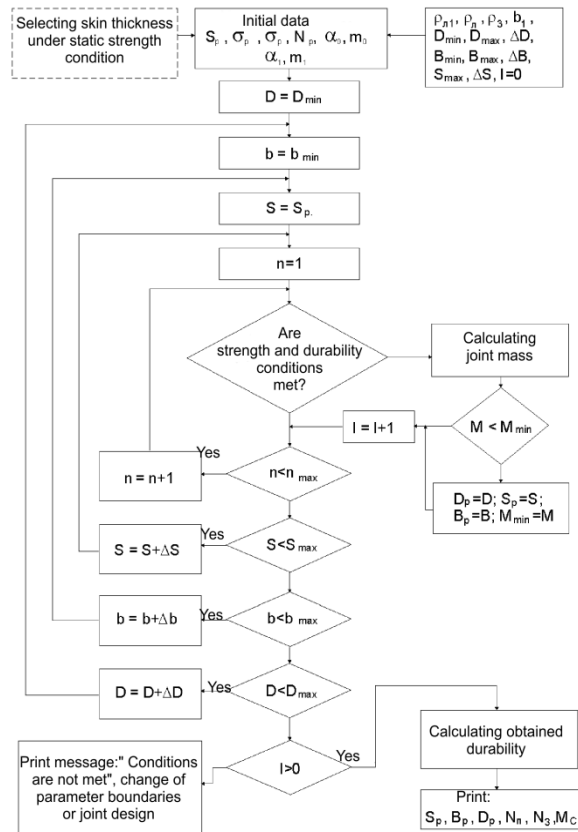
$$b_1/d \geq 0.56b/d + 0.28;$$

$$b/d \geq 2.58;$$

$$S_1 + S_2 \leq 2d;$$

$$\alpha_0 N^{m_0} \geq \alpha_1 N^{m_1} \frac{\eta S_p b \sigma_0}{d S_1} \frac{\theta_m}{\theta_6} + (1 - \eta) \frac{S_p \sigma_0}{S_1} + K_1 \sigma_1$$

For rivets by OCT1 34040-79     $\alpha_0 = 589,1; m_0 = -0.13;$   
 $\alpha_1 = 0.059; m_1 = 0.143.$



CHANGING REASONABLE PARAMETERS AND JOINT MASS DEPENDING ON SPECIFIED DURABILITY

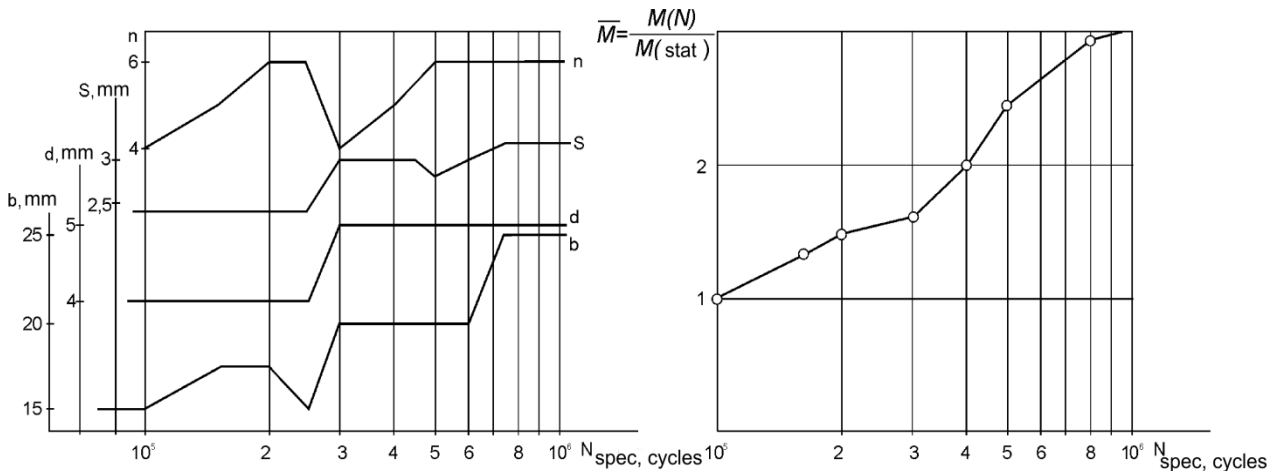


Fig. 3.30 – Skin Riveted Joint Design Procedure of Specified Endurance at Draft Design Phase

According to geometric data of assembly structures and their riveted joints obtained before three dimensional geometric models are constructed with the use of Siemens NX system [7, 8]. All constructions are based on aircraft master-geometry. Strong members models (frames, stringers, skins) are offset made inside the unit: at first-skin, then, frames and stringers. Gusset model is made at the end as a member of technological compensation. Modelling is performed phase by phase. Joint constituent parts are under modelling (stringers, frames, gusset, skin); parts joining in unit; creation of hole solids and subtraction of their elements; modelling of rivets and their setting in holes (Fig. 3.29).

Application of this procedure enables to create riveted joints of minimum mass with a specified static strength and endurance.

3. Procedure in analyzing effect produced by structural and production data on characteristics accounts elastoplastic strain of rivets and coupling interaction between joint elements.

This procedure has been implemented by the use of ANSYS finite elements analysis shown in Fig. 3.31.

Results of this procedure application are shown in Fig. 3.32 under analysis of strain-stress State characteristics in the elements of three row singles hear joint made by using AHY 0314 rivets.

The rivet strain nature and distribution of equivalent stresses in plates have been determined during analysis. In doing so, it has been found that the highest values of equivalent stresses in plates can be observed at a distance of  $1.5...2.5d_3$  from rivet axis but not in the rivet coupling areas. Clearance between a rivet and plate does not exceed 0.055 mm at any area under applying tensile stresses of  $\sigma_{gr} = 150\text{MPa}$  proving joint proofness within the total range of equivalent loads. Pocket tightening value  $\Delta_y$  is 0.1 mm while expansion is  $\Delta_e = 0.2$  mm.

4. Estimation procedure of efforts distribution between the rows of shear riveted joint with the use of ANSYS system accounting rivet setting procedure (Fig. 3.33).

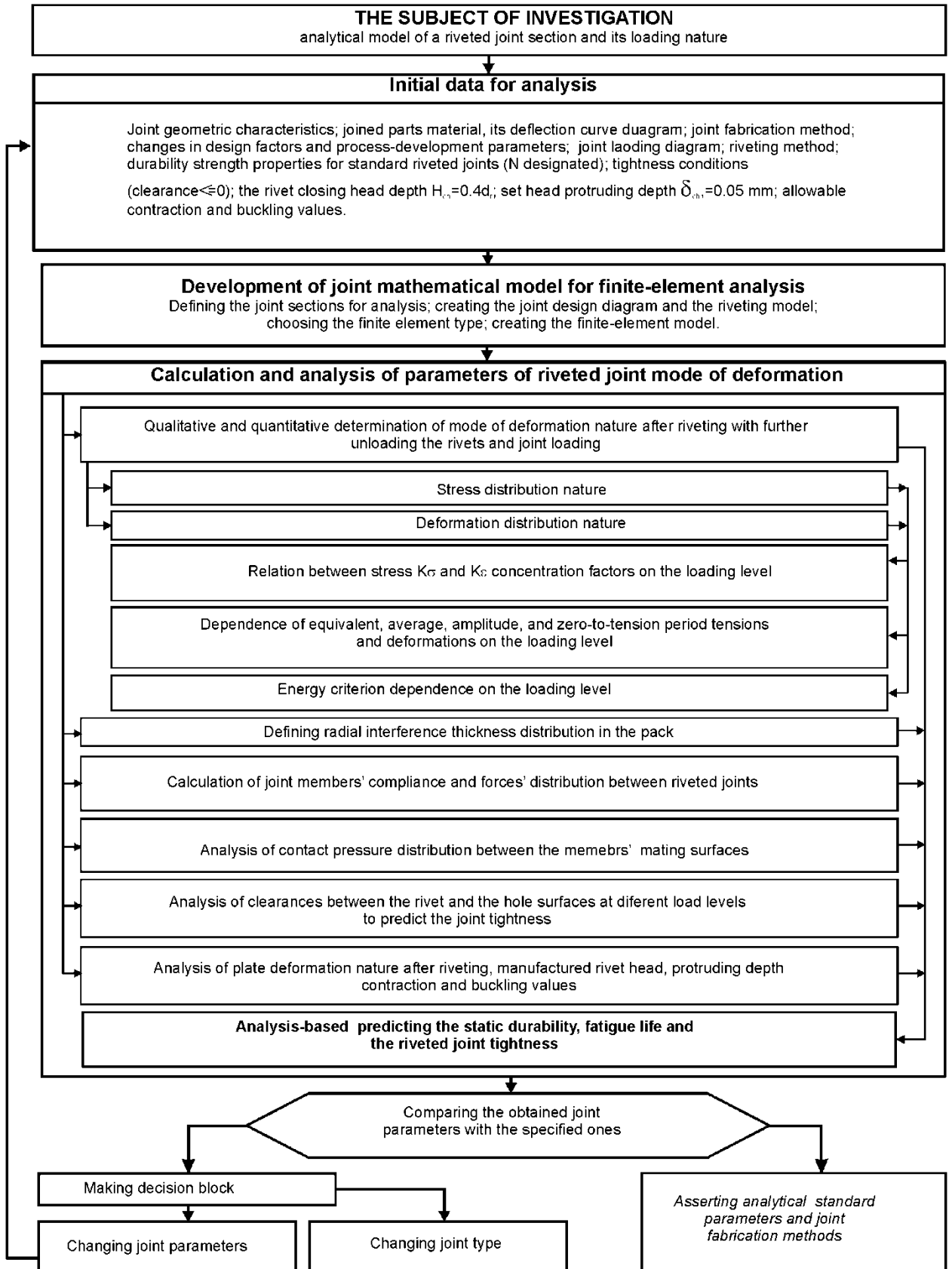


Fig. 3.31– Procedure for Analyzing Structural and Production Data on Characteristics Riveted Joint Local Stress-Strain State

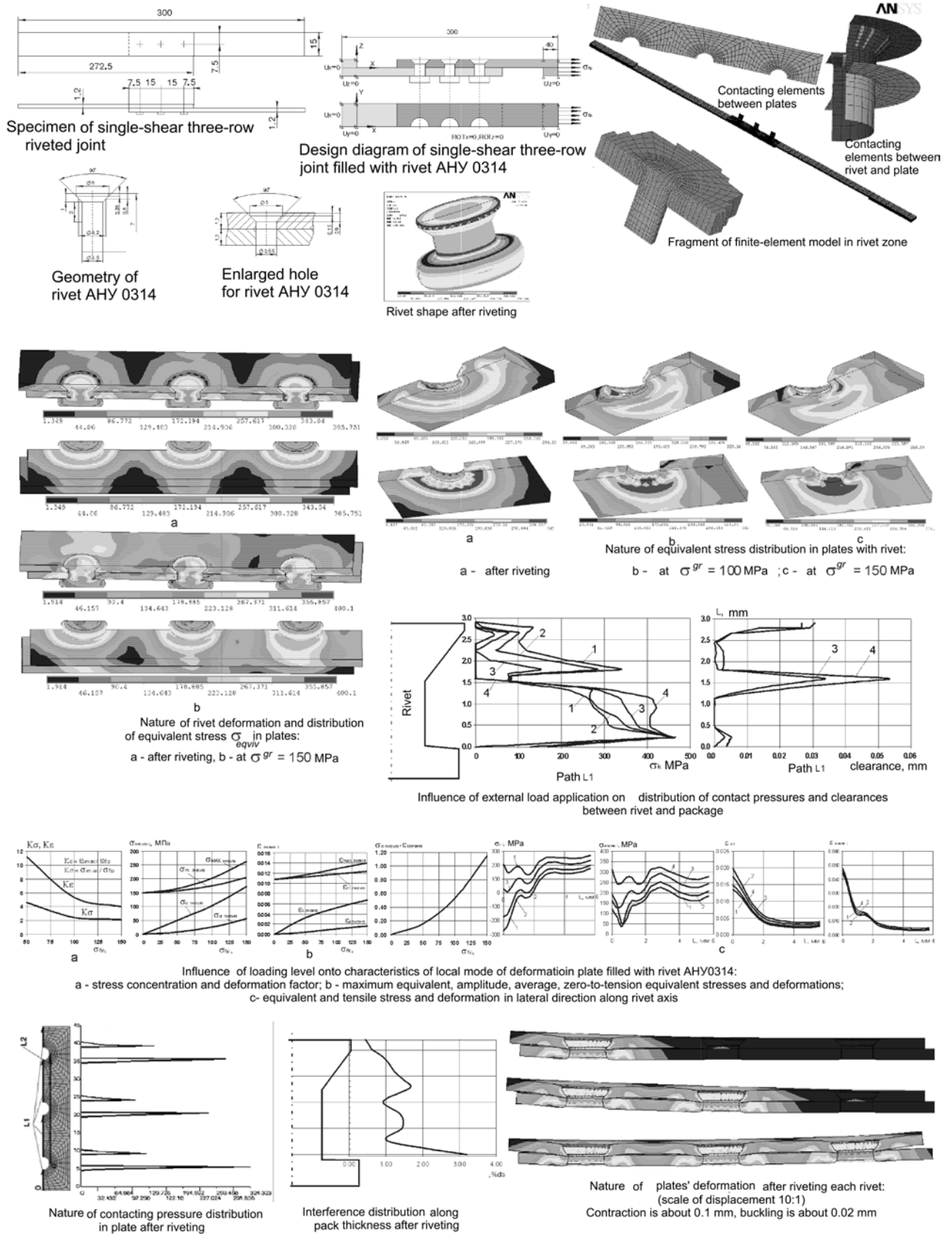


Fig. 3.32 – Characteristics Analysis of Local Stress-Strain State in Elements of Three Row Single Shear Joint Filled with ANU 0314 Rivets

1  
SELECTING STANDARD SPECIMEN OF COUNTERSUNK RIVETED JOINT AND ITS PARAMETERS. DEVELOPING 3-D COMPUTER MODEL.

DIVIDING STRUCTURE TO ZONES INCLUDING INDIVIDUAL FASTENERS. DEVELOPING DESIGN DIAGRAM OF SINGLE-ROW JOINT. DEVELOPING FINITE-ELEMENT MODEL INCLUDING CONTACT ELEMENTS. MODELLING RIVETING PROCESS. CALCULATING MODE OF DEFORMATION IN JOINT MEMBERS USING ANSYS PROGRAM. DETERMINING "LOAD-DISPLACEMENT" RELATION FOR EVERY VARIANT OF JOINT ACCOUNTING RIVET INSTALLATION WAY.

DEVELOPING DESIGN DIAGRAM FOR MULTI-ROW JOINT. REPLACING RIVETS WITH SPECIAL ELEMENTS COMBIN39 HAVING PROPERTIES OF NON-LINEAR SPRINGS AND REPRESENTED IN CAD/CAE ANSYS. SPECIFYING DEFORMATION LAW FOR ELEMENTS COMBIN39 USING 6-7 POINTS THAT CORRESPONDS TO NATURE OF MUTUAL DISPLACEMENT OF PLATES GOT FOR EVERY VARIANT OF JOINT ACCOUNTING RIVET INSTALLATION WAY. SPECIFYING APPROPRIATE CONDITIONS OF ATTACHMENT AND APPLYING ACTING LOADS

DETERMINING FORCES BEING RESULTS OF PROBLEM SOLUTION IN ELEMENTS COMBIN39. ANALYSING NATURE OF FORCE DISTRIBUTION IN RIVET ROWS AND COMPARING THEM WITH EXPERIMENTAL DATA

2

SELECTING STANDARD SPECIMEN OF COUNTERSUNK RIVETED JOINT AND ITS PARAMETERS. DEVELOPING 3-D MODEL.

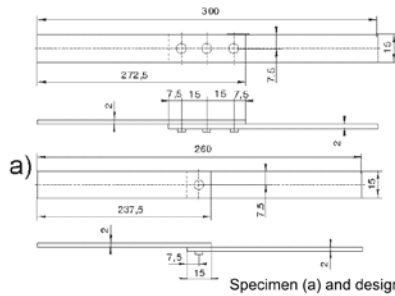
DEVELOPING DESIGN DIAGRAM OF MULTI-ROW JOINT. DEVELOPING FINITE-ELEMENT MODEL INCLUDING CONTACT MEMBERS. MODELLING RIVETING PROCESS. CALCULATING MODE OF DEFORMATION IN JOINT MEMBERS USING ANSYS UNDER DIFFERENT VARIANTS OF LOADING LEVEL.

DETERMINING DISTRIBUTION FIELD OF TENSILE STRESSES HAVING UNEVEN NATURE IN SECTIONS 1, 2, 3 OF UPPER AND LOWER PLATES. CALCULATING FORCES BETWEEN ROWS OF RIVETED JOINTS BY MULTIPLYING MEAN INTEGRAL STRESS IN EACH SECTION AREA. CALCULATING FORCE DISTRIBUTION BETWEEN RIVET ROWS. CALCULATING SHARE OF LOAD TAKEN BY EACH RIVET. ANALYZING FORCE DISTRIBUTION NATURE IN RIVET ROWS AND COMPARING THEM WITH EXPERIMENTAL DATA

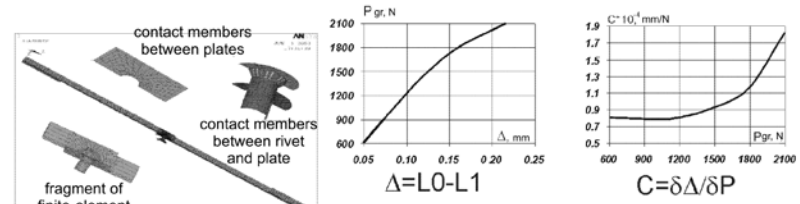
COMPARING METHODS:

1 First method does not account residual stresses and deformations occurring after riveting process; it is easier; it does not require powerful computer resources and can be used at stage of draft design.

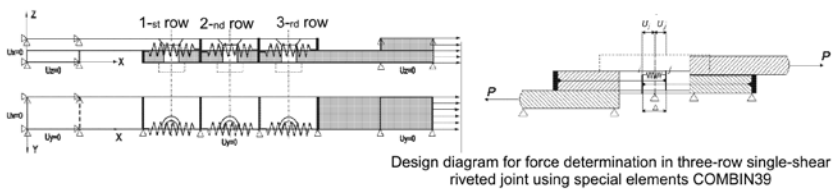
2 Second method accounts residual stresses and deformations occurring after riveting process, and, therefore, is more precise. Great computer resources for calculations are required.



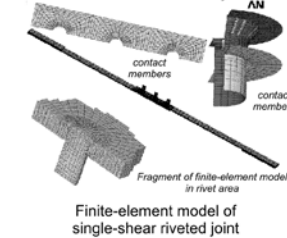
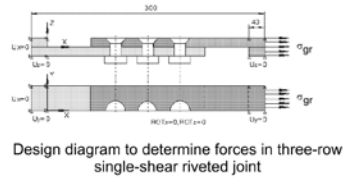
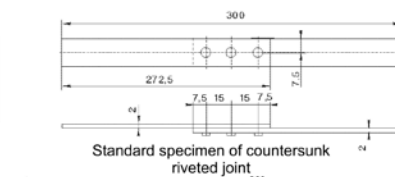
Standard specimen of countersunk riveted joint



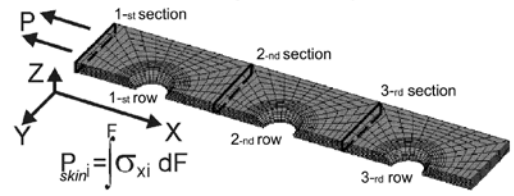
Influence of external tensile force  $P_{gr}$  on nature of change: a) mutual displacement of plates to be joined; b) compliance under external tensile load.



Design diagram for force determination in three-row single-shear riveted joint using special elements COMBIN39



Finite-element model of single-shear riveted joint



Section arrangement in plate used in calculating force distribution between rivet rows

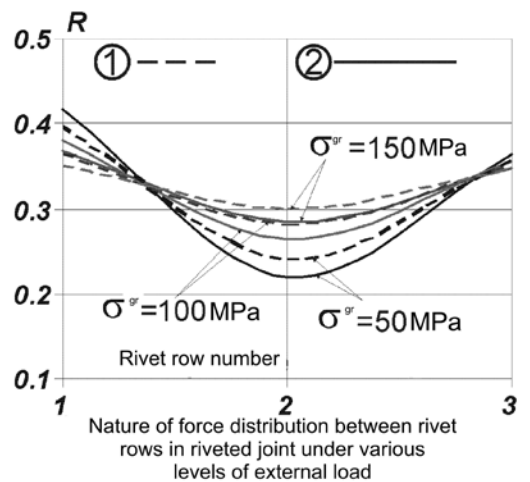
$$P_{rivet i} = P_{skin i} - P_{skin (i+1)}$$

$i$  - number of rivet joint

$P_{rivet i}$  - load transmitted through  $i$ -numbered rivet

$$R_i = \frac{P_{rivet i}}{P}$$

$R_i$  (load share taken by  $i$ -numbered rivet) - ratio of load  $P_{rivet i}$  transmitted through the rivet to total load  $P$



Nature of force distribution between rivet rows in riveted joint under various levels of external load

Fig. 3.33 – Procedure in Estimation of Efforts Distribution between Rows of Shear Riveted Joint

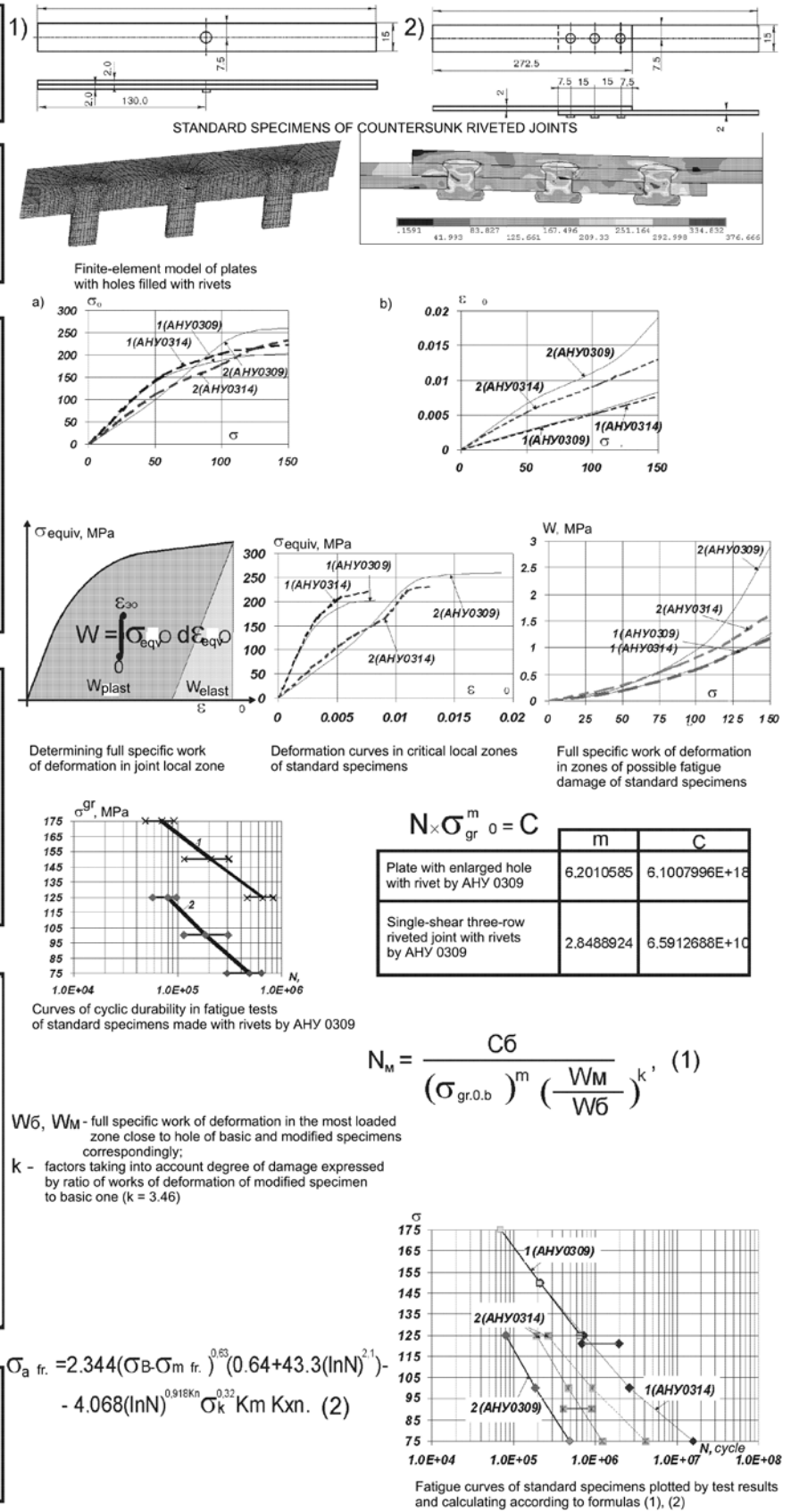
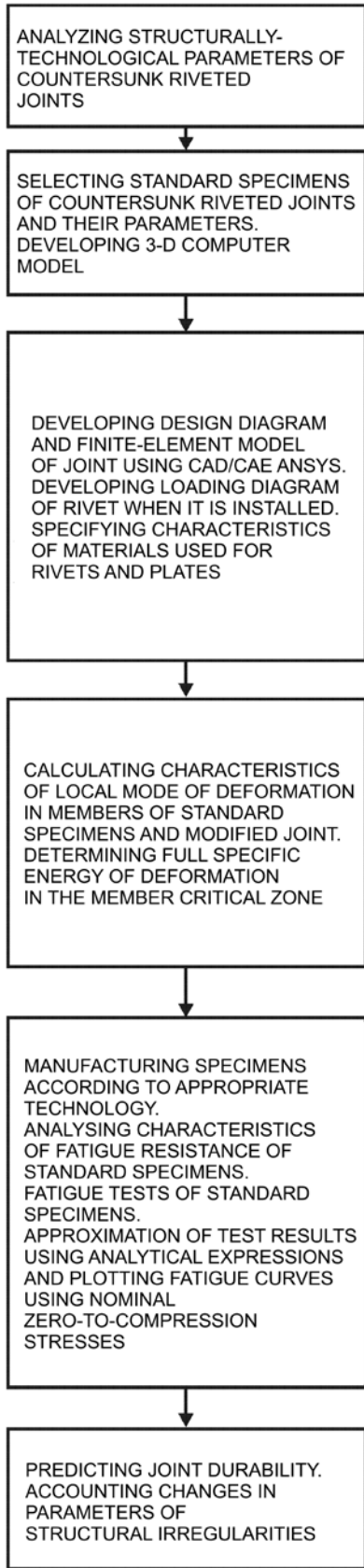


Fig. 3.34 – Procedure Predicting Dependence between Structural and Production Data of Countersunk Riveted Joints and Their Endurance

It should be noted the second procedure accounting residual stresses and

strains originating after riveting to be more accurate than the first one. Due to this fact it has been found that when thin skins become narrower and more curved after riveting it results in degradation of aircraft skin outer surface quality and it leads to more unequal distribution of efforts between the rows of riveted joints (Fig. 3.33). The second procedure requires introduction of finite elements between interacting surfaces and, therefore, it needs significant computer resources for computation. In the first procedure the rivets are replaced by the special elements COMBIN39. The finite elements are not involved in computation process, thus, this method is less accurate but it has any restrictions as far as the number of rows are concerned.

5. Prediction procedure in influence produced by the structural and production fastener parameters of the countersunk riveted joints on their endurance with the account once made for the change of the specific strain energy in the area of the probable fatigue failure. This procedure makes it possible to predict endurance of the modified test-pieces on the base of testing standard test-pieces of riveted joints. Procedure algorithm and the results of its application on the example of the joints made by the rivets AHY309 and AHY314 are shown in Fig. 3.34.

Investigation analysis demonstrates that the endurance of the modified joints depends on relation of specific strain actions in the highest loaded areas close to hole of the based and modified test-pieces, respectively (Fig. 3.34). Endurance of these test-pieces obtained by calculation to meet this procedure lies within the range of values spread obtained in experimental way.

Developed procedure in computer-aided designing of shear riveted joints serves as a base for creation of new riveted joints with specified endurance to meet static strength, proofness and outer surface quality requirements.

### 3.5. NEW STRUCTURAL-PRODUCTION CONCEPTS FOR SHEAR RIVETED JOINTS OF AIRCRAFT ASSEMBLY THIN-WALL STRUCTURES

New structural and production concepts for shear riveted joints of aircraft thin wall assembly structures have been developed using computer-aided design procedure to obtain specified endurance.

An important problem in creation of airframe riveted joints operating under corrosive media conditions is to ensure high level quality of outer surfaces [OS], endurance and pressurizations (proofness) along the total pack thickness of joined parts. Production procedures for mechanical cleaning of protruded manufactured rivet heads used at aircraft manufacturing factories do not meet specified guaranteed requirements of specifications resulting in significant expenses for heads machining and restoration of their protective coating. A number of rivets (Fig. 3.35) as well as their setting procedures have been developed to provide specified protrusion of manufactured rivet heads free of any mechanical cleaning after riveting.

Rivet set head butt includes straight circular cylindrical compensator with diameter equal to cylindrical portion of a countersunk primary head.

Пам. 2066003

Joint rivets have reduced countersunk set head with cylindrical compensator placed on the head butt.

(AHY 0314)

Joint rivets a plane compensator in truncated cone shaped adjacent to the set head with smaller base.

(AHY 0310)

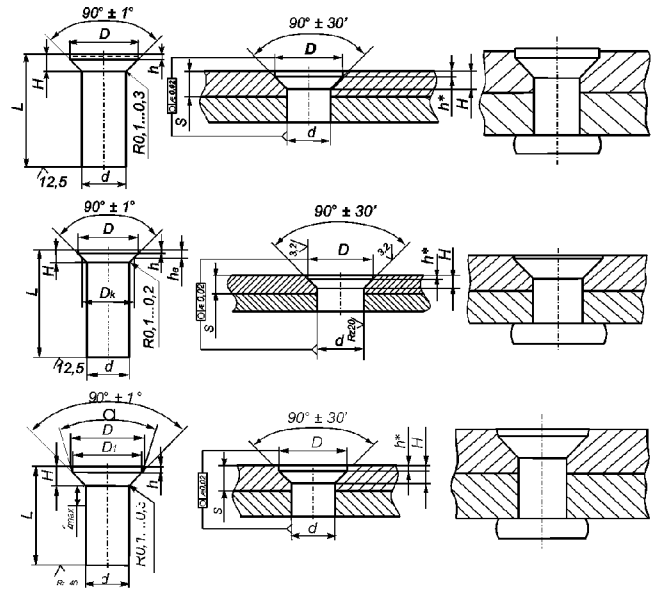


Fig. 3.35 – New Countersunk Rivet Structure with Cylindrical Compensator and Holes for Their Setting

Joints based on these rivets have been subjected to test for tightness and endurance (Fig. 3.36).

As far as the main quality criteria are concerned these rivets have higher quality level in compare with the modern riveted joints used in aviation industry. Special attention should be paid at joints made with the use of AHY 0314 rivet. Skin outer surface quality is directly ensured within the riveting process without use of any additional rather labor intensive finishing operations.

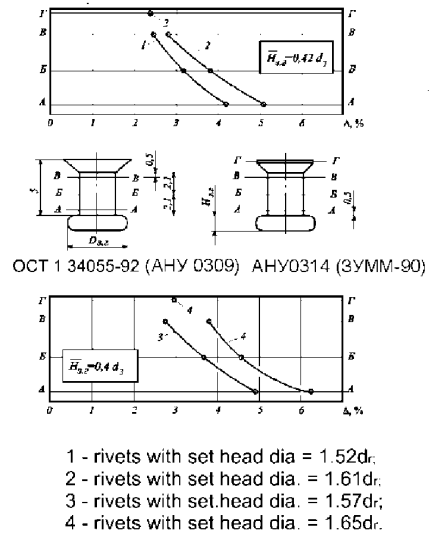
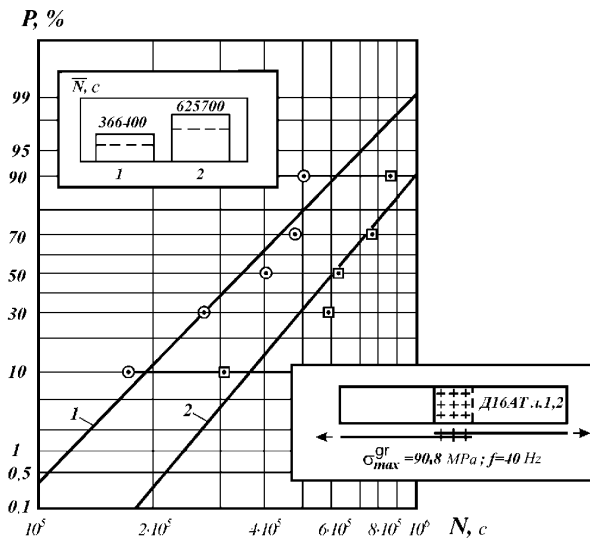


Fig. 3.36 – Fatigue Test Results of New Countersunk Rivets

In this case in addition to criteria of countersunk set rivet protrusion on the skin, the skin tightening in the area of fastener points meet desired specifications “Quilted” effect is practically unavailable and it makes good grounds for increasing competitive ability of riveted structures used at thin skins. These properties as well as high manufacturing ability of this rivet, high tightness and en-



durance of joints assembled on this base made it possible to use this rivet under designing and manufacturing of the “Antonov’s” AN-148 aircraft.

Riveting technique and procedure also produce significant effect on service life of riveted joints and outer surface quality. Facility for press riveting has been developed (AC No.1765966, Fig. 3.37) enabling to provide desired height of rivet heads, outer surface quality, tightness and service life of assembled joint under riveting.

Flat washer 8 is installed on the surface of the press unit being a peculiar feature of the stamp and, in this case, press unit diameter is equal to the diameter of the washer. Pressing sleeve 6 on the unit arranged above the rivet snap has a conical inner surface 9 with its height being equal to the plane protrusion value of the pressing sleeve operating and face on the operating surface 3 of the press unit.

An operating load is transferred with eccentricity relatively to regular zone sections of strong members in longitudinal and lateral single shear riveted joints of the wing and fuselage, in skin joints with stringer tip in repair plate-to-airframe strong members joints.

Availability of eccentricity under load transfer results in originating of bending strains in parts to be joined.

They cause stress concentration increase in the area of utmost high loaded rows of multi-row joints resulting in decrease of single shear joints fatigue endurance.

Techniques for upgrading of fatigue endurance have been developed based on stress-strain state analysis of single-shear joint plates (Fig. 3.38) comprising as follows:

setting of rivets utmost rows with clearance in parts forming overlapping edge and with interference in the second joined part;

additional rivet row setting at the overlapping edge (see Fig. 3.39) involving end (tip) of joined parts for accepting bending moment and non-operating for shear.

Experimental studies done prove the fact that setting of fasteners utmost rows with the clearance of the parts forming overlapping edge results in increase of fatigue endurance averagely at:

- 1.5 – 6.0 times for five rows overlapping joints;
- 2.2 – 3.0 times for three row plate joints;

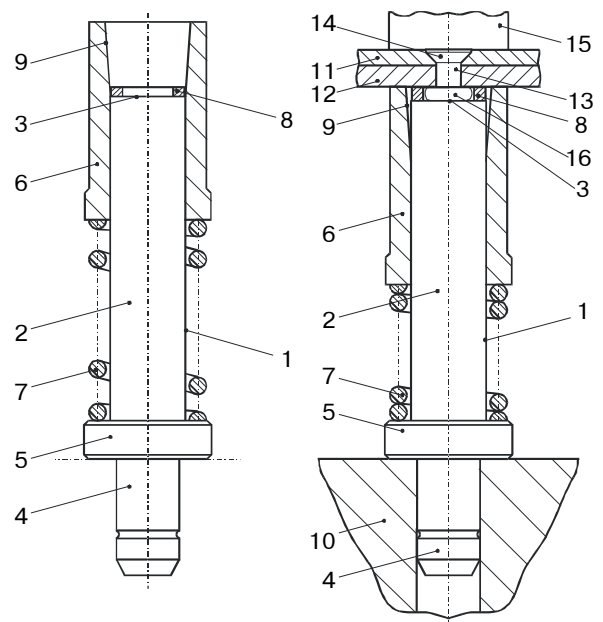
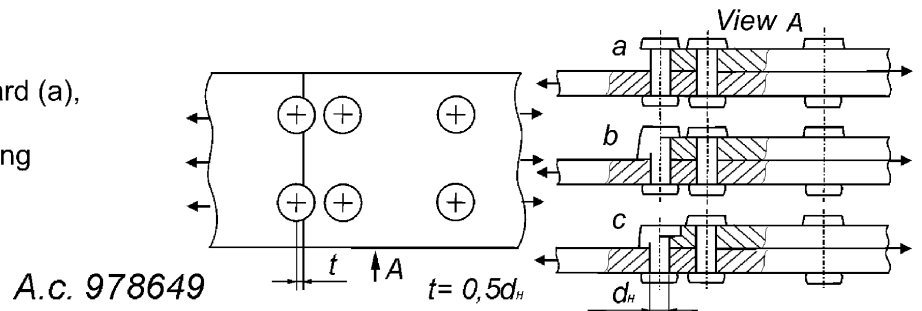


Fig. 3.37 – Stamp Structure for Single Shear Press Riveting

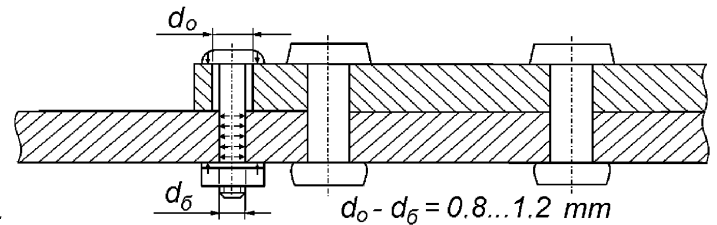
- 2.3 times for four row overlapping joints and 1.9 times in case of using countersunk rivets for joints;
- 2.6 – 4.2 times for four rows joints on plate;
- 1.2 – 1.9 times for four row overlapping joints with the rivets of utmost rows being set with clearance at one rivet;
- 5.9 – 31.6 times for skin joints with end stringer in compare with fatigue endurance of the joints free of utmost rows loading.

Additional rivet row with standard (a), segmental (b) c-stepped (c) set heads is installed overlapping at the joint edge at distance of half pivot diameter.



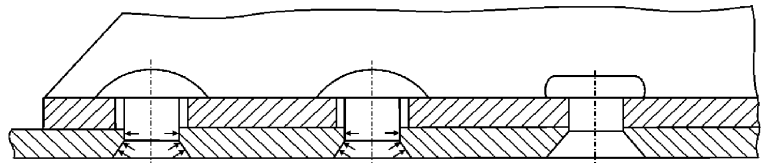
Shear joint shank ends are additionally attached to the mating parts with fasteners installed with a shank end clearance and the radial interference in mating part.

A.c. 1010325



The extreme rivets in the skin and left stringer are installed with a stringer grip clearance and with the skin radial interference. The rivet closing heads may be countersunk and cone.

A.c. 1418524



The shank end edge of the joined part is attached to the loaded part near the location where the cantilever head edges are leant against the additional strap attached to the mating part. The fastener bars are installed with hole clearances at the junction of the strap and the shank end edge with radial interference in loaded part.

A.c. 1186844

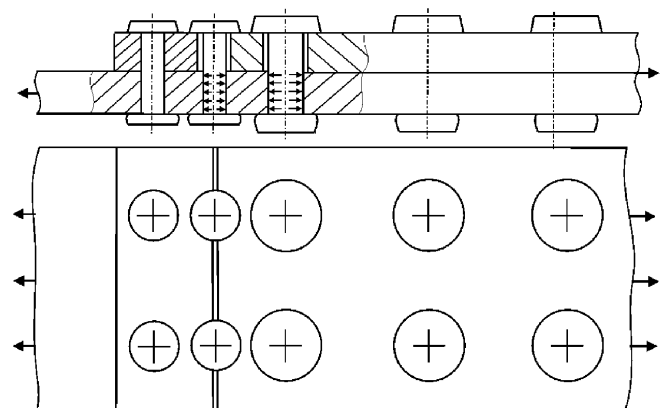


Fig. 3.38 – New Structural and Process Concepts Upgrading Cyclic Endurance of Aircraft Structure Single Shear Riveted Joints

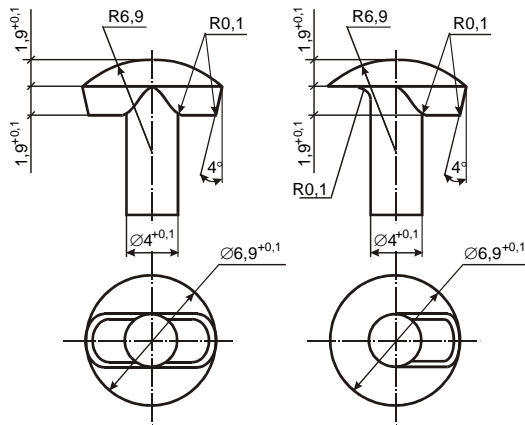


Fig. 3.39 – Special Rivets with Flat-Convex Head and Double (Single) Protrusion From Experimental Batch

Test pieces have been subjected to endurance test with their utmost rows being set with clearance in parts forming an overlapping edge assembled under availability of Y30MЭC-5 seal at joined surfaces anodized by “HX” and coated with ФЛ-086 primer as well as test pieces assembled from parts under delivery condition. Under availability of the used coatings fatigue endurance of the joins becomes averagely higher at 1.7-6.7 times being true under availability of clearance between the rivet shank and hole walls in part forming an overlapping edge.

Fatigue endurance becomes higher under placement of additional single shear joined fasteners rows involving part tails in combination with bending moment being non-operating for shear:

- overlapping rivet joints – averagely at 2.3 – 3 times;
- skin-to-ending stringer joins-averagely at 3.9 – 4.8 times in compare with the fatigue endurance of the joins free of additional fastening members.

It has been demonstrated that setting of additional fastening members with a process linear under the rivet head having 0.3, 0.6, 0.9 of total lifetime at the edge of overlapping joins results in increase of joins residual endurance at averagely 3.5, 5.8 and 11.7 times respectively.

New structural and process concepts for shear riveted joins of aircraft assembled thin-wall structures have been developed and implemented at national aircraft manufacturing companies. It enables to upgrade outer surface quality of these joins, their tightness and service life.

### 3.6. NEW STRUCTURAL-PROCESS PROCEDURES AND TECHNIQUES IN DELAY OF FATIGUE CRACKS GROWTH FAVORABLE FOR SERVICE LIFE INCREASE OF ASSEMBLED STRUCTURAL COMPONENTS

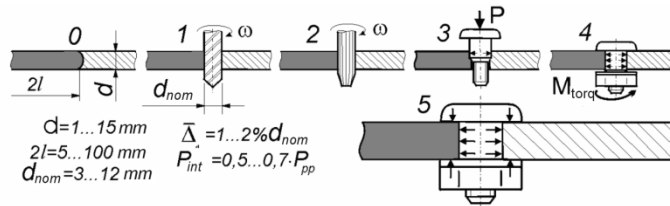
Fatigue cracks growth new structural-process procedures and techniques in delay of fatigue cracks growth favorable for service life increase of assembled structural components have been developed (Fig. 3.40).

Effect of length  $2 \cdot l$  and external load level  $\sigma^{gr}$  on the crack edges spread has been subjected to study (opening  $2 \cdot u_y$ ). Holes  $\theta$  made at crack tip (apex of crack) and at its length mid in plate from D16AT have been made oval. Obtained data make it possible to select reasonably feasible values of radial interference  $\Delta_d$  for fasteners into holes. Analysis of study results has demonstrated that for cracks at a length of  $2 \cdot l \leq 80$  mm with a load level corresponding to  $\sigma_{gr} \leq 100 \dots 150$  MPa, fabrication of holes of  $\varnothing 6$  mm at the apex of crack results in decrease of stress concentration factors at 1.5–2 times;

Efficiency of bolts setting with axial tightening at the cracks tip has been estimates (using ANSYS). It has been proved that axial tightening reduces stress concentration factors at 1.3 – 2.8 times decreasing extension stress amplitude at apex of cracks at 1.3 – 4 times.

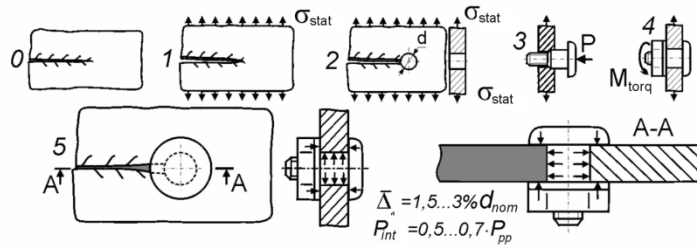
Installation of bolts with radial interference and axial tightening in holes made in crack apices

A.C. 725862



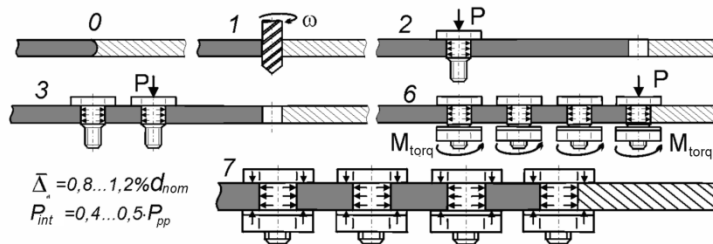
Loading of structure by static effort opening the crack. Effort is removed after installation of bolts with radial interference and axial tightening in holes made in crack apices

A.C. 1054006



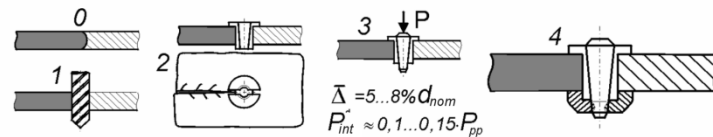
Opening and fastening of crack edges with the bolts installed in series with radial interference in holes made along crack length beginning from crack middle point

A.C. 1374670



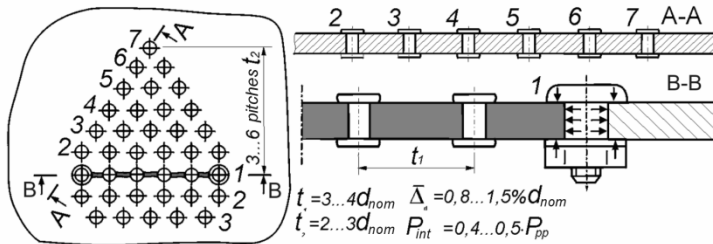
Installation of wedge fastener in hole made in crack apex

A.C. 1165552



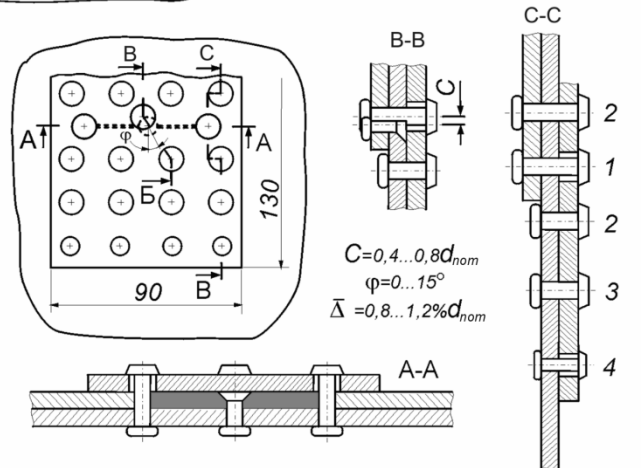
Making the holes in crack apices and near crack edges and installation of fasteners in the holes with radial interference and axial tightening

A.C. 1191247



Attaching the repair strap with fasteners shifted from their centers according to "battle" filled holes along panel tension direction and with radial interference and axial tightening in the panel and strap but with clearance in strap along the hole in crack apex

A.C. 1516287



1, 2, 3, 4, 5, 6, 7 – number of the main technology steps of establishment of fasteners in area of fatigue crack

Fig. 3.40 – Fatigue Crack Delay Integrated Techniques in Structures with Fasteners

Effect produced by bolts set with radial interference at holes made at the

apex of cracks and in the middle of its length on the plate stress-strain state has been studied using ANSYS system. It has been proved that bolt set with radial interference in the hole at the apex of crack result in displacement of maximal extension stresses  $\sigma_x$  from hole walls at 35 % of its length. It has been proved that stresses amplitude as a result of bolt setting with radial interference at the apex of crack becomes shorter in the areas closing to hole walls at 2 – 3.8 times. In this case zero-to-stress state cycle  $\sigma_0$  is reduced in the plate critical section by 1.9 – 3 times while a decrease of stress concentration factors at levels of  $\sigma_{gr} \leq 100$  MPa relatively to the plate with unfilled holes is equal to 7 – 15 %.

Plates from aluminium alloys different in width and thickness having centrally located cracks of different length with the holes made at the apex and with the bolts set therein have been subjected to experimental investigation to determine efficiency of radial interference as the means of residual stress creation (leading to delay of cracks growth).

It has been experimentally revealed that creation of radial interference equal to 1 % of bolt diameter in the hole made in the crack tip increased fatigue endurance of plates fabricated from D1A-T I. 2.5 – 2 times, from D16A-T I. 2.0 2.3–6 times, from V95pchAT1SVI5 – 3.7 times. Initiation of radial interference at 2 % of bolt diameter has resulted in residual endurance increase of just the same plates at 7.0; 15.5 and 14 times respectively.

Plates from D1A-T I. 2.5 with centrally located crack  $2 \cdot l = 40$  mm having bolts  $\varnothing 6$  mm set at the apex with radially tightened nuts have been subjected to experimental study of fatigue endurance to show efficiency of nuts tightening as the means of creating residual stresses, strengthening of crack edges initiation of friction forces to prevent crack spreading and to delay crack growth with their tips drilled. Tests have shown that nuts tightening resulted in increase of plates residual endurance at 8 and 15 times under  $M_t = 5$  and 8 N×m, respectively.

Effect produced by static extending load which makes the crack open under as a result of fasteners action set with radial interference has been subjected to experimental study. Fatigue tests have shown that application of static load to plate equal to cycle maximal load with the holes made in crack tips and bolts set-therein at 1 % radial interference increased residual fatigue endurance of plates from D16ATI2 at 8 – 14 times.

Efficiency of the developed FCDM has been subjected to study for radial interferences and tightening obtained under setting standard fasteners according to serial assembly procedure with application of standard drilling and counter-sunk tools and equipment used in aircraft manufacturing industry alongside with facilities for bolts pressing, bolt nuts tightening manufactured rivet heads forming [13, 14].

Fatigue test result analysis demonstrates the following (Fig. 3.41).

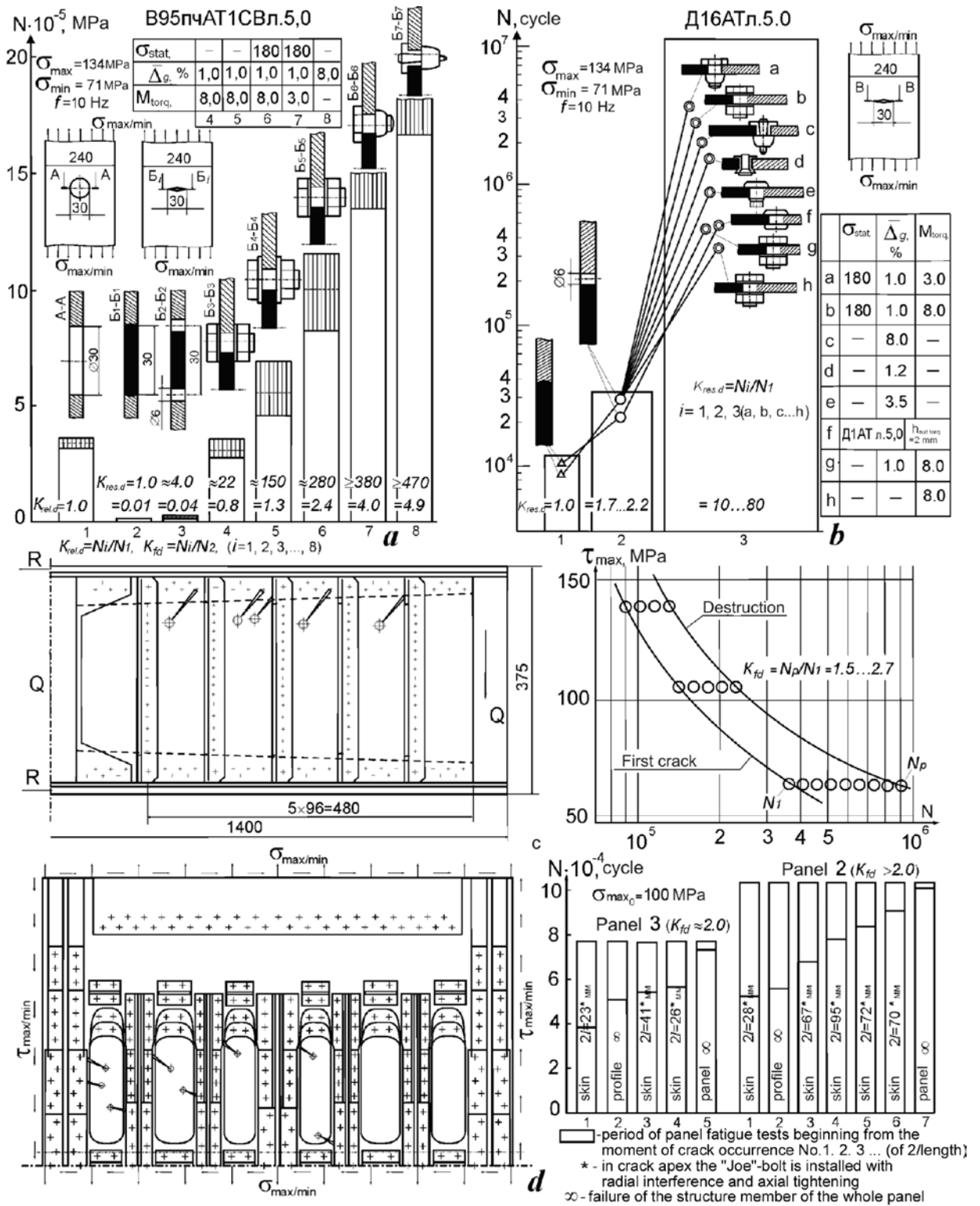


Fig. 3.41 – Fatigue Crack Growth Delay Techniques Efficiency by Setting Fasteners with Radial Interference and Tightening

FCDM application according to innovator’s certificate 725862 (Fig. 3.40) has demonstrated that residual fatigue endurance of loaded plates form D1AT I. 2.5 is 22 – 25.3 times higher, from D16AT I. 2 – 47 times and more, D16AT I. 5 – 12.6 times, from V95пчАТ1СВ – 18.5 times higher in compare with the endurance of plates having centrally located crack with  $\varnothing 6$  mm holes being fabricated at the apex.

FCDM application according to i. c. 1054006 has shown residual fatigue endurance of plates to be higher from D16AT I 5 and V95pchAT1SV at 7.8 and 3.7 times respectively under the use of 5009A-C bolts and Ø6 mm “joe”-bolts being 56 and 34.7 times higher in compare with the endurance of plates where crack growth is prevented just by setting fasteners wit radial interference and tightening without preloading.

FCDM application according to i.c. 1374670 has shown residual fatigue endurance of plates from D16AT to be 17.3 times higher in compare with the endurance of plates having cracks apex drilled.

FCDM application according to i. c. 1516287 has shown residual fatigue endurance of plates from D16ATI2 to be more than 2 times higher in compare with the endurance of plates with cracks apex drilled and repair overlays used. Under setting rivets of utmost rows with clearance in overlay (that is unloading of plate-to-overlay join utmost rows) endurance has additionally increased at 1.8 times under the presence of U-30MES-5 sealant and at 2.6 times without use of the sealant..

Application of the developed FCDM under fatigue tests of one-to-one size test pieces of spar sections and stringers panels has increased their fatigue endurance at 1.5 – 2.7 and 1.7 – 2.1 times, respectively.

Developed techniques of cracks growth delay and manufacturing procedure have been implemented in to industry making possible to upgrade laboratory test informability and to increased aircraft service life.

### 3.7. CONCLUSIONS

1. Scientific methodological grounds of integrated to achieve specified endurance of aircraft assembly structures have been developed and realized due to CAD/CAM/CAE systems for solving great scientific-technical problem to provide high service life of modern passenger and transport aircraft.

New conceptual philosophy of aircraft assembly structure integrated designing at every stage of aircraft life cycle in unified information media due to computer-aided system provide quality upgrading in development of parametric, analytical models of assembly structures, in quality upgrading and higher labor intensity of the designer, in creation of bolted and riveted joins in mass minimizing, in higher endurance, airtightness and quality of it's outer surface.

2. A set of new scientific principles, methods and techniques has been proposed to solve newly arisen problems under development of aircraft assembly structures and their joins with specified endurance:

- Principle in analytical models development of aircraft assembly structures;
- Creation principle of aircraft skin master-geometry;
- Principle in designing regular zones of aircraft assembly structures;
- Principle in designing irregular zones of aircraft assembly structures;
- Principle in supporting and achieving serviceability of aircraft assembly structures;



- Master geometry creating technique using computer-aided systems;
- Integrated method designing and computer-aided modelling of aircraft wing, fuselage, tail unit with the use of CAD/CAM/CAE systems;
- Integrated designing technique in joining regular zone members of aircraft assembly structures with specified service life;
- Structural members endurance design technique for assembly structure joints with an allowance made for fretting-corrosion;
- Method of integrated designing and computer-aided modelling aircraft assembly structure shear-bolted joints with specified endurance;
- Integrated analysis method for defining effect produced by structural and process properties on characteristics of local stress-strain state and coupling interaction between members of shear bolted joints by the use of ANSYS;
- Technique for determining effect produced by structural-process properties on compliance and distribution of efforts between the rows of shear bolted joints using ANSYS system;
- Designing technique for defining effect produced by structural and process properties on shear bolted joints in area of probable fatigue failure based on energy criteria and fatigue curves of standard joint test-pieces;
- Integrated design and 3D computer-aided modelling technique for standard riveted joints of aircraft assembly structures;
- Analysis technique for defining effect produced by structural and process properties of countersunk riveted joints on their endurance;
- Calculation technique for distribution of efforts between the rows of shear riveted joints accounting fatigue property and rivet design;
- Skin riveted joints design technique having specified endurance;
- Fatigue crack growth delay procedure in airframe thin-wall structures by setting fasteners with interference in the holes made in the crack tip.

3. Aircraft assembly structure geometry forming method has been proposed using CAD/CAM/CAE system based on unified computer model of aircraft outer surface made by analytical geometry method.

4. Specified endurance of aircraft assembly structure has been firstly provided in combination with the basic phases of aircraft service life cycles, that is, designing, manufacturing and operation.

5. New estimation and experimental method has been proposed for design and design estimation phases to predict effects produced by structural and process properties on the endurance of bolted and riveted joints accounting variation of specific strain energy and coupling pressures in the area of joint members probable fatigue failure.



New techniques in unloading utmost rows of shear joints have been proposed by using additional overlays and lightening holes providing endurance increase at 1.6–2 times.

New design of countersunk bolts and their setting procedure have been developed on the basis of the new method for analyzing of local stress-strain state properties of bolted joints to provide joints tightness and endurance upgrading at 2–7 times.

New design of high life countersunk rivets with cylindrical compensators and their setting procedure has been developed to provide specified endurance, tightness and high outer surface quality without machining rivet heads after riveting that results in decrease of labour intensity.

6. Countersunk bolted and riveted joints for the manufacturing phase of aircraft assembly structures have been proposed to perform with local elastic-plastic radial and axial interference. It's efficiency has been proved by the significant scope of stress-strain state property study in joining parts by finite elements method realized in CAD/CAM/ANSYS system as well as by experimental endurance study of standard joints, assembly spars and panels. A method has been proposed, studied and realized to reduce a negative effect produced by fretting corrosion on the endurance of shear bolted joints made with some manufacturing deviations along the mated surfaces by applying polymeric fillers on their surfaces to provide endurance increase of bolted joints at 1.8 – 3.6 times.

7. New structural and process procedures to delay fatigue cracks growth have been developed basing on new SSS analysis method for plate with fatigue cracks at holes tips by setting fasteners in the holes with radial interference providing service life increase at 1.5 – 2 times.

8. Reliability of scientific results and recommendations is proved by a great scope of numerical experiments with the use of ANSYS certified system, computer-aided modeling of aircraft structural components using UNIGRAPHICS and Siemens integrated systems and by experimental study of aircraft assembly structure models endurance performed a KhAI laboratory.

9. Developed methodology of aircraft assembly structure integrated designing with specified endurance has been used under development of AN-74TK-300, AN-140, AN-148, AN-158 aircraft and in training aviation specialists at National Aerospace University named after N. E. Zhukovsky "Kharkov Aviation Institute".

## Chapter 4

## STRUCTURAL-PROCESS METHODS AIRCRAFT TITANIUM STRUCTURAL COMPONENT BOLTED JOINTS. FATIGUE ENDURANCE UPGRADING WITH FRETTING-CORROSION TAKEN INTO ACCOUNT

### 4.1. ESTIMATION-EXPERIMENTAL METHOD TO DETERMINE EFFECT PRODUCED BY FRETTING-CORROSION FATIGUE ENDURANCE OF TITANIUM STRUCTURAL MEMBERS PRODUCED FROM BT6 ALLOY

Fretting corrosion effect has been proposed to determine by a value of maximal stresses decrease in smooth strip test-pieces under fretting-corrosion condition ( $\sigma_{\max 0f}$ ) in compare with maximal stresses in test-pieces free of fretting corrosion ( $\sigma_{\max 0}$ ) at identical number of loading cycles and asymmetry factor of loading cycle  $r = 0$  [8, 10, 13]:

$$\Delta\sigma_{\max 0f} = \sigma_{\max 0} - \sigma_{\max 0f}. \quad (4.1)$$

Fatigue endurance of smooth strip test-pieces under fretting corrosion conditions (Figs 4.1, 4.2) has been subjected to experimental study and fatigue curves have been plotted following their results  $\sigma_{\max 0f}^m N = C$  (Fig. 4.3).

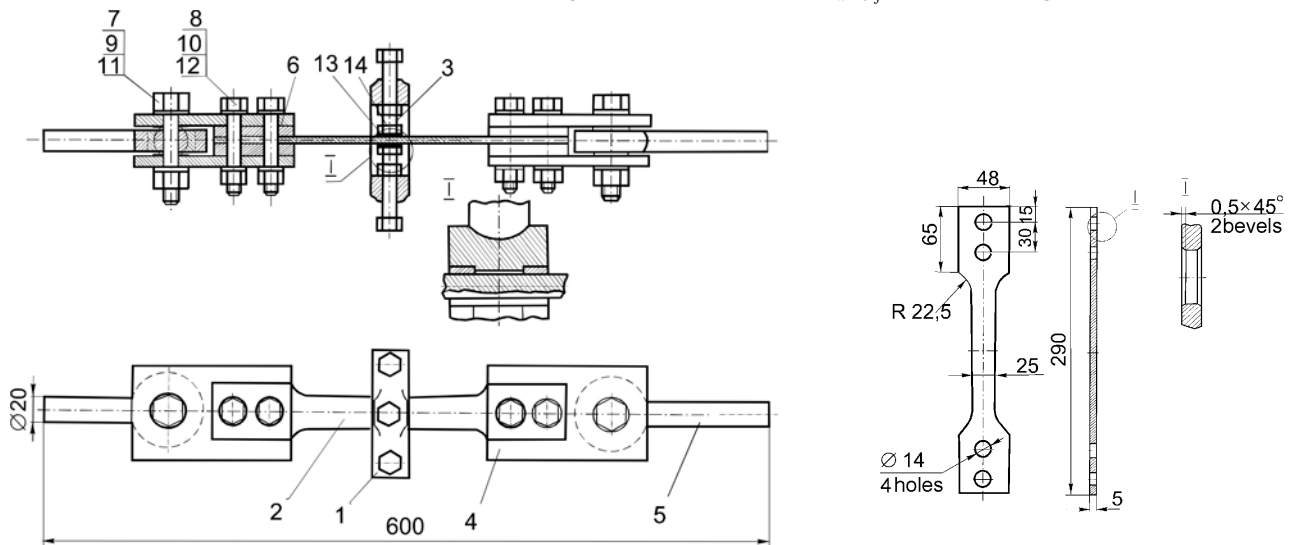


Fig. 4.1 – Test-Piece and Facility for Studying Effect Produced by Coupling Pressure Value and Combination of Materials in Coupling Pair for Fatigue Endurance of Smooth Strip under Fretting-Corrosion Condition; 1 – clamp; 2 – test-piece; 3 – pressing bolt; 4 – plate; 5 – clamp; 6 – linear; 7-12 – fasteners; 13 – washer; 14 – pressing fixture

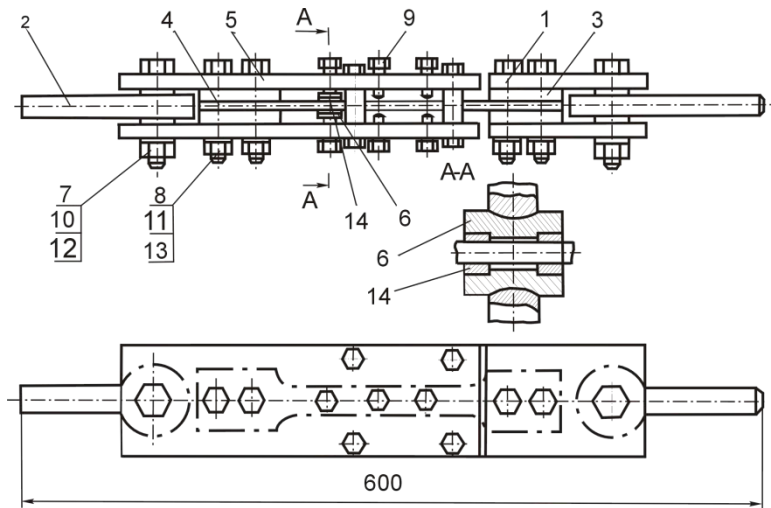


Fig. 4.2 – Facility for Studying Effect Produced by Relative Displacement Amplitude on Fatigue Endurance of Smooth Strip under Fretting-Corrosion Condition:

- 1 – plate; 2 – clamp;  
 3 – linear; 4 – smooth strip test-piece; 5 – adaptation plate;  
 6 – clip; 7 – 13 – fasteners;  
 14 – washer

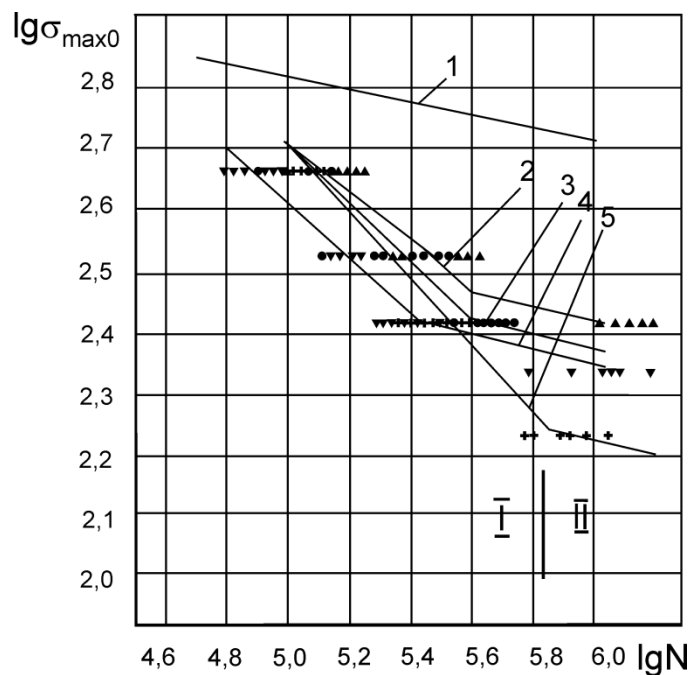


Fig. 4.3 – Smooth Strip from VT6 Alloy. Fatigue Test Results:  
 1 – VT6 alloy fatigue curve free of fretting-corrosion;  
 2, 3, 4, 5 – VT6 alloy fatigue curves and experimental data under fretting-corrosion with washers made from different alloys  
 2 –  $\blacktriangle$  – D16AT,  $\sigma_c = 106$  MPa; 3 –  $\bullet$  – 30HGSA,  $\sigma_c = 106$  MPa;  
 4 –  $\blacktriangledown$  – VT3 – 1,  $\sigma_c = 106$  MPa; 5 –  $+$  – 30HGSA,  $\sigma_c = 82$  MPa

VT6 alloy ( $\sigma_{max0} = 1993 N^{0.101}$ ) fatigue curve expression and formula for stress amplitude estimation of loading cycle with an asymmetry factor of  $0 < r < 0.6$  in maximal stresses of repeated-stress cycle equal to damage effect have been defined following fatigue endurance test results of smooth strip test-pieces free of fretting corrosion:

$$\sigma_{max0} = 2\sigma_a / (1-r)^{0.7} . \quad (4.2)$$

At study of VT6 alloy fatigue characteristics under fretting-corrosion condition multi-factor experiment has been subjected to correlative and regressive

analysis. Effect produced by coupling pressure values  $\sigma_c$ , relative displacement amplitude in coupling pair (a) of smooth strip been determined as well as washer material and coating test for fatigue endurance of smooth strip.

Due to this fact and based on formula (4.1) an estimation-experimental regularity has been derived for determination and prediction of fatigue endurance for smooth strip from VT6 alloy under fretting-corrosion condition [13]:

$$\begin{aligned}\sigma_{\max 0f} &= 1993N^{-0.101} - 20.8N^{0.0524K_c}\sigma_c^{0.48}; N > 2 \cdot 10^5; \sigma_c \leq 78MPa; \\ \sigma_{\max 0f} &= 1993N^{-0.101} - 2594N^{0.048K_c}\sigma_c^{-0.618}; N > 2 \cdot 10^5; \sigma_c > 78MPa,\end{aligned}\quad (4.3)$$

where  $N$  – fatigue endurance;  $K_c$  – a factor specifying effect produced by washer material and its coating on fatigue endurance ( $K_c = 1; 0.92; 1.14$  respectively for pairs VT6+30HGSA; VT6+D16AT; VT6+VT3-1).

Local stress-strain state (SSS) properties and coupling interaction characteristics under extension of titanium strip test-pieces with pressed to it washers have been studied by the use of finite element method realized in CAD/CAM/ANSYS system. Also, probable fatigue failure area under fretting corrosion condition have been determined. Effect produced by coupling pressure values on variations of local SSS properties has been found in strip for all combination of materials involved in this investigation under our discussion. Coupling pressure values increase from 50 to 150 MPa results in growth of maximal main extending stresses at 1.04 – 1.2 times, strains at 1.04 – 1.1 times and specific strain energy equal to repeated-stress cycle at 1.15 – 1.35 times.

Experimental studies have shown that fretting corrosion of titanium parts depends on washers material, coupling pressure values and reduces fatigue endurance of titanium strip at 2-3 times in compare with fatigue endurance of VT16 titanium alloy free of fretting corrosion. In this case fatigue endurance is decreased at: 40 – 80 times under maximal loading of repeated-stress cycle equal to 400 MPa; 400 – 750 times under 300 MPa; 1500 – 3000 times under 250 MPa. Analysis of experimental results has shown that effect produced by relative displacement amplitude values in coupling pare on fatigue endurance is insignificant and therefore, is neglected in dependencies (4.3).

#### 4.2. DETERMINATION METHOD OF EFFECT PRODUCED BY STRUCTURAL AND PROCESS DATA OF BOLTED JOINTS ON PARTS COUPLING INTERACTION CHARACTERISTICS

Load transfer excentricity in single-shear bolted join causes bending stresses in its elements (Fig. 4.4) and linear force irregular distribution of interaction along the total bolt coupling area including a hole wall [11, 12].

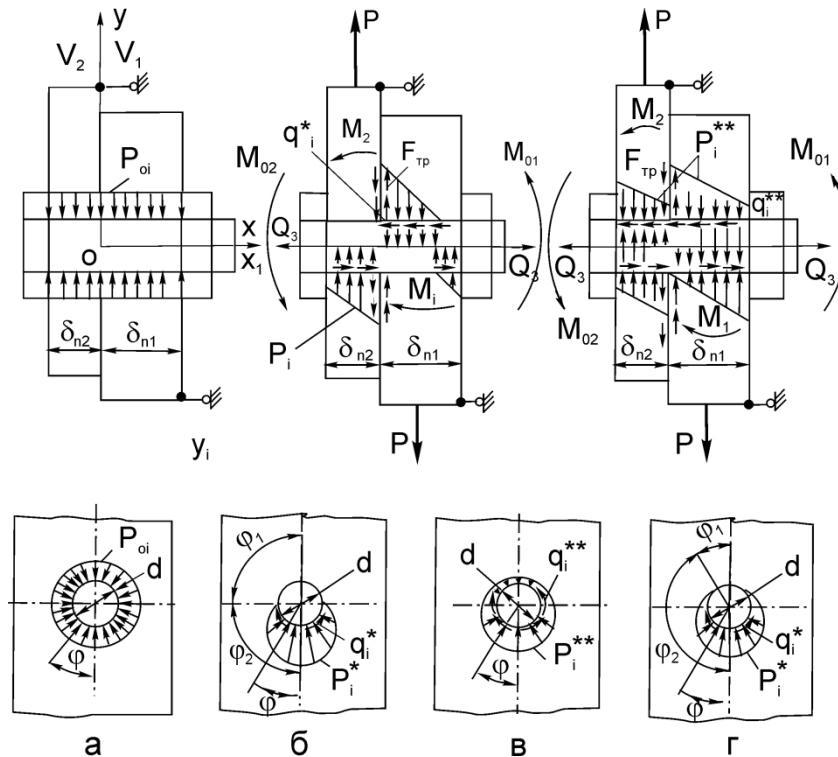


Fig. 4.4 – Single Bolted Joint Estimation Diagram

Generally, a bolt in shear joint of two parts can transfer force  $P$  and moment  $M_i$ .

Under coupling interaction modelling plates and bolt in single joint, the plates are presents as an elastic foundation. Under operation in progress the bolt is loaded as a beam working for bend and shift through the elastic foundation of normal  $p_i(x)$  and targent  $q_i(x)$  load, reactive basic moments ( $M_{0i}$ ) in sections along the coupling planes between a nut and bolt head with joined plates. Bolt tightening effort  $Q_3$  is acting on bolt and joined plates.

In addition to everything mentioned above, normal  $p_{0i}$  and targent (friction forces)  $q_{0i}$  of bolt load caused by radial interference acting on coupling interaction nature have been taken into account in the proposed model.

A method has been developed to determine characteristics of bolt coupling interaction with joined plates under elastic-plastic interferences with an account made for probable bolt tearing from its hole under high external loads that result in bolt coupling with hole wall along the total circumference length ( $0 \leq \varphi_1 < \pi/2$ , see Fig. 4.4, d). This method involves:

- Analysis of physical interaction between single shear single bolted joint elements and defining the main structural-technical factors specifying its fatigue endurance, development of joint estimation diagram with an account made for coupling interaction loading history;

- Development of differential equation demonstating coupling interaction between bolt and plates in single-shear joint;

– Definition of boundary condition for differential equation of bolt axis elasticity in area of nut and bolt head connection with joined plates and plates with each other;

– Integration of bolt axis elasticity differential equation with an account made for boundary conditions;

– Iteration search for solution of formulated boundary problem of bolt axis elasticity bending;

– Determination of coupling pressure value in joint parts mating area.

Irregularity factors of linear normal contact loading  $[p(x)]$  with reference to bolt length are defined by the following formula  $k_{\theta i} = \frac{p_i(x)\delta_{ni}}{P}$  [14].

Joined plate thickness-to-bolt diameter  $\delta_n/d$  ratio effect on linear loading irregularity factors is shown in Fig. 4.5.

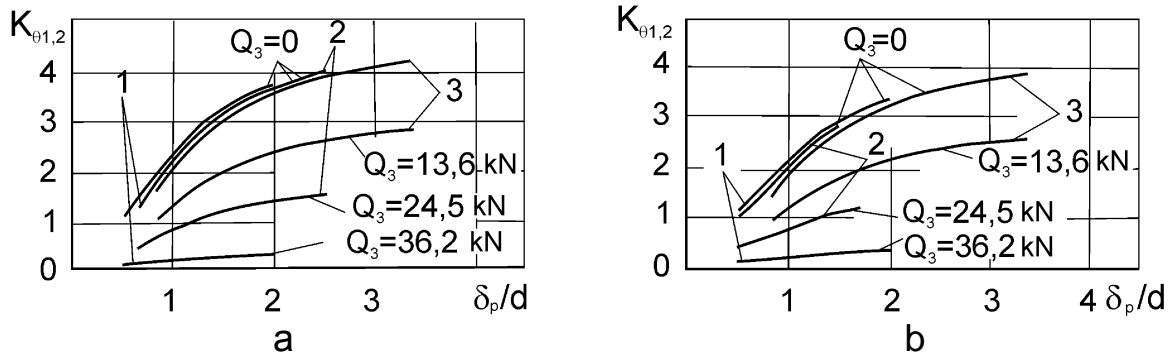


Fig. 4.5 –  $\delta_n/d$  Ratio Effect on Irregularity Factors of Linear Normal Coupling Loading with Reference to Bolt Length in Single-Shear Joint:

a) bolt 30HGSA steel;

b) bolt – VT16 titanium alloy; 1 –  $d = 10$  mm; 2 –  $d = 8$  mm;

3 –  $d = 6$  mm;  $P = 10$  kN;  $K_{\theta 1} = K_{\theta 2}$

Following  $\delta_n/d$  value increase from 0.5 to 3,  $K_{\theta 1}$  is increased within the range from 1.0 to 3.8 for bolts from 30HGSA steel (at 2.6 – 2.8 times) for every studied bolt diameter:  $d = 6$ ; 8; 10 mm.

For joints with the use of bolt  $d = 8$  mm from 30HGSA steel under specified thickness of  $\delta_{n2} = 5$  mm, thickness increase  $\delta_{n1}$  at 4 times results in  $K_{\theta 1}$  increase from 1.1 to 4.0 while for joints using bolt from VT16 titanium alloy,  $K_{\theta 1}$  from 1.3 to 5.7.

Tightening effort  $Q_3$  increase from 5 to 25 kN decreases coupling pressure irregularity factors under bolt head  $v_{Hb}$  from 7 to 2.0 – 2.5. Value  $v_n$  under the nut for the variants of joints under discussion varies within the range from 3 to 1 (Fig. 4.6).

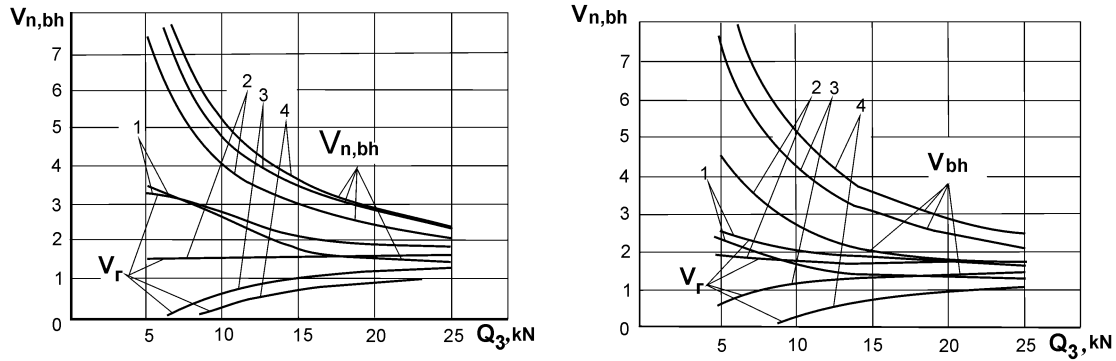


Fig. 4.6 – Tightening Effort Effect on Coupling Pressure Irregularity Factors under the Nut and Bolt Head: a –  $\bar{\delta}_{n2} = 4$  mm; 1 –  $\bar{\delta}_{n1} = 4$  mm; 2 –  $\bar{\delta}_{n1} = 8$  mm; 3 –  $\bar{\delta}_{n1} = 12$  mm; 4 –  $\bar{\delta}_{n1} = 16$  mm; b –  $\bar{\delta}_{n1} = 16$  mm; 1 –  $\bar{\delta}_{n2} = 16$  mm; 2 –  $\bar{\delta}_{n2} = 12$  mm; 3 –  $\bar{\delta}_{n2} = 8$  mm; 4 –  $\bar{\delta}_{n2} = 4$  mm;  $P = 30$  kN;  $E_1 = 210$  GPa;  $\bar{\Psi} = 0$ ;  $d = 8$  mm

Application of radial interference decrease irregularity factors value of linear normal coupling load up to 5 times (Fig. 4.7).

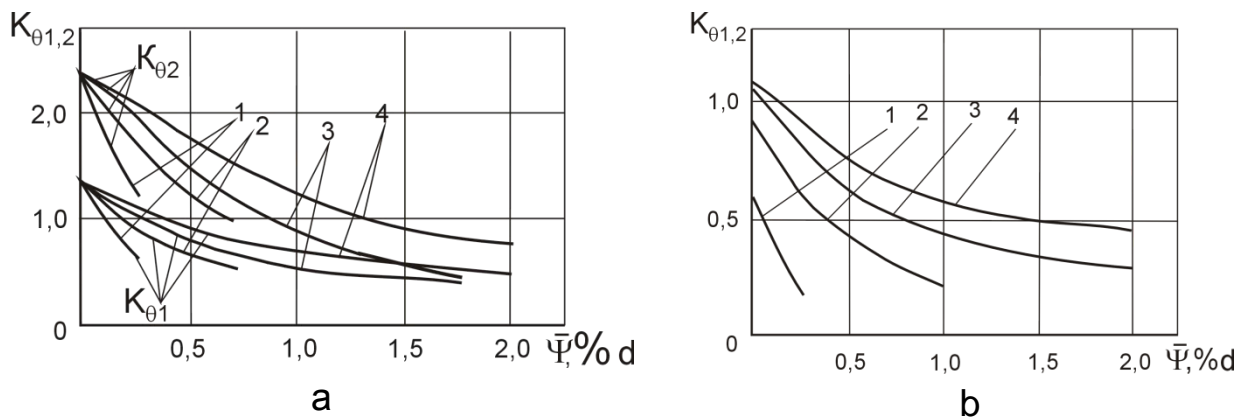


Fig. 4.7 – Radial Interference Effect on Irregularity Factors for Linear Normal Coupling Load with Reference to Bolt Length in Single Shear Joint:

a – free of tightening

$\bar{\delta}_{n1} = 5$  mm;  $\bar{\delta}_{n2} = 10$  mm; b – under tightening condition of 10 kN;

$\bar{\delta}_{n1} = \bar{\delta}_{n2} = 5$  mm;  $K_{\theta1} = K_{\theta2}$ ; 1 –  $P = 10$  kN; 2 –  $P = 20$  kN; 3 –  $P = 30$  kN;

4 –  $P = 40$  kN

#### 4.3. EXPERIMENTAL STUDY OF EFFECT PRODUCED BY STRUCTURAL-PROCESS PARAMETERS ON FATIGUE ENDURANCE OF STRUCTURAL MEMBERS JOINTS FROM VT6 ALLOY

Fatigue endurance experimental study results have been presented (Fig. 4.8) and dependencies have been developed for determination of strip fatigue endurance with the holes filled by VT-6 alloy under the bolt set in the hole ( $d = 10$  mm [12, 13]). Fatigue failure nature of double shear joint members is shown in Fig. 4.9.

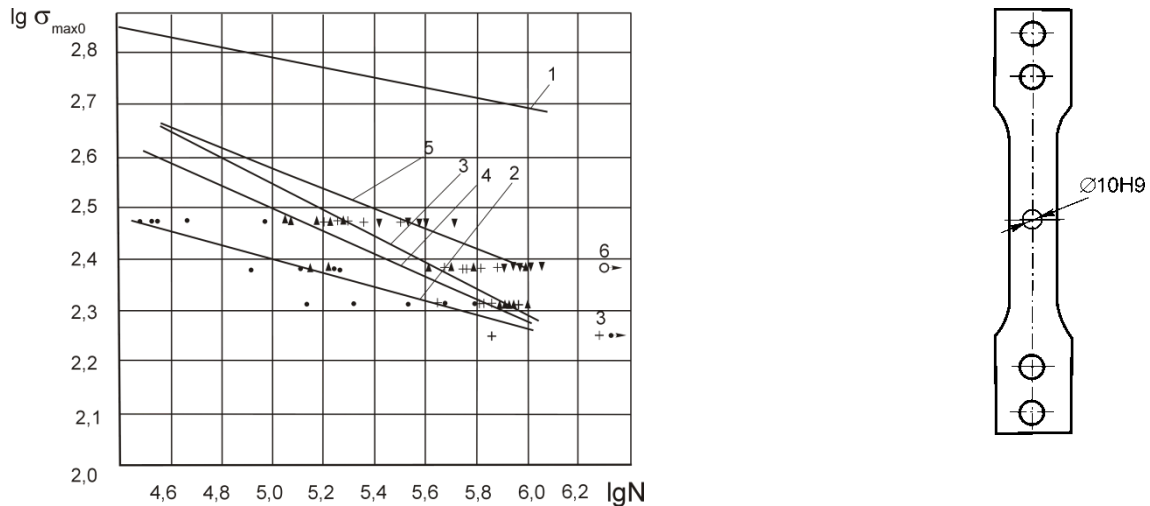


Fig.4.8 – Fatigue Test Results of Strip With a Hole under Different Variants of Bolt Setting: 1 – VT6 alloy fatigue curve; 2, 3, 4 – fatigue curve of strip with hole form VT6 alloy;

2 – ● –  $\bar{\Psi}=0$ ;  $M_3=0$ ; 3 – + –  $M_3=40$  N·m ( $\sigma_C=90$  MPa);

4 – ▲ –  $M_3=20$  N·m ( $\sigma_C=45$  MPa);

5 – ▼ –  $\bar{\Psi}=0.6\%$  d;  $M_3=20$  N·m; 6 – O –  $\bar{\Psi}=0.6\%$  d;  $M_3=0$

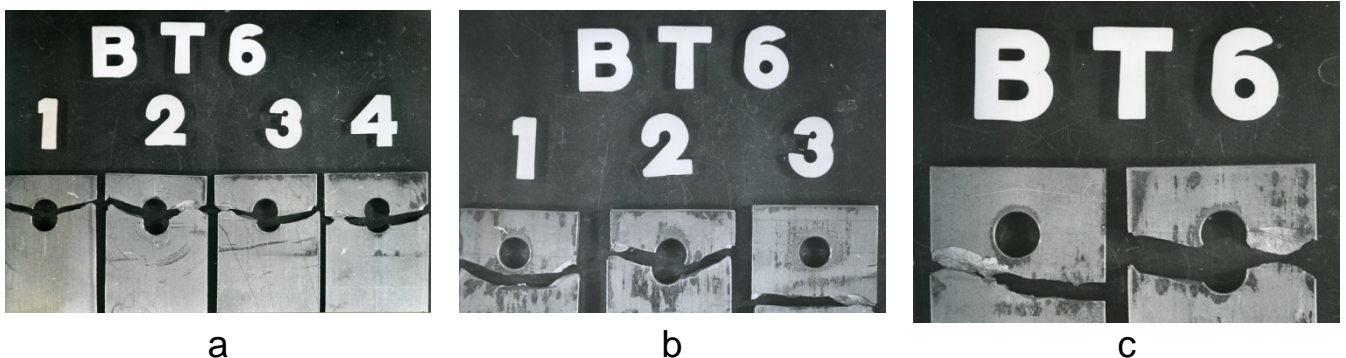


Fig.4.9 – Fatigue Failure Nature of Two-Shear Joint Elements Form VT6 Titanium Alloy under Bolt Setting: a – 1, 2 free of radial interference and tightening;

3, 4 – with radial interference and free of tightening; b – with tightening

$M_3=20$  N·m free of radial interference;

c – tightening  $M_3=20$  N·m and interference  $\psi=(0.7...1.1\%)d$

Fatigue test results of single-bolted ( $d=10$  mm) two-shear joints are shown in Fig. 4.10. Application of specified axial tightening upgrades fatigue endurance of aircraft structural members titanium two-shear joints are 20 times under maximal loads of repeated stress cycle 200 MPa and 35 times under 140 MPa in compare with fatigue interference 1.5 – 1.9 %) d free of tightening upgrades fatigue endurance of two-shear joint 1.2 – 2 times in compare with two-shear joint with bolts tightening [13, 14, 16].



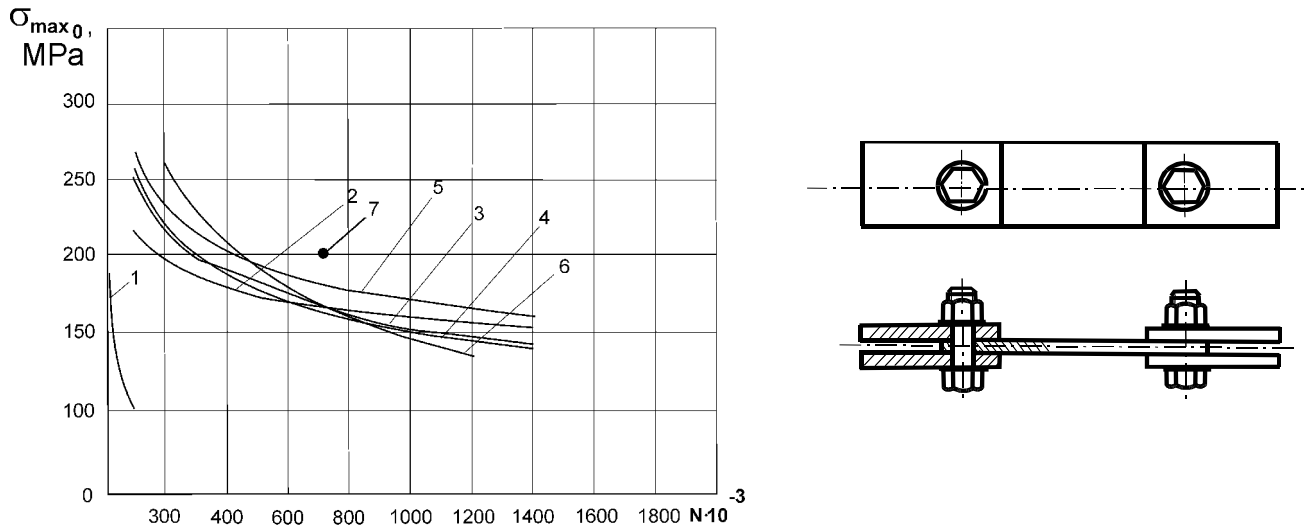


Fig. 4.10– Effect of Radial Interference and Axial Bolt Tightening on Fatigue Endurance of Two-Shear Joint from VT6 Alloy: 1 –  $\bar{\psi} = 0$ ,  $M_3 = 0$ ; 2 –  $\bar{\psi} = (0.7...1.1 \%) d$ ,  $M_3 = 0$ ; 3 –  $\bar{\psi} = (0.7...1.1 \%) d$ ,  $M_3 = 20 \text{ N}\cdot\text{m}$ ; 4 –  $\bar{\psi} = 0$ ,  $M_3 = 20 \text{ N}\cdot\text{m}$ ; 5 –  $\bar{\psi} = (1.5 \dots 1.9 \%) d$ ,  $M_3 = 0$ ; 6 – calculation according to formula  $\sigma_{max_{of}} = 1993 \text{ N}^{-0,101} - 20.8 \text{ N}^{0.0524K} / \sigma_C^{0,48} K_{CC}$ ; 7 – total coupling surface strengthening of internal element,  $\bar{\psi} = (1.5...1.9 \%) d$ ,  $M_3 = 20 \text{ N}\cdot\text{m}$

Process peculiarities in making titanium bolted joint with radial interference have been experimentally studied. Probabilities of high quality setting of bolt from 16HSN, 30HGSA and VT16 titanium alloy in pack from VT6 alloy have been determined. Admissible values of radial interference and bolt material effect as well as its coating and lubrication on setting effort value have been defined. Limit thickness values of joined parts packs have been calculated for different values of radial interference under the use of bolts from 30HGSA steel and VT6 titanium alloy.

#### 4.4. STUDY OF STRUCTURAL PROCESS METHOD APPLICATION TO UPGRADE FATIGUE OF BOLTED JOINTS IN AIRCRAFT TITANIUM STRUCTURAL MEMBERS WITH AN ACCOUNT MADE FOR FRETTING CORROSION

Strengthening of joint plate internal area has been studied to reduce negative effect of fretting corrosion in fatigue endurance of two-shear bolted joints (Fig. 4.11).

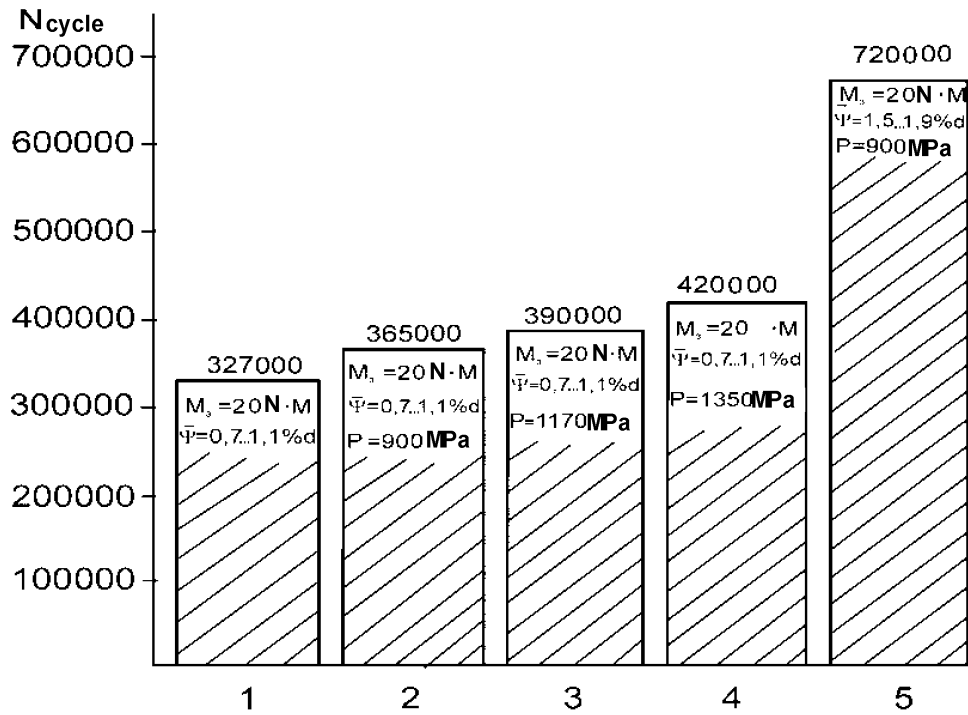


Fig. 4.11 – Internal Plate Surface Strengthening Effect on Fatigue Endurance of Two-Shear Joints Made from VT6 alloy: 1 – free of strengthening; 2, 3, 4 – circular area strengthening around the hole and area under the edges of joint external plate; 5 – total coupling surface strengthening of joint internal plate

Studies performed have demonstrated that combination of using surface strengthening of plastic strain ( $P_{str} = 0.95 \dots 0.99 \sigma_u$ ) of radial interference  $\psi = (1.5 \dots 1.9 \%) d$  and bolts axial tightening to  $M_3 = 20 \text{ N}\cdot\text{m}$  is the most efficient way to upgrade fatigue endurance of two-shear joint from VT6 alloy resulting in endurance increase at 2.3 times in compare with endurance of joints with radial interference and specified tightening.

Effect of axial tightening and radial interference on compliance of single-shear single-bolted joint (Fig. 4.12) has been studied.

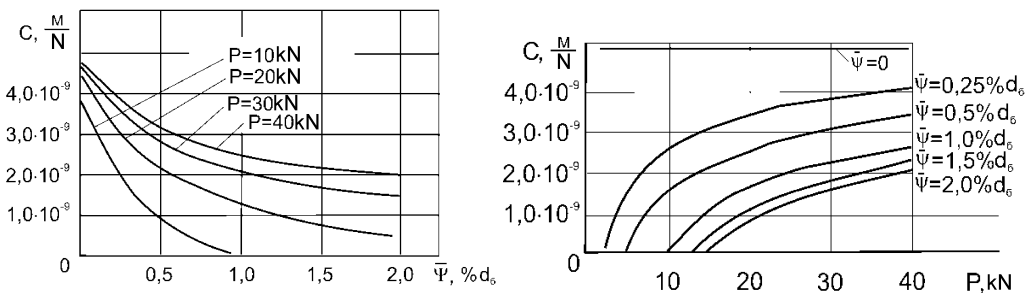


Fig. 4.12 – Influence of Radial Interference and Efforts Transferred by Single-Shear Bolted Joint on United Compliance Factor: a –  $Q_3 = 0$ ; b –  $Q_3 = 10 \text{ kN}$ ;  $d = 8 \text{ mm}$ ; bolt – 30HGSA; VT6 plates ( $\delta_{n1} = \delta_{n2} = 5 \text{ mm}$ )

Compliance factor  $C$  does not depend on outer load value and for this joint:  $C = 5.0 \cdot 10^{-9}$  m/N at joints free of radial interference and tightening ( $\psi = 0$ ,  $M_3 = 0$ ). Use of radial interference  $\psi = 1.0\%$   $d$  in single-bolted joint ( $d = 8$  mm,  $\bar{\delta}_{n1} = \bar{\delta}_{n2} = 5$  mm) reduces compliance at more than 5 times under load effort values of  $P_{oper} < 20$  kN. For the load range  $P = 0 \dots 40$  kN compliance factor value within the range from 0 to  $5 \cdot 10^{-9}$  m/N for different variety of joints. The most compliance factor dependence on load effort value can be observed under low levels from 10 to 15 kN. Bolt axial tightening reduces compliance factor at 15...20% in compare with compliance factor of joints free of tightening.

Use of radial interference in bolted joint reduces compliance factor under  $\psi = 0.5\%$   $d$  at more than 1.4 times  $\psi = 1.0\%$   $d$ , at 1.9 times,  $\psi = 2.0\%$   $d$  at 2.3 times.

Load distribution between bolt rows has been studied for prediction of multibolted joint fatigue endurance [13, 14, 16].

The first bolt load in joints with radial interference grows following interference value increase to achieve a value of 0.62 for this joint (Fig. 4.13).

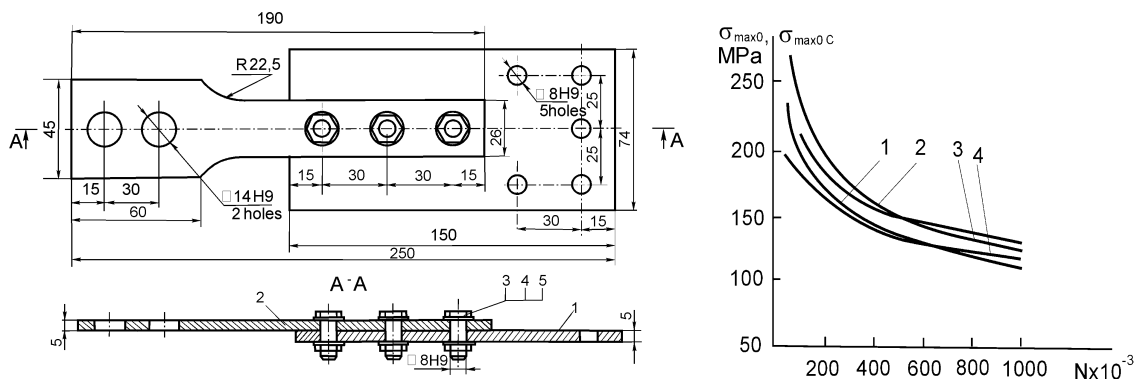


Fig. 4.13 – Joint Test Piece from VT6 Steel and its Fatigue Endurance Curve:

Experimental Curves – 1 –  $\psi = 0$ ;  $M_3 = 10$  N·m;

2 –  $\psi = (1.5 \dots 1.8\%)$   $d$ ;  $M_3 = 10$  N·m;

3 –  $\psi = 1.5 \dots 1.8\%$   $d$ ;  $M_3 = 10$  N·m; 4 –  $\psi = 0$ ;  $M_3 = 10$  N·m

Based on conducted studies and in accordance with the specified characteristics of fatigue endurance in areas of probable fatigue failure it has been proposed to estimate its geometric parameters – along hole axis at points of joint geometric parameters variation at area of intensive fretting corrosion action.

Fatigue endurance of shear bolted joint,  $N_{sbj}$  must be higher than endurance of the skin-to-stringer and to-spar longitudinal joint  $N_{lj}$  or to be equal to it:

$N_{\text{sbj}} \geq N_{\text{lj}}$ . Estimated-analytical dependence [13, 14] is used for fatigue endurance estimation of titanium shear bolted joints along hole axis

$$A_1 N^{\zeta_1} = A_2 N^{\zeta_2} \frac{k_{\theta i}}{k_{\theta i}} \sigma_{r \max 0} + \sigma_{sgr \max 0} + A_3 N^{\zeta_3} \sigma_{ugr \max 0} \cdot \quad (4.4)$$

$A_1, A_2$  factors values and degree index  $\zeta_1, \zeta_2$  have been defined according to the fatigue test results of the strip with hole. Nominal strains in part section for which estimation is conducted, –  $\sigma_{\sigma \max 0}, \sigma_{\text{flgr} \max 0}, \sigma_{\text{Bgr} \max 0}$  – respectively, are caused by the action of loads transferred by the bolt going through the plate and from the bending moment.

Dependence accounting bolt fitting nature and joint bending [13, 14] is taken for fatigue endurance estimation in fretting-corrosion area:

$$\sigma_{\max 0f} = 1993 N^{-0.101} - 20.8 N^{0.0524K_c} (\sigma_{ce} \cdot v_i)^{0.48} K_{cc} K_b; \quad (4.5)$$

$$\sigma_{ce} \cdot v_i \leq 78 \text{ MPa};$$

$$\sigma_{\max 0f} = 1993 N^{-0.101} - 2594 N^{0.0481K_c} (\sigma_{ce} \cdot v_i)^{-0.6176} K_{CC} K_b;$$

$$\sigma_{ce} \cdot v_i > 78 \text{ MPa},$$

Where  $K_{CC}$  is a factor accounting radial interference effect;  $K_b$  is a factor accounting joint bending effect;  $K_{CC}=0.94$  for the joints with radial interference and specified tightening  $\bar{\nu}=(1.0 \dots 1.5 \%) d$ ;  $K_{CC}=1.0$  for joints free of radial interference with the specified bolt tightening;  $K_v=1.13$  for single shear joints;  $v_i$  – coupling pressure irregularity factor under the nut and bolt accounting effect of joint structural and process parameters.

Fatigue endurance estimation in area of the most loaded row of bolts (Ref to Fig. 4.13) has been performed for single shear three-bolted joint according to dependencies (4.4).

Fatigue endurance estimation of single shear joint according to utmost dependencies has been demonstrated satisfactory compliance with the test results.

#### 4.5. CONCLUSIONS

1. Experimental tests have shown that fretting-corrosion intensity depends on inashers material, coupling pressure value decreasing fatigue endurance of titanium strip at 2 – 3 times in compare with fatigue strength of VT6 titanium alloy free of fretting-corrosion. In this case, fatigue endurance reduction of the main titanium structural members caused by fretting-corrosion is in progress: at 40 – 80 times under maximal strains of repeated stress cycle – 400 MPa; at

400 – 750 times under 300 MPa; at 1500–3000 times under 250 MPa in compare with the endurance of the smooth test-pieces.

2. Developed model of a single shear bolted joint enables to determine distribution of linear standard coupling load with reference to use obtained estimates-experimental dependencies for determination of fatigue endurance of joint structural members in regular zone where failure takes place under the action of fretting-corrosion.

3. Application of standard axial tightening makes fatigue endurance of titanium structural members joints higher at 20 times under maximal strains of repeated stress cycle 200 MPa and at 35 times under 140 MPa in compare with fatigue endurance of the joints free of bolts tightening.

4. Application of radial interference (0.5...1.5 %)  $d$  reduces irregularity factor values of linear normal coupling load with reference to bolt length at 2-3 times and increase fatigue endurance of single shear bolted joint at 1.5-2 times in compare with the endurance of the joints using bolt tightening only.

5. Application of coupling surface strengthening by plastic strain method [strengthening pressure  $P_{str} = (0.95 - 0.99) \sigma_u$ ], radial interference (1.5...1.9 %)  $d$  and standard axial tightening is the most efficient method to increase fatigue endurance of double shear titanium joints resulting in endurance increase at 2.3 times in compare with endurance of joints with interference and standard tightening.

6. Practical application of the proposed structural-process methods of increasing fatigue endurance and fatigue endurance determination method of shear bolted joints make it possible to design joints of specifies fatigue endurance with an account made for fretting-corrosion.

*Chapter 5***STRUCTURAL-PROCESS METHOD TO INCREASE FATIGUE ENDURANCE OF AIRCRAFT AIRFRAME MEMBERS DETACHABLE BOLTED JOINTS**

---

**5.1. SCIENTIFIC JUSTIFICATION OF FATIGUE ENDURANCE INCREASE METHOD FOR STRUCTURAL ELEMENTS OF DETACHABLE BOLTED JOINTS BY LOCAL AND BARRIER REDUCTION**

Resulting in structural process peculiarities analysis of strong structural members detachable bolted joints it has been stated that they significance specify strength lifetime, tightness and weight of assembly units.

Anchor countersunk joints with self-locking nuts (Fig. 5.1) occupy special place among them to be used in structural members with one way access for fastening detachable panels of wing, tail unit and fuselage, hatch covers as well as nose and tail sections of wing, stabilizers and fairings.

Analysis of bolt setting process at manufacturing factory has shown that wing assembly process using series production procedure revealed systematic damage of hole wells in joined members of bolt thread section (depth to 0.2 mm). damage is caused by availability of production holes originated within production of self-locking nuts and assembly joints.

Therefore, it's time to modify procedure in making bolted detachable joints excluding possibility of hole wall damage.

Fatigue failure of shear countersunk bolted joints during operation occurs in stress and strain concentration technique.

At experimental levels of loads endurance of countersunk bolted joint models is practically two times less than endurance of strip with a cylindrical hole specifying lifetime of wing strong longitudinal members.

Production techniques in processing joined parts in holes area by burnishing ( $\delta = 2...4\%$ ), barrier reduction (reduction depth 0.2...0.3 mm) are used to increase endurance of strips with holes. But analysis of literature sources has shown that there are any scientific justification of fatigue endurance increase techniques for such joints. There are no practical recommendations for making highlife thread countersunk bolted joints and for predicting lifetime characteristics of such joints based on characteristics analysis of the local stress-strain state.

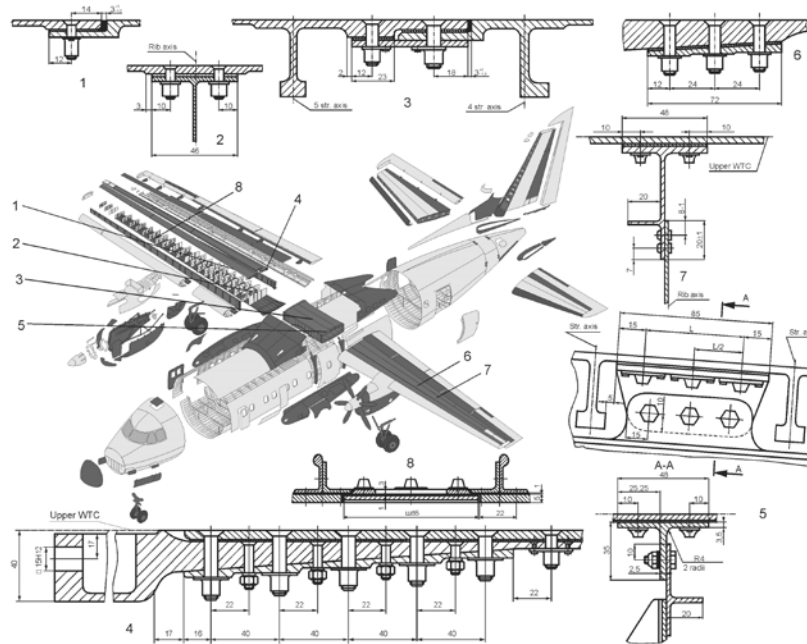


Fig. 5.1 – Airframe Structural Members Titanium Anchor Joints:

- 1 – outer wing panel longitudinal joint; 2 – rib-to-panel attachment joint;
- 3 – center section panel joint; 4 – panel-to spar cap joint (lengthwise section);
- 5 – center section panel-to-rib joint; 6 – panel-to-overlay joint; 7 – panel-to-rib joint;
- 8 – drain valve location point

Analysis has shown that the use of just a single type of processing (burnishing or rolling, deep plastic strain) does not allow to obtain specified lifetime characteristics of detachable bolted joint structural elements. Therefore, combined local (with a relative interference of 0.6 and 7 %) and barrier reduction (reduction depth – 0.3 mm) effect on characteristics of local SSS of extended strip with a cylindrical hole has been subjected to analysis with an account made for the properties of materials and production peculiarities of strip processing in the area of the holes.

Developed method for analyzing characteristics of strip with cylindrical hole local SSS (Fig. 5.2) under combined local and barrier reduction includes:

- Development of three-dimensional parametric models of crimps and strips with cylindrical hole (Fig. 5.3);
- Estimation diagram development for strip with hole;
- Specifying curve for strained material;
- Development of finite element models for strip with cylindrical hole and crimps (Fig. 5.4) an allowance for coupling interaction between strip and crimps area;
- Specifying limit conditions with reference to symmetry plane;
- Modeling lower crimp movement at the phase of combined local and barrier reduction application of external extending efforts corresponding to the level of extension strains in gross section;

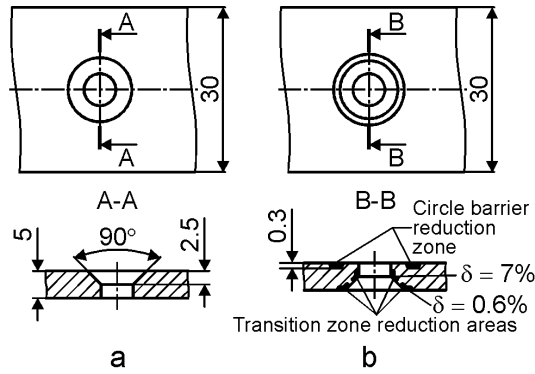


Fig. 5.2 – Strip with Cylindrical Hole Test-Piece:  
a – reduction free; b – with reduction

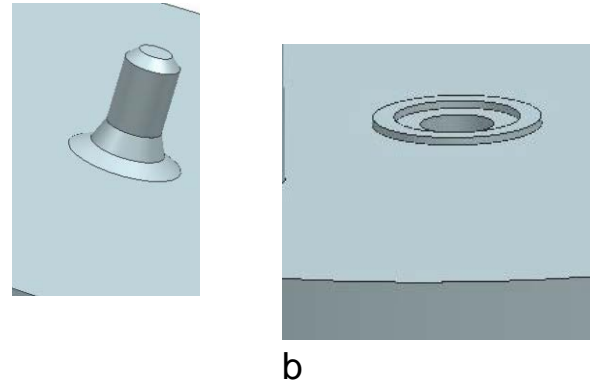


Fig. 5.3 – Segments. Crimp Three-Dimensional Models for:  
a – transition area;  
b – circular barrier reduction

- Modelling an unloading process by removing actions of external extension efforts analysis of main extension strains distribution with reference to the depth in section along the hole axis;
- Estimation of strip local SSS characteristics with reference to hole axis and reduction area;
- Determination of amplitude and maximal extension stresses, strains and specific strain energy equivalent to repeated stress cycle ( $W_{1max0}$ ) in combination with reference to hole axis and reduction area (Fig. 5.5).

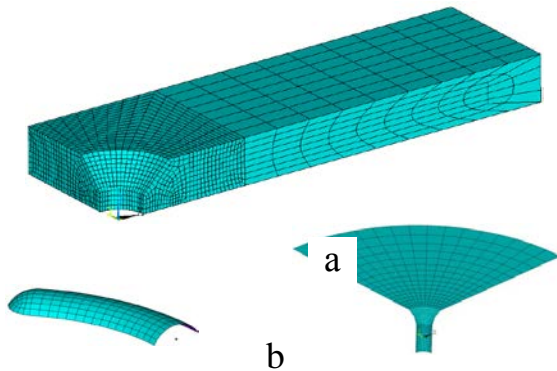


Fig. 5.4 – Finite elements:  
a – models – strips with a cylinder-conical hole; b – crimp

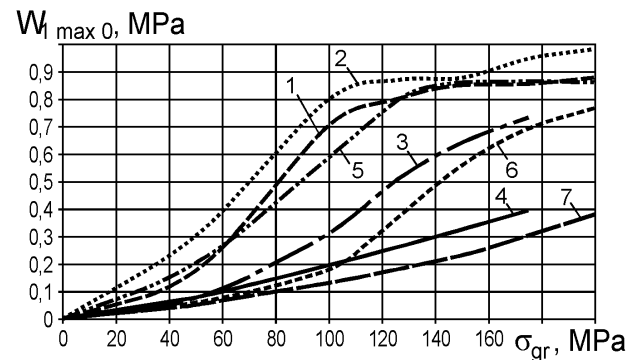


Fig. 5.5 – Load level and process technique effect on distribution  $W_{1max0}$  in strip with cylindrical hole under extension

Strip dependencies curves  $W_{1max0} = f(\sigma_{gr})$  are shown in Fig. 5.5: 1 – with cylindrical hole; 2 – with cylinder-conical hole; 3 – with cylindrical hole processed by craters stamping technique with segment configuration; 4 – with cylindrical hole processed by craters stamping technique with segment configuration in stamping area; 5 – with cylinder-conical hole processed by local reduction technique in section with reference to hole axis; 6 – with cylinder-conical hole processed by combined technique in section with reference to hole



axis; 7 – with cylinder-conical hole processed by combined technique in annular stamping area.

As a result of conducted analysis within the range of extension stresses  $\sigma_{gr} = 50 \dots 175$  MPa it has been stated that: segment configuration craters stamping with a depth of 0.3 mm at lower strip surface results in reduction of maximal main extension stresses value equivalent to repeated stress cycle of 1.17 – 2.03 times, main extension strains equivalent to repeated stress cycle of 1.1 – 1.9 times and maximal specific strain energy value equivalent to repeated stress cycle of 1.29 – 4.01 times in compare with the respective values for unprocessed strip with cylinder-conical hole (it was compared in section with reference to hole axis); combined processing by combined local and barrier reduction of the strip results in reduction of maximal main extension stresses value equivalent to repeated stress cycle at 1.17 – 2.4 times; main extension maximal strain values equivalent to repeated stress cycle at 1.29 – 2.26 times and maximal specific strain energy value equivalent to repeated stress cycle at 1.37 – 5.43 times in compare with respective values for unprocessed strip with cylinder-conical hole.

Experimental studies have been conducted to determine effect produced by processing technique endurance characteristics of the strip with cylinder-conical hole. The following characteristics of the strip fatigue endurance have been determined:

- With cylindrical hole;
- With cylinder-conical hole;
- By processing in area of cylinder-conical hole using reduction of cylinder-conical hole transitional area (at a depth of 0.5 mm);
- By processing in area of cylinder-conical hole using reduction of cylinder-conical hole transitional area (at a depth of 0.3 mm);
- By combined reduction and circular barrier reduction of transitional area using TsDM-10PU under  $\sigma_{0gr\ max} = 130$  MPa.

Fatigue failure nature of test-pieces is shown in Fig. 5.6.

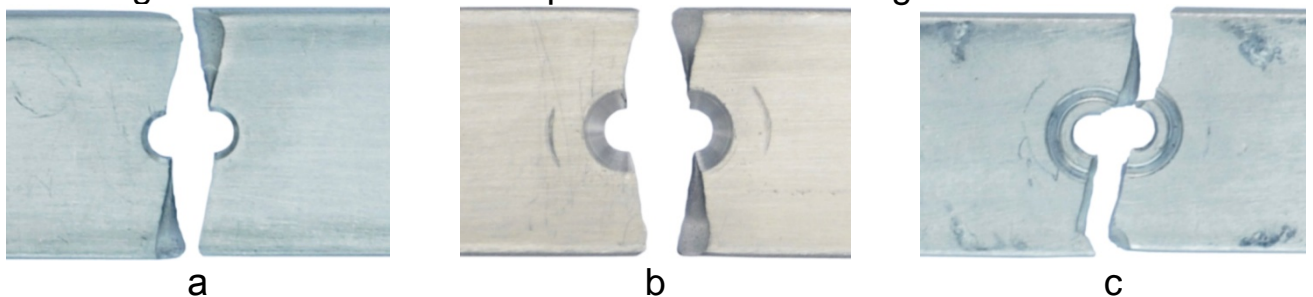


Fig.5.6 – Fatigue Failure Nature of Test-Pieces: a – strip with cylindrical hole; b – strip with cylinder-conical hole; c – strip with cylinder-conical hole processed in hole area by circular barrier reduction

The fatigue tests have resulted in the following:

- Fatigue endurance of the strip with cylinder-conical hole is equal to

0.5 fatigue endurance of the strip with cylindrical hole;

- Fatigue endurance of the strip with cylinder-conical hole processed in hole area by reduction of transitional area is equal to 0.75 fatigue endurance of the strip with cylindrical hole;

- Fatigue endurance of the strip with cylinder-conical hole processed in hole area by barrier circular reduction or by combined reduction of cylinder-conical transitional area is at 7.5 times higher than fatigue endurance of the strip with cylindrical hole and at 14.9 times higher than the strip with cylinder – conical hole.

Analytical expression has been developed for prediction of finite elements fatigue endurance in hole area on the basis of local SSS characteristics – specific strain energy in its local concentration area (probable fatigue area).

Analytical expression for the fatigue endurance curve can be presented as  $W^{m_w} \cdot N = C_W$ , where  $W$  – strain specific energy elastic component, MPa. Analytical expression for prediction in the following way:

$$N_{mW} = \frac{C_{Wm}}{C_{Wb}} \cdot N_b \cdot \frac{W_b^{m_{wb}}}{W_m^{m_{wm}}},$$

where  $m_{wb}$ ,  $m_{wm}$ ,  $C_{Wb}$ ,  $C_{Wm}$  – fatigue curve equation factors  $W^{m_w} \cdot N = C_W$ , obtained a within processing of fatigue tests results with reference to basic and modified test pieces.

For non-loaded for shear detachable bolted joint processed by strip burning technique in cylindrical hole area and combined reduction of transitional area and circular barrier reduction in cylinder-conical hole area can be expressed as following

$$N_{mW} = 21.8 \cdot N_b \cdot \frac{W_b^{36.3}}{W_m^4}.$$

Analysis of endurance estimation results according to the proposed technique has proved compliance and truthiness of the suggested prediction method and has shown that predicted endurance values of test pieces lie within dispersion boundaries range of fatigue characteristics obtained experimentally.

## 5.2. LOCAL SSS AND FATIGUE ENDURANCE CHARACTERISTICS STUDY OF AIRFRAME STRUCTURAL MEMBERS TEST-PIECES IN AREA OF DETACHABLE BOLTED JOINTS

Technique has been developed to determine variations of local SSS characteristics using ANSYS engineering analysis system in anchor joints within the process of its creation and loading. Technique involves determination of residual stresses in panel formed after riveting process during anchor nut setting, equivalent stresses distribution field in joint elements, equivalent maximal average amplitude and normal repeated stress and strain cycle, stress and strain concentration factors, specific strain energy, clearance change state in anchor joint elements with the similar characteristics of the similar joint with low hexagone nut.

Longitudinal joints (width 25 mm) of single-axis loaded test-piece of AN-74 aircraft wing detachable panel have been taken as a model for analysis of local strain-stress state (SSS) (Fig. 5.7).

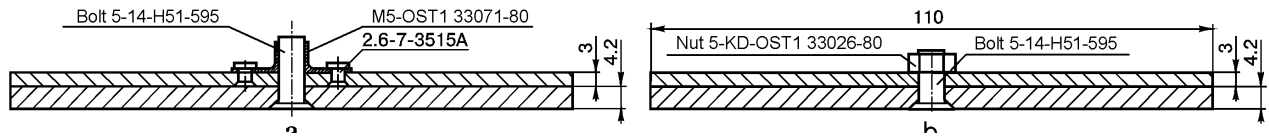


Fig. 5.7 – Test-Piece Non-Loaded for Shear Longitudinal Countersunk Joint:  
a – with anchor nut; b – with low hexagon nut

As a result of local SSS analysis performed under stud the nature of distribution of the equivalent stresses in strips after application of extension load it has been stated that the most dangerous zones are located in the cylindrical portion of the hole and transitional area between conical and cylindrical parts. The highest stresses in anchor joint are observed in strip with conical countersunk under an anchor bolt. Equivalent stresses equal to 185 MPa are originated in conical portion after application of tightening effort. Stresses in this area are growing followed by extension load increase and they reach 365 MPa under  $\sigma_{gr} = 200$  MPa. In strip with hole for anchor nut a specific strain energy in cross section within the field of hole for bolt is a 25 % higher than in the area of the hole for rivet for extension decreased to be 8 %. It is so because a part of extension load is transferred through the anchor nut itself and holes filled with rivets reduce local stresses and strains in area of cylindrical hole.

Results obtained under the study of local SSS characteristics became a basis for determination of specific strain energy critical concentration points and for developed of structural-process method to increase the fatigue endurance of structural members in detachable bolted joints area.

A method has been developed to determine variations in characteristics of local SSS using ANSYS engineering analysis system in elements of doubleshear, single row countersunk detachable bolted joint within the process of its creation and loading as well as to make comparable estimation of effect produced by two-hole self-locking nut on characteristics of local SSS in joint of skin and thin hexagon nut (Fig. 5.8).

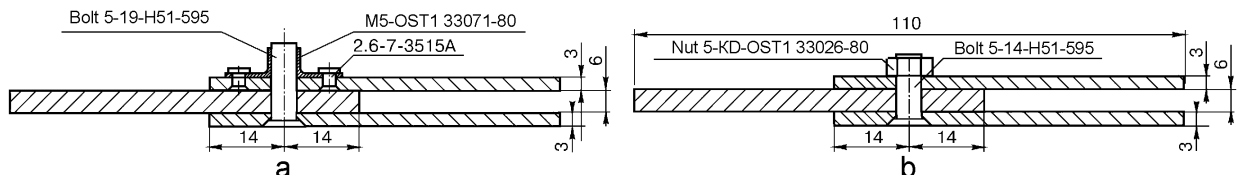


Fig. 5.8 – Doubleshear Single Row Countersunk Detachable Bolted Joint Test-Piece:

a – with anchor nut; b – with thin hexagon nut

This technique comprises determination of residual stresses in panel originated due to riveting during anchor nut setting, equivalent stresses distribution

field in joint elements medium amplitude and repeated stress and strain cycles of loading cycle, stress and strain concentration factors, specific strain energy, variation of coupling pressures in joints between mated surfaces and comparing stress-strain state in anchor joint elements with similar characteristics of the similar joint having thin sextagone nut is a result of local SSS analysis performed in compliance with the developed technique it has been stated as following:

- Use of two-holes self-locking nut results in hole under anchor bolt in strip where in available in compare with joint having standard hexagon nut. So within the range of loads corresponding to  $\sigma_{gr} = 0...100$  MPa in anchor joint maximal stresses are  $\sigma_{x\ max}$  at 30 %, repeated stress cycles  $\sigma_{0\ max}$  at 10 %, amplitude stresses  $\sigma_{a\ max}$  at 35 %, specific strain energy at 37 % and coupling pressure  $\sigma_{c\ max}$  at 10 % less than in joint with standard hexagon nut;

- Local SSS characteristics in central strip and lower overlay of anchor joint and joint with standard hexagon nut are as high as 5 %.

Data obtained as a result of analysis became the grounds for studying effect produced by structural and process parameters on characteristics of local SSS in elements of detachable bolted joints of aircraft structural components and their fatigue strength.

Technique has been developed in studying fatigue strength in longitudinal joints of detachable wing panel to determine critically dangerous area with reference to fatigue endurance conditions in elements of detachable bolted joints structure. Longitudinal joint of wing detachable panel has been subjected to modeling with the use of single-axis loaded test-pieces to study a fatigue strength (Fig. 5.9) as well as test-pieces simulating panel segment loaded for shear with reference to displacement conditions (Fig. 5.10).

Analysis of fatigue test results has shown that failure of the total test pieces (under  $\sigma_{0\ gr\ max} = 134...137$  MPa) takes place due to fatigue cracks in the element modelling detachable wing panel. Failure is originated from countersunk holes for countersunk bolt. Cracks are initiated from the cylindrical hole portion. Fatigue cracks development in test-pieces modeling panels segment is firstly in progress perpendicular to longitudinal joint axis. Following further crack growth and its spreading from joint area to regular panel portion the cracks turned in direction perpendicular to applied load. This fact has been proved by the results of a great number of studies showing that cylinder-conical hole area is the most dangerous with reference to stress concentration. Fatigue tests have been conducted using TsDM-10PU and MUP-50 unit respectively.

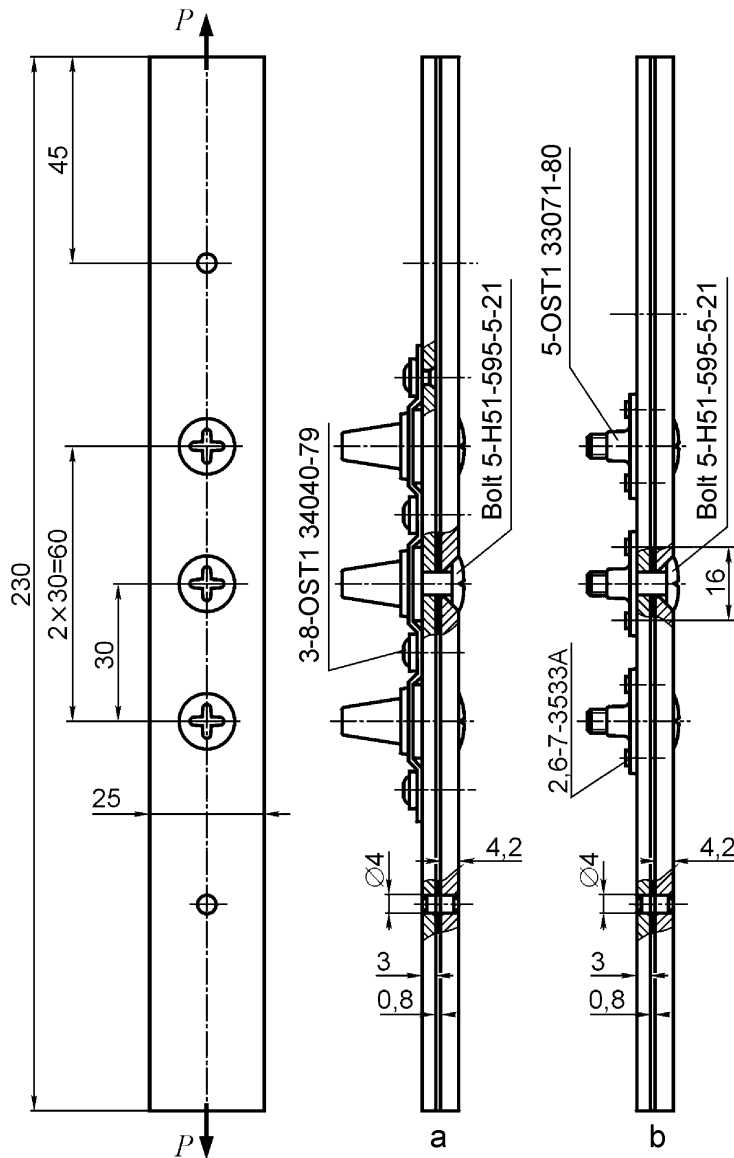


Fig. 5.9 – Longitudinal Not Loaded For Shear Joint Test Piece: a – nut-to-section attachment; b – double-ear self-locking nuts setting

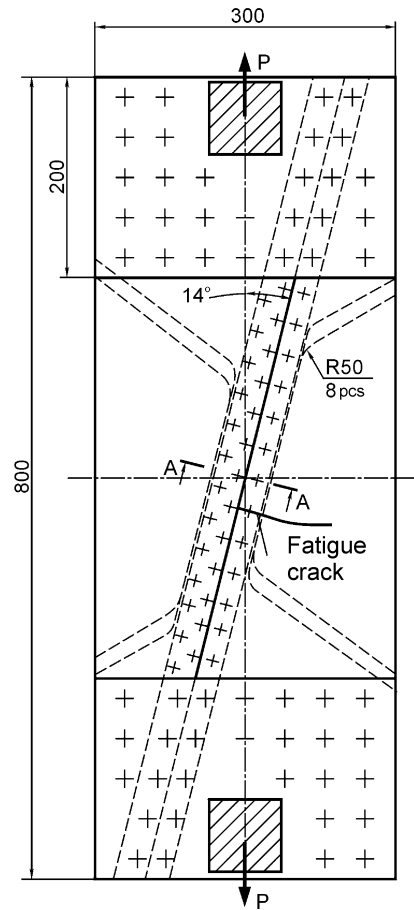


Fig. 5.10 – Detachable Wing Panel Longitudinal Loaded Joint Test Piece and Fatigue Cracks Spreading Nature

In this case fatigue endurance of longitudinal non-loaded for shear joints has been: under nut attachment to section (Fig. 5.9, a) – 20 800; under setting two-ears self-locking nuts (Fig. 5.9, b) – 42 600 loading cycles. Fatigue endurance of the joint loaded for shear is as following: under nut attachment to section – 22 400; under setting two-ears self-locking nuts – 24 700 loading cycles.

Fatigue test results have proved feasibility and necessity to develop new structural and processing techniques in upgrading of fatigue endurance of airframe structural members in detachable bolted joint area.

### 5.3. FATIGUE ENDURANCE CHARACTERISTICS EXPERIMENTAL STUDIES OF AIRFRAME STRUCTURAL MEMBERS STANDARD MODELS IN DETACHABLE BOLTED JOINTS AREA

Experimental studies have been performed using TsDM-10PU unit under operating level of extension cyclic loading ( $\sigma_{0\text{ gr max}} = 130 \text{ MPa}$ ) for the following

versions of test-pieces:

- Strip-to-cylindrical hole and cylindrical hole joints;
- Strip-to-cylindrical hole joint processed by burnishing of hole walls and cylindrical hole;
- Longitudinal detachable bolted joint not loaded for shear;
- Longitudinal detachable bolted joint not loaded for shear with its structural elements being processed in cylindrical hole area by burnishing of hole walls while in cylindrical hole area by transitional area reduction and barrier circular reduction.

Standard fatigue failure nature of test-pieces is illustrated in Fig. 5.11.

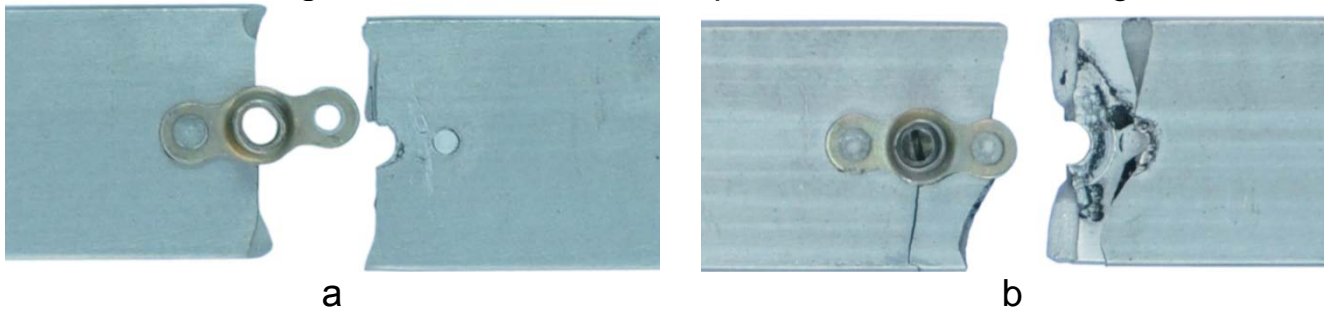


Fig. 5.11 – Fatigue Failure Nature of Test Pieces:

- a – strip-to-cylindrical hole and anchor nut joints;
- b – detachable bolted joint not loaded for shear processed in cylindrical hole area by reduction of transitional area and circular barrier reduction

Analysis of test-piece failure nature demonstrates that fatigue failure of strip-to-cylindrical hole and anchor nut joint of detachable bolted joint not loaded for shear processed in cylinder-conical hole area by reduction of transitional area and circular barrier reduction takes part in cylinder hole area. Fatigue failure of longitudinal detachable bolted joint not loaded for shear takes place in cylinder-conical hole area.

Test pieces of strip-to-cylindrical hole processed by burnishing hole walls and anchor nut as well as test-pieces of not-loaded for shear longitudinal detachable bolted joint with its structural elements being processed in cylinder-conical hole area by reduction of transitional and barrier circular reduction have not been subjected to failure under reaching  $N = 1\,000\,000$  loading cycles and their tests have been in progress under  $\sigma_{0\,gr\,max} = 150$  MPa to determine fatigue failure area.

It has been found in this case that fatigue endurance of detachable bolted joint models of airframe structural members processed in holes area by burnishing walls of cylinder-conical hole and combined local reduction of cylinder-conical hole transitional area barrier circular reduction upgrades at more than 8.1 times in compare with strip with cylindrical hole and at more than 16 times in compare with strip having cylinder-conical hole and as high as 9.7 times in compare with longitudinal detachable joint model not loaded for shear.

Fatigue test results for structural element test-pieces are shown in Fig. 5.12 in the graphic form: 1 – strips with cylindrical hole; 2 – strips with cyl-

inder-conical hole; 3 – strips with cylinder-conical hole processed in hole area by transitional area reduction of cylinder-conical hole; 4 – strips with cylinder-conical hole processed in hole area by circular barrier reduction; 5 – strips with cylinder hole processed in hole area by combined reduction of transitional area and circular barrier reduction; 6 – strips with cylindrical hole and riveted anchor nut; 7 – strips with cylindrical hole processed by burnishing hole walls with a relative interference of  $\delta = 4\%$  and riveted anchor nut; 8 – detachable bolted joint not loaded for shear; 9 – detachable bolted joint not loaded for shear (strips with cylindrical hole free of burnishing hole walls, strip with cylinder-conical hole processed by reduction of transitional area and circular barrier reduction); 10 – longitudinal detachable bolted joint not loaded for shear with structural elements processed in cylindrical hole area by burnishing hole walls in area of cylinder conical hole by reduction of transitional area and barrier circular reduction.

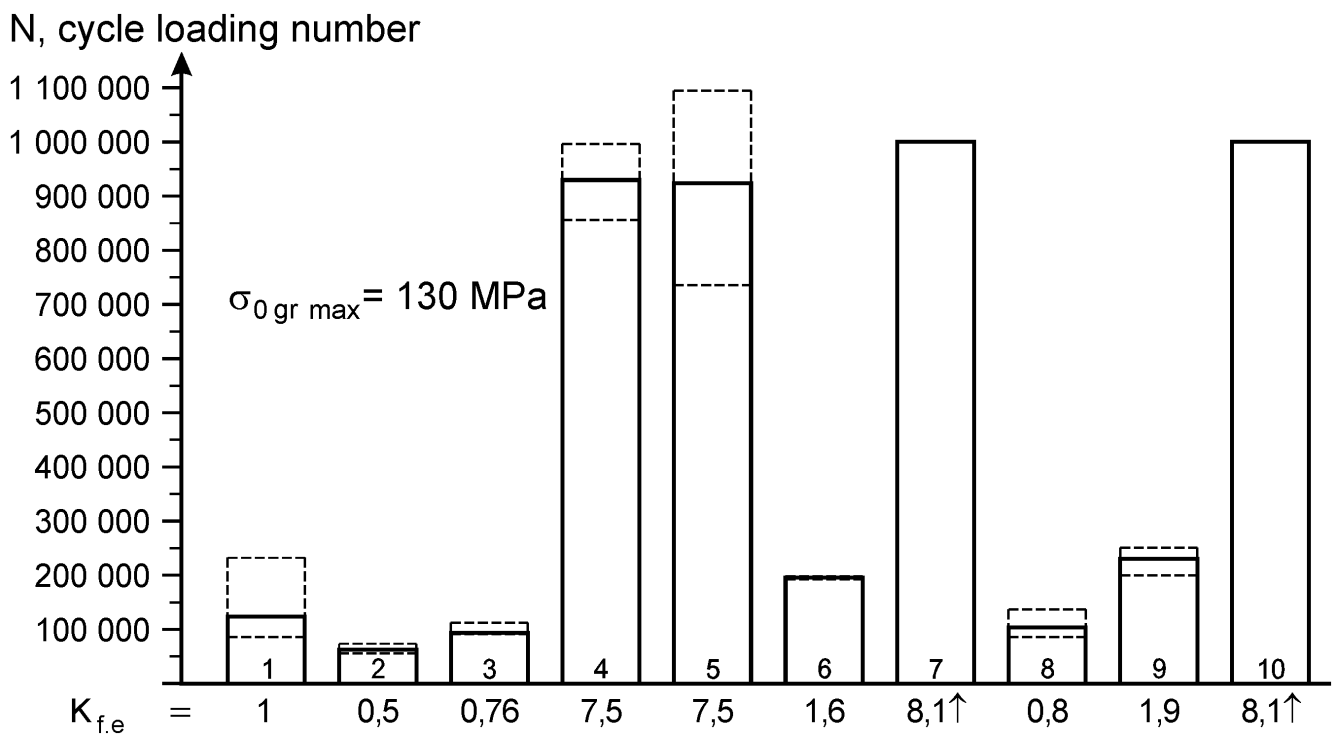


Fig. 5.12 – Structural Elements Processing Technique Effect Produced in Detachable Bolted Joints on Fatigue Endurance Characteristics of Test-Pieces at Operating Loading Level of  $\sigma_{0gr\ max} = 130\ MPa$

Test-pieces fatigue endurance upgrading factors area also presented graphically:

$$K_s = N_e / N_{stwh}$$

where  $N_e$  – fatigue endurance of structural and fabrication variants of samples;  $N_{stwh}$  – fatigue endurance of strip with cylindrical hole.

#### 5.4. STRUCTURAL-PROCESSING TECHNIQUE TO UPGRADE FATIGUE ENDURANCE OF DETACHABLE BOLTED JOINTS

Hole walls damage under anchor nuts setting is one of the reason resulting in fatigue endurance decrease at two times. Therefore, wing detachable panel assembly technique has been developed to avoid damage of hole walls by thread portion of temporary and permanent bolts.

Due to application of newly developed squeezing fixture for riveting to join self-locking nut to panel and to temporary bolt structure enabling to secure nut in permanent position within hole making for rivets and their riveting, it became possible to avoid hole walls damage. Interaction diagram of developed squeezing fixtures and temporary bolt is presented in Fig. 5.13.

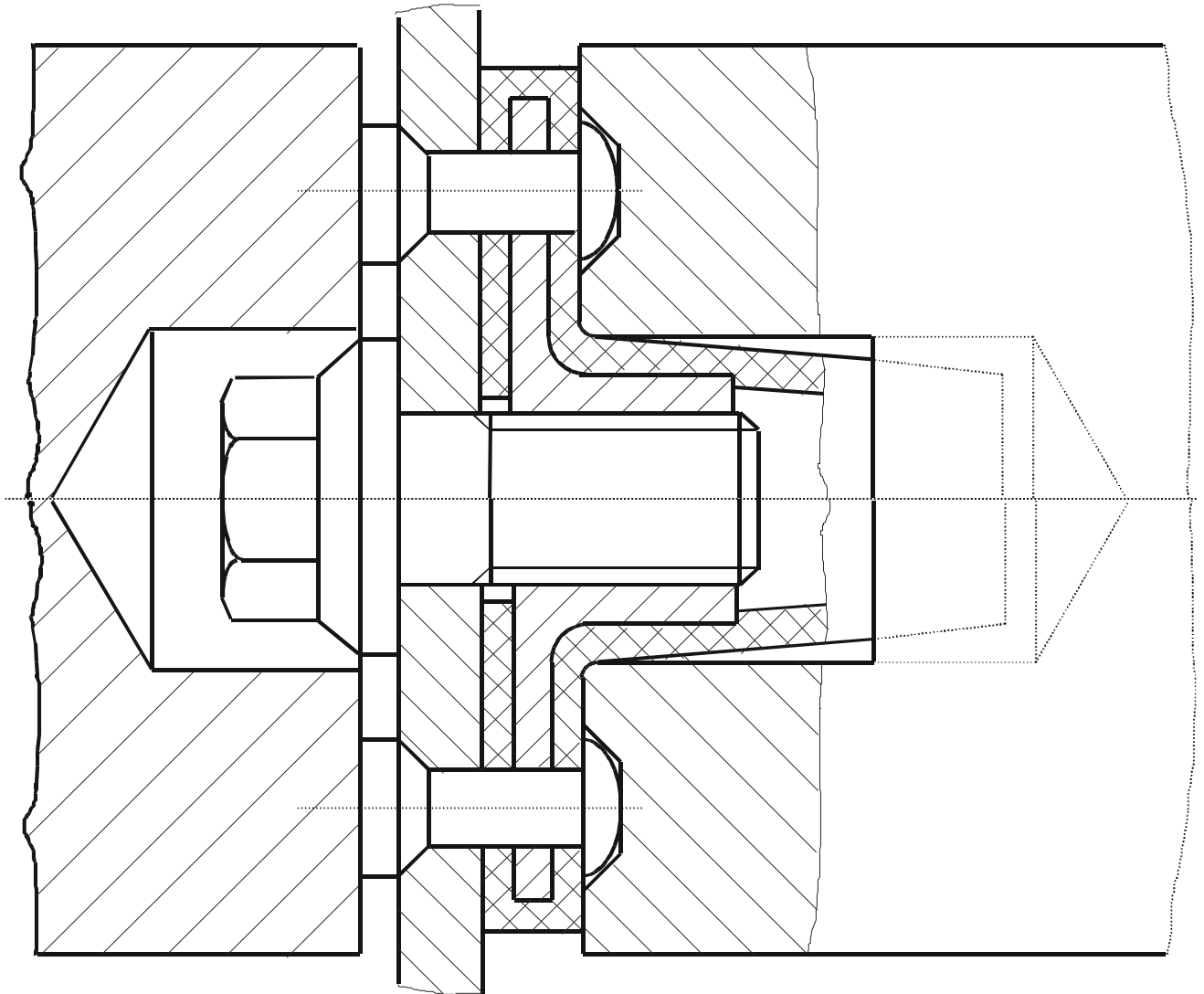


Fig. 5.13 – Interaction between Processing Squeezing Fixtures and Bolt under Riveting



Developed structural-processing technique to upgrade fatigue endurance of detachable bolted joints comprises:

- Making holes with insignificant tolerance;
- Burnishing cylindrical hole walls of detachable bolted joint elements;
- Setting self-locking nuts with guaranteed axial interference using specially developed temporary bolts;
- Making rivets holes for self-locking nuts and burrs removal;
- Making riveted joints to join self-locking nuts with structural members;
- Temporary bolts removal;
- Structural elements processing in cylindrical holes area by combined reduction of transitional area and circular barrier reduction;
- Attachment bolts setting and pack tightening check.

Fatigue tests of joint models loaded for shear at a loading level of  $\sigma_{0\ gr\ max} = 150$  MPa have been conducted to prove efficiency of structural-processing technique to improve fatigue endurance of detachable bolted joints.

In doing so, it has been stated that fatigue endurance of strong test-pieces models has been 30 000 loading cycles. Fatigue endurance has been 310 000 loading cycles for test-piece models loaded for shear longitudinal detachable bolted joint with their structural elements being processed in cylindrical hole area by burnishing hole walls with a relative interference of 4 % while in an area of cylinder-conical holes by reduction of transitional area (reduction depth – 0.3 mm). So, application of the developed structural-processing technique resulted in upgrading of fatigue endurance at more than 10 times.

As a result of application of the developed structural processing technique to improve fatigue endurance of the detachable bolted joints, the service life of such joints has been determined by dividing the number of cycles prior to failure ( $N$ ) obtained under laboratory conditions at an operational loading level into reliability factor determined in correspondence to Airworthiness Rules and Regulations:

$$T = N/\eta,$$

where  $\eta$  is a reliability factor with its minimal value be accepted equal to six under specifying service life according to the results of the test-pieces laboratory tests.

Then, joint lifetime under equivalent flight loading cycle corresponding to  $\sigma_{0\ gr\ max} = 130$  MPa:  $T = N/\eta = 10^6 / 6$  is equivalent to 165 000 flights.

Obtained value is 3 times higher than aircraft designed service life (50 thousand flights) proving that the target of this study has been met.

## 5.5. CONCLUSIONS

1. Fatigue endurance upgrading technique of joint elements by determining

of local SSS characteristics in strips with cylindrical and cylinder-conical holes for countersunk anchor with self-locking nuts has been scientifically proved based on analysis of structural-processing peculiarities of airframe structural members detachable bolted joints local SSS characteristics determination techniques and airframe structural members fatigue endurance in the area of detachable bolted joints. Strain specific energy value obtained with an account made for processing procedure of joined parts using elastic-plastic strain methods has been taken as a criteria to specify endurance.

2. Technique has been developed to analyze effect produced by combined local barrier reduction on local SSS characteristics of the strip with cylinder-conical hole. In this case it has been found that application of local and barrier reduction results in decrease of maximal specific strain energy value being equivalent to repeated stress cycle in area of probable fatigue failure to be 1.37 – 5.43 times in compare with its value for the strip with cylinder-conical hole.

3. Effect produced by strip processing technique in the area of cylinder-conical holes on fatigue endurance characteristics has been studied. It has been found that fatigue endurance of the strip with cylinder-conical hole processed in hole area by combined reduction of cylinder-conical hole transitional area and by circular barrier reduction is at 7.5 times higher than fatigue endurance of the strip with cylindrical hole and 14.9 times higher than endurance of the strip with cylinder-conical hole at an operational level of cyclic loading ( $\sigma_{0\text{ gr max}} = 130$  MPa).

4. Application of the developed technique to upgrade fatigue endurance by combined reduction of cylinder-conical hole transitional area and by circular barrier reduction results in fatigue endurance upgrading non-loaded for shear detachable bolted joint at more than 9.7 times under operational loading level ( $\sigma_{0\text{ gr max}} = 130$  MPa).

5. Structural-processing technique has been developed to upgrade fatigue endurance of airframe structural members detachable bolted joints by combined reduction of transitional area and by burnishing wall of cylindrical holes as well as by local and barrier reduction of structural members in area of cylinder-conical holes.

6. Application of the developed technique to upgrade fatigue endurance results in achieving specified service life of aircraft structural members in area of detachable bolted joints.

7. Study results have been implemented into practice at “Antonov” State Company, Kharkov’s State Aircraft Manufacturing Company and in a training course at the National Aerospace University by N. E. Zhukovsky (“KhAI”).

## Chapter 6

## STRUCTURAL-PROCESSING TECHNIQUE TO PROVIDE AIRFRAME SERVICE LIFE IN FUNCTIONAL HOLES AREA

### 6.1. SCIENTIFIC BACKGROUNDS OF STRUCTURAL-PROCESSING TECHNIQUES TO PROVIDE AIRFRAME FATIGUE ENDURANCE IN FUNCTIONAL HOLES AREA

Fatigue endurance of structural members ( $N$ ) with free holes under operational loads is determined by specific strain energy value ( $W = \sigma_{0eq} \cdot \varepsilon_{0eq}$ ) in the local area of its concentration. Fatigue endurance change is predicted according to change of local SSS characteristics in area of probable fatigue failure ( $N = C/W^m$ ).

It is quite clear that elastic component value decrease of specific strain energy in area of probable fatigue failure is required to upgrade fatigue endurance and service life of structural members in functional holes area (Fig. 6.1).

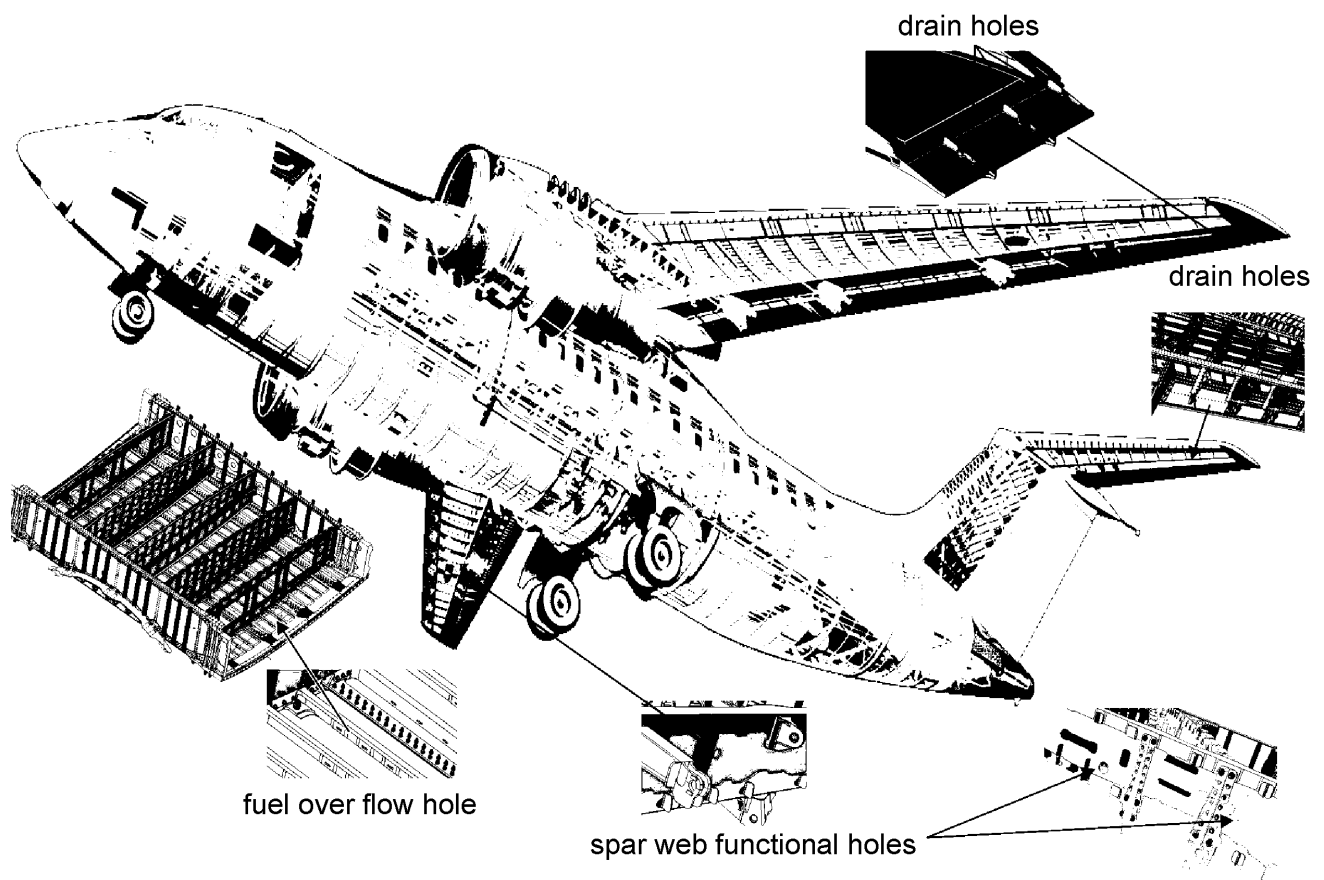


Fig. 6.1 – Airframe Structural Members with Functional Holes

Specific strain energy decreasing factor  $k_{W_{0eq}} = W_{0eq_i} / W_{0eq_b}$  (where

$W_{0eq_i}$  – specific strain energy value in functional holes area processed by local elastic strain techniques;  $W_{0eq_b}$  – specific strain energy value of basic test piece (strip with free holes) specifies endurance change level of structural members with functional holes.

A method (Fig. 6.2) has been developed to analyze effect produced by thickening, rolling, burnishing, reduction on local SSS characteristics of airframe structural members in functional holes area with an account made for structural and processing parameters.

Effect has been studied produced by one-side thickening value (*thk* parameter) variable within the range between 1 and 3.5 mm  $[(0.2...0.7) \delta_s]$  and two-side thickening value variable within the range between 0.5 and 1.75 mm  $[(0.2...0.7) \delta_{st}]$  in hole area on local SSS characteristics of a strip with  $\delta_{st} = 5$  mm thickness,  $B = 48$  mm width, 150 mm length with a hole of 8 mm diameter under extension. Extending stresses value in gross section is taken equal to 0, 50, 100, 130, 150 and 200 MPa.

Geometrical parameters of strips with holes accepted for analysis are shown in Fig. 6.3. Strips estimated diagrams are presented in Fig. 6.4 while finite elements models are shown in Fig. 6.5.

Strip material is 1163T aluminium alloy. Material behavior model is polylinear elastic-plastic with kinematic strengthening.

Fig. 6.6 demonstrates test results of the effect produced by loading level and one-side thickening value while Fig. 6.7 shows level value and two-side thickening in hole area on specific strain energy value being equivalent to repeated stress cycle.

As a result of studies performed is has been found that one-side strip thickening in hole area does not result in significant change (as high as 3 %) of maximal main extending stresses being equivalent to repeated stress cycle in section along the hole axis. Application of two-side thickening in hole area at 1.2–1.7 times results in decrease of maximal main extending stresses equivalent to repeated stress cycle at 1.1–1.7 times in compare with stress in strip with hole free of strengthening. In this case, maximal main extending strain value and maximal specific strain energy of the equivalent repeated stress cycle are decreased at 1.02 – 1.67 and 1.2 – 2.8 times respectively.

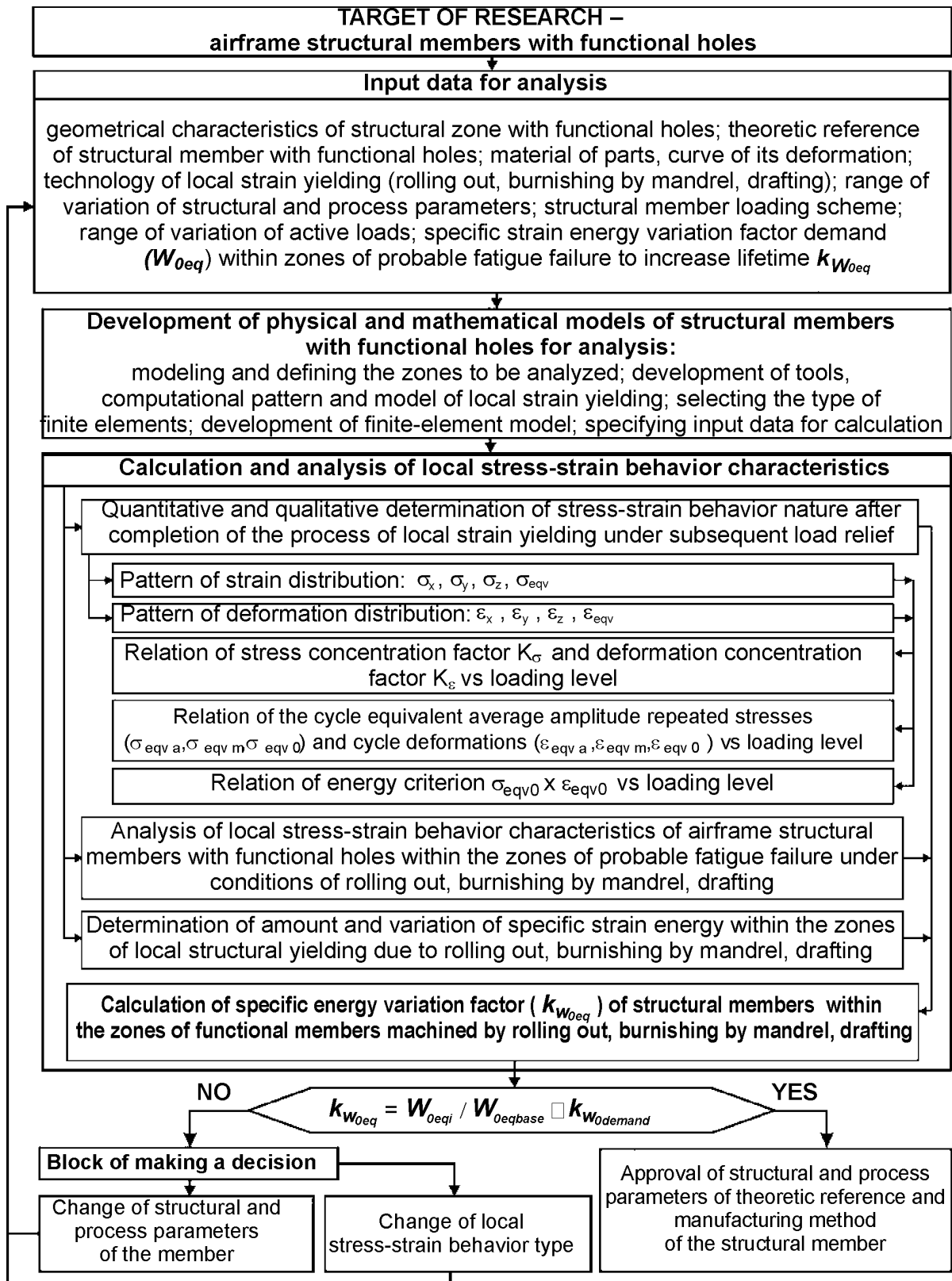


Fig. 6.2 – Method for Analyzing Effect Produced by Structural Processing Parameters in Local SSS Characteristics of Airframe Structural Members with Functional Holes

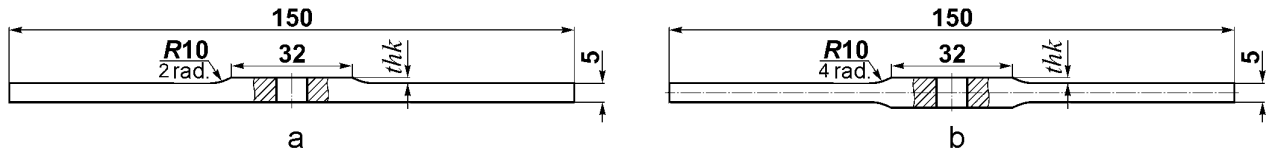


Fig. 6.3 – Geometrical Dimension of Strip with Hole:  
a – one-side thickening; b – two-side thickening

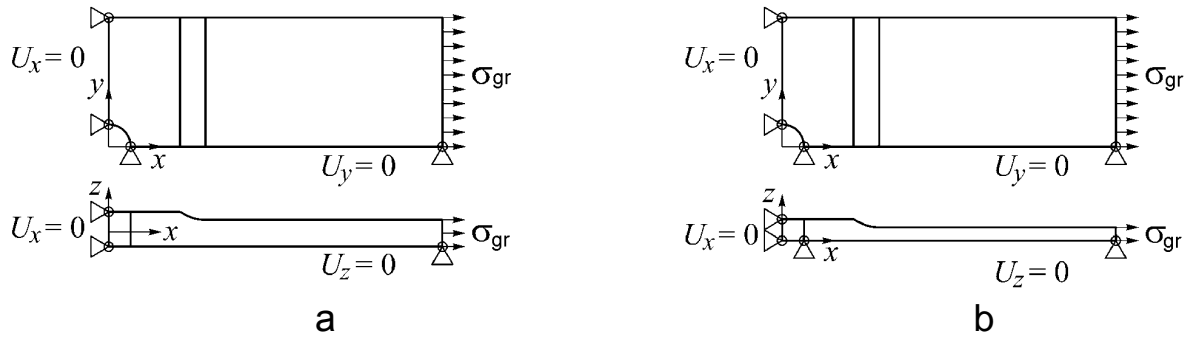


Fig. 6.4 – Estimation Diagram:  
a – 1/4 of strip with hole and one-side thickening;  
b – 1/8 of strip with hole and two-side thickening

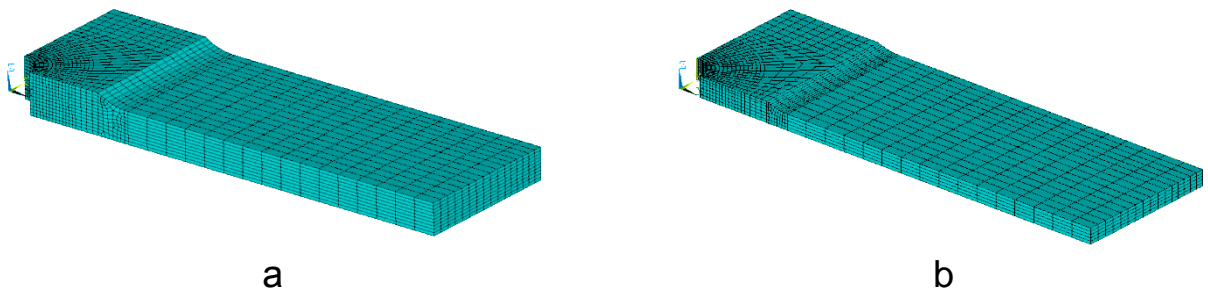


Fig. 6.5 – Finite Element Model:  
a – 1/4 of strip with hole and one-side thickening;  
b – 1/8 of strip with hole and two-side thickening

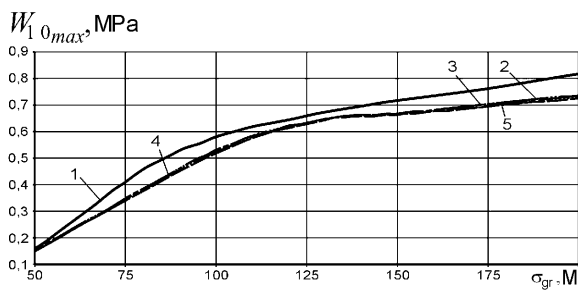


Fig. 6.6 – Effect Produced by Loading Level and One-Side Thickening Value on  $W_{10max}$  change of equivalent repeated stress cycle in strip with hole:  
1 – free of thickening;  
2 – 1.0 mm thickening; 3 – 1.5 mm;  
4 – 2.5 mm; 5 – 3.5 mm

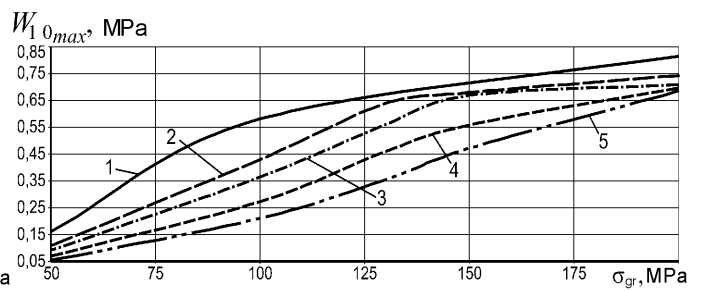


Fig. 6.7 – Effect Produced by Loading Level and Two-Side Thickening Value on  $W_{10max}$  change of equivalent repeated stress cycle in strip with hole: 1 – strip with hole;  
2 – 0.5 mm thickening; 3 – 0.7 mm thickening; 4 – 1.25 mm thickening;  
5 – 1.75 mm thickening

Effect has been studied produced by relative radial interference under burnishing  $\Delta = (d_{ins} - d_h)/d_h$ , of barrier reduction and loading level under extension on local SSS characteristics of strip with hole.

Geometrical burnishing tool dimension are shown in Fig. 6.8; clamping tools for stamping segment craters are presented in Fig. 6.9.

During analysis the following values of relative radial interference under burnishing have been studied: 0; 0.5; 1.0; 1.5; 2.0; 2.5 and 3.0 %. Reduction depth has been taken equal to 0.3 mm.

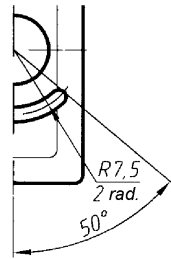


Fig. 6.9 – Crimping Tool Drawing Part for Stamping Segment Craters

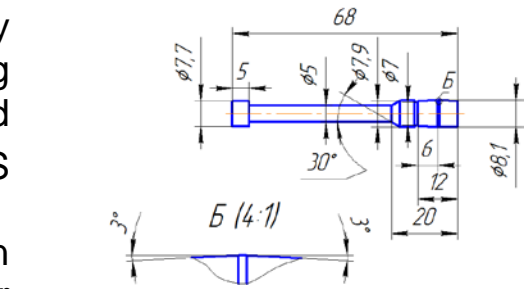
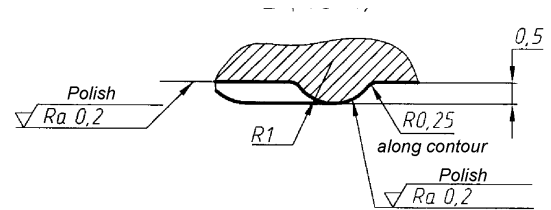


Fig. 6.8 – Geometric Burnishing Tool Characteristics



Extension stress values in gross section have been discretely taken equal to 0, 50, 100, 130, 150 and 200 MPa.

The analysis has demonstrated that material displacement is observed under burnishing in contacting area between burnishing tool and hole wall in axial direction. As a result material beading is formed on strip free surfaces. It is just clearly seen under high values of relative radial interference (Fig. 6.10).

Contact interaction problem between a strip with hole and crimping tool has been solved. As a result a distribution nature has been obtained between axial displacement equivalent stresses according to Moses (Fig. 6.11) in hole area

As a result of conducted tests it has been found that strips with holes within the range of stress values in gross section from 100 to 200 MPa at burnishing holes with relative radial interference from 1 to 3 % result in decrease of maximal main extending stresses of equivalent repeated stress cycle at 1.1 – 2.2 times if compared with stress in strip with hole.

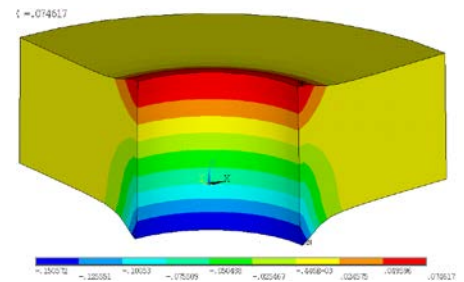


Fig. 6.10 – Axial Displacement Distribution Nature ( $U_z$ , mm) after Burnishing (interference – 3 %)

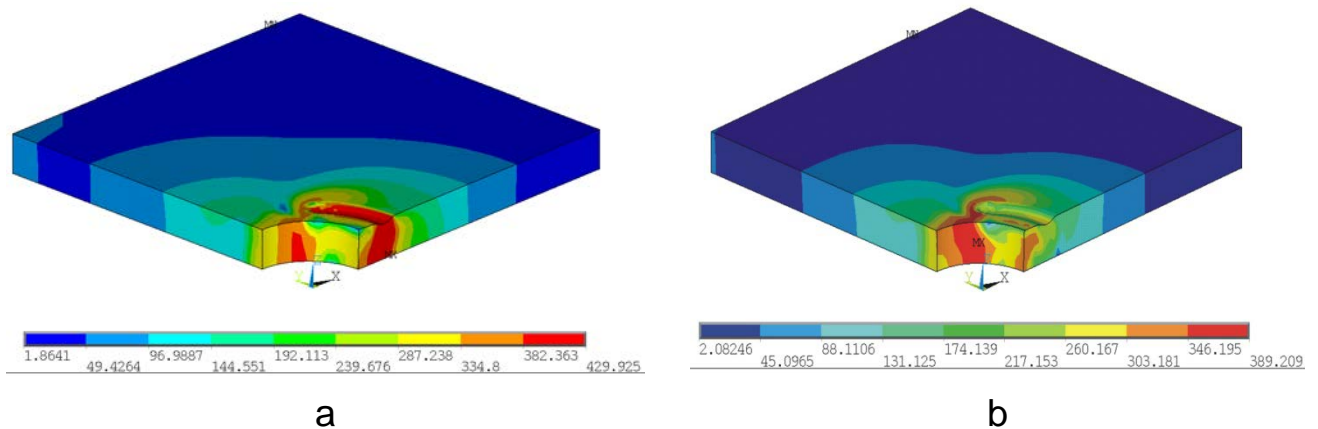


Fig. 6.11 – Equivalent Stresses Distribution Nature according to Moses ( $\sigma_{eq}$ , MPa) in Strip at Hole Area:  
 a – after reduction at depth of 0.3 mm;  
 b – after removal of crimping tool

In doing so, maximal main extending strain values and maximal specific strain energy of equivalent repeated stress cycle become less at 1.2 – 2 and 1.4 – 4.5 times, respectively. Application of barrier reduction by segment creators stamping at a depth of 0.3 mm results in decreasing maximal main extending strains of equivalent repeated stress cycle at 1.5 – 2.22 times in section along hole axis and at 1.4 – 1.7 times in reduction area with reference to stresses for strip with hole.

In aircraft airframe structure spar, frame and rib webs are loaded by shear. Holes of different diameters and functional purpose are made therein with stress and strain concentration being originated in this area.

Effect has been studied produced by the hole diameter and two-side reduction depth on local SSS characteristics of the strip with hole under displacement condition. It has been found that strip with hole under loading for shear within the range of stress values in gross section lies from 50 to 200 MPa. Application of circular reduction at a depth of 0.3 mm results in decrease maximal main extending stresses of repeated stress cycle at 1.03 – 2.22 times. In this case, values of maximal main extending stresses and maximal specific strain energy of repeated stress cycle are decreased at 1.03 – 1.8 and 1.05 – 3.9 times respectively. Experimental studies have been performed to determine fatigue endurance characteristics of basic test-pieces from 1163T material: strip with hole ( $B/d = 6$ ) and strip with three holes (distance between hole centers  $l = 12$  mm). Analytical dependencies for endurance prediction have been developed with reference to the results of the strips fatigue tests (Fig. 6.12):



- Strip with single hole:

$$\sigma^{4.88317} N = 2.26879 \cdot 10^{15}$$

$$\text{or } \sigma = 1.39521 \cdot 10^3 N^{-0.204785};$$

- Strip with three holes:

$$\sigma^{5.35564} N = 3.77761 \cdot 10^{16}$$

$$\text{or } \sigma = 1.24532 \cdot 10^3 N^{-0.186719}.$$

Methods have been developed in the second section to analyze effect produced by local plastic strain in functional holes area of airframe structural member on local SSS characteristics and experiment studies performance are scientific concepts for structural-processing techniques to provide airframe service life in area of functional holes.

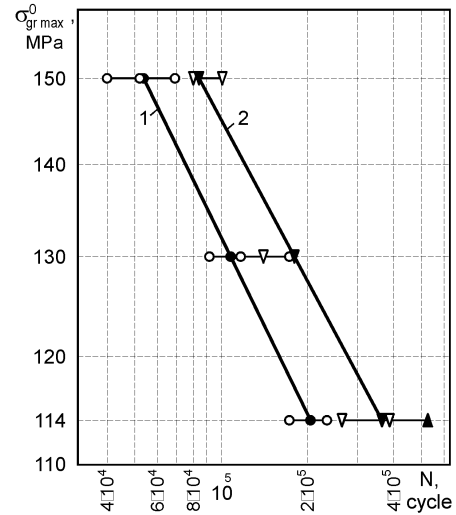


Fig. 6.12 – Fatigue Curves;  
1 – strip with hole;  
2 – strip with three holes

## 6.2. STUDIES TO DETERMINE EFFECT PRODUCED BY LOCAL PLASTIC STRAIN METHODS ON AIRFRAME STRUCTURAL MEMBERS SSS CHARACTERISTICS IN AREA OF FUNCTIONAL HOLES

Three dimensional geometric models of strip test-pieces and production tools (Ref. to Fig. 6.13 through 6.14) for processing strip in area of holes have been created using Siemens NX system.

Strip material steel D16chT. Burnishing tool material – steel HVG GOST 5950-73, crimping tool material – steel Y48A GOST 1345-90. Operating load values under studies at  $\sigma_{gr} = 0; 100; 130; 150$  MPa.

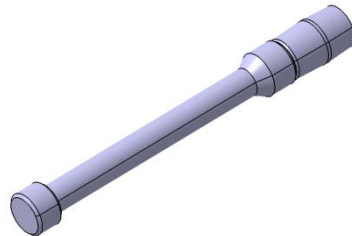
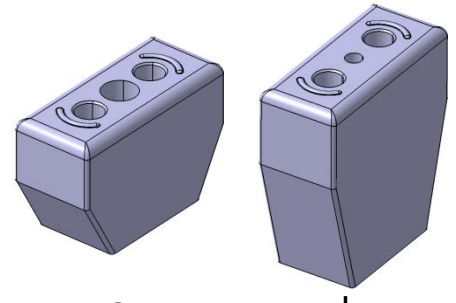


Fig. 6.13 – Three-dimensional burnishing tool model



a  
b  
Fig. 6.14 – Three-dimensional models:  
a – upper crimping tool;  
b – lower crimping tool

Studies results of effect produced by strip processing technique holes area on variations of maximal specific strain energy of repeated stress cycle at a loading level of  $\sigma_{0gr} = 130$  MPa are shown in Fig. 6.15. The following version of strip are digitally specified: 1 – with  $\varnothing 8$  mm hole, chamfers  $0.5 \times 45^\circ$ ; 2 – with three holes of  $\varnothing 8$  mm, distance between centers of holes  $l = 12$  mm; chamfers  $0.5 \times 45^\circ$ ; 3 – three holes of  $\varnothing 8$  mm,  $l = 12$  mm, chamfers  $0.5 \times 45^\circ$ , formed by using extension technique with radial interference of 0.2 %; 4 – with three holes of  $\varnothing 8$  mm,  $l = 12$  mm, chamfers  $0.5 \times 45^\circ$  formed by using rolling technique with a radial interference of 0.6 %; 5 – with three holes of

Ø7.9 mm,  $l = 12$  mm, chamfers  $0.5 \times 45^\circ$  formed by the use of burnishing technique with a radial interference of 2%; 6 – with three holes of Ø8 mm,  $l = 12$  mm, chamfers  $0.5 \times 45^\circ$  formed by use of stamping technique to produce segment craters with a reduction depth of 0.3 mm, angle of segment craters equal to  $60^\circ$  in reduction area; 7 – with three holes of Ø8 mm,  $l = 12$  mm, chamfers  $0.5 \times 45^\circ$  formed by stamping segment craters with a reduction depth of 0.3 mm and craters angle equal to  $50^\circ$  in reduction area; 8 – with three holes of Ø8 mm,  $l = 12$  mm, chamfers  $0.5 \times 45^\circ$  formed by stamping segment craters with a reduction depth of 0.3 mm, craters angle equal to  $60^\circ$  in area along utmost hole axis; 9 – with three holes of Ø8 mm,  $l = 12$  mm, chamfers  $0.5 \times 45^\circ$  formed by stamping segment craters with a reduction depth of 0.3 mm, craters angle of  $50^\circ$  in area along utmost hole axis.

As a result of studying SSS of strip with hole it has been found that application of specified processing methods and techniques results in decrease of maximal specific strain energy at 1.03 – 3.9 times in compare with a strip having single hole and at 1.03 – 4.75 times in comparison with a strip having holes system.

Effect has been studied produced by thickness values, holes shapes, arrangement of holes relatively to each other, rolling, burnishing and barrier reduction of airframe structural members in area of functional holes on local SSS characteristics.

The following versions have been studied under analyzing effect produced by processing techniques and parameters in area of stringer functional holes:

1) Stringer with three holes of Ø8 mm ( $l = 40$  mm, chamfers  $0.8 \times 45^\circ$ ) for fuel flow made on upright strip (Fig. 6.16);

2) Stringer with three holes of Ø8 mm ( $l = 40$  mm, chamfers  $0.8 \times 45^\circ$ ) for fuel flow made on upright strip processed in holes area:

– By burnishing holes walls with a relative radial interference of  $\Delta = 1; 2; 3\%$ ;

– By burnishing with the use of processing sleeve Relative radial interference under burnishing (burnishing tool-sleeve)  $\Delta = 2; 3\%$ ;

– By extending holes with a relative radial interference  $\Delta = 0,4; 0,6\%$ ;

– By stamping concentric platform around hole edge (stamping diameter 12 mm stamping depth  $h = 0.2; 0.3; 0.4; 0.5$  mm);

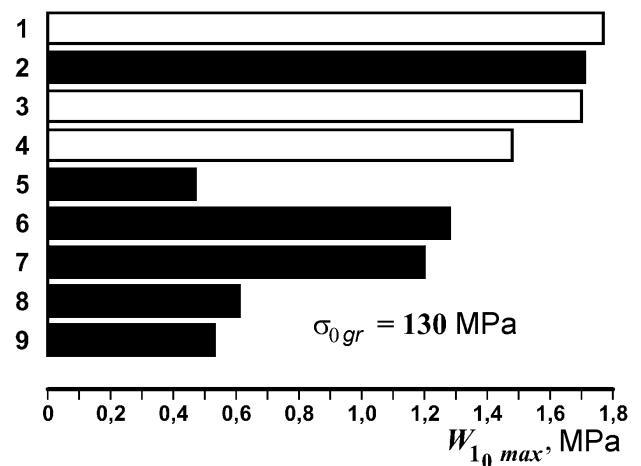


Fig. 6.15– Effect Produced by Strip Processing Techniques in Holes Area on Variations of Maximal Specific Strain Energy of Repeated Stress Cycle

3) Stringer with three holes of  $\varnothing 7.5$ ; 9; 7.5 mm (chamfer  $0.5 \times 45^\circ$ ) processed in area of holes by stamping segment craters (stamping depth  $h = 0.2$ ; 0.3; 0.4; 0.5 mm) (Fig. 6.17);

4) Stringer with hole having an oval shape (chamfer  $0.5 \times 45^\circ$ ) processed in hole area by stamping segment craters (stamping depth  $h = 0.2$ ; 0.3; 0.4; 0.5 mm) (Fig. 6.18);

5) Stringer with three holes  $\varnothing 8$  mm ( $l = 12$  mm, chamfers  $0.5 \times 45^\circ$ ) (Fig. 6.19):

6) Stringer with three holes  $\varnothing 8$  mm ( $l = 12$  mm, chamfers  $0.8 \times 45^\circ$ ) processed in holes area (Fig. 6.19):

- By burnishing holes with relative radial interference of 3 %;
- By rolling hole walls with a radial relative interference of 0.6 %;

7) Stringer with three holes of  $\varnothing 8$  mm ( $l = 12$  mm, chamfers  $0.5 \times 45^\circ$ ) processed by stamping segment craters (stamping depth  $h = 0.2$ ; 0.3; 0.4; 0.5 mm) (Fig. 6.20);

Stringer with three holes of  $\varnothing 8$  mm (chamfers  $0.8 \times 45^\circ$ ) and 4 mm spacing between holes processed by cylindrical reduction at a depth of 0.2 mm (Fig. 6.19).

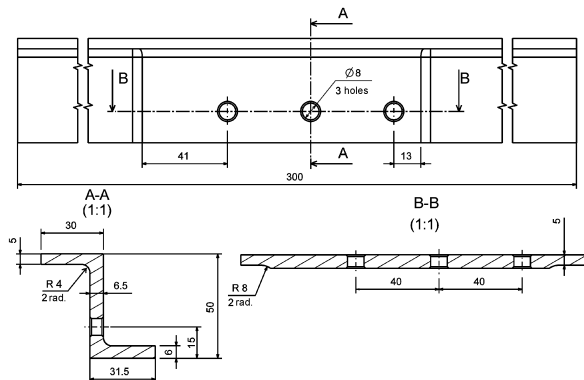


Fig. 6.16 – Stringer with Holes Test-pieces

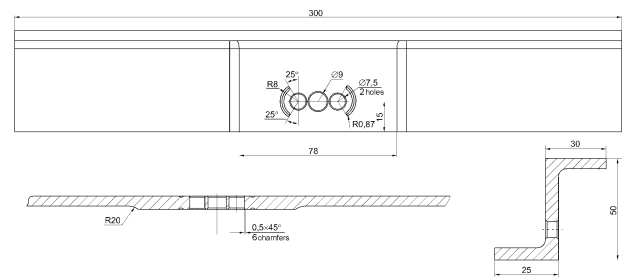


Fig.6.17 – Stringer with Three Holes of  $\varnothing 7.5$ – $9$ – $7.5$  mm Processed by Stamping Segment Shape Craters Test-Piece

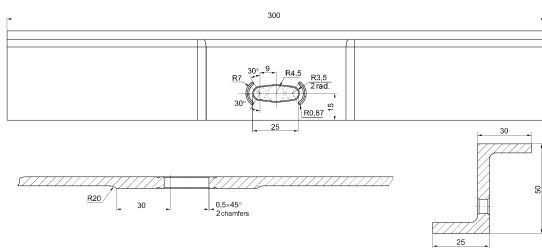


Fig. 6.18 – Stringer with Holes Giving Oval Shape Processed by Stamping Craters of Segment Shape Test-Piece

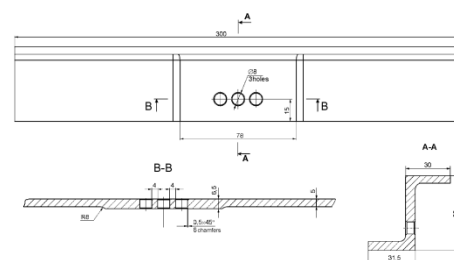


Fig. 6.19 – Stringer with Three Holes of  $\varnothing 8$  mm (Distance Between Center of Holes – 12 mm) Test-piece

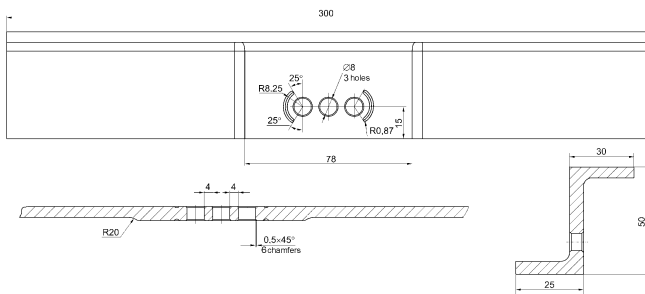


Fig. 6.20 – Stringer with Three Holes of  $\varnothing 8$  mm (distance between center of holes – 12 mm), Processed in Holes Area by Stamping Craters of Segment Shape Test-Piece

Stringer material is 1163T aluminium alloy.

A number of parameters values have been obtained as a result of study to specify stringer SSS in area of functional holes.

Under analysis of stringer SSS it has been found that application of the specified structural and processing techniques results in decrease of maximal specific strain energy of equivalent repeated stress cycle at 1.1 – 3.9 times in compare with basic version ( $k_{W_{0eq}} = 0.9...0.26$ ).

As a result of studying structural and processing parameters of strip and stringers with a number of functional holes it has been found as following:

- Relative interference under burnishing hole walls shall be 2...3 %;
- Relative interference under rolling the holes produces insignificant effect on variation of specific strain energy and may be 0.2...0.6 %;
- Barrier reduction depth with the range of values under study produces insignificant effect on variation of specific strain energy and under processing can be 0.2...0.6 mm.

As a result of studies performed the following version has been taken as the basic one for making holes: three holes with a diameter of 8 mm under holes spacing of 12 mm and production techniques for processing structural members in holes area:

- Holes rolling with a relative interference of 0.2...0.6 %;
- Burnishing holes walls with a relative radial interference of 2 and 3 %;
- Barrier reduction by stamping segment craters with a reduction depth of 0.3 mm.

### 6.3. EXPERIMENTAL STUDIES TO DETERMINE EFFECT PRODUCED BY METHODS OF PROCESSING AIRFRAME STRUCTURAL MEMBERS IN AREA OF FUNCTIONAL HOLES ON STATIC STRENGTH AND FATIGUE ENDURANCE

Experimental studies have been performed using facilities for conduction of fatigue and static tests МУП-50, electromechanical unit YMM-02 and hydraulic unit for fatigue and static tests ЦДМ-10ПУ.

Test-pieces have been tested at an experimental loading level/ the following versions of processing have been investigated:

- Rolling of holes at a relative radial interference of 0.2 and 0.6 %;
- Burnishing holes at a relative radial interference of 2 and 3 %;

- Burnishing holes at a relative radial interference of 2 % followed by chamfer reduction;
- Strip processing in holes area by barrier reduction with stamping segment craters;
- Strip processing in holes area by barrier reduction with stamping segment craters and chamfer reduction;
- Chamfer reduction.
- Chamfer squeezing.



Fig. 6.21 – Fatigue Failure Nature of Strips with Three Holes

Fig. 6.21 demonstrates fatigue nature of strips with three holes processed in holes area by barrier reduction using stamping technique of segment craters and chamfer reduction made from pressed section (material D16T).

Analysis of fatigue test results as for strips with three functional holes processed in holes area enables to represent an analytical expressions for the fatigue curves in the way as follows:

- under processing holes walls by rolling at a relative radial interference of  $\Delta = 0.2\%$ :

$$\sigma^{3.69299} N = 2.07643 \cdot 10^{13} \text{ or } \sigma = 4.03744 \cdot 10^3 N^{-0.270783};$$

- under processing holes walls by rolling at  $\Delta = 0.6\%$ :

$$\sigma^{4.47043} N = 9.24922 \cdot 10^{14} \text{ or } \sigma = 2.22742 \cdot 10^3 N^{-0.223692};$$

- under processing holes walls by burnishing at  $\Delta = 2\%$ :

$$\sigma^{6.11416} N = 3.18877 \cdot 10^{18} \text{ or } \sigma = 1.06257 \cdot 10^3 N^{-0.163555};$$

- under processing holes walls by burnishing at  $\Delta = 3\%$ :

$$\sigma^{5.42147} N = 1.54531 \cdot 10^{17} \text{ or } \sigma = 1.48096 \cdot 10^3 N^{-0.184452};$$

- under processing strips in holes area by barrier reduction stamping segment craters:

$$\sigma^{5.14986} N = 5.39036 \cdot 10^{16} \text{ or } \sigma = 1.77396 \cdot 10^3 N^{-0.19418},$$

Where  $\sigma = \sigma_{0 \text{ gr max}}$ , MPa.

Fatigue curves graphs for strip with hole (Fig. 6.12) have been plotted according to data of analytical dependencies.

Fig. 6.22 digitally specifies the fatigue curves of the strip ( $B/d = 6$ ): 1 – with single hole of  $\varnothing 8$  mm from D16T; 2 – ▽ with three holes of  $\varnothing 8$  mm (distance between centers of holes  $l = 12$  mm); 3 – with three holes of  $\varnothing 8$  mm ( $l = 12$  mm) processed in holes area by rolling with a relative interference of  $\Delta = 0.2\%$ ; 4 – ◇ with three holes of  $\varnothing 8$  mm ( $l = 12$  mm) processed in holes area by rolling  $\Delta = 0.6\%$ ; 5 – ● with single hole from D16T material tested in TsA61; 6 – ◆ with three holes of  $\varnothing 8$  mm ( $l = 12$  mm) processed in holes area by burnishing with a relative interference of  $\Delta = 2\%$ ; 7 – ☆ with three holes of  $\varnothing 8$  mm ( $l = 12$  mm) processed in holes area by burnishing with a relative interference of

$\Delta = 3\%$ ; 8 – \* with three holes of  $\varnothing 8$  mm ( $l = 12$  mm) processed in holes area by burnishing with a relative interference ( $\Delta = 2\%$ ) and holes chamfer reduction; 9 – □ with three holes of  $\varnothing 8$  mm ( $l = 12$  mm) processed in holes area by chamfers reduction; 10 – ◻ with three holes  $\varnothing 8$  mm ( $l = 12$  mm) processed in holes area by chamfers rolling and reduction; 11 – ◁ with three holes of  $\varnothing 8$  mm ( $l = 12$  mm) processed in holes area by barrier reduction in the form of segment craters shape free of chamfers reduction; 12 – ▷ with three holes of  $\varnothing 8$  mm ( $l = 12$  mm) processed in holes area by barrier reduction in the form of segment craters shape and chamfers reduction; ☆→ – test-piece failure from fretting corrosion at clamps.

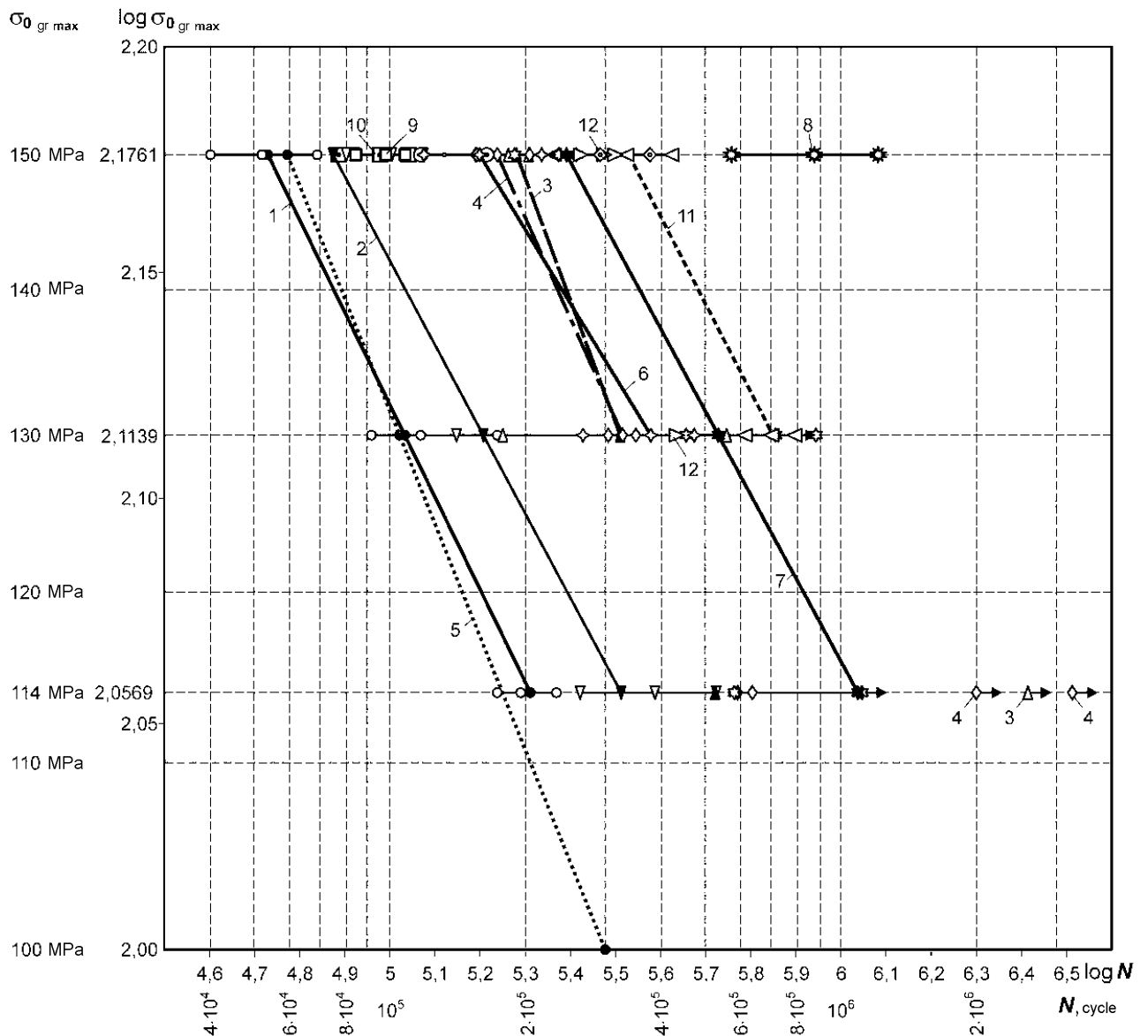


Fig. 6.22 – Strip Endurance Curves

Experimental studies have been performed to specify an effect produced by processing techniques on fatigue endurance of stringer structural test-pieces (Fig. 6.23).

After making holes and stringer processing in area of functional holes by rolling with a relative radial interference of  $\Delta = 0.3\%$ , by burnishing hole walls

( $\Delta = 3\%$ ), by barrier reduction stamping segment craters they were subjected to shot-blasting of stringer walls (both sides) in holes area. After shot-blasting the test-pieces have been coated by АН.Окс.Нхр. in compliance with series production procedure at aircraft manufacturing factory.

It has been found that under processing structural stringer-like test-pieces in holes area by barrier reduction stamping segment craters, stringer endurance in area of holes for dual flowing at a loading level of  $\sigma_{gr\ min} = -30\text{ MPa}$ ,  $\sigma_{gr\ max} = 100\text{ MPa}$  exceeds  $10^6$  loading cycles and provides achievement of design life time.

Areas and fatigue failure nature of studied test-pieces at a loading level of  $\sigma_{gr\ min} = -30\text{ MPa}$ ,  $\sigma_{gr\ max} = 100\text{ MPa}$  are shown in Fig. 6.24.

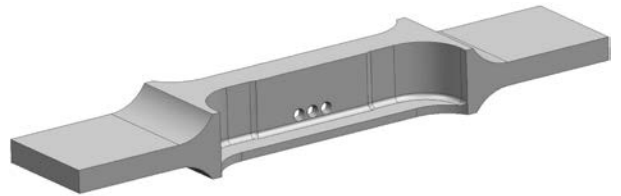


Fig. 6.23 – Three dimensional Model. Stringer Like Structural Test Piece with a Number of Holes



Fig. 6.24 – Structural Stringer-Like Test-Pieces with Functional Holes. Fatigue Failure Area and Nature

Stringers are alphabetically specified in Fig. 6.24: a – processed in holes by burnishing holes walls with relative interference of  $3\%$ ; b – processed in holes area by barrier reduction in the form of segment shape craters.

#### 6.4. CONCLUSIONS

1. Structural-processing methods have been scientifically proved to provide airframe fatigue endurance in area of functional holes by analyzing local SSS characteristics in probable fatigue failure area. Technique has been developed to analyze an effect produced by local thickening rolling, burnishing barrier reduction on local SSS characteristics of airframe structural members with func-

tional holes and an account made for loading history. It has been found that application of the developed techniques results in decreasing specific strain energy in an area of single functional hole at 1.03–4.5 times under operating loading levels.

2. Experimental studies of fatigue endurance of basic test-pieces of strip with hole and holes system have shown that fatigue endurance of strip with three holes is higher than fatigue endurance of strip with single hole at 1.6–2 times as for equivalent loading level.

3. Effect has been studied produced by extension burnishing and barrier reduction of strips with hole and system of holes on local SSS characteristics showing that application of the specified processing techniques results in decrease of maximal specific strain energy at 1.03 – 3.9 times in compare with  $W_{0eq}$  strip having single hole and at 1.03 – 4.75 times if compared with  $W_{0eq}$  strip having a system of holes.

4. Conducted studies of the effect produced by holes thickening, shape and arrangement, extension, burnishing and barrier reduction of airframe structural members in area of functional holes on local SSS characteristics have demonstrated that application of the specified methods and techniques results in decrease of maximal specific strain energy of the equivalent repeated stress cycle at 1.1-3.9 times in compare with the basic versions.

5. Conducted experimental studies if the effect produced by techniques for processing airframe structural members in the area of functional holes on fatigue endurance have shown that rolling with a relative radial interference between 0.2 % and 0.6 % at an experimental loading level makes fatigue endurance higher at 1.3–4 %; holes walls burnishing with relative radial interference 2...3 % at 3.4–6.3 times; barrier reduction at a depth of 0.2...0.3 mm by stamping segment craters at 4.3–5.7 times that make it possible to provide specified life time characteristics of airframe in the area of functional holes.

6. Procedure and techniques have been developed to provide processing of airframe structural members in the area of functional holes by rolling, burnishing and barrier reduction.

7. Based on data estimation procedure of technical and economical efficiency of processing techniques to provide airframe structural members life time made from aluminium alloys in area of functional holes it is recommended to arrange techniques in the following order:

- 1) burnishing with a relative radial interference of 2 to 3 %;
- 2) barrier reduction by stamping segment craters with a depth from 0.2 to 0.4 mm;
- 3) rolling with a relative radial interference from 0.25 to 0.6 %.

8. Results of these studies have been implemented into practice at "Antonov" Co., KhSAMC, and National Aerospace University (KhAI) named after N. E. Zhukovsky.



*Chapter 7***ANALYSIS IN SPECIFYING SERVICE LIFE PECULIARITIES FOR  
TRANSPORT CATEGORY AIRCRAFT**

---

Requirements for specifying aircraft life time with reference to structure strength conditions under long-term operation are specified by Airworthiness Rules and Regulations (NLGS-3 [20]), Aviation Rules AR-25 [2] and approved in 1996 as a Supplement to Airworthiness Regulation (AR-25.571) [21].

Structure safety with reference to fatigue strength condition should be proved at the following phases of aircraft operation:

- Prior to regular operation under stating initial specified service life;
- Within operation following usage of prior specified life time; in this case, subsequent (phase by phase) clarification of specified life time increased values (including time required for disposal) based on obtaining true data as for structure loading conditions and its fatigue strength characteristics as well as on analysis and accounting effect produced by operating conditions and accumulation of operation experience.

Assigned service life is summerized operating hours and when achieved, operation must be terminated irrespective of aircraft state. Continuous aircraft operation is provided by timely extension of the newly specified life time. Aircraft structure specified life time is expressed by a number of flying hours and a number of flights of quantity of operation cycles and should not exceed neither:

- Admissible operating hours with reference to structure endurance condition;
- Admissible operating hours with an account made for survivability (safety damage).

Admissible operating hours with reference to endurance conditions of the structure is determined basing on results of laboratory tests for structure endurance as a whole and (or) such endurance condition and determination of weak points.

Admissible structure operating hours accounting survivability (safety damage) is determined on the basic of laboratory test results for endurance and survivability of the structure in a whole corresponding to operating estimation as well as such laboratory test for survivability which are close to structure tests as a whole according to loading condition.

When specifying assigned life time according to endurance condition (safety life principle) any damages resulting in strength reduction should not originate in airframe structural members to less than admissible level and, there fore, special check is not required.

Application of operating survival principle allows origination of cracks in airframe strong structural components or failure of some members during operation but in this case, the following is required to:

- Know in advance where they may be originated (critical points);
- Provide slow cracks development from moment of crack origination to

the critical point to ensure its timely detection;

- Know what method should be used to detect cracks origination (visual or instrumental);
- Know dimension of critical damage.

Survivability is a property of the structure to keep strength under damage origination. Safety damage is a damage of the surface that does not result in residual strength reduction to be less than admissible level.

Under life time characteristics of an airframe structural components we understand as following:

- Structure ability to resist origination of the fatigue cracks being characterized by operating hours required for availability of fatigue cracks;
- Structure ability to keep specified strength under origination and growth of cracks (an operating hours between crack origination and reaching f critical size when structure has a loss of desired carrying ability).

Restrictions as per assigned life associated with a probable reduction of airframe structure load-bearing ability as a result of corrosive processes are specified to meet the following requirements: Norm: When specifying service life an account should be made probable reduction of structure strength characteristics caused by corrosion. During operation structure condition should be systematically checked to provide detection of troubles leading to reduction of structure fatigue endurance (corrosion, accidental damages).

Determination of life characteristics and definition of assigned service life is a complicated and complex problem. To prove this statement it is just enough to define problems to be solved in this case.

#### 1. Determination of the probable operation conditions

Total variety of an aircraft probable usage must be defined as a single standard flight as a combination of standard flights alongside with a relative portion of condition using expert's evaluation and experience for aircraft use close to its category.

#### 2. Load specification corresponding to these standard flights:

- Repetition of loads under the action of atmospheric turbulence with an account made for different flight altitudes and different geographic regions corresponding to air routes of aircraft operation;
- Repetition of loads at ground flight phase involving towing, taxiing to start, ground engines test, running to take off, running after landing, taxiing to parking area;
- Loads related with operation of units during a flight.

Estimation methods loads measurement results during flying tests of the prototypes and loads measurement results at aircraft of similar type are used at this stage.

#### 3. Development of aircraft fatigue test programs both for total aircraft and its separate members and components.

Laboratory flight should last 10 through 15 minutes maximum otherwise such tests would be too long and expensive. Estimation procedures of transition between loads are used under development of loading programs to present to-

tal operating loads as several cycles of loading airframe structure at flight air and ground phase.

In case of loading programs application of "TWIST" type when total amount of expected loads during operating period without recalculation of load are applied, it is necessary to solve the problem of neglecting small and high loads. Neglecting of small loads is done because they produce insignificant damage effect but being available in great amount they result in long duration of tests. Neglecting high loads but occurring very seldom is required because they may result in increasing endurance of tested structure but may never happen during operation of some aircraft. For every specific structure it is necessary to solve the problem what loads small or high can be neglected individually resulting in increasing endurance avoiding loss of expected loading cycles.

#### 4. Conduction of tests for endurance and survivability

During test it is necessary: to provide monitoring of cracks growth; to study their development rate; to provide techniques of instrumental monitoring. Cracks reached large sizes close to critical ones should be subjected to repair and tests should be continued to reveal as many critical points and cases as possible corresponding to two-three design life times. Repair efficiency is checked during tests. At this stage, artificial damages are introduced into critical points if not originated naturally.

#### 5. Residual strength test conduction

Tests for endurance and survivability should be terminated by tests for residual strength to determine critical damage size. In case, if the structure sustains maximum operating load under the first loading it is necessary to remove repair overlays one by one every time applying maximum operating load. If all overlays removed but the structure keeps its carrying ability the load is continuously applied until failure. In doing so, damage size resulting in failure of airframe structure should be registered.

#### 6. Dismounting and defects detection

After termination of laboratory tests for endurance and survivability, the structure shall be subjected to check for condition involving instrumentation monitoring followed by disassembling (disconnection) of undetectable components to reveal probable fatigue damages which detection is difficult during tests or impossible.

#### 7. Conduction of fractographic studies

Main fatigue cracks are made open and subjected to fractographic studies to determine true values of cracks growth rate and damage critical sizes.

8. Study of operation conditions. Analysis and account of differences in operation conditions of some aircraft and aircraft groups.

9. Measurement of loads at this type of aircraft according to flight data recorders under operation conditions.

10. Determination of equivalents both at stage of fatigue cracks initiation and at their development stage. Estimation procedures are used.

11. Study of technical condition under operation. Equivalents clarification based on comparing results of laboratory tests and operation experience data.

12. Tests for endurance and survivability of an aircraft with a great number of flying hours, and etc.

Highly qualified work of design agencies TzAGI, civil and military aviation specialists is required to specify assigned service (life) time assigned life time specification system itself and requirements are subject of continuous modification. Airworthiness norms and regulations (3) allow application of operation survivability principle while according to AP-25 it is obligatory to use. A system of safety factors specified in rules and regulations (2) [22] with reference to fatigue endurance and survivability is a subject of modification and improvement, assigned service life.

The system of life time determination can and would be improved by clarifying and differentiating some of its segment.

First of all, the following aspects are a subject of improvement:

- Fatigue damage accumulation laws;
- Procedures for equivalent transition between loading both at cracks origination stage and at its development stage;
- Effect produced by small and large loads on damage accumulation;
- Effect produced by positive and negative accelerations as well as small loads on cracks growth rate;
- Cycles asymmetry effect;
- Determination of cycles interaction effect;
- Determination of critical sizes of damage;
- Techniques for determination of individual life time consumption;
- Estimation procedures for determination of fatigue cracks growth rate and damage critical sizes, etc.

The scientists and specialists of TzAGI, Institute of problematic strength NAS of Ukraine, Mechanical Institute, Institute of civil and military aviation (GosNIIGA), National Aerospace University, Ministry of Education and Science of Ukraine, Aircraft Operation and Maintenance Research Institute (NIERAT), aviation and design agencies have made the main contribution to the development of scientific grounds of metal fatigue, procedures and techniques as for specifying and implementing life characteristics of airframe strong structural components.

#### 7.1. DETECTION OF LIFE TIME CHARACTERISTICS AT THE PHASE OF LABORATORY STUDIES

To prove life time characteristics of airframe strong structural components specified during design, laboratory studies are conducted according to Airworthiness Rules and Regulations [20] for endurance and survivability of structure in general or such laboratory studies which are close to structure test condition as a whole according to loading and attachment conditions.

A program of fatigue test is under development. It takes conditions of expected standard operation into account and contains a single or several standard flights and covers the total amount of expected loads as far as damage possibility is concerned.

With tests in progress under achieving hours corresponding to single (or

more) design life time the fatigue cracks appear at critical points. Cracks development is under visual observation and using cracks detectors or instrumentation techniques.

Maximal damages close to critical ones are covered by overlays and continued to structure limit condition at two and more times with reference to operating hours exceeding design life time. Fatigue tests are ended by static strength test, total dismounting and defect detection at every airframe structural member. Then, fatigue cracks are subjected to opening and fractographic studies.

It is done so, because, firstly, it is difficult to detect timely all cracks. Many of them are adjoining cracks developed from nearby openings or they stop reaching the opening, that is, crack covers a complicated way of development. Secondly, many cracks are developed unseen being located at points difficult to approach and observation for example, in packs or under overlays and often require termination of tests to provide their detection and monitoring or dismount of airframe units and loading system members or to use non-destructive test, for instance, X-ray with its limited resolving capabilities. Everything mentioned results in tests delay and makes labor intensity high. Thirdly, unpredicted cracks can be originated and developed undetected until reaching certain sizes, for example as a result of production defects (burrs, cuts, etc), Therefore, fractographic studies become a single possibility to obtain data and information on cracks growth rate and sequence of their development. Conduction of fractographic studies is possible provided that symptoms can be observed on cracks surface which may be in correspondence to realized loading, for example, fatigue grooves originated under cyclic loading [23–25].

Cracks growth rate data are obtained using fractography by measuring distance between observed test-pieces (ref., for example, to work [6]).

But due to a long chain of reasons an accuracy of information obtained is not definite under the application of these procedure but study of fatigue fractures takes a long time to be highly labor intensive. As for reasons we may underline as following:

- Grooves are not always arranged continuously but area can be observed where failure takes place by convergence of micro hollows forming pit structure (Fig. 7.1) and in so doing, a number of area is increased followed by cracks growth;
- At some area of fracture surface grooves location does not the route of fatigue crack development;
- In developing the crack goes through the holes which may result in its partial delay.

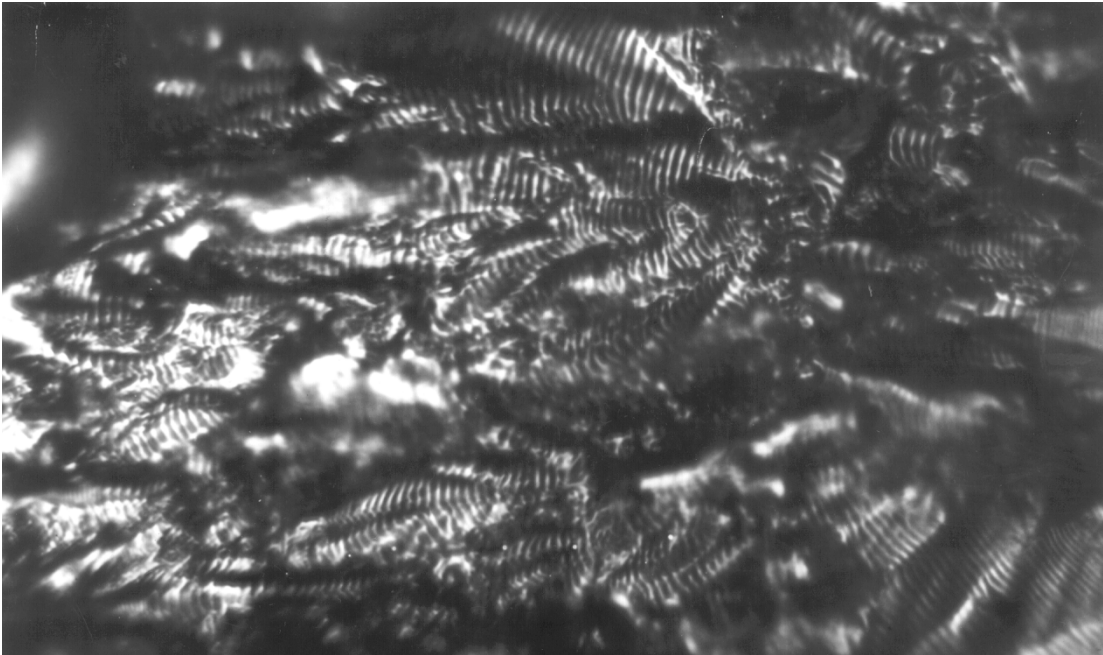


Fig. 7.1 – Fatigue Crack Surface View in D16T Material to Illustrate that Fatigue Grooves Are not always Arranged Continuously (optical fractogram X2000)

Fractographic study process can be simplified and truthiness of obtained result can become higher provided that fatigue fracture surface have symptoms allowing to regard it not as a separate cycle but, more or less, as a major part of loading program. To create such symptoms loads are periodically introduced into programmable in spite of the fact that a way of marking by the use of periodic accelerations provide easily distinctive marking symptoms in the form of macrolines but have a disadvantage that may lead to endurance increase. In addition, if number of macrolines in facture for one or another reason does not equal to a number of accelerations a difficulty may arise that may be overcome accounting grooves corresponding to every loading cycle but as demonstrated above it becomes not always possible. Therefore, a problem of loading marking to technique development is a subject of solution in this work under survivability test enabling to obtain true information on crack kinetics under next fractographic studies and significantly, at several times, to make labor intensity of fractographic studies less irrespective of cracks location and their development history (para. 8.1).

It is known, the preliminary positive accelerations may result in fatigue endurance increase of airframe strong structural components under cyclic loading that follows. But there is a poorly studied problems as for separation of this effect between stages prior to crack origination and its development as well as for effect produced by the next loading nature [24, 34 – 60].

This problem becomes especially important after adoption of concept at ANTONOV Co as for combining fatigue and static tests of AN-124 aircraft using just a single piece.

Such concept can be explained by the following reasons:

- Aircraft high cost;
- Long terms and high cost of tests conduction to be explained, in its turn, by large size of aircraft;
- Desire to obtain information as soon as possible on airframe life time characteristics and to have enough time for making required revisions in aircraft design at early stage of production and so, to avoid any modifications at aircraft already produced;
- Static tests to be mostly representative because they are performed not on brand new aircraft but at an aircraft with flying hours corresponding approximately, at least, to one design life time;
- Performed analysis of aircraft flying tests standard program to demonstrate that 75 % of total flights envisaged by flying test program have outer loads not exceeding 50 % in values as for maximal operating loads while at 90 % of total flights – they do not exceed 70 % of maximal operating load values; based on this analysis results the sequence and terms of conducting static tests have been specified to cancel timely restrictions as far as flying tests are concerned;
- Probability of outer wing asymmetric loading under static tests to provide minimal higher level of the standard flight subsequent cyclic load t one of outer wings and etc.

With the possibilities taken into account one of this work problem is to study effect produced by preliminary positive accelerations on fatigue endurance characteristics at prior to origination and development of fatigue crack to provide correct planning of combined tests at AN-124 aircraft and correct estimation of the obtained results (para. 8.2).

Necessity to determine ratio for cyclic loads damage actions (in between equivalent transition) is arisen under solving different problems in aviation engineering. The problems, for example, can be as following:

- Fatigue tests program development for airframe strong structural components when necessity is arisen to specify different operating cyclic loads acting at different flight phases as their certain number feasible from test period point of view;
- Interpretation of fatigue test-results when starting actual operation;
- Test result interpretation of structural test-pieces tested according to simple loading programs, for instance, repeated stress cycles and etc.

For modern strength norms and regulation (20) envisage probability to operate airplanes using principle of operating survivability, it is also necessary to have a transition mechanism between loads even at cracks growth stage. Despite multiple studies in this field an equivalent problem still remains actual. It is explained, first of all, by complication and multi-aspects of the problem itself as well as by high labor intensity of the studies [51, 52].

Procedure is known to determine damage action of cyclic loads at cracks growth stages based on the dependence

$$dL/dn = f(\Delta K, R),$$

where  $dL/dn$  – cracks growth rate;  $\Delta K$  – cycle intensity factor range;  $R = (\sigma_{min})/(\sigma_{max})$  – cycle asymmetry factor;  $\sigma_{max}$ ,  $\sigma_{min}$  – maximal and minimal stresses of the cycles.

Dependence  $dL/dn \sim f(\Delta K, R)$  is obtained based on test-piece test results.

The following operations are performed for a single load type with  $\Delta\sigma_i$  and  $R_i$  parameters:

- A group of test pieces is subjected to cyclic test (at least, six) under specified type of loading;
- Averaged dependencies between cracks growth rate and crack length  $L$  are plotted (according to data observed during tests or results of fractographic studies).

The same operations are performed for every type of comparable loads.

An equivalent  $\varepsilon$  between two types of loads is specified as a ratio of rates corresponding to loads compared under the same lengths of cracks.

Specified procedure to determine equivalents of loading damage action at cracks growth stage requires a great number of test-pieces to be tested for obtaining dependence of cracks growth rate from  $\Delta K$  and  $R$  parameters.

A great required number of test-pieces subjected to testing can be explained by the following:

- Test-pieces are required to be tested for every type of loads under investigation;
- For dispersion of test results true for fatigue phenomena several test-pieces should be subjected to testing for every type of load.

As a result that test cycle becomes long, labor intensity becomes high associated with the need to use a great number of tested test-pieces.

For the next problem of this work is the development of procedure to estimate damage action of cyclic loads at cracks growth stage allowing to determine equivalents between loads at much less labor intensity in compare with the known ones (ref. para. 8.3).

A problem as for equivalents and, in particular, effect of compressing loads on fatigue cracks growth rate irrespective of multiple studies in this field due to high labor intensity remains poorly investigated, therefore, obtaining any additional information on this problem remains rather actual [64–77].

Effective recommendations on determination of equivalents at the stage of cracks growth cover as following.

In connection with the peculiarities of stress state at apex of the cracks as a result of stresses growth associated with opening of the crack are much higher than stresses associated with its mating. The last one is considered to be practically neglected. Under investigation of the stresses field far from crack (or external loads, bending moments efforts) it means that two combination of timely variable loads – initial combination and combination obtained by excluding a point of those loading part which results in initiation of compressing loads at crack apex – are practically equivalent to value of stresses specifying cracks growth.



In addition, it is noted in this recommendations that variable loads with a relatively low amplitude play more significant role at the stage of cracks growth being revealed in decrease of degree index value  $m$  of endurance curve as

$$N\sigma^m = const,$$

where  $\sigma$  – stress;  $N$  – endurance;  $m$  – endurance curve degree index.

In this connection accumulation of relatively reliable equivalent data at estimating equivalents at the stage of fatigue cracks development is recommended to perform as two phases. At the first phase, the equivalents are estimated to compare two initial combination of loads with reference to their fatigue damage value (for example, aircraft standard flight loads and a number of loads within laboratory tests). In doing so, the order and procedure of estimation fully correspond to equivalent estimation procedure at the stage prior to cracks origination with the exception degree index value according to endurance curve.

Every individual cycle characterized by amplitude  $2\sigma_a$  and mean value  $\sigma_m$  (or maximal  $\sigma_{max}$  or minimal  $\sigma_{min}$  values) is reduced to equivalent repeated stress cycle with a maximal value of cycle  $\sigma_o$  as precondition

$$\sigma_o = \begin{cases} \sqrt{2\sigma_a\sigma_{max}}, & \text{at } \sigma_m \geq 0, \\ \sqrt{2}(\sigma_a + 0,2\sigma_{max}), & \text{at } \sigma_{max} < 0, \\ 0, & \text{at } \sigma_m \leq 0 \text{ and } \sigma_{max}. \end{cases}$$

Endurance curve degree index  $m$  is taken for structures from aluminum alloys with geometric concentration of stresses  $K_t = 2...6$  and joins equal to  $m = 3$ .

At the second phase the equivalents are calculated to compare two transformed combination of loads with reference to fatigue damage value. Each of transformed loads combinations is formed from corresponding initial combination by excluding negative part of loading. Transformed combination of loads is formed according to “full cycles” procedures and thereafter calculation is performed in a way similar to I phase. Less among two values obtained at estimation phases I and II is taken at the crack growth stage as a reasonable equivalent.

It is obvious that application of such approach is caused by insufficient study of this problem. Therefore, conduction of studies in estimation of effect produced compressing loads at the stage of fatigue crack growth and check for fundamental fit of available recommendations, that is, neglecting negative portion of cyclic loads lading to cracks mating is one among the problems of this work (ref. para. 8.4).

Tolerable size of fatigue damage under specified level of operating load (as a rule, maximal operating load) is required to know as important condition for airframe operation in compliance with survivability principle. For available estimation procedures to determine critical sizes of actual structure damage do not give sufficiently reliable results, one-to-one size structural components are subjected to test followed by simulation of respective fatigue damage.

For the reason that just a single copy of structural member is available,

there is always a threat to obtain unsatisfactory results due to damage size to be selected either too big or too small. In the first case, it results in damage under the load less than required while in the second case, the sizes of the tolerable damage can be less.

Additional problems can arise when critical structural members can not be observed during study making impossible to monitor fatigue crack growth in this element.

Procedure is known (Procedure I) to determine critical length of the fatigue crack involving dependence construction “failure load – critical damage size” ( $P = f(L)$ ).

Then, critical crack length ( $L_{cr}$ ) is determined at specified load ( $P_{cr}$ ) (Fig. 7.2).

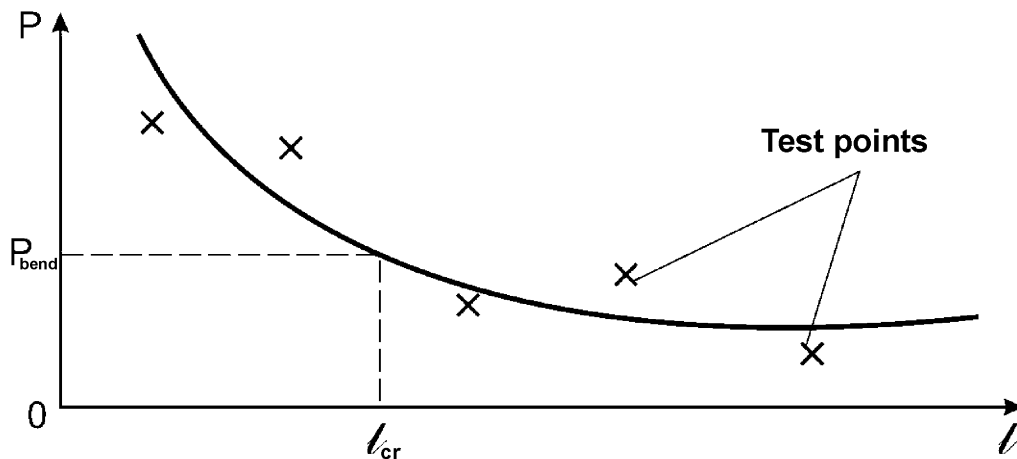


Fig. 7.2. – “Failure Load – Critical Damage Size” ( $P = f(L)$ ). Dependence view, obtained in compliance with procedure I of critical damage size determination

To plot specified dependence several test-pieces are subjected to cyclic loading until fatigue cracks of different sizes have been originated followed by static loading of every test-piece until failure.

Cyclic loading is performed within the range of useful loads (for wing – within cycle maximum “Ground – Air – Ground” (G-A-G)).

Crack size under application of the failure load is not exactly known: it is estimated according to size observed on the surface provided that test-piece type allows to do so, or in compliance with a number of fatigue loading cycles determined by preliminary tests.

Actual crack size is determined by fractographic investigation of the fracture, determined of fatigue area boundaries is not difficult under free program of cyclic loading. For this procedure envisages analysis of, at least, several test-

pieces it can be applied just to relatively simple test-pieces poorly representing an actual structure. Even loading simulation with loaded test-piece requires the application of rather complicated and expensive test-pieces while investigation conduction becomes difficult because crack growth monitoring during tests becomes practically impossible. It is obvious that this procedure is not feasible for testing structures by loading.

But, it has advantages in firstly, the crack is formed under condition close to actual ones (loads do not exceed cycle maximum (G-A-G)) and secondly, due to rather great difference between cyclic loads and load applied under final fracture of test-piece the fatigue are boundary becomes mostly clear and its determination becomes the most difficult. This test procedure enables also to obtain data on cracks growth rate.

Procedure is known (procedure II) [34] to determine critical length of fatigue crack covering test-piece is subjected to cyclic loading until initiation of fatigue crack while acoustic emission parameters are registered in the course of loading and according to change of this parameter we may regard achievement of crack length critical value. Thereafter cyclic loading is terminated and for measuring critical length of the crack the test-piece is finally broken by static loading. Relief boundary on broken section separates area of cyclic loading (pre-critical crack growth) and final fracture area (beyond critical growth of the crack).

For application of this procedure it necessary to know acoustic emission parameters (intensity, summarized emission of amplitude separation) corresponding to critical crack length and in our case it should be found, it becomes obvious that this procedure is not acceptable for solving assigned problem.

## 7.2. ASSIGNED LIFE TIME SPECIFYING AT OPERATION PHASE

As it has been underlined above, assigned life time of aircraft structure according to Airworthiness Norms and Regulations [20] is expressed by a number of hours and flights or amount of operational cycles. When any among specified life time values is reached (in flying hours, flights, operational cycles) an aircraft operation shall be terminated irrespective of its operational condition.

Fatigue test results of aircraft full size structure are initial for determination of aircraft allowable hours during operation.

Test program for endurance of every structural component according to Airworthiness rules and regulations should reflect all loading condition originating within aircraft operation for which a combination of variable loads values and an amount of loading cycles may produce an effect on service lifetime.

Test program, for endurance should be based on standard flight (or combi-

nation of standard flights alongside with a relative portion of their conduction). Admissible operating hours corresponding to endurance characteristics obtained under laboratory test of the identical structure according to one and the same program is determined by division on summarized reliability factor  $\eta$  of average number of test cycles (sets) the structure has been able to sustain.

Summarized reliability factor value  $\eta$  shall be determine as a product of several reliability factors accounting different factors:

$$\eta = \eta_1 \eta_2 \eta_3 \eta_4 \eta_5 .$$

Let's discuss  $\eta_3$  factor value associated with a subject under discussion.

$\eta_3$  factor value accounting truthiness of load repetition data acting on aircraft is taken equal to:

- $\eta_3 = 1.0$  provided that reliable experimental data on repetition of loads are used being obtained at this type of airplane (or for characteristics of atmospheric turbulence at airplanes with the parameters close to aircraft under discussion for rather longer period of operation) and accounting probable differences in loading associated with the peculiarities of operation, geographic condition, route length and etc.;

- $\eta_3 = 1.5$  provided that mean experimental data on repetition of loads are used without analysis of probable differences in loading some groups or types of aircraft.

Depending on accounting rate of probable differences in loading  $\eta_3$  value according to the results of special analysis may be taken within the range  $1.0 < \eta_3 < 1.5$ .

As it goes from above-specified definition of  $\eta_3$  factor, it account reliability estimation level of standard loading to be extra for going to the most loaded test-piece that is, “responsible” for correct determination of dynamic loads and correct selection of standard flight or their combination.

Let's discuss aircraft wing loading change diagram in root section (at wing-to fuselage attachment point), during flight where stresses are maximal (Fig. 7.3).

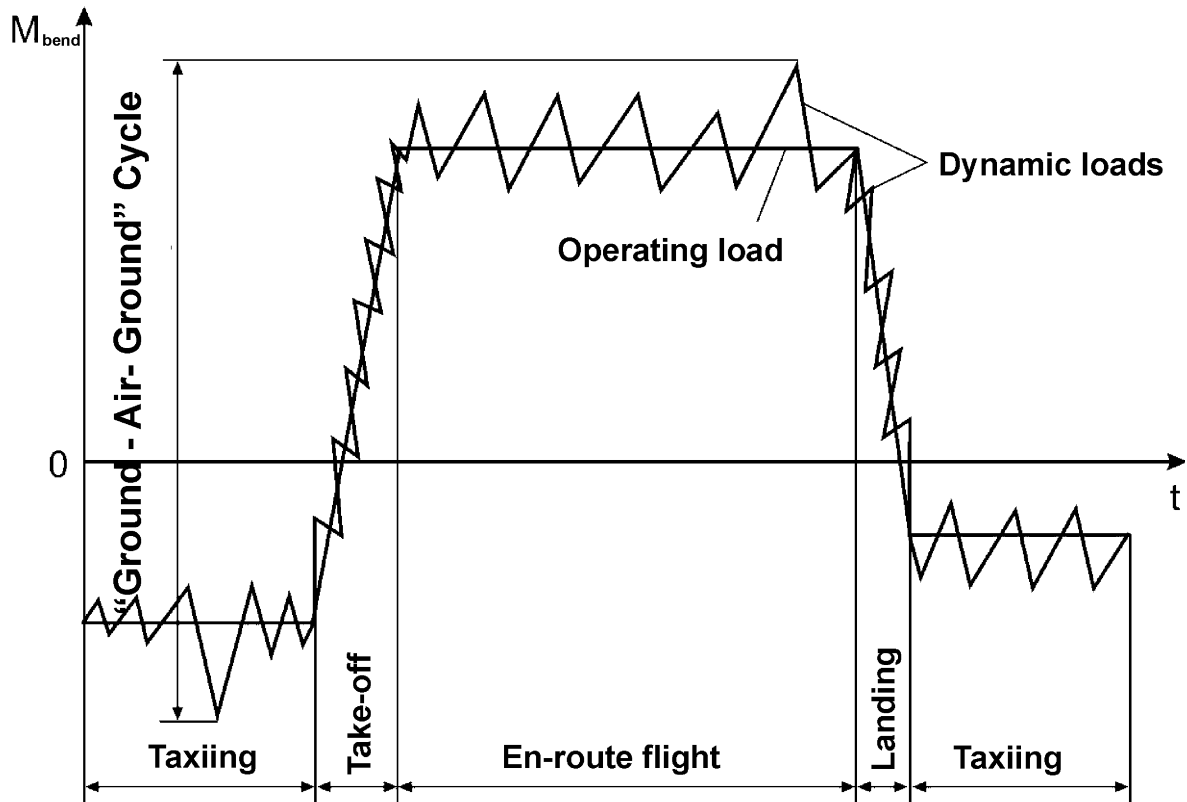


Fig. 7.3 – Wing Bending Moment Variation in Root Section during Flight

It demonstrates that summarized damageability of the wing during flight is determined both by dynamic loads caused by atmospheric turbulence maneuvers, runway uneven pavement and etc. and by operating load. Such subdivision is conventional because damageability from dynamic loads, for instance, atmospheric turbulence depends both on turbulence intensity and flight time and on operating load value to which they are applied to. Such aircraft have taken off landed on extremely smooth runway and have flown in absolutely calm atmosphere, practically total damageability. Could be determined by variations of operating loads being specified, in this case, as cycle G-A-G.

For mid-class airplanes, for example, AN-24, AN-26, AN-32 it is not difficult to select correctly the standard flight or a set of flights just because operating load varies insignificantly from flight and damageability share from cycle G-A-G caused mainly by operating load is as high as 50 % from summarized damageability per flight. So, for AN-24 aircraft a standard two-hours flight has been with an average payload of 3.5 tf. More than 30-years experience of operation has proved correctness of this selection. Average flight time does not exceed 2 hours for this period of operation with reference to this park of aircraft or for individual article. Maximum admissible values of hours and flights for AN-24 aircraft account 40 000 flight and 57 000 flying hours. Following aircraft dimension increase an operating range of flights parameters becomes higher such as take-off weight ( $G_{to}$ ), fuel quantity in wing ( $G_f$ ), payload ( $G_c$ ), height ( $H_f$ ), flight time ( $T_{fl}$ ) and just their combination dictates variation of operating load.

So, for instance, for AN-24 airplane probable range of specified parameters variation is given in Table 7.1.

Table 7.1

Flight Parameters Variation Range for AN-22 Aircraft

Flight Parameters	Variation Range
$G_{to}$	(140...225) tf
$G_f$	(10...80) tf
$G_c$	(0...100) tf
$H_l$	(300...10000) m
$T_{fl}$	10 min – 13 h

An operating load depending on combination of these parameters may greatly vary from flight to flight with reference both to cycle amplitude and asymmetry (Fig. 7.4) while repetition of cycle G-A-G for such airplanes lies within 50 – 80 % from the total repetition per flight.

It is natural that wing structure damageability of heavy transport category airplane may significantly (at several times) vary from flight to flight being known at “ANTONOV” company since 1975 [79]. Actually, for instance, wing damageability for the AN-22 airplane with the parameters  $G_{to} = 225$  tf,  $G_c = 60$  tf,  $H_l = 7000$  m,  $T_{fl} = 5$  h would be more than 5 times higher than wing damageability at transport category aircraft free from payload to have take-off-landing with the parameters  $G_{to} = 150...180$  tf,  $H_{fl} = 500$  m,  $T_{fl} = 10...30$  min. In addition, lower or upper wing surface may become decisive from the lifetime expenditure point of view depending on different flight parameters combination dictating operating load variations as well as on different combination of flights from paved and unpaved runway.

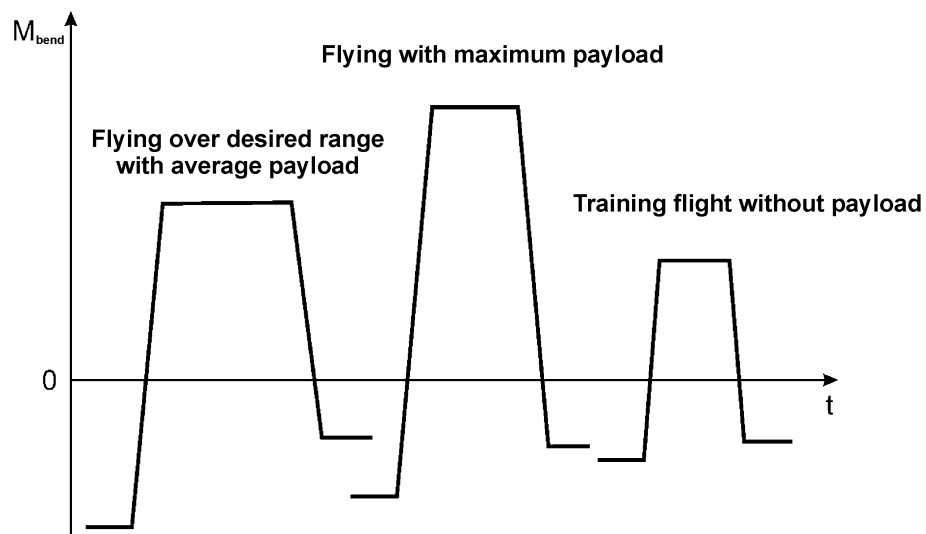


Fig. 7.4 – Operating Load Variation (wing bending moment in root section) Depending on Different Combination of Flight Parameters

In this case, it is difficult to select correctly a single standard flight in compliance with Airworthiness norms and regulations (2) and even several standard

flights according to Airworthiness norms and regulations (3) which could be regarded as averaged standard flights with reference to damageability. Such selection under development of fatigue test program and specifying initial assigned lifetime is based on predicted operating condition which may turn out to be another one for some group of airplanes or some articles. Therefore, reliability factor value  $\eta_3$  equal to 1.5 seemed to be excessive may become insufficient or its actual value may be less than one. It means that life depletion determination by comparing flying hours at actual flight and lifetime hours specified on the basis of standard flights may result, in some cases, in life depletion of this aircraft prior to termination of the assigned lifetime or end of operation operable from aircraft endurance point of view.

Airworthiness norms and regulations dictate under determination of the assigned lifetime to account operation experience and make corrections in standard loading condition. But, if not to do so starting from aircraft operation, later it becomes impossible to restore flights parameters.

For aircraft with a great operating range of flight parameter variations specifying operating load, it is required to specify lifetime with reference to standard flights but not in actual ones specify transition mechanism between them. Aircraft lifetime depletion should be registered starting since beginning of operation for every aircraft or for some groups with the same conditions of application. So, accounting procedure development of individual wing lifetime depletion is one among the problem of this work with an account made for actual data of aircraft operating (para. 11.1).

Flight crew training programs involve training flights to master flying skills under conduction of take-off-landing. So called circle flights cover the following stages:

- Taxiing to runway;
- Running and take-off;
- Circle flight at low altitude;
- Landing and landing run;
- Taxiing from runway and taxiing to runway start.

The main disadvantage of this procedure is availability of control operations – total running, taxiing and total take-off run, producing significant effect on airframe strength lifetime, fuel consumption and restrictions to operation for required long length of runway.

Airframe structure damageability (and particularly, wing as a component dictating mainly strength lifetime of airplane) can be decreased provided that general circle flights (with all stages included) be replaced by flight with sequential take-off just after landing (conveyer flights). Airframe damageability reduction would be achieved due to undoing intermediate taxiing while for wing additionally due to decrease of “Ground-Air-Ground” time cycle.

### 7.3. STUDIES TARGET AND PROBLEMS

Basing on specified analysis of the problems solved under specifying assigned lifetime of transport aircraft the target lies in development of procedure to achieve desired lifetime characteristics under operation of transport aircraft structural components by their revealing during laboratory tests with an individual loading under operation taken into account.

The following problems are defined to achieve specified goals:

- Procedure development to reveal designed lifetime characteristics of transport aircraft structural components with the use of marked loading programs at the stage of laboratory tests;
- Procedure development in determination of fatigue crack critical length under test for residual strength of single article structure;
- Procedure development in realizing available life characteristics of airframe structure at operation stage with an account made for individual loading;
- Implement procedure and techniques to reveal and realize available lifetime characteristics into practical defining and extending assigned life for transport airplane.

This work is the next development of some constituent portion of complicated system in assigning lifetime of airframe strong structural members with an account made for individual loading being insufficiently developed and requiring clarification (paras 7.1 and 7.2) and that is exactly as following:

- Procedure development of marked programmable loading under conduction of laboratory tests for survive ability to upgrade accuracy of the next fractographic studies and making their labor intensity lower;
- Investigation of effect produced by preliminary positive accelerations on lifetime characteristics of aircraft structural members;
- Development of procedure in determination of ratio between the damage action of cyclic loads and fatigue crack growth;
- Study of effect produced by compressing loads on fatigue crack growth rate;
- Procedure development of individual accounting in lifetime depletion of heavy transport aircraft wing;
- Procedure development in conduction of airplanes training flights to reduce strength life depletion of wing structure.



*Chapter 8***PROCEDURE DEVELOPMENT IN REVEALING AVAILABLE LIFE  
CHARACTERISTICS OF TRANSPORT AIRCRAFT AIRFRAME STRUCTURE  
USING MARKED LOADING PROGRAM AT LABORATORY TESTS STAGE**

---

**8.1. PROCEDURE DEVELOPMENT IN MARKING PROGRAMMABLE LOADING UNDER  
CONDUCTION OF LABORATORY SURVIVABILITY TESTS**

As specified in item 7.1 due to different kinds of reasons (fatigue cracks are developed at points heavy accessible for observation, for instance, shear joint pack or under overlays, join together in the course of development, end at holes and etc) fractographic studies of fatigue fractures often become a single probability to obtain information on periods of origination and duration of cracks growth. But such studies are rather labor intensive and their accuracy depends on some factors, for instance, poor detection of grooves corresponding to loading cycles of grooves availability on fracture surface when they are arranged not continuously but area are observed where failure takes place by convergence of micro hollows followed by formation of pit structure and etc.

Fractographic study process will be simplified while truthiness of obtained results be upgraded provided that fatigue fracture surface has symptoms allowing to conduct accounting by more or less big portions but not by separate cycles of loading program. Under some conditions grooves pitch change or fracture structural variations can be used as such symptoms originating under variations of amplitude and average level of loading cycles. The loading program itself can contain variations of loads leaving in fracture different marking symptoms. In other cases, for this purpose this program may contain variations of loading sequence or additions by special cycles of marking loads. As for the later, loads exceeding all the rest program levels have been often and periodically applied or so-called accelerations. But, marking technique by the use periodic accelerations though providing easy detectable marking symptoms in the form of macrolines has a disadvantage that may result in endurance upgrading. In addition, if number of macrolines in fracture, for some reasons, does not equal to the number of accelerations a problem arises that can be solved just by counting grooves corresponding to every cycle of accelerations but as it has been mentioned above it is not always probable. Due to this fact a target has been specified to develop such marking techniques for programmable loading under conduction of laboratory tests for survivability to have next fractographical tests to be less labor intensive with their accuracy to be ensured.

Marking symptoms formation procedure should meet the following conditions:

1. It should not produce significant effect on characteristics detected under tests, for instance, for endurance and cracks growth rate. For determination of this effect fully is not probable, such marking technique becomes more feasible when variation of obtained characteristics improves reliability or even makes then more accurate. The last case obtained may take place when for marking

purpose the cycles are introduced than in the opposite.

2. Marking symptoms should be easily detectable and errors in detection of some marking symptoms should not distort obtained results of investigation.

From the point of view of peculiarities in use of marking symptoms in fractographic test process it is feasible to distinguish two types of their location in loading program:

1. One and the same marking symptom is multiply repeated within the range of some program portion, for example, in every laboratory flight of one unit. Detection of some marking symptom in some or another article point demonstrates that at the moment of the crack front passing through this point those units of loading program are realized that corresponds to this marking symptom. Marking symptoms are changed at the boundaries for unit.

2. Single or group marking symptoms are located so to specify boundaries of some loading program portion.

The following variations of loads can be used to obtain marking symptoms:

- Transition from loading unit with a single constant amplitude to the unit with another constant amplitude;

- Insertion of load units with low amplitude;

- Variation of a number of low amplitude cycles under laboratory flight;

- Periodic unloading and etc.

Selection of optimal marking symptom or their combination as well as type of marking symptoms arrangement in program depends on the material of the tested part or loading program nature and stress levels used.

This publication presents firstly developed procedures of loading program marking [26–30] under solving two problems:

- Investigation of kinetics and duration of fatigue crack development in wing under cyclic loading not exceeding the level of loads in Ground-Air-Ground;

- Determination of critical crack length in one-to-one size wing.

Simple flat test-pieces fabricated from D16 and B95 alloys have been subjected to test to determine conditions under which the grooves are different. Test-piece test programs envisaged wide range of variations in level, variety and sequence of loading.

Data have been obtained using fractographic method allowing to compare cracks lengths and loading level with the reveal of grooves. The same data have made it possible to find association between revealing stress intensity factor values  $K_{max}$  and cycle asymmetry factor  $R$ . For visual and summarized representation obtained data have been plotted on graph depending on  $K_{max}$  and  $R$  parameters. Example of such dependence for B95 material plotted with reference to electronic-fractographical analysis results is shown in Fig. 8.1.

Studies performed [27] have made it possible to develop a number of programmable loading marking procedures based on distinguishing some grooves.

The first procedure – wing loading marking of “flight-by flight” type varying number of cycles in flight from unit to unit.

Study of structural test-pieces by the use of E2-21-788 simulating joint be-

tween spar cap, lower panel and wing detachable section has been performed to determine endurance characteristics and crack growth duration in detachable sections. Test-pieces have been consisted of two pressed sections made from V-93Pch alloy while overlays from D16chT pressed panel and T-shape section from D16chT material. Overlay simulated skin of wing lower panel and was made as a continuous panel section simulated mid-spar cap. Test-piece overlay and spar cap were joined by two sections of joint, by five rows of steel bolts with the first and last rows having  $\text{Ø}10A_3$  while the second, third and fourth having  $\text{Ø}12A_3$ .

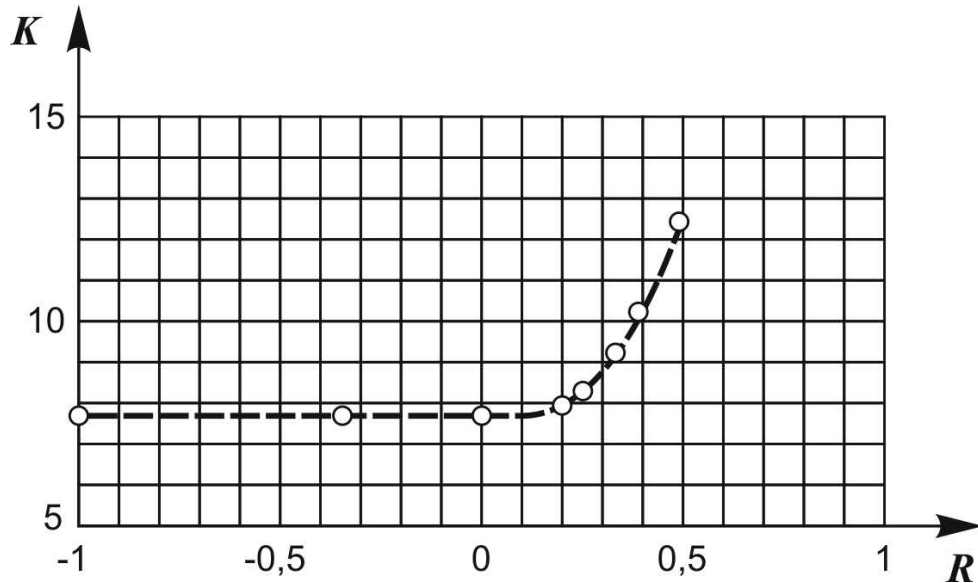


Fig. 8.1 – Dependence between Lower Boundary of Grooves Detection and  $K_{max}$  and  $R$  Parameters for Test-Pieces from Pressed Panel, material B95 Pch (according to electronic microscopy data)

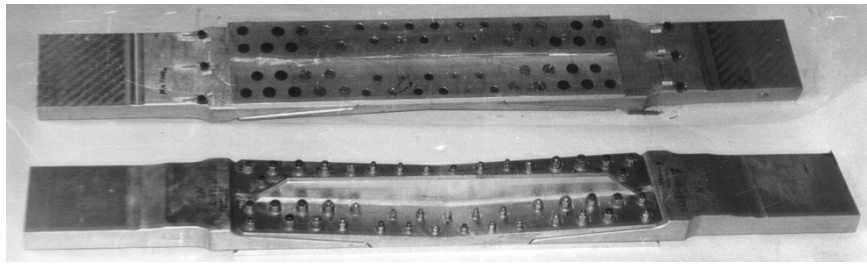
Joint section failure occurs in section where thickness 28 mm and maximum average net stress  $\sigma_{ex} = 122$  MPa. Original test-piece photo and after failure is depicted in Fig. 8.2.

Loading has been done using MTS-500 test machine at a frequency  $f = 0.5 \dots 1.5$  Hz. Tested section has been inaccessible for visual observation.

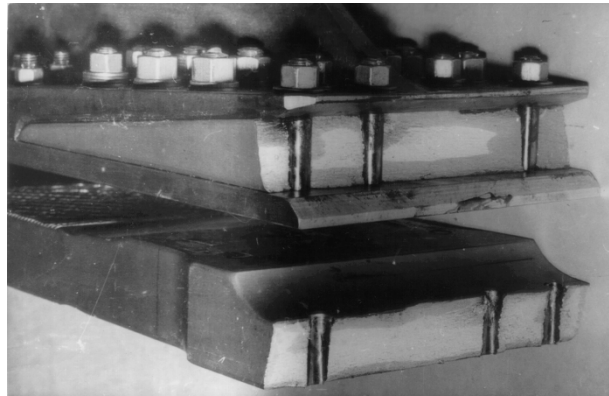
As an example Fig. 8.3 demonstrates view of fracture surface structure for test-piece E22-21-788 No. 24.

Marking procedure has been used including variations of “cycles” numbers incorporated in laboratory flight without entering additional loads to the program. This procedure is feasible from the point of view of the effect produced of the obtained endurance characteristics provided that average number of cycles in flight remains constant within some period of loading program to be as short as possible.

Loading program used as shown in Fig. 8.4.



a



b

Fig. 8.2 – Structural Test-Piece View of dr. E22-21-788, Simulating Wing Detachable Section: a – before test; b – fractured at the first mostly loaded row of bolts after fatigue tests

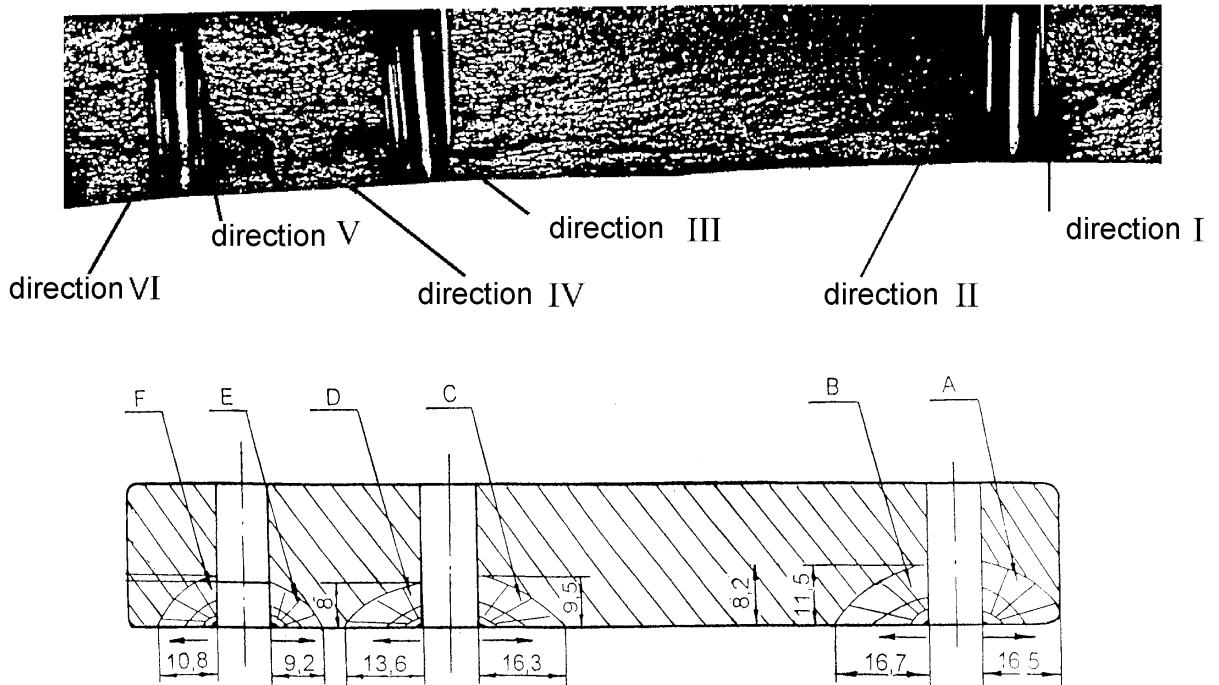

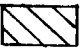


Fig. 8.3 – Fracture Surface View and Diagram of dr. E22-21-788 No. 24:  
 –fatigue area;  – static final fracture area; → – crack development direction

Total area of fatigue failure is approximately equal to 600 mm<sup>2</sup>.

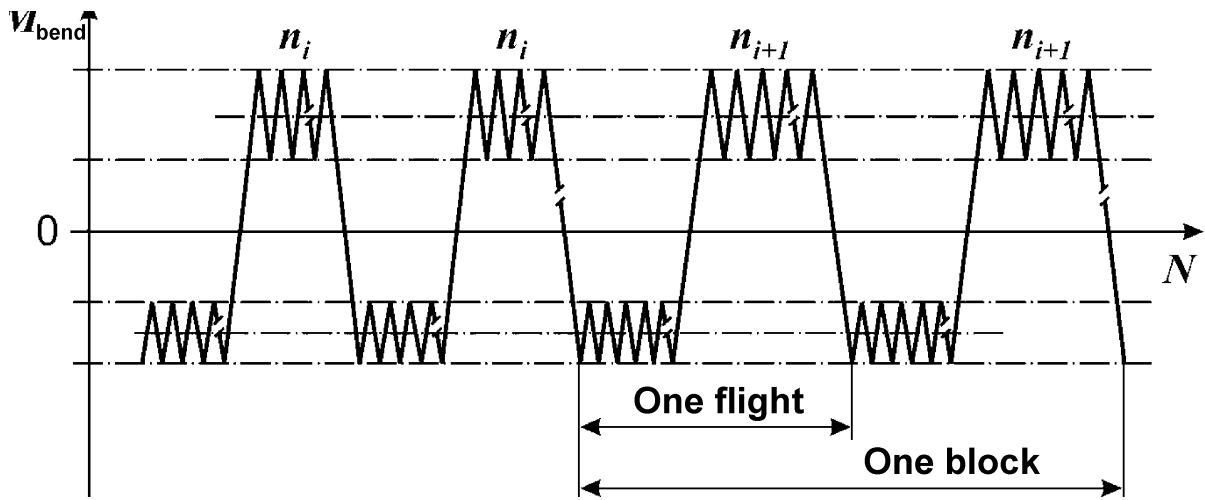


Fig. 8.4 – Structure Test-Piece Loading Program View of dr. E22-21-788 with Varying Number of “Dynamic” Cycles Incorporated in Laboratory Flight

Values of  $n_i$  of flight air phase at crack growth stage are tabulated in Table 8.1.

Table 8.1.

Values of  $n_i$  of Flight Air Phase at Crack Growth Stage

Unit number $i$	1	2	3	4	5	6
Number of cycles, $n_i$	8	5	10	7	9	6

Number of “dynamic” cycles flight varied after every thousand flights making up one unit in the following sequence:  $n_i = 5, 10, 7, 9, 6, 11, 5, 8, 12, 7$  under average value of “standard” flight  $n = 8$ .

To make favourable condition under fractographic investigation the sequence of cycles “dynamic” number variations is selected in a way to provide their difference in neighbouring unit equal, at least, to two. The program has been repeated after every ten (10) units.

The following results of investigation have been obtained.

The grooves just close to focus have been observed on fracture surface of broken test-pieces demonstrating direction of crack spreading within a single flight. Smaller grooves have been revealed under electronic microscope following crack growth. The first among these grooves was wider. It was in correspondence with crack spreading in going from compressing loads to tensile (stretching) loads (cycle G-A-G), the rest subjected to loading by “dynamics” cycles (Fig. 8.5).



Fig. 8.5 – Test-Piece Fatigue Crack Surface View in Units Replacement Area under Testing in Accordance with Program, Fig. 8.4 (electronic fractogram X6000)

Fracture has been subjected to sequential investigation in crack development direction to specify test-piece failure kinetics and defined the length specifying front position at a moment of “dynamic” cycles number of variations (program unit transition points). If grooves corresponding to flights were so small that smaller grooves therein could not be distinguished under magnification by optical microscope and fractures have been subjected to investigation with the use of electronic microscope.

Graphs of dependence “crack length – number of flights” have been plotted in compliance with the results of fractographical investigations. Determination of operating hours prior to the first and after the last transition has been performed by estimation according to the results of grooves pitch measurement or by their direct calculation.

Optical and electronic fractograms, obtained under subsequent investigation of fracture surface, have been demonstrated as an example in Fig. 8.6, in Fig. 8.7 – graphs have been plotted to show curves of fatigue crack development duration in single test-piece according to the results of units transition points determination.

Under program development (Fig. 8.4) the test-pieces have been subjected to testing with the use of three different loading programs (Table 8.2).

Table 8.2.

Loading Programs

$\sigma_{nett}$ , MPa	Loading program		
	I	II	III
$\sigma_{max}$	134	122	134
$2\sigma_a$	49	68	82
$\sigma_{min}$	-75	-76	-75

Grooves associated with the crack development during a flight were always very clear. But small grooves associated with “dynamic” were, in the first case, very poorly distinctive. As dynamic have been increased, the distinctiveness of the grooves became better – in the third case of testing the small grooves were visible close to fatigue crack focus even when magnified by the use optical microscope.

So, revealing of small grooves number at any point of fracture surface have enabled to find association with some program unit of loading and as a result, to define operating hours for the cracks of any length. Developed marking technique makes it possible to obtain information even if fracture has been partially damaged.

The second procedure – loading marking by repeated stress cycles or symmetrical cycles of inserting flight units with a variable number of cycles in flight.

Under study of An-24 power plant pylon attachment units when loaded by symmetrical cycles of constant amplitude (cycles G-A-G) to form marking symptoms on fracture surfaces, program insertions have been entered the program with a variable “dynamic” and in this case, this entry was in correspondence with a different number of cycles in flight.

Grooves have been observed of fracture surfaces of crashed test-pieces when magnified by an optical microscope with their pitch being varied at inserts points. Definition of length corresponding to crack format at a moment of program variation and revealing a number of dynamic cycles in flight in inserts have made it possible to determine Kinetic of test-piece failure. Fig. 8.8 demonstrates fractography of pylon beam with crack, loading program view with marking inserts and diagram of standard electronic fractogram at point of transition from cycles to marking insert.

Developed marking technique can be used under another programmable testing, for instance, under unpredicted loading.

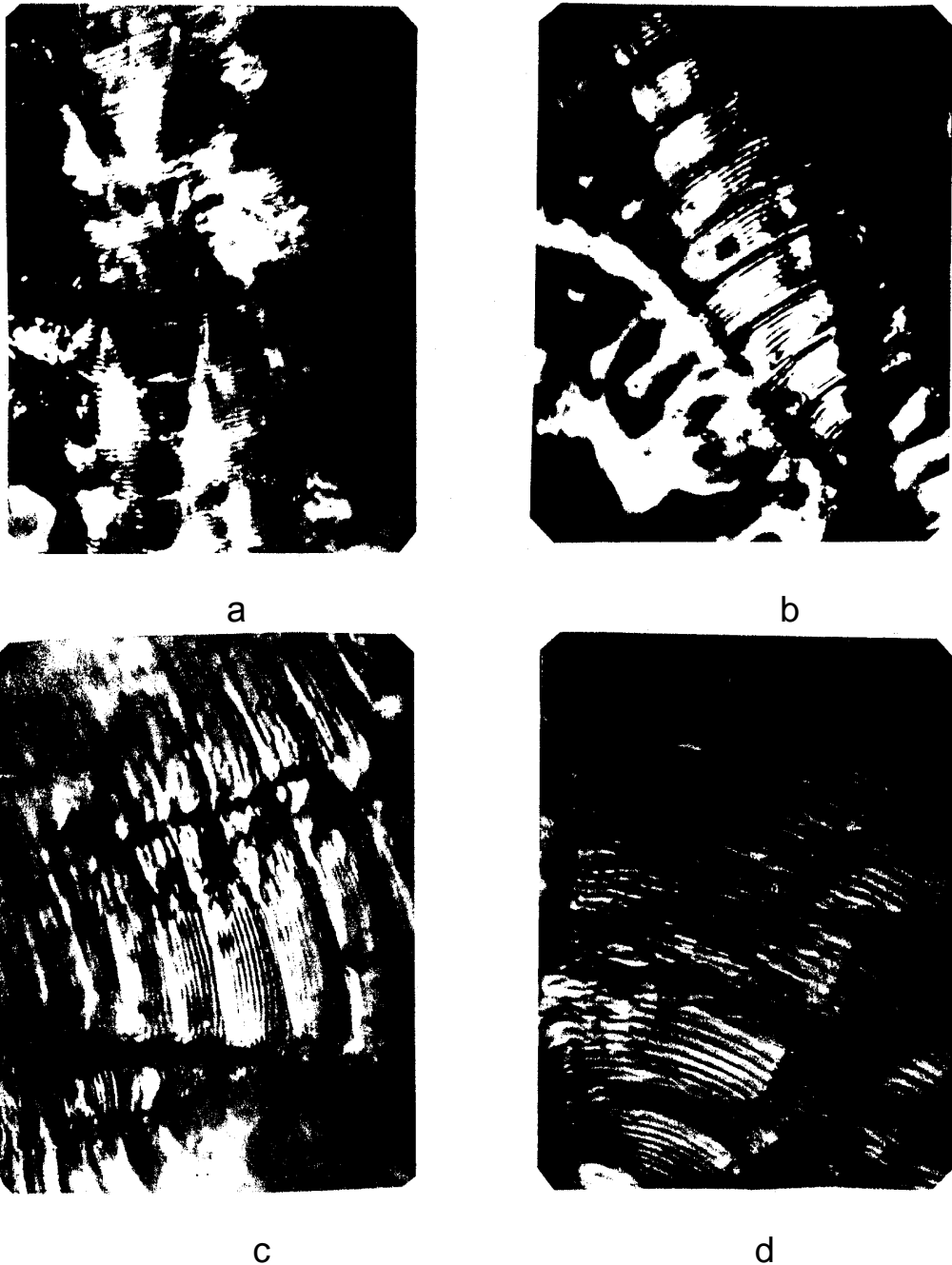


Fig. 8.6 – Test-piece fracture surface optical fractograms, dr. E22-21-788, area A (direction 1): a –  $L = 0.5$  mm,  $n = 10$ , X2000; b –  $L = 7.6$  mm,  $n = 7$ , X2000; c –  $L = 9.4$  mm, X2000, transition  $n = 7 - 9$ ; d –  $L = 11.6$  mm,  $n = 9$ , X2000

The third procedure – loading marking under determination of critical crack length in one-to-one size wing with different combination of inserts from an amount of loads of low amplitude and periodic unloadings.

Wing tests to determine critical size of fatigue failure have been conducted by cracks equalizing under cyclic loading with constant amplitude when while lower one –  $0.85 P^o$  ( $M_2$ , Fig. 8.9).



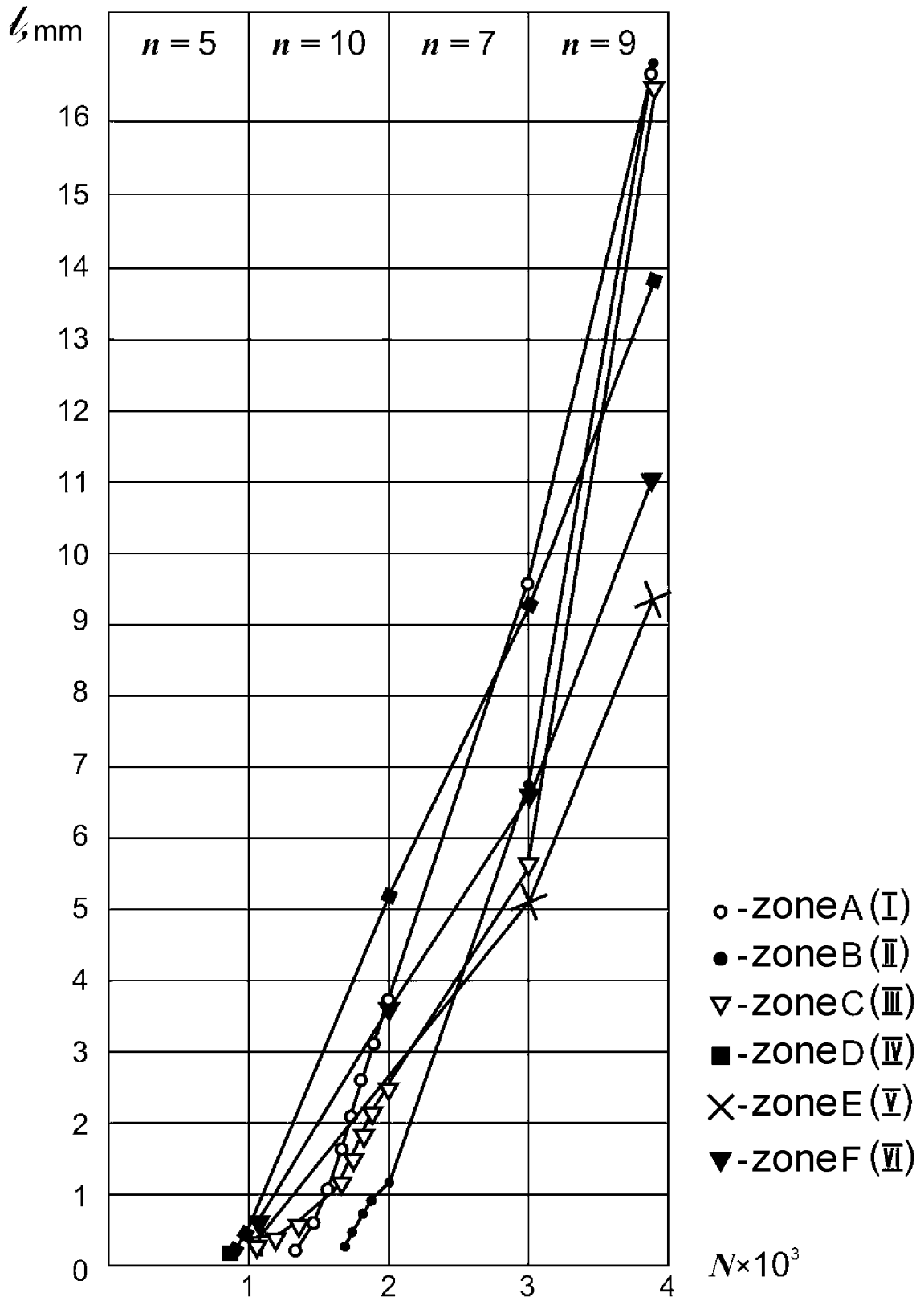
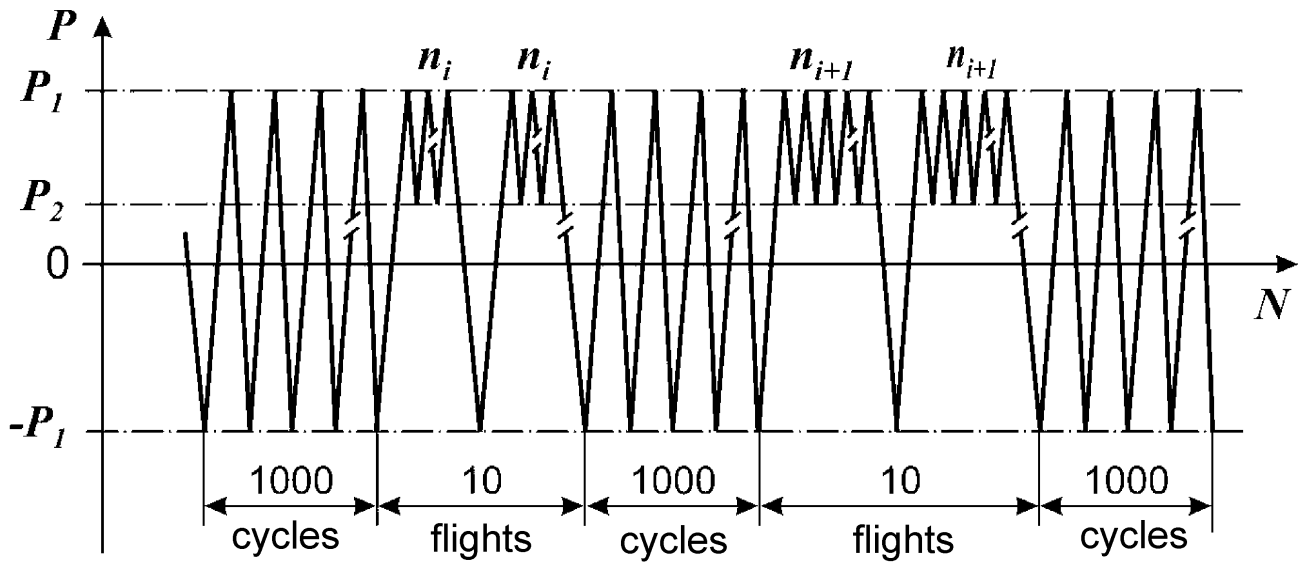
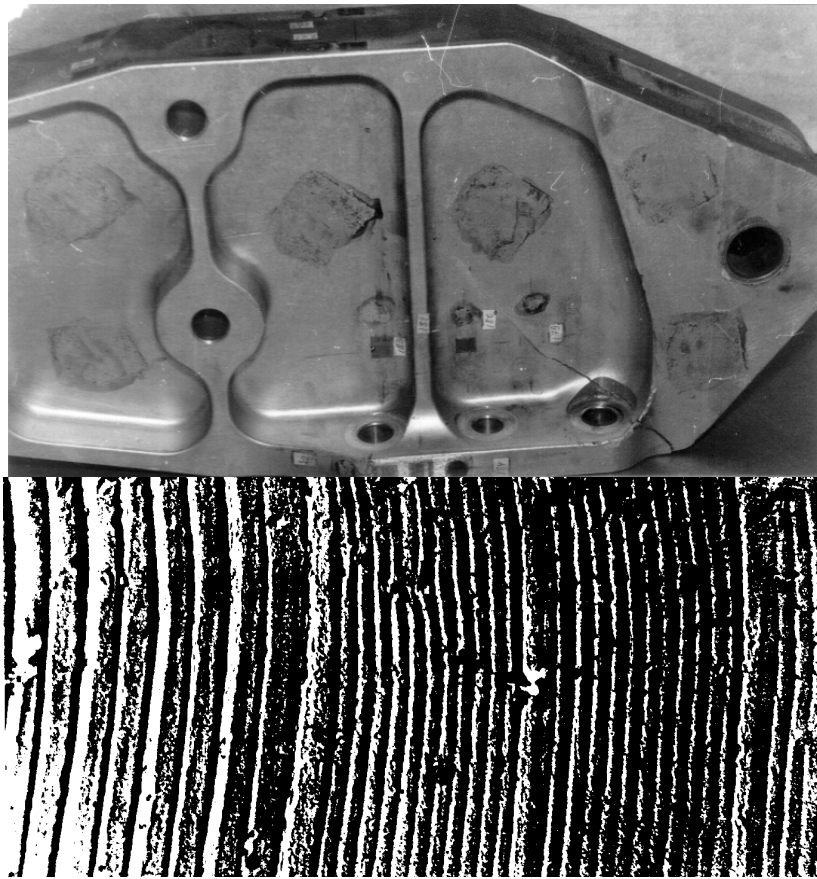


Fig. 8.7 – Crack Length Dependence From a Number of Laboratory Flights  $N$  in Directions I-VI Area ABCDEF Test-Piece E22.21.788:  
 $n$  – laboratory flights number



$$P_2 = 0,35P_1$$

Fig. 8.8 – Power Plant Pylon Beam View with Crack, Beam Loading Program View with Marking Inserts. Standard Electronic Fractogram Diagram at Point of Transition from Cycles to Marking Insert

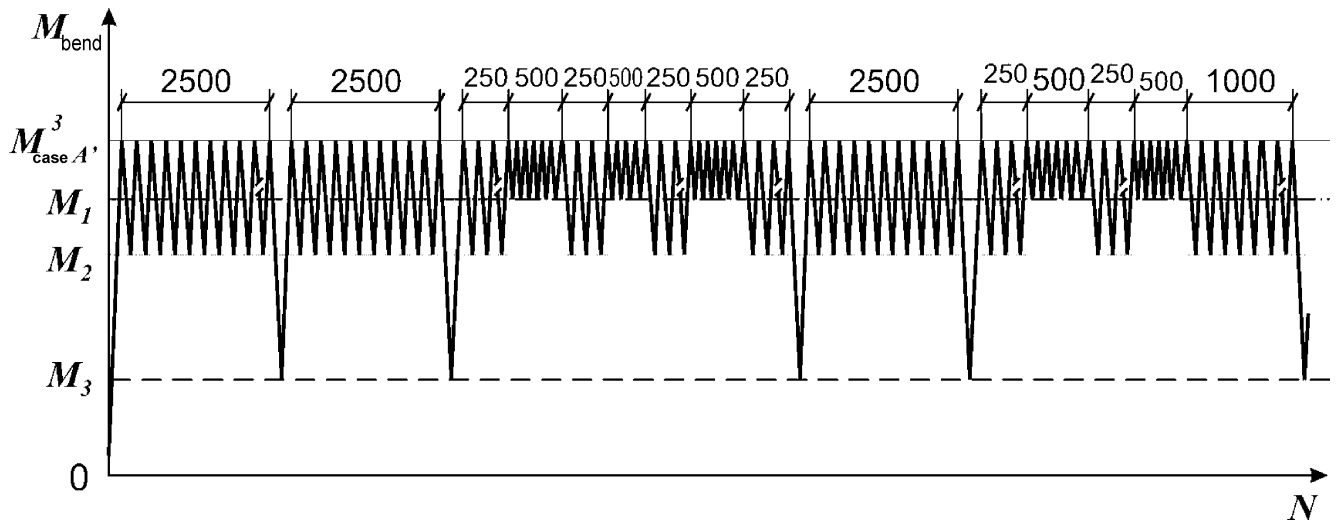


Fig. 8.9 – Wing Test Program Fragment for Residual Strength:  
 $M_1 = 0.05 M_{c.A}^0$ ;  $M_2 = 0.85 M_{c.A}^0$ ;  $M_3 = 0.5 M_{c.A}^0$

In that case to obtain marking sign the following was used:

- a) Decreasing of loading amplitude ( $M_1$ );
- b) Load relief to  $0.5 P^0$  ( $M_3$ ).

Maximal mean net stresses under tested condition have been equal under tests to  $\sigma \approx 250$  MPa. Reduced amplitude sets involved 500 loading cycles. Both types of marking loads in tests program have been combined into five marking groups different from each other in such a way to obtain unrepeated system of markers. Marking loads in this groups have been applied after every 250 loading cycles between marking groups – 1000, 2000, 2500 loading cycles at a range of  $0.15 P^0$ .

The program incorporated three phases differing from each other by sequence of marking loads groups. An allowance has been made for the repeated loading after completion of these phases.

As fractographical tests have shown, a set of loads applied having less range and relief have left strips-marks at fracture surface at a width of 0.4...10 mk showing cracks front position at a moment of their application and loads, in this case, have resulted in formation of more rough marks.

Electronic fractograms of wing section fracture surface is illustrated in Fig. 8.10.

Summarized growth corresponding to marking loading was 1.5...2.0 % of total crack length. This value is associated with the selection of loading program aimed at obtained reliably distinguishable marks under minimal time of testing.

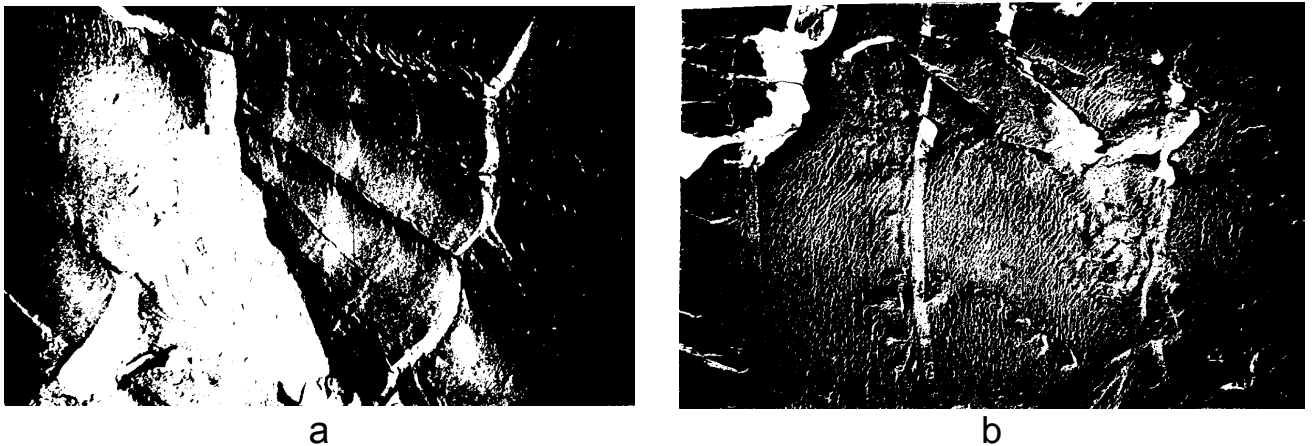


Fig. 8.10 – Electronic Fractograms of Wing Joint Section Fracture Surface:  
 a – at a distance of 0.19 mm from fracture focus;  
 b – at a distance of 0.36 mm from fracture focus X7000

Macrostructure study of wing joint section fracture surface has made it possible to detect fatigue damage centre and main directions of crack development. After even accelerated crack development stage in two maximal area, the fatigue surface has been interrupted and pit structure has been observed on fracture surface standard for a single rupture. Prior to its drastic increase of crack development rate could be seen at a small segment of one of these area being detected under distance measurement between marking groups marks. Strong shock has been registered with tests in progress.

As investigations have demonstrated operating hours at the moment of pit surface detection in fracture turned out to be close to operating hours at the moment of shock proving that crack sliding occurred at this time. So, it could be noted that fatigue damage size at a moment of crack drastic growth was critical for section studied.

Under fracture surface study at the end of other fatigue area there were no crack drastic development. Zones have been drastically interrupted and wavy like surface has been seen specific for fractures of test-pieces with cracks under single failure. Such fracture structure proves that failure at these points took place under approaching of the main crack front and fatigue damage dimension at these areas is not critical. Application of marking loading programs and detection of peculiar features in fracture structure have enabled to specify sequence of wing failure and define dimension of crack critical value.

According to the results of crack length measurement corresponding to front at a moment of marking loads application the graphs have been plotted to show dependence “crack length – operating hours”. So, to have true information on failure process under fatigue tests and investigations for residual strength using fractographical analysis for investigation labour intensity reduction different marking techniques of programmable loading have been developed:

- Variations in number of cycles in flight in mating sets at least, two cycles of wing programmable loading of the type “flight – after flight”;
- Inserting flight sets with a variable number of cycles in flight from insert-to insert, at least two cycles under loading by repeated stress or symmetrical cycles;
- Inserts of different combination from a set of low amplitude and periodic load relief under wing test for residual strength.

Developed marking technique has enable to solve the following problems:

- Determine origination moment and fatigue crack development kinetics in area inaccessible for observation under tests of structural test-pieces and structural members for survival;
- Determine the sequence, the kinetics of failure and the critical size of the fatigue damage in the lower airfoil of the An-22 aircraft wing joint;
- Reduce significantly (by times) the complexity of fractographic studies.

With the application of the developed method for marking of software loading, tests for the survivability of airplanes An-12, An-22, An 24, An-32, An-28, An-72, An-124 and design samples of An-22 and An-124 aircraft have been conducted (or are in process).

## 8.2. INVESTIGATION OF PRELIMINARY POSITIVE OVERLOAD EFFECT UPON STRUCTURAL ELEMENT LIFETIME

As noted in subsection 7.1, preliminary positive overloads can lead to an increase in the fatigue life of the airframe load-bearing structure under subsequent cyclic loading. However, the problem of dividing this influence between the stages prior to crack initiation and its propagation remains unknown, as well as the subsequent loading nature effect [24, 34-60].

This issue became especially acute after the Antonov State Company accepted the concept of combining the fatigue and static tests of the An-124 aircraft on a single test piece. Therefore, the task was set to investigate the effect of preliminary positive overloads on the service life characteristics under the subsequent loading simulating the loading of the An-124 wing, and experimental studies were performed on specimens with an aperture made in a D16chT pressed panel. The specimen general view is shown in Fig. 8.11.

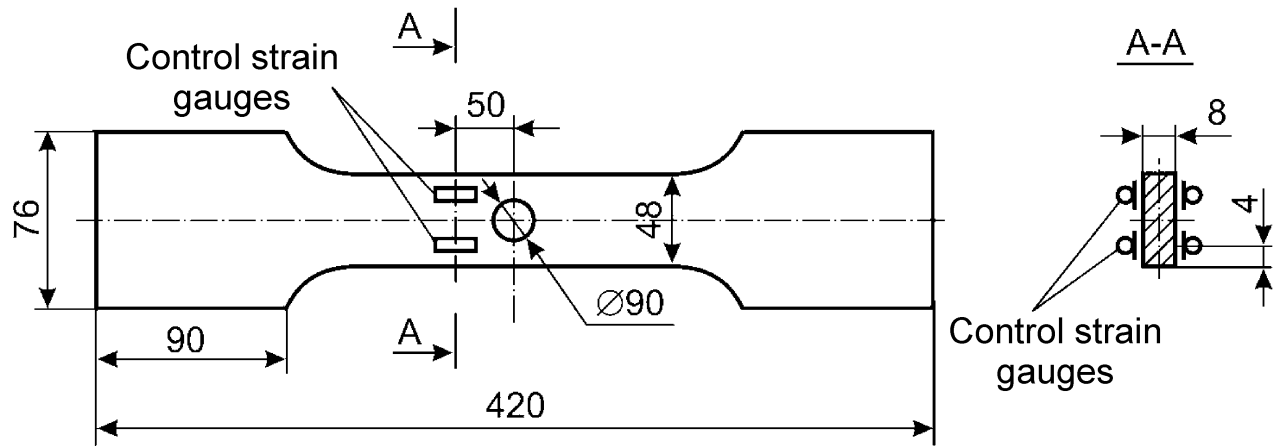


Fig. 8.11. Arrangement of Specimens and Strain Gauges

Tests of the specimens were carried out as blocks consisting of 20 flights of three types (Table 8.3) on a UIM-25 test machine (Fig. 8.12).

The test loading frequency was 5 Hz. Prior to testing, the specimens were subjected to single positive overloads. The coefficients of the preliminary overload (being the ratio of the stresses under overload to the maximum stresses under program loading) were:  $K = 1.25; 1.53; 1.82; 2.12$ . Under overloads, the loading occurred at a rate of 1 ts/s. The specimens were held under the given overload for 3 s, after which they were provided with "rest" before loading with repeated loads having duration of at least two days. Correctness of the specimen positioning in the testing machine was monitored by means of strain gauges. The tests were carried out with holding of given loads till failure.

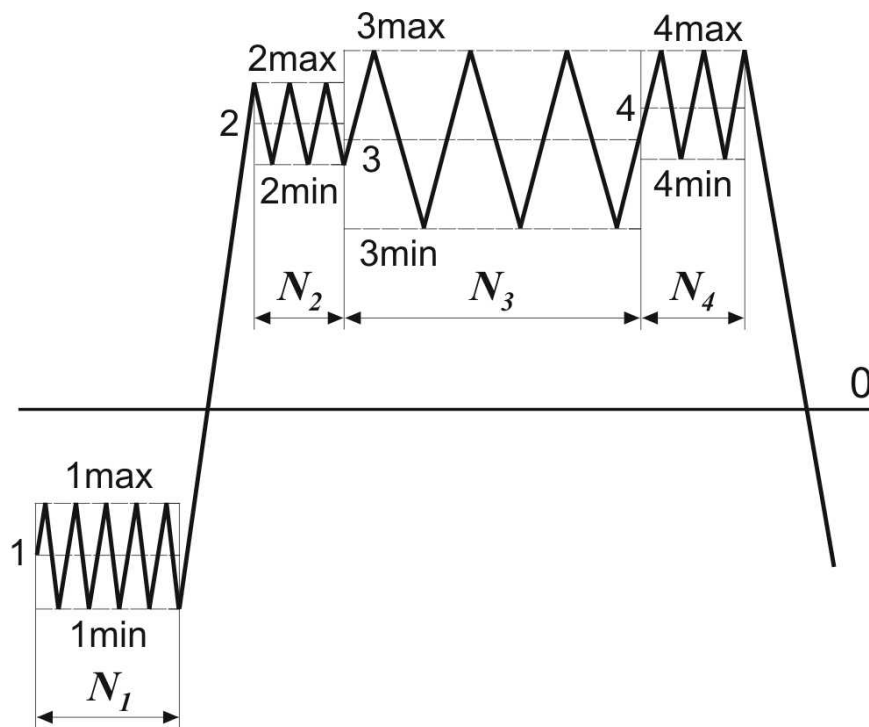


Fig. 8.12. Loading Scheme for Specimens

Table 8.3.

## Loading Parameters for Standard Flights

Number of Flights in Block	Point Number	$\sigma_{gr}$ , MPa	$\sigma_{gr}$ , MPa
II	1	-53.8	-91.5
	2	67.5	56.3
	3	81.2	31.0
	4	81.2	55.1
8	1	-42.5	-89.4
	2	95.1	79.3
	3	112.0	48.4
	4	112.0	74.2
I	1	-40.2	-79.3
	2	116.7	98.2
	3	137.1	67.8
	4	137.1	91.9

A separate group of specimens was also tested, which first were loaded with a maximum overload of 2.12, after that the central hole was made in every specimen.

When performing main loading, insertions of marker loads were introduced through each thousand standard flights. With the help of the fractographic method, decoding of the breaks was performed and the dependences of the crack rate and length vs the operating time were built. Due to the fact that the fatigue grooves near the outbreaks began to differ at crack lengths of more than 0.2 mm, a work-time was obtained for the period before the crack nucleation, corresponding to the achievement of this crack length.

Figures 8.13 to 8.15 and Table 8.4 summarize the results of the tests and studies.

Note:  $\bar{N}_{ini}(\bar{N}_K)$  and  $\Delta\bar{N}_{ini}(\Delta\bar{N}_K)$  are average values of the total durability and duration of crack propagation in the original specimens respectively (specimens with preliminary overload  $K$ ).

From the data obtained, it follows that, with an increase in the overload, a monotonic increase in the durability is observed both at the stage prior to the crack nucleation and at the stage of its propagation.

Preliminary overload  $K = 1.25$  had practically no effect on the fatigue characteristics of the specimens. Overload  $K = 1.5$  resulted in an increase in the durability of the specimens by 1.07 times. At the same time, duration of the crack propagation increased by 1.12 times, and the period before nucleation – by 1.04 times.

## Summary Results of Tests and Studies

Coefficient of Increase	Overload Coefficient (number of tested specimens)				
	1.00 (16)	1.25 (14)	1.53 (12)	1.82 (8)	2.12 (7)
Total durability $\eta_{dur} = N_k/N_{ini}$	1	1.02	1.09	1.41	1.93
Period before crack nucleation $\eta_{nuc} = (N_k - \Delta N_k)/(N_{ini} - \Delta N_{ini})$	1	1.02	1.05	1.32	1.83
Duration of propagation $\eta_{dev} = \Delta N_k/\Delta N_{ini}$	1	1.02	1.14	1.59	2.09

Further increase in the overload resulted in a greater increase in durability. So, with the preliminary overload  $K = 2.0$ , the increase in durability was approximately 1.7 times (the period before nucleation and duration of the crack propagation increased by 1.6 and 1.9 times, respectively).

It can be seen from Fig. 8.14 that with increasing overload, the crack propagation rate decreases, with the maximum decrease occurring in the zone directly adjacent to the hole edge, i.e. the zone of maximum stresses under overloads, where the local yielding of the material took place.

For clarity, graph of this rate is plotted in relative coordinates and given in Fig. 8.16.

It follows from Fig. 8.16 that:

1. With increasing preload, the area size where the crack propagation becomes slower increases, which is obviously due to an increase in the plasticity zone.

2. With increasing the distance from the concentrator for the same overload, the effect of preliminary overload on the crack propagation rate becomes less significant and at distances greater than  $L = 12$  mm, was practically absent even under the maximum overload  $K = 2.12$ . This means that change in duration of crack propagation under application of preliminary overload is mainly due to a change in the crack propagation rate in the zone of the concentrator, where plastic deformation was achieved under preliminary overloading.

To verify this conclusion, a group of specimens was tested, where specimens without a hole were applied with maximum overload of 2.12, after that a central hole was made. In other respects, the test procedure and fractographic studies did not differ from those described above.

Tests showed that durability to failure of the original specimens (without overloading) and the specimens with maximum overload of 2.12 applied prior to the hole had been done was practically the same. The rates also were the same, and



hence duration of crack propagation. This confirms the conclusion that change in the duration of crack propagation with the application of preload was mainly due to change in the crack propagation rate in the zone of the concentrator.

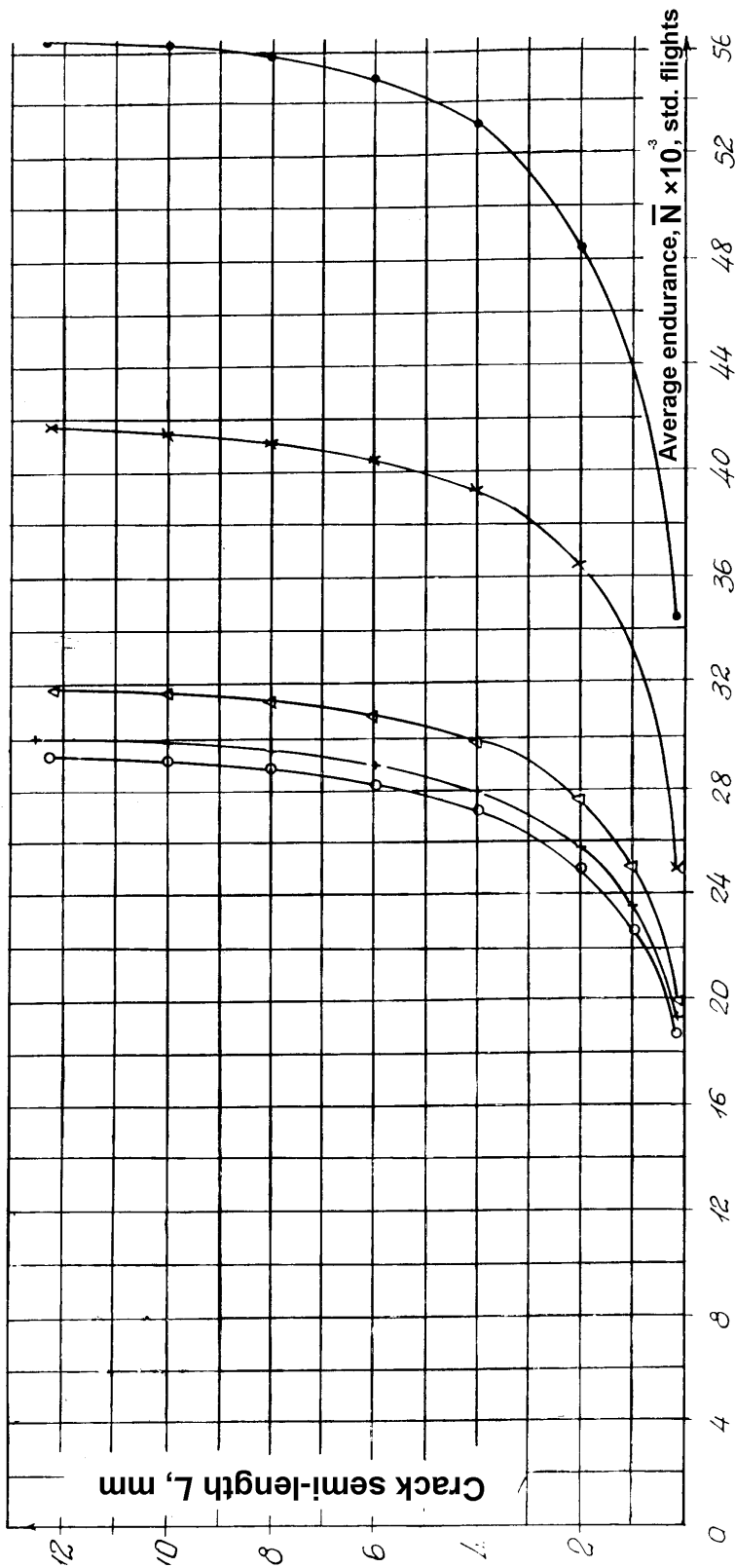


Fig. 8.13. Function  $L-N$  for Original Specimens with Preliminary Overloads:  
 ○ — original specimens; + —  $K=1.25$ ; △ —  $K=1.53$ ; x —  $K=1.83$ ; ● —  $K=2.12$

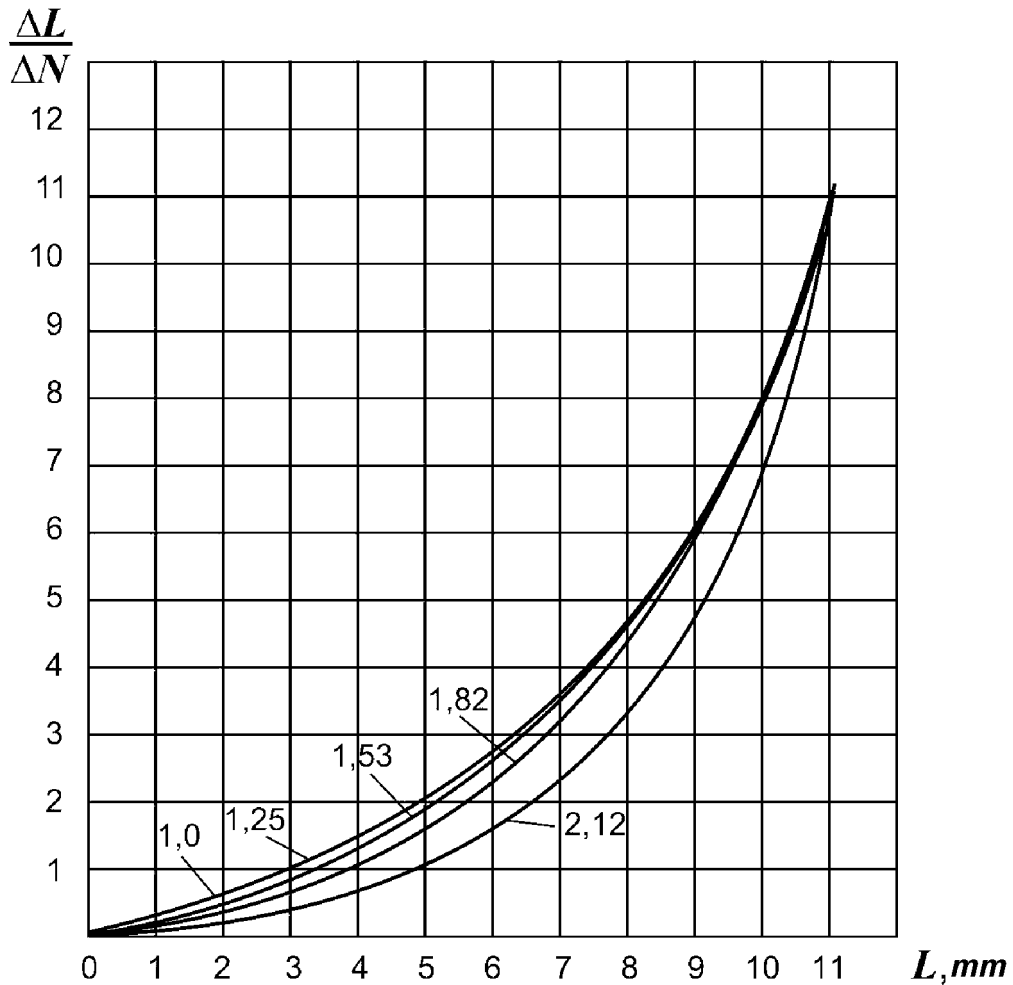


Fig. 8.14. Average Propagation Rate vs Crack Semi-length in Original Specimens ( $K = 1.0$ ) and in Specimens Preliminary Overloaded ( $K = 1.25$ ;  $1.53$ ;  $1.82$ ;  $2.12$ )

Hence:

1. The experimental investigation of the regularity of preliminary single overload effect on the characteristics of fatigue endurance of specimens with a hole made of D16chT alloy under loading simulating the loading of the wing of a transport airplane has been performed.

2. It has been shown that preliminary overload leads to an increase in fatigue life both at the stage preceding crack appearance and at the stage of its propagation.

3. The effect of preliminary overloads was monotonous and increased with rising in their amount.

Thus, loading with overload  $K = 1.25$  had practically no effect on the fatigue characteristics both at the stage preceding the crack appearance (up to  $L_{cr} = 0.2$  mm) and at the crack propagation stage.

Under overload  $K = 1.5$ , the overall durability increased by 1.07 times. At the same time, duration of crack propagation increased by 1.12 times, the period preceding its nucleation – by 1.04 times.

Overload  $K = 2.0$  increased durability by approximately 1.7 times, and the period preceding nucleation and duration of crack propagation by 1.6 and 1.9

times, respectively.

4. The increase in durability at the stage of crack propagation was achieved mainly due to decrease in the rates in the zone of the concentrator (hole), which was obviously due to formation of a plasticity zone caused by overload.

5. With the distancing from the concentrator under the same overload, the effect of preloading on the rate of crack propagation decreased and at length  $L \geq 12$  mm was practically absent even under maximum overload  $K = 2.12$ .

6. The obtained results of studies of the effect of positive preliminary single overload on the characteristics of fatigue life were used to justify the service life of the airframe load-bearing structure of An-12, An 124 and An-124-100 aircraft.

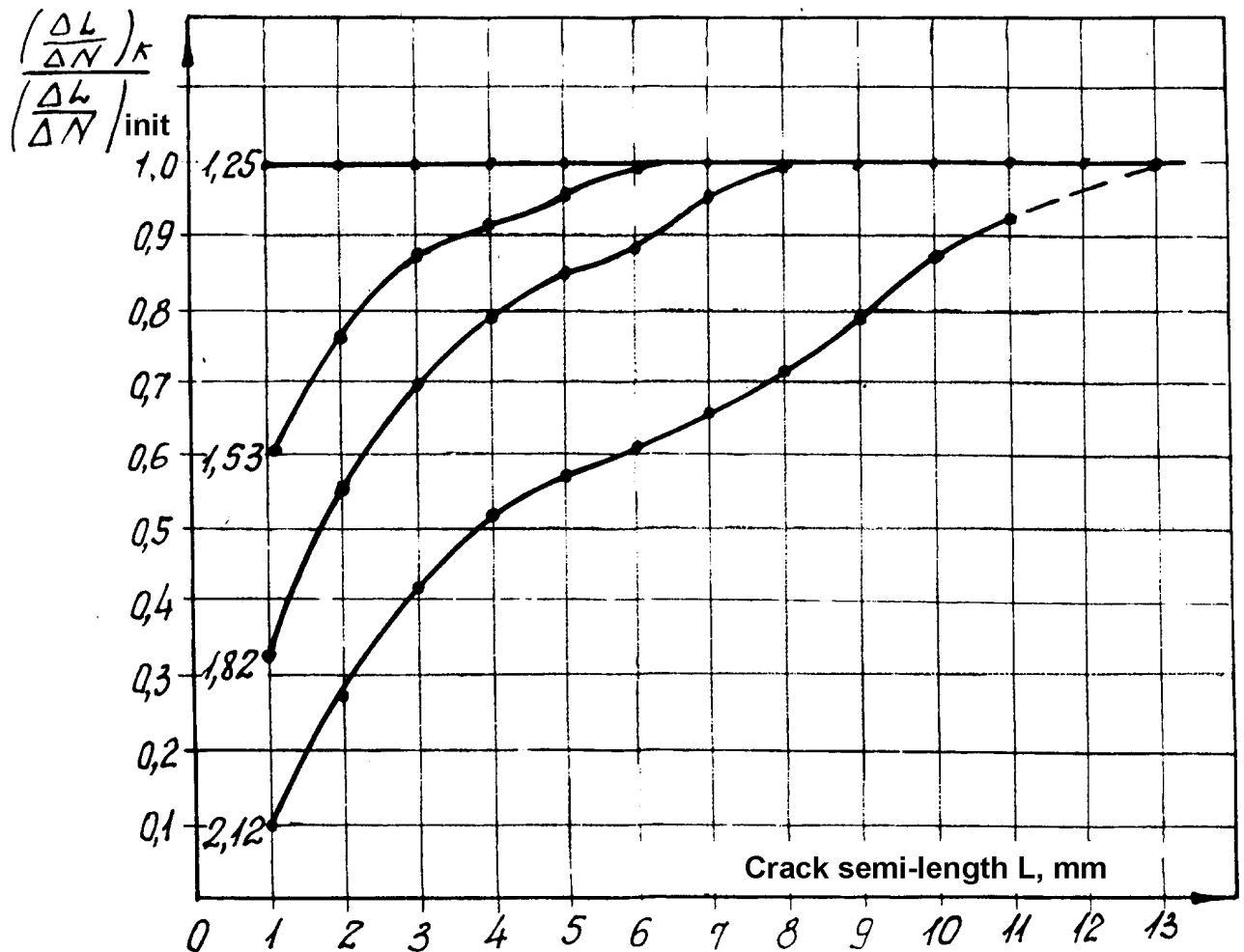


Fig. 8.15. Crack Propagation Relative Rate Under Different Overloads in Relation to Crack Semi-length

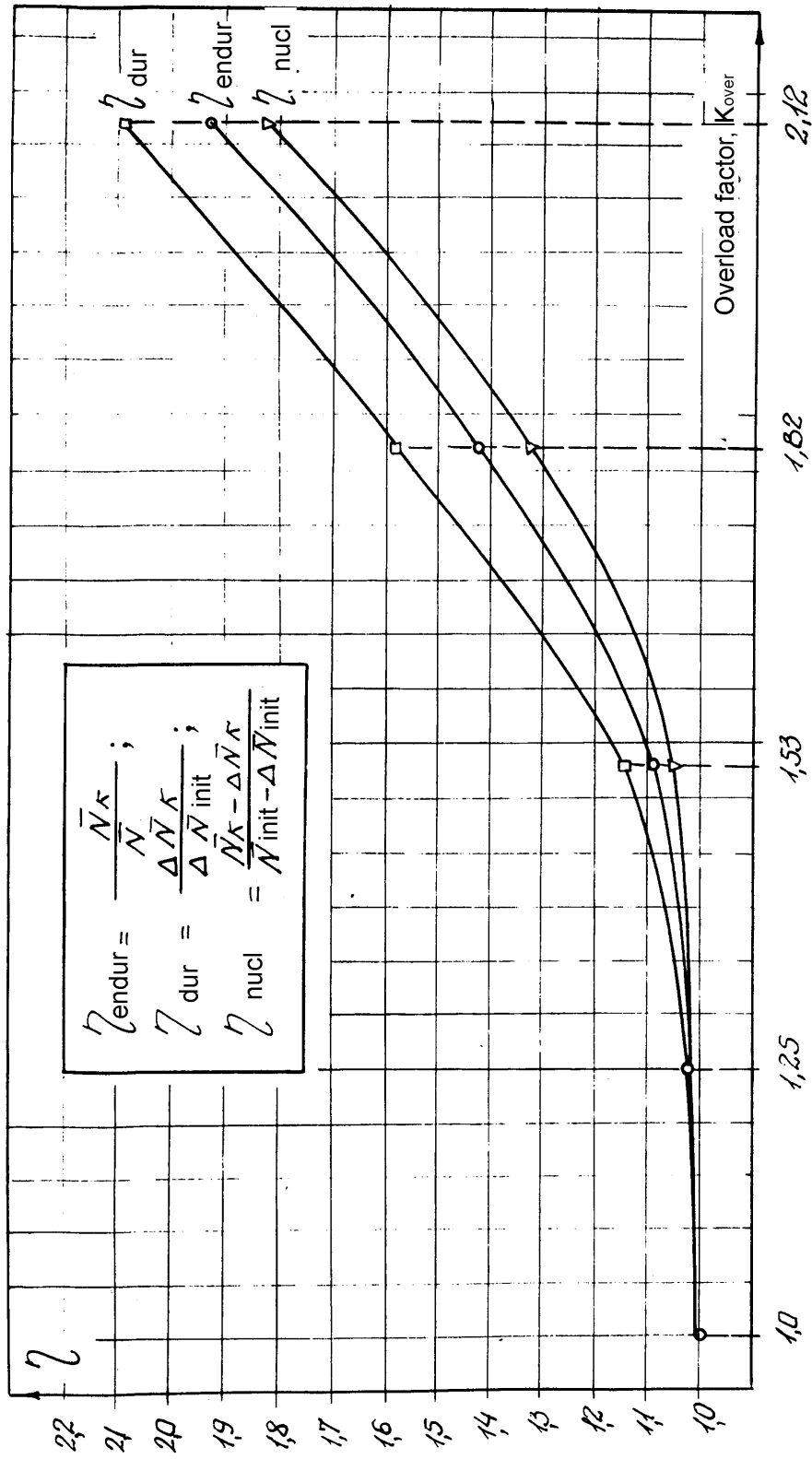


Fig. 8.16. Effect of Overload Factor  $K_{over}$  Upon Period Preceding Nucleation, Duration of Crack Propagation and Durability of Specimens

### 8.3. DEVELOPMENT OF METHOD INTENDED TO DETERMINE DAMAGE RATIO CAUSED BY CYCLIC LOADS AT STAGE OF FATIGUE CRACK PROPAGATION

As noted in subsection 7.1, the known method for determining the equivalents of the load damaging effect at the crack propagation stage requires testing a large number of specimens to obtain a relation between the crack propagation rate and load parameters  $\Delta\sigma$  and  $R$ .

The large number of test specimens required is determined by the following:

- testing of specimens should be carried out for each type of load;
- due to scattering of the test results for each type of load inherent to fatigue phenomenon, several specimens should be tested.

As a result, the test cycle is extended, labor intensity is increased, due to the need to manufacture a large number of specimens and test them. Therefore, the task was set to develop a technique for assessing the damaging effect of cyclic loads at the stage of fatigue crack propagation, which allows one to determine the equivalents between loads with a significantly lower labor intensity than the known one.

A significant reduction in the labor intensity of determining the equivalent of the load damaging effect at the stage of crack propagation in comparison with the known technique is achieved with the aid of the developed technique (Ref. [63]), which includes the same operations of loading specimens with comparable cyclical loads and determining the rate of crack propagation for each compared load, and operation of determining the equivalents of the load damaging action with respect to the crack propagation rate. However, in this technique, the types of loads with different parameters  $\Delta\sigma$  и  $R$ , compared with respect to the damaging action, are included in one loading implementation of one specimen, whereas in the known technique only one type of loads is included in one implementation.

Another difference of the technique [63] is that, when used, it is not necessary to construct the dependences of the  $da/dn \sim f(\Delta\sigma, R)$  form for each type of load compared. The load damaging effect can be judged by the width of non-fatigue grooves detected by the methods of electronic fractography, which correspond to the compared loading cycles. On the local sections of the fracture surface, the average value of the groove pitch step of the compared load cycles is calculated at certain intervals and equivalents are defined as the ratio of the average values of the groove pitch for different crack lengths. In order to exclude the phenomena of the load interaction, the measurements were carried out on the sections of the grooves became stable after the load change.

The essence of this technique is explained by the following example of a specific application. Equivalents of the damaging action of symmetrical loads in a specimen made of aluminum alloy B95pch were determined. The loading program (Fig. 8.17) contained five groups of compared loads (I-V), periodically repeated during the loading process. The average load value remained constant and was  $\sigma_m = 80$  MPa.

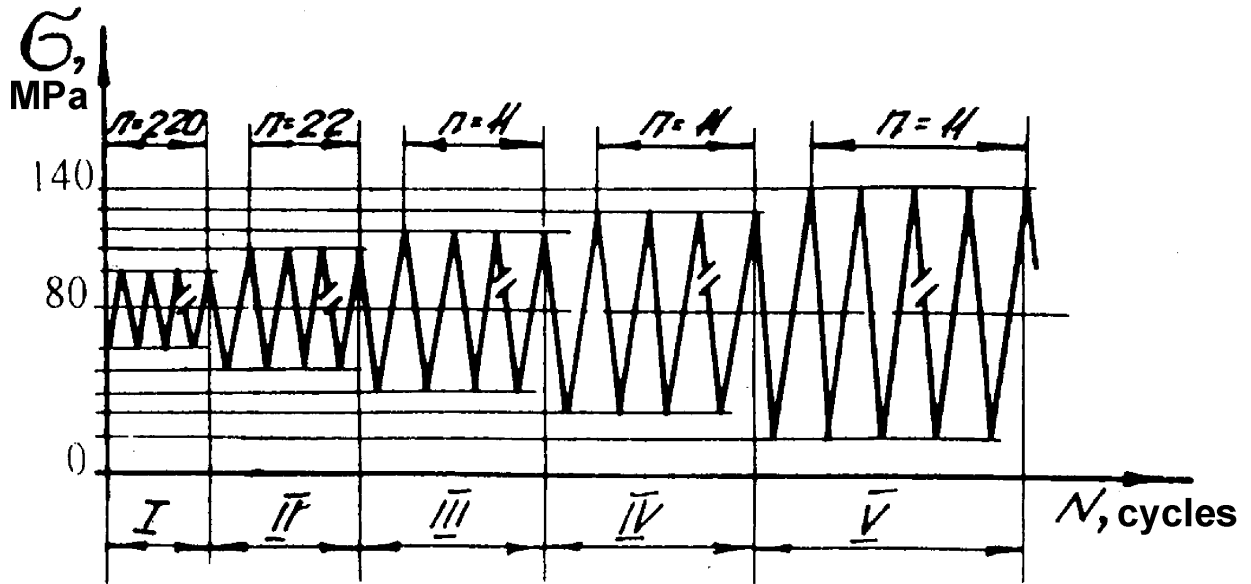


Fig. 8.17. Loading Program Having Five Types of Compared Loads.  
Top Figures Show Numbers of Cycles in Group

The amplitude of compared loads was as follows:  $\sigma_{aI} = 20$  MPa,  $\sigma_{aII} = 30$  MPa,  $\sigma_{aIII} = 40$  MPa,  $\sigma_{aIV} = 50$  MPa,  $\sigma_{aV} = 60$  MPa.

The number of cycles in the groups was variable – groups of cycles with smaller amplitudes included more cycles.

To identify fatigue grooves, the fracture of a specimen broken during testing was subjected to fractographic study using electronic microscope with magnification of 5,000 to 10,000 times.

On the fracture surface groups of grooves were identified, which pitch varied depending on the amplitudes of the program load cycles (Fig. 8.18).

With a successive study of the fracture in the direction of crack propagation, measurements of the groove pitch corresponding to different loads were periodically carried out with intervals ensuring sufficiently representative values.

Based on the obtained data of the groove pitch, averaged over the results of at least three measurements in one field of view, equivalents of the damaging effect of compared loads were calculated:

$$\varepsilon = b_i/b_j,$$

where  $\varepsilon$  is the equivalent of the damaging effect of compared loads;  $b_i$  is the groove pitch corresponding to the unit load cycle of group  $i$ ;  $b_j$  is the pitch increment corresponding to the unit load cycle of group  $j$ .

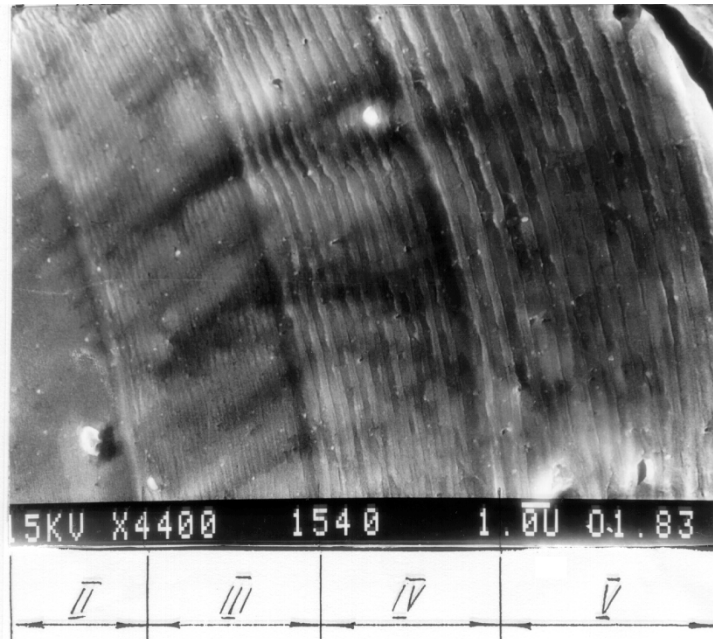


Fig. 8.18. Electronic Fractogram of Fracture Surface Area with Fatigue Grooves Corresponding to Cycle Groups (See Fig. 8.17)

Fig. 8.19 shows, as an example, the graphical dependence of the change in the equivalent of  $\varepsilon$  on crack length for loads of the *V* and *I* groups.

The developed procedure for determining the equivalents between loads at stage of crack propagation has a number of advantages:

1. Comparison of the groove pitch (microscopic values of crack propagation rate) corresponding to different loads is performed at local fracture surface areas, which virtually eliminates the effect of the heterogeneity of the material structure.

2. Since comparison of the load damaging effect was carried out on the fracture surface of the same specimen, then influence of scattering of the material properties, manufacturing technology, installation of the specimen in the testing machine, test conditions etc. was eliminated.

3. Elimination of the above-mentioned factors affecting the scattering of the crack propagation rate leads to significant reduction in the labor intensity and time of the experiment by reducing the required number of specimens.

4. For the determination of equivalents, the fatigue fractures of various test pieces, tested for other purposes in loading programs, can be used, for which it is possible to establish a unique mating of the loads and grooves.

5. Due to decrease in the number of factors affecting the dispersion of the results, and also due to combination of the compared loads in one load realization, in determining the equivalents by the proposed method, much smaller amount of experimental work is required. Thus, in the example given, one specimen was needed to determine the equivalents of the five different loads, and in the above method, approximately 30 specimens would be required.

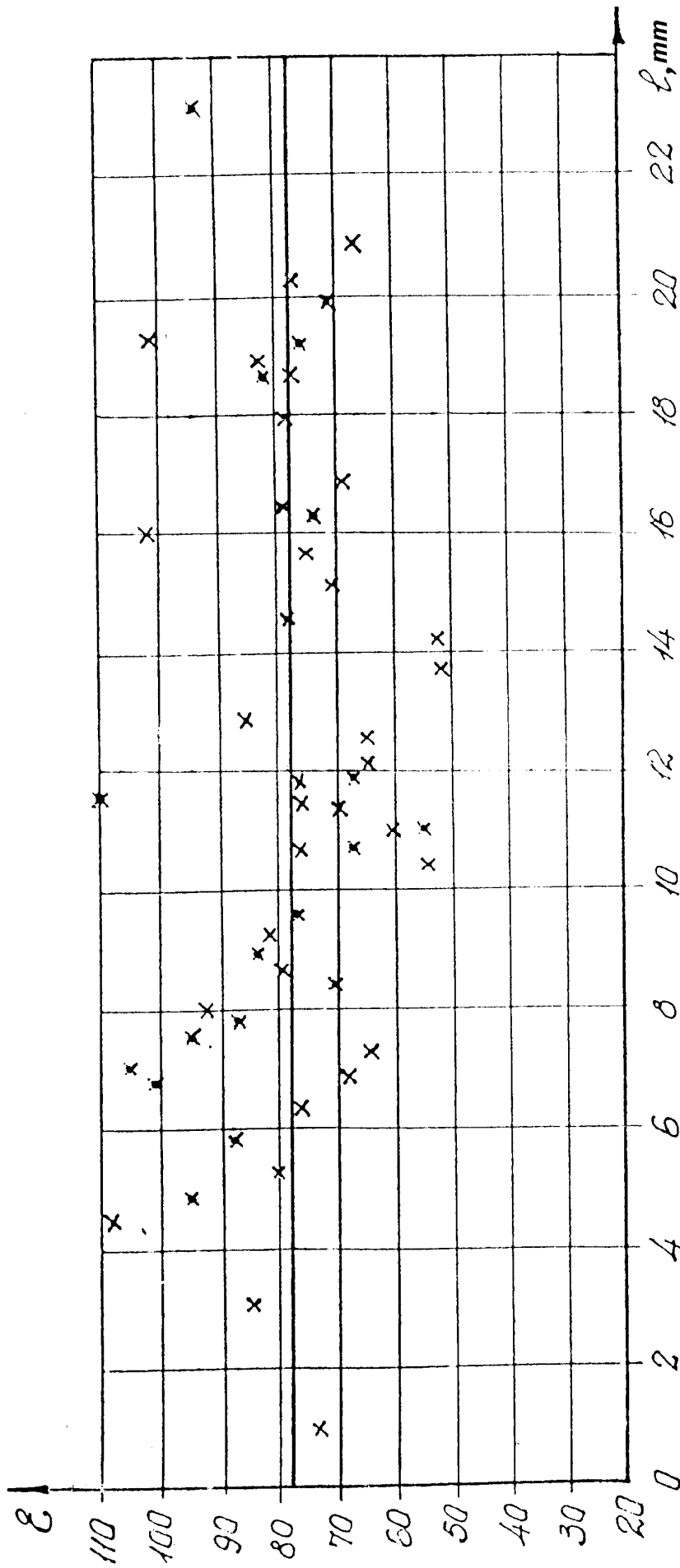


Fig. 8.19. Relation of Equivalent Stress ( $\varepsilon$ ) of Cycles with  $\sigma_a = 60$  MPa and 20 MPa and Crack Length  $L_{crack}$  under constant  $\sigma_m = 80$  MPa for B95pch Material



Application of the fractography method to determine the equivalents between loadings has a number of limitations associated with the conditions of groove formation and phenomena of mutual influence.

Thus, a technique has been developed for determining correlation of the damaging effect of cyclic loads at the stage of a fatigue crack propagation using the method of fractography and obtaining an author's certificate for an invention [63].

#### 8.4. INVESTIGATION OF COMPRESSION LOADS EFFECT UPON PROPAGATION RATE OF FATIGUE CRACK

The issue of the compressive loads effect at the fatigue crack propagation stage, despite numerous studies in this field, remains poorly understood due to the great complexity of the studies (see Subsection 7.1), therefore, obtaining any additional information on this issue is very actual [77]. The problem urgency rises in connection with the need to calculate the equivalents between cyclic loads at the stage of fatigue crack propagation (see subsection 8.5). The developed methods for marking the program loading (see subsection 8.1) allow such studies to be carried out with considerably less labor intensity. Because of the foregoing, the task was set to conduct an experimental study of the compressive loads effect at the fatigue crack propagation stage.

The studies were carried out with the help of the method for assessing the damaging effect of cyclic loads [63] (see subsection 8.3) on flat specimens cut from the pressed wing panels PK 0211 made of D16dchT and PK 14755 made of B95PhT1. The mechanical properties of the panels are given in Table 8.5.

Table 8.5.

Mechanical Properties of Panels

Panel Type	$\sigma_6$ , MPa	$\sigma_{0.2}$ , MPa	$\delta$ , %
Panel PK 0211	Length-wise 500...523 Cross-wise 512...528	382...417 373...400	106...116 120...134
Panel PK 14755	Length-wise 602...620 Cross-wise 615...621	560...580 575...578	125...130 105...125

Specimens were cut from the panel web in the longitudinal direction and processed by milling to a thickness of 10 mm. The shape and dimensions of the specimens are shown in Figure 8.20, a.

To accelerate propagation of the cracks the corner cuts were made from both sides of the holes made in specimens. The cuts were made mechanically.

The correctness of installation of the specimens in the testing machine was controlled by means of stress strain gauges.

Specimens were tested using the electrohydraulic test machine for 40 tf with a control computer.

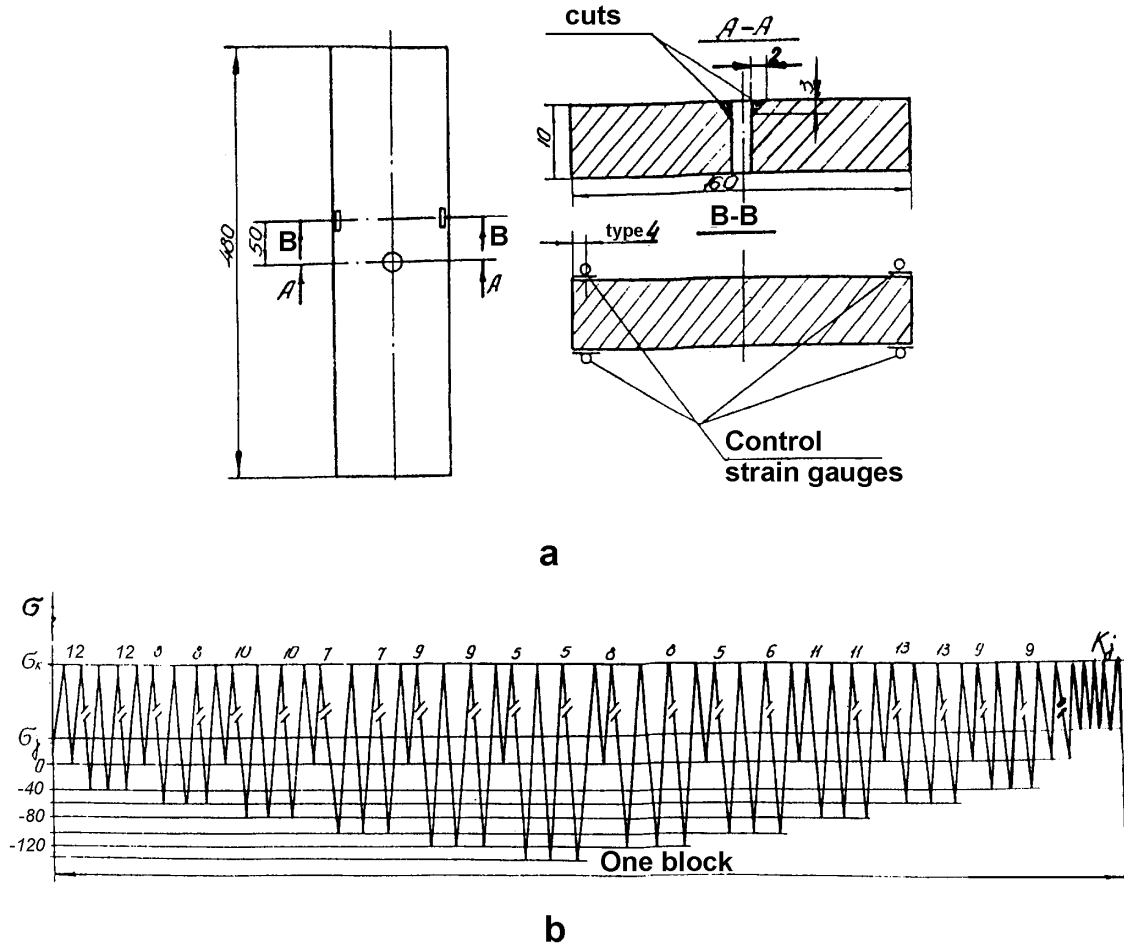


Fig. 8.20. Specimens Made of D16chT and V95Pch (a) and Loading Program (b) to Determine Compressive Load Effect upon Crack Propagation Rate: a – Specimens; b – Loading Program

The tests were carried out under laboratory ambient conditions at room temperature. The loading frequency was  $f = 0.5 \dots 1.5$  Hz. The tests were carried out to failure of the specimens. Several load programs were used. The type of load program type I is shown in Fig. 8.20, b.

The program contained a sequence of groups of symmetrical and repeated stress cycles with a constant maximum stress level for each specimen. During tests, maximum values were as follows:  $\sigma_{max} = 80, 100, 120$  and  $140$  MPa.

Minimum values of the groups of symmetrical cycles gradually decreased from group to group with a step  $\Delta\sigma = -20$  MPa (from the level  $\sigma_{min} = -40$  MPa to the level  $\sigma_{min} = -140$  MPa), and then increased with the same step to the original minimum level.

Change in the loading sequence (decrease-increase) was envisaged in order to exclude (or detect) possible mutual influence of cycles. For convenience of fractographic analysis, the loading program was marked (see subsection 8.1):

After working out 10 blocks, the values of  $K_j$  were repeated. The number of

cycles should be determined from the number of upper peaks.

The number of cycles from group to group changed in the block; after each block of loads, one "laboratory flight" was inserted into the loading sequence with the variable number of dynamics cycles in flight from block to block (Tables 8.6 and 8.7, Fig. 8.20, b).

Table 8.6

Variable Number of Dynamics Cycles in Flight from Block to Block

Specimen Number	10	11	12	13
$\sigma_k$ , MPa	140	120	100	80
$\sigma_j$ , MPa	50	40	30	30

Values of  $K_j$  for different blocks are given in Table 8.7.

Table 8.7.

Values of  $K_j$  for different blocks

Block number, $j$	1	2	3	4	5	6	7	8	9	10
Value of $K_j$	5	10	7	9	6	11	5	8	12	7

This is the main test program, the results of which had revealed the effect of the cyclic load negative part.

The load program of type II (Figure 8.21) was a sequence of symmetrical cycles  $\sigma_u = \pm 100$  MPa, and the load program of type III (figure 8.22) was a sequence of zero-to-tension cycles  $\sigma_{max} = +100$  MPa. These programs were also marked. After every 1000 cycles (a block), marks were introduced in the loading sequences of program II and III, consisting of ten "laboratory flights" with number of flight cycles, which varies from the block to the block.

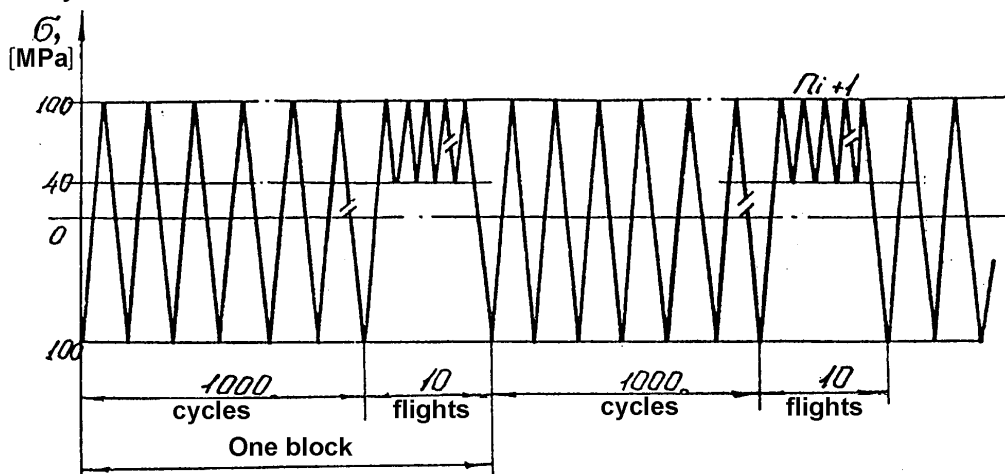


Fig. 8.21. Loading Sequence for Specimens (Program II)

Values of  $n_i$  for different blocks are given in Table 8.8.

Table 8.8.

Values of  $n_i$  for Different Blocks

Block Number, $I$	1	2	3	4	5	6	7	8	9	10
Value of $n_i$	5	10	7	9	6	11	5	8	12	7

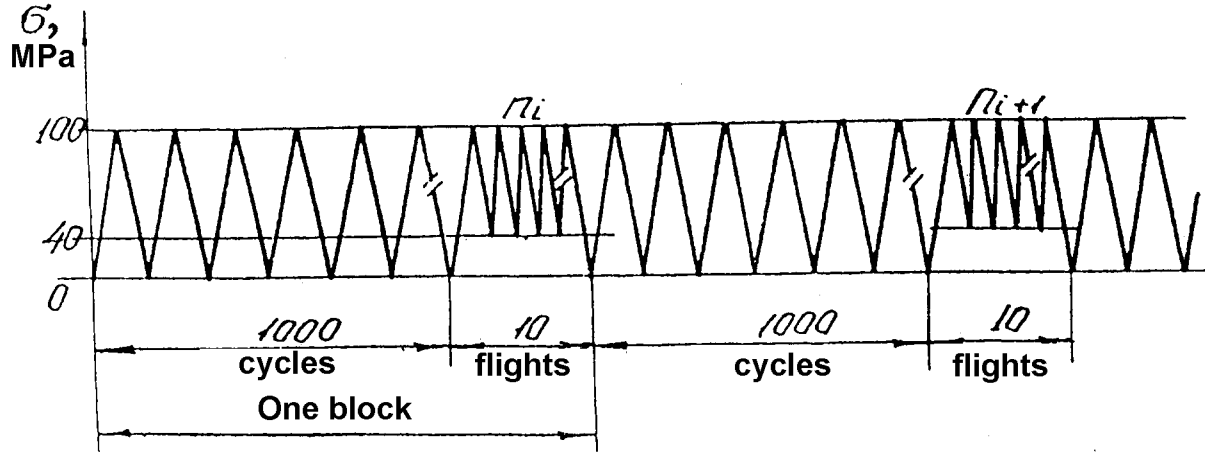


Fig. 8.22. Loading Sequence for Specimens (Program III)

The number of cycles was determined by the number of upper peaks. After working out 10 blocks, the loading was repeated.

The loads in programs II and III corresponded to the existing method of determining the equivalents (see subsection 8.4) and were intended to verify the results obtained for program I for a single value of symmetrical and repeated stress cycles ( $\sigma_a = \pm 100$  MPa and  $\sigma_m = + 100$  MPa, respectively).

8 specimens were tested under program I (4 of them were made from material D16chT and 4 of them were made from material V95pch). Maximum stress levels and mean time to failure are given in Table 8.9. Change in the compressive loads remained the same for all the specimens.

Table 8.9.

## Maximum Stress Levels and Mean Time to Failure

Specimen Number	$\sigma_{max}$ , MPa	Mean Time to Failure (Blocks + Cycles)	
		D16chT	V95pch
1	80	220 bl. + 86 cl.	253 bl. + 91 cl.
2	100	130 bl. + 167 cl.	149 bl. + 75 cl.
3	120	61 bl. + 107 cl.	91 bl. + 15 cl.
4	140	43 cl. + 20 cl.	52 bl. + 156 cl.

12 specimens were tested under programs II and III, 6 specimens were made of D16chT and V95pch materials.

Values of mean time to failure are given in Table 8.10.

Values of Mean Time to Failure

Specimen Number	Type of Loading	Mean Time to Failure (Cycles + Standard flights)	
		D16chT	V95pch
5	Symmetrical cycle $\sigma_a = \pm 100$ MPa	24437 cl. + 240 t.fl.	24542 cl. + 240 t.fl.
6		20114 cl. + 200 t.fl.	21613 cl. + 210 t.fl.
7		21855 cl. + 210 t.fl.	28450 cl. + 280 t.fl.
8	Repeated stress cycle $\sigma_{max} = +100$ MPa	29680 cl. + 290 t.fl.	33189 cl. + 330 t.fl.
9		39538 cl. + 390 t.fl.	31519 cl. + 310 t.fl.
10		31424 cl. + 310 t.fl.	27737 cl. + 270 t.fl.

The failure of the specimens occurred due to cracks that propagated from the cut at the central hole.

The fractures of the destroyed specimens were subjected to fractographic investigation with the help of an optical microscope having magnification of 1500, the EVM-100L electronic transmission microscope and the JSM-35c scanning microscope. The fractures were photographed, the schemes of their structure were compiled. The research directions were chosen parallel to the lateral surface of the specimens at a distance of 1 mm. Measurements of the coordinates of crack lengths using the optical microscope were carried out with a dial gauge having a 0.01 mm division value.

While testing in the transmission electron microscope a two-step plastic-carbon replica technique was applied with chromium shade in the direction of crack growth. Replicas were cut in such a way that their centers were located along the chosen direction of research. When studying replicas with the electron microscope, the groups of grooves were identified and correspondence of these groups to the cycles of various program loads was established. Orientation on the replica was allowed because of the presence of grooves, corresponding to the inserts of laboratory flights  $K_j$  between the blocks of loads, as well as the fact that the first groove corresponding to the pulsating cycle in each group differed in color.

The replicas were studied in the region of stable crack growth, as long as the possibility of linking the observed grooves to the test program remained. The replica sites with groups of grooves were photographed with magnifications that provide clear outline of the groove boundaries and their optimal dimensions. When photographing, areas with continuous striation were selected, which do not have defects that distort the dimensions of discontinuities, deformations, and distortions. The accuracy of determining the coordinates on the replica was  $\pm 0.1$  mm. In order to increase the amount of data and reliability of the results the replicas were repeatedly duplicated. When examined with the scanning electron microscope, fractures were subjected to preliminary ultrasonic cleaning, ion etching and decoration. The fracture was exposed in the micro-

scope chamber in such a way that the direction of the investigation was parallel to the direction of one of the objective table displacements. The scale division value of the adjusting wheel to measure the movement was 2 microns. Accelerating voltages of 15 ... 30 kV were used.

To obtain objective data and possibility of duplication, the groove pitch measurements were carried out using electronic fractograms. As an example, Fig. 8.23 shows electronic fractograms of the surface portions of the specimen from D16chT material with groups of repeated stress and symmetrical cycles obtained on the transmission electron microscope. The fractograms show the groups of grooves corresponding to repeated stress and symmetrical cycles.

The marking of the fractograms was carried out perpendicularly to the front of the cracks in the direction of their propagation. Measurements of the groove pitch were carried out using the MBS-2 microscope, the scale division value was of 0.1 mm. The pitch of a single groove was determined as the average value of the pitch of the measured group of grooves, referred to their number:

$$\delta = \Delta L/n.$$

The values of the pitch of the grooves of the repeated-stress cycles  $\delta_n$  and symmetrical cycles  $\delta_s$ , as well as their ratios-equivalents  $\varepsilon$  were recorded in the tables. Based on the data obtained, graphical dependences of crack growth rate on crack length, as well as graphs for equivalents, were built. The values of the equivalents were determined starting from crack lengths  $L_{crack} \approx 2.0$  mm (including the cut).

Approximation of the experimental results was carried out by the least squares method according to the linear law and the second-order curve for the equivalents (both dependences were plotted on one graph) and the second-order curve for crack propagation rates. The mathematical processing of data and the construction of graphs were carried out with the help of the computer.

Specimens tested according to programs II and III were analyzed with the optical and electronic scanning microscopes in order to plot the cracks propagation rates. With a consistent study of the fracture surface in the direction of the investigation, separated from the lateral surface of the specimen by distance of 1 mm, identification of the laboratory flight marks was carried out.

The increment of crack length over the loading interval between inserts (1000 cycles) was measured. The accuracy of the displacement measurement was 0.005 mm. According to the obtained data, graphical dependences of the crack propagation rate vs length were constructed. Approximation of the experimental results was carried out using the method of least squares. Equivalents ( $\varepsilon$ ) between the loads of programs II and III were determined from the corresponding crack growth curves.

### **Results of Studying Specimens Tested Under Program I**

In accordance with the described procedure, specimens No. 1, 2, 3, 4 (material B95) and specimen No. 1 (material D16) tested under program I were investigated. Usage of marked loading programs made it possible to find clear correspondence between the observed grooves and those causing their loading cycles.

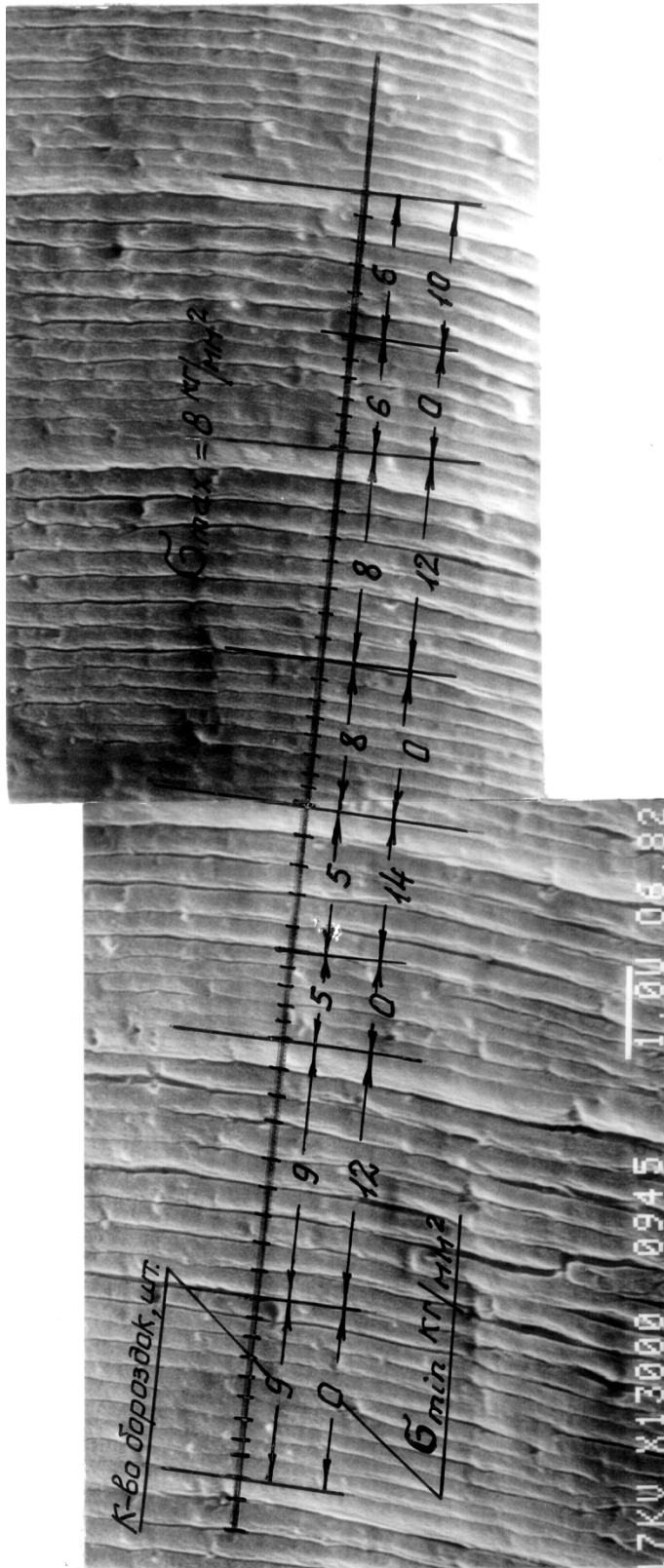


Fig. 8.23. Electronic Fractograms of Fracture Surface Sites of Specimen from D16chT, Tested According to Program Given in Fig. 8.20 (Magnification of 7000)

When analyzing the fractograms of specimens tested under program I, it was established that the grooves corresponding to the symmetrical cycles have larger step than grooves corresponding to repeated-stress cycles. The greatest difference in the step was observed for small crack lengths.

Measurements of the groove pitch have shown that an increase in the

compressive stress causes an increase in the groove pitch, i. e. contributes to an increase in the damaging effect of the load. However, as the crack grows, the difference between the grooves corresponding to the compared cycles decreases and the grooves of the repeated-stress and symmetrical cycles become commensurable. Fig. 8.24 shows the graph of change in pitch of grooves for symmetrical cycles along the crack length as a function of  $\sigma_{min}$  in specimen No. 1 (material B95). Maximum stresses for this specimen were  $\sigma_{max} = 80$  MPa. It can be seen from the figure that as the compression ratio increases, the growth rates of cracks increase.

When measuring the groove pitch of repeated-stress cycles in groups adjacent to groups of symmetrical cycles with different compressive stresses, no significant spread of the grooves of repeated stress cycles was observed. The graph of the pitch change of these grooves in specimen No. 1 is shown in Fig. 8.25.

While studying the remaining specimens, similar regularities were revealed. Determination of the correlation of the damaging action of symmetrical and repeated stress cycles in specimens No. 1 ... 4 (material B95pch) and specimen No. 1 (material D16hT) was carried out in two ways:

1. By the ratios of the groove pitch of various cycles measured on fractograms in local zones. In this case, there was no need to determine the true values of the groove pitch, it was sufficient to measure their dimensions on the same electronic fractogram. The resulting length ratios were then approximated by the least squares method using linear relationship.

2. From the approximated growth rates of cracks for symmetrical and repeated stress cycles, determined with allowance for the increase in fractograms.

The first way to determine the ratios of the damaging action of loads is less time-consuming, since it is not necessary to determine the absolute values of the rates. However, since the nature of the equivalents variation along the crack length was not known in advance, an uncertainty appeared in the approximation of the obtained data.

The second way to determine the equivalents by comparing the crack growth rates with the approximated curves in this case was a test, since the general nature of the dependence of the rate vs crack length was known.

This method is more laborious, since it requires construction of three curves (two for rates and one for equivalents) instead of one curve for equivalents in the first way. In this work, both methods described were used to develop the technique.



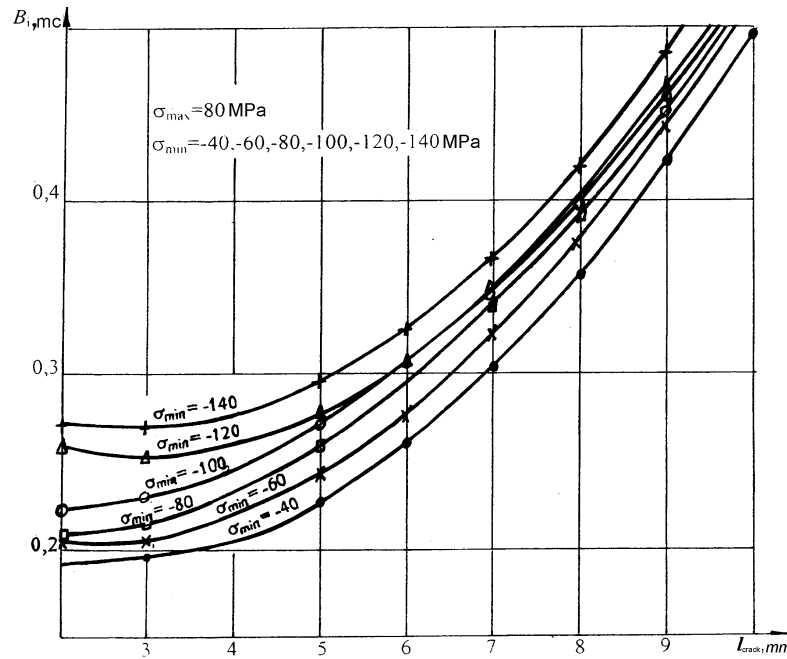


Fig.8.24. Change of Groove Pitch  $B_i$  over Crack Length  $L_{crack}$  in Relation to  $\sigma_{min}$  in Specimen No. 1 Made of V95 Under Symmetrical Load  $\pm (-140)$ ;

$\Delta$  - (-120);  $\circ$  - (-100);  $\square$  - (-80);  $x$  - (-60);  $\bullet$  - (-40)

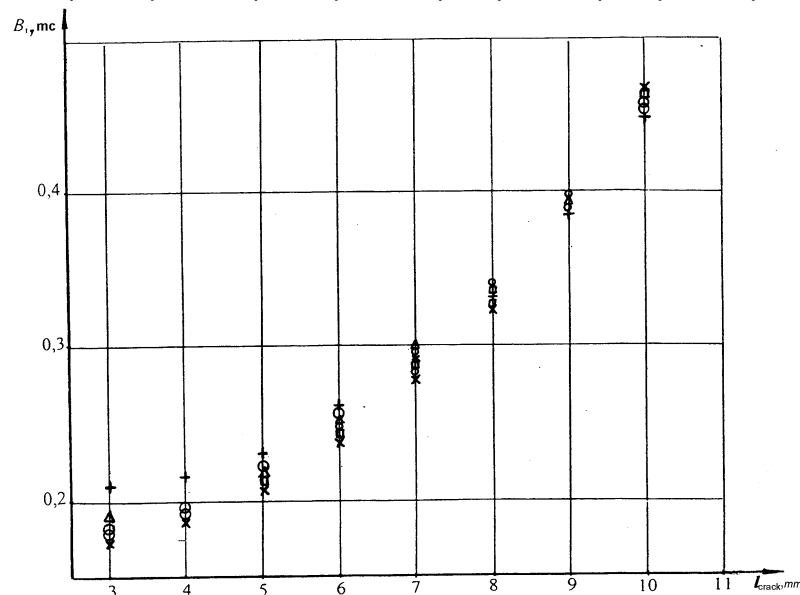


Fig. 8.25. Change of Groove Pitch  $B_i$ , Corresponding to Repeated-Stress Cycles, Adjacent to Symmetrical Cycles of Different Degree of Compression ( $\sigma_{min}$ ), Specimen No. 1, Material V95:

$\bullet$  - (-40);  $x$  - (-60);  $\square$  - (-80);  $\circ$  - (-100);  $\Delta$  - (-120);  $+$  - (-140)

Results of data processing in both cases were practically the same and values of  $\varepsilon$  were described with linear dependence rather well. Grafical dependences of equivalents  $\varepsilon$  vs crack length under different parameters of loads  $\sigma_{max}$  and  $\sigma_{min}$  for materials V95pch and D16chT are shown in Figs 8.26, 8.27.

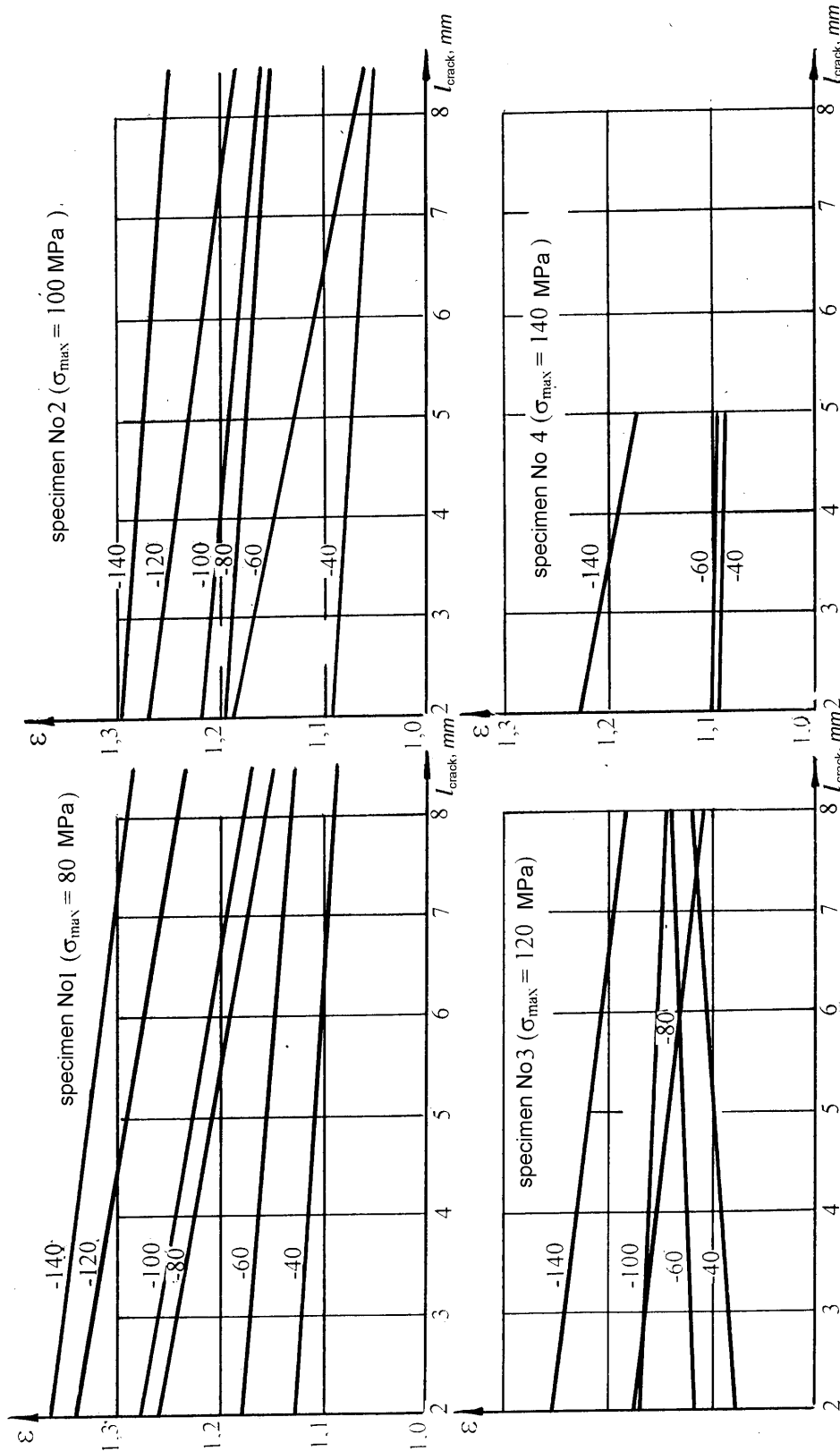


Fig.8.26. Ratios of Damaging effect of Symmetrical and Repeated Stress Cycles  $\varepsilon$  over Crack Length  $L_{crack}$  in Relation to  $\sigma_{max}$  and  $\sigma_{min}$  in Specimens Made of V95

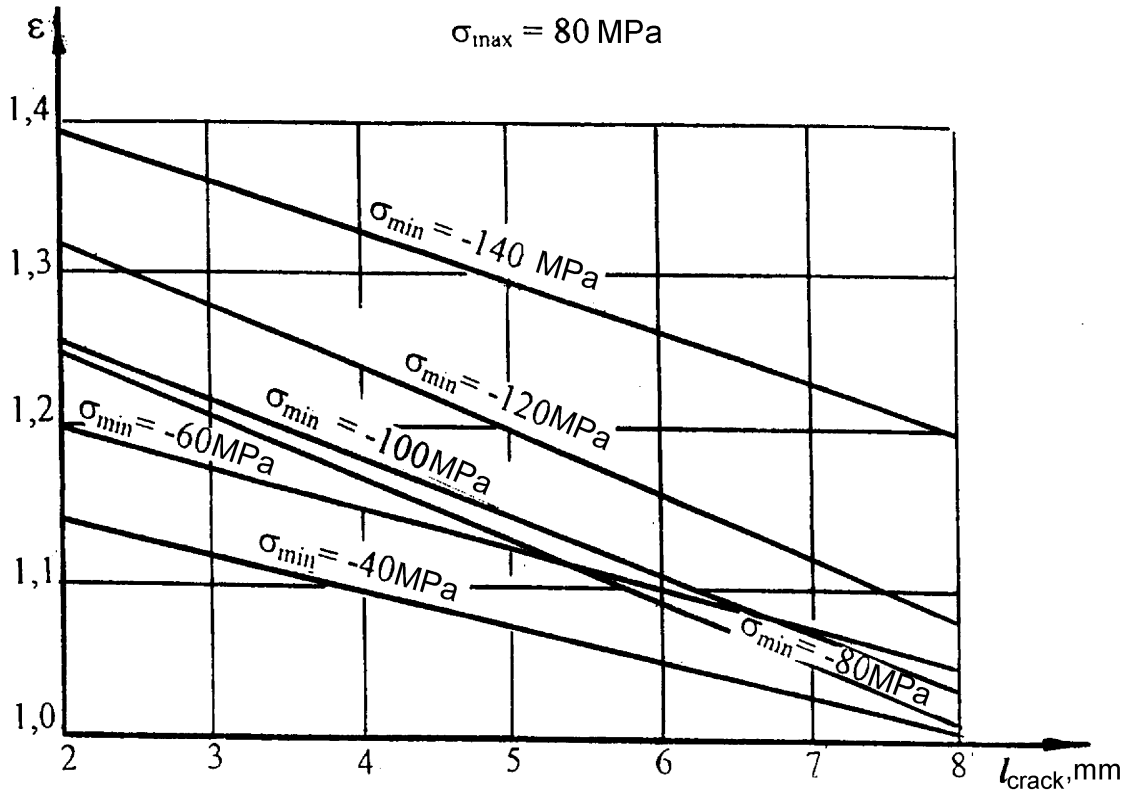
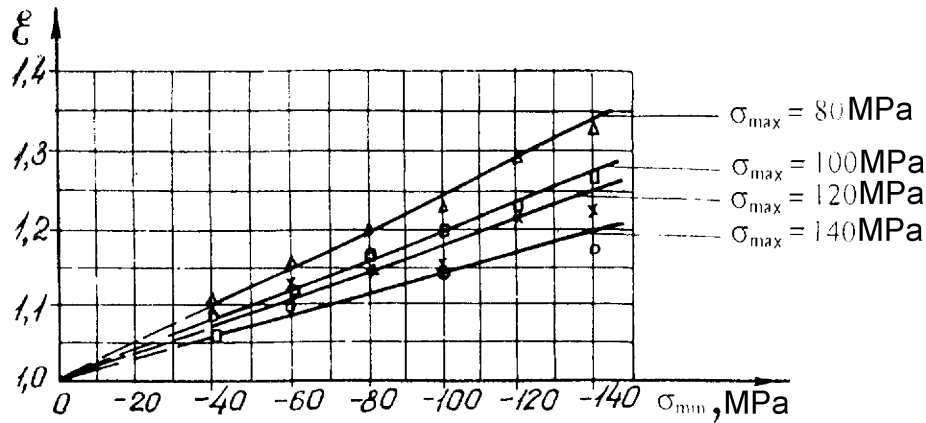


Fig. 8.27. Ratio of Damaging Effect of Symmetrical and Repeated Stress Cycles  $\varepsilon$  Over Crack Length  $L_{crack}$  in Relation to  $\sigma_{min}$ , Specimen No. 1, D16chT

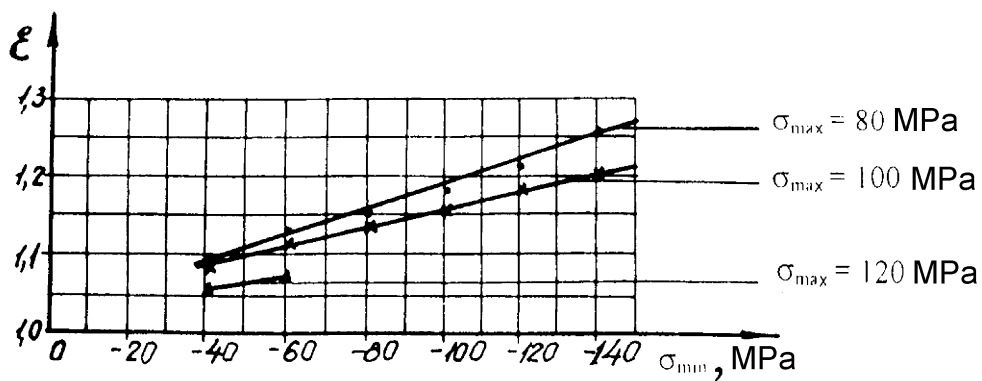
Fig. 8.28 shows sections of these dependences for materials V95Pch and D16chT for crack length  $L = 5 \text{ mm}$ . The dependences given above show that symmetrical loads have greater damaging effect in comparison to repeated stress cycle loads of the same maximum level. Their damaging effect depends on several parameters – the magnitude of compressive and tensile loads and the crack length. This dependence is manifested as follows:

- when the compressive stresses increase, damaging effect of the load increases;
- with increasing tensile stresses, the effect of compressive loads decreases;
- with increasing crack length, damaging effect of the compressive loads also decreases.

However, even for the case of the largest compressive stresses studied,  $\sigma_{min} = -140 \text{ MPa}$  and the smallest maximum load studied,  $\sigma_{max} = 80 \text{ MPa}$ , the compression effect did not exceed 40% for both materials. The minimum impact value was not less than 8%. It should be noted that with an increase in maximum load level and corresponding increase in the rate of crack propagation, the scatter of the  $\varepsilon$  values (in specimens No. 3 and 4) increased. In this case, there were some deviations from the regularity of the mutual arrangement of the  $\varepsilon$  graphs. However, the  $\varepsilon$  average values along the crack length retained the tendency of a monotonic increase with increasing compressive stresses.



a



b

Fig. 8.28. Change of Damaging Effect Ratios of Symmetrical and Repeated Stress Cycles  $\epsilon$  in Relation to  $\sigma_{min}$  and  $\sigma_{max}$ ,  $L_{crack} = 5$  mm: a – V95; b – D16

### Checking for Absence of Cycles Mutual Influence

The damaging effect of compressive loads may be invoked by the following factors:

- their direct influence on the crack development;
- an adverse effect of loads interaction.

It is known that for cycles with constant maximum loading level and positive asymmetry coefficient, the loading sequence does not have significant effect on the crack growth rate [62]. In this paper, maximum level remained constant throughout the loading process. However, since the program contained compressive loads of different amounts, it became necessary to establish whether the cycles had mutual effect.

The greatest effect could be expected where the repeated stress load was placed next to the cycles with the maximum compression, i.e. where there was maximum amplitude difference. Therefore, the sequence of loading was chosen according to the principle of increasing-decreasing of the influencing factor. In such an implementation (see Fig. 8.20, b), the consecutive increase of the compressive loads was replaced with the same decrease. Then, in the presence of mutual influence, it was possible to consider only the growth rates of

cracks corresponding to the stages of increase in compressive loads, assuming that under inverse loading sequences, mutual influence of the previous stage will be removed. And, on the contrary, in the absence of mutual influence, an entire implementation could be used to estimate the equivalents.

The presence or absence of mutual influence could be detected by comparing the groove pitch corresponding to different groups of repeated stress cycles in the area of increasing and decreasing compressive loads, and also by changing their step inside the groups.

A comparison of the groove pitch of the groups of repeated stress cycles following the different groups of symmetrical cycles did not reveal any patterns that indicate presence of mutual influence, while for the symmetrical cycles themselves, which differ in compressive loads, such regularities were obvious.

The ratios of the groove pitch of repeated stress cycles before and after groups of symmetrical cycles were both exceeding and smaller the unit, regardless of the stage of increasing-decreasing compressive loads. On average, the difference in the groove pitch did not exceed 4%, which was commensurate with the local spread and the error of measurements (see Figs 8.29, 8.31).

Analysis of the fractograms of the tested pieces has shown that within the groove groups of repeated stress cycles there was also no systematic change in their pitch.

Thus, it can be assumed that in the load programs used there was practically no mutual influence of the cycles.

### Checking the results

The results obtained were checked for one of the values of cyclic loads, namely: symmetrical cycles with  $\sigma_a = \pm 100$  MPa and repeated stress cycles with  $\sigma_a = 100$  MPa in the traditional way for programs of type II and type III.

The load program of type II was a sequence of symmetrical cycles  $\sigma_a = \pm 100$  MPa, and the load program of type III was a sequence of repeated stress cycles  $\sigma_a = + 100$  MPa.

For marking every 1000 cycles (a block) in the loading sequence II and III marks were introduced, consisting of 10 "laboratory flights" with a variable number of flight cycles in a flight from block to block.

The specimens No. 5, 6, 7 and No. 8, 9, 10 of materials B95 and D16 were tested under programs II and III, respectively. As already noted, for programs II and III, the values of equivalents were determined by comparing the growth rates of cracks in specimens tested with the application of symmetric and repeated stress loads. Since in these programs mutual influence of cycles was deliberately excluded, as each of them contained the same type of load, the comparison of the obtained data with the results of program I made it possible to additionally verify that mutual influence of the cycles in program I did not take place.

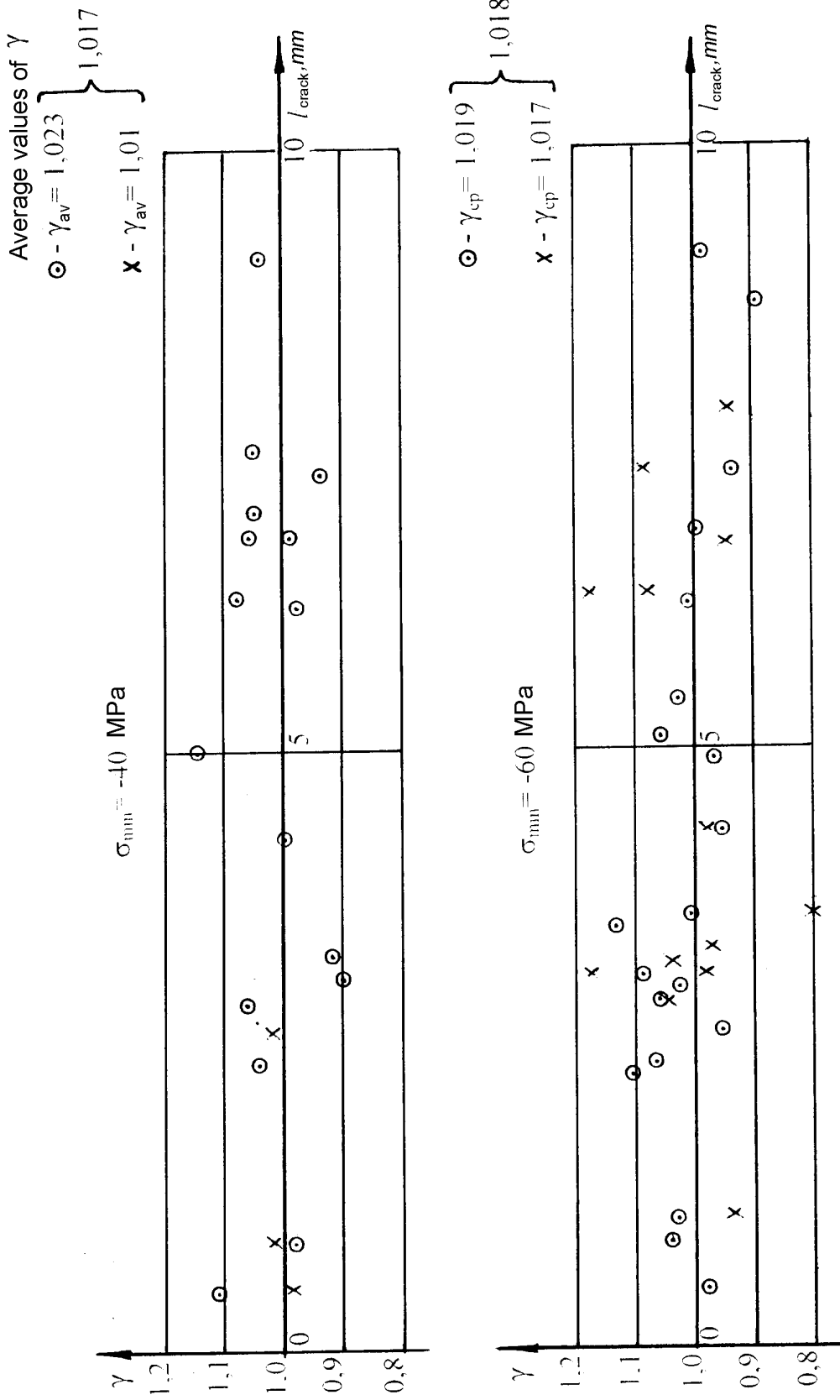


Fig. 8.29. Groove Pitch Ratios  $\gamma$  of Repeated Stress Cycles Following Groups of Symmetrical cycles to Groove Pitch of Previous Repeated Stress-cycle Along Crack in Material B95:  
 O - in Zone of Decreasing Compression, X - in Zone of Increasing Compression

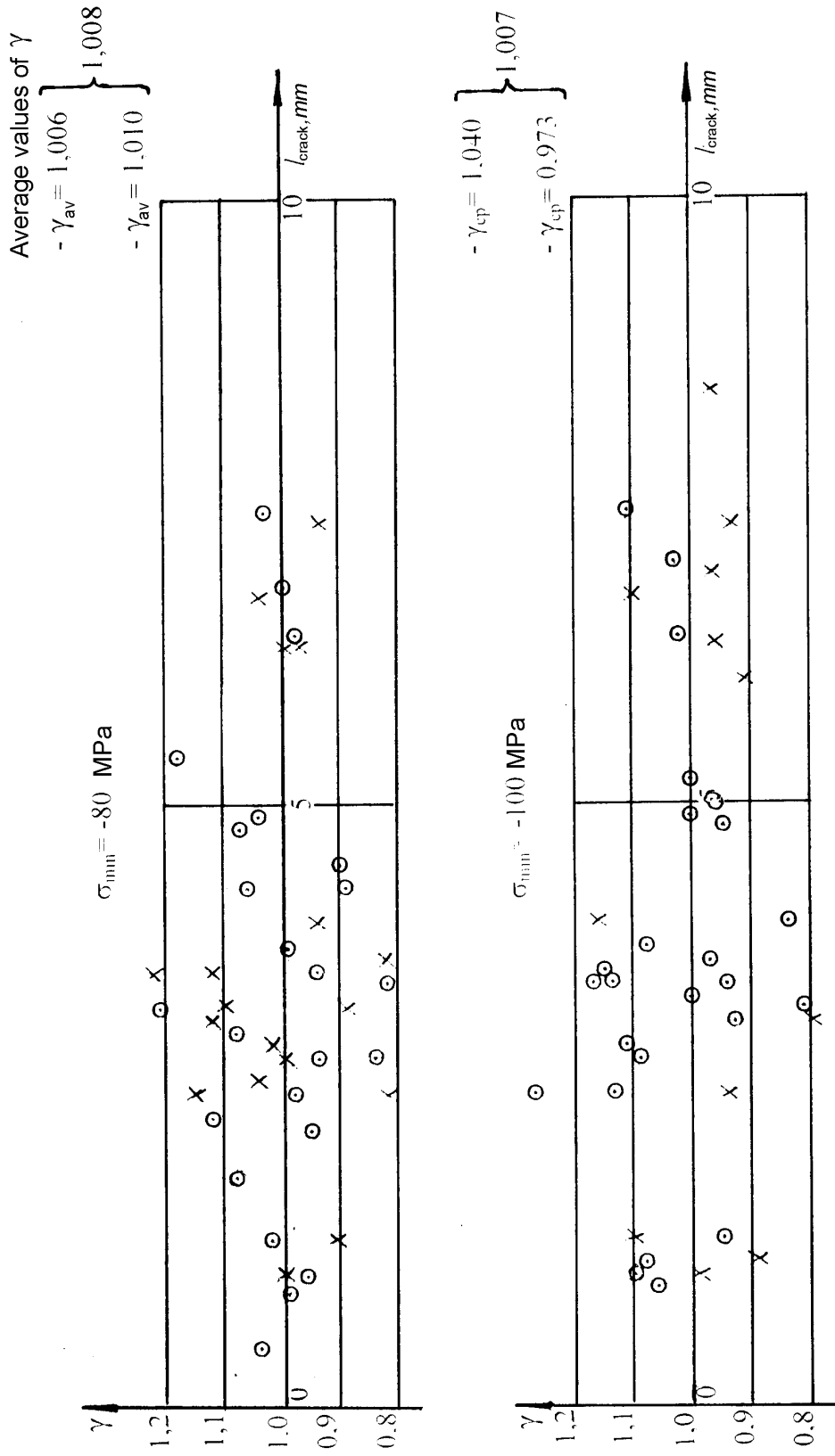


Fig. 8.30. Ratio of Groove Pitch  $\gamma$  of Repeated Stress Cycles Following Groups of Symmetrical cycles to Groove Pitch of Previous Repeated Stress Cycle Along Crack in Material B95:  
 O - in Zone of Increasing Compression, X - in Zone of Decreasing Compression

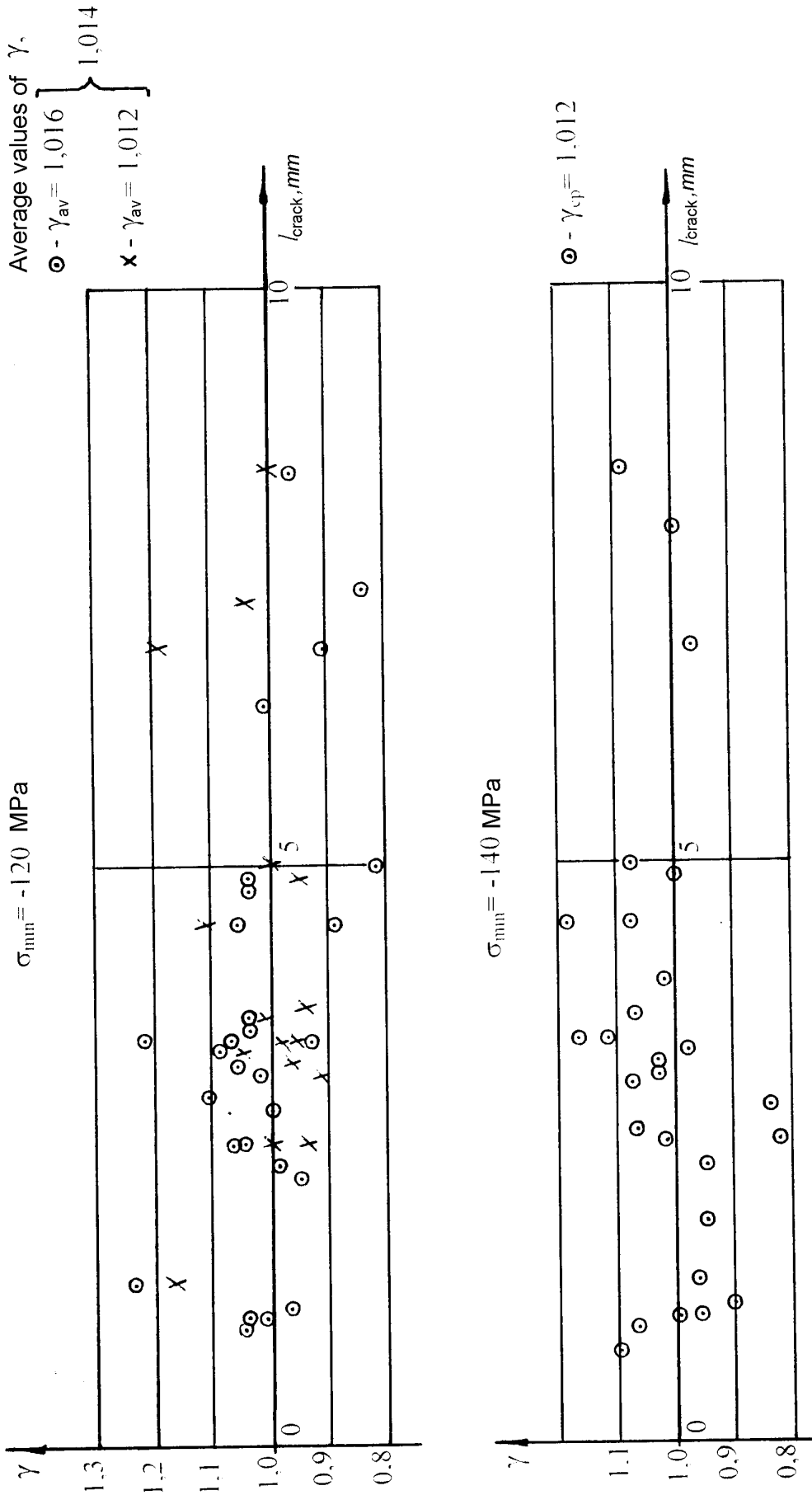


Fig. 8.31. Groove Pitch Ratios  $\gamma$  of Repeated Stress Cycles Following Groups of Symmetrical Cycles to Groove Pitch of Previous Repeated Stress Cycles Along Crack in Material B95:  
 O - in Zone of Increasing Compression, X - in Zone of Decreasing Compression



It should be noted that when using the methodology with the application of program I, the amount of experimental studies on the number of required specimens is an order of magnitude lower than in the comparative trials under programs II and III. Indeed, in order to obtain the data for  $\varepsilon$  shown in Fig. 8.26, four specimens were required for the testing under program I, while for the production of the same data under programs II and III, 84 specimens would be required, from the condition of three specimens per load. In addition, the program I trial eliminated variability of data associated with differences in test conditions. All this increased the reliability of the data obtained.

Under programs II and III, 12 specimens were tested - six specimens of D16hT and six specimens of B95pch.

The operating time before failure is shown in Table 8.11.

Table 8.11.

## Operating Time Before Failure

Specimen No.	Type of Loading	Operating time before failure (cycles + lab flights)	
		D16chT	B95pch
5	Symmetrical cycle $\sigma_a = \pm 100$ MPa	24437 ccl + 240 lab.fl.	24542 ccl + 240 lab.fl.
6		20114 ccl + 200 lab.fl.	21613 ccl + 210 lab.fl.
7		21855 ccl + 210 lab.fl.	28450 ccl + 280 lab.fl.
8	Repeated-stress cycle $\sigma_{max} = 100$ MPa	29680 ccl + 290 lab.fl.	33189 ccl + 330 lab.fl.
9		39538 ccl + 390 lab.fl.	31519 ccl + 310 lab.fl.
10		31424 ccl + 310 lab.fl.	27737 ccl + 270 lab.fl.

Determination of the crack growth rates in the specimens tested according to programs II and III was carried out on the basis of measurements of the crack increments over the loading intervals between the marks. In accordance with the measurement data, graphs of the crack growth rates in the specimens for symmetric and repeated loads in materials B95 and D16 were constructed. These graphs are given in Fig. 8.32.

For each load, the graphs were plotted on the basis of averaging the results of studying three specimens (crack growth rates were measured in six fatigue zones within stable growth areas  $L_{crack} = 2 \dots 15$  mm). It can be seen from the graphs that the crack growth rates for symmetrical loads are higher than for repeated loads. Based on the comparison of the curves, the graphs of the change in ratio of the load damaging effect  $\varepsilon$  along the crack length for materials B95 and D16 (Fig. 8.33) were plotted. It follows from the figure that the ratio of the damaging effect of the symmetric and repeated stress cycles, which was maximal at small crack lengths, was  $\varepsilon = 1.3$  for  $L = 2$  mm. As the cracks grew up to a length  $L = 15$  mm, it decreased.

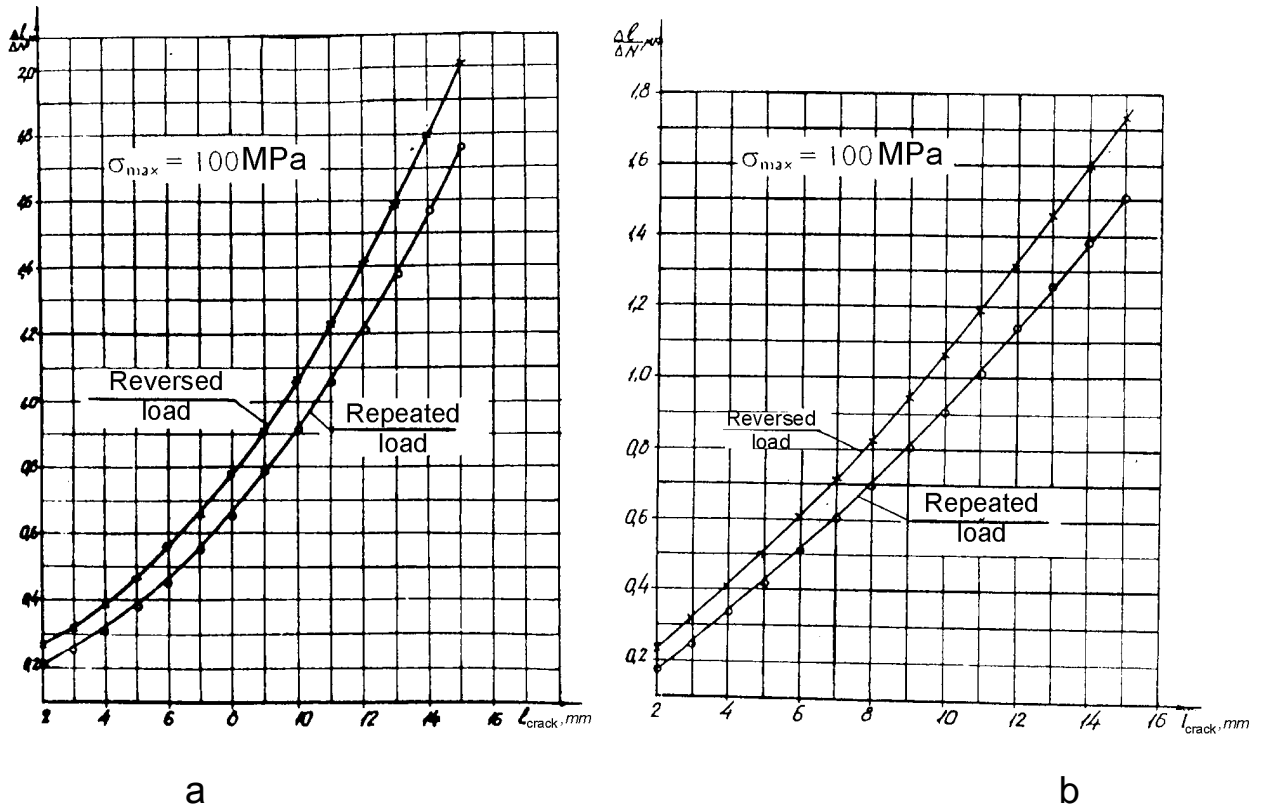


Fig. 8.32. Relation of Crack Growth Rate ( $\Delta L/\Delta N$ ) vs Length  $L_{crack}$  in Specimens Tested Under Programs Given in Figs 8.25, 8.26: a – D16; b – B95

Comparison of the dependence of  $\varepsilon$  (Fig. 8.33), obtained during testing the specimens according to programs II and III, with the dependence for the same loading conditions determined during testing of specimen No. 2 under program I (see Fig. 8.26) has revealed that these data practically coincide. This confirms the correctness of the experimental results obtained under the program of type I.

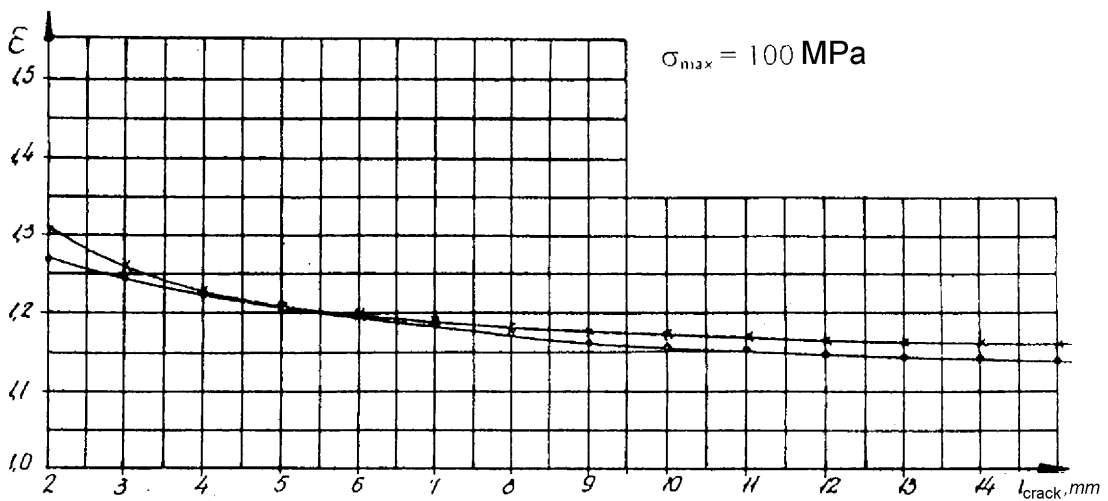


Fig. 8.33. Ratio of Damaging Effect of Symmetric and Repeated-stress Cycles  $\varepsilon$  Along Crack  $L_{crack}$  in Specimens Tested Under Programs Given in Figs 8.21 and 8.22: x – V95; o – D16

Thus, influence of the negative part of the cyclic loads at the stage of fatigue crack growth in the specimens of aluminum alloys B95 and D16 was studied using the technique [63] (see subsection 8.3). The following has been established:

- application of the compression half-cycle increases the load damaging effect in comparison with the repeated-stress cycle of the same maximum level;
- with increasing compressive stresses, their damaging effect increases;
- with increasing tensile stresses at constant compressive stress, relative effect of the compressive loads decreases;
- with increasing crack length, damaging effect of compressive stresses decreases;
- under the investigated conditions of crack lengths ( $L_{crack} \leq 15$  mm) and the ratios of maximum and minimum stresses ( $\sigma_{max} = 140$  MPa,  $\sigma_{min} = -40 \dots -140$  MPa) the effect of compressive loads did not exceed 40% and was not less than 8%.

#### 8.5. RECOMMENDATIONS ON ACCOUNT OF COMPRESSIVE LOAD EFFECT WHEN CALCULATING EQUIVALENTS BETWEEN CYCLIC LOADS AT THE STAGE OF FATIGUE CRACK GROWTH

Effective recommendations for determination of equivalents at the stage of fatigue crack growth are based on the assumption that in connection with the strained state peculiarity at the crack end due to the fact that the stress growth associated with crack opening significantly exceeds the stresses associated with its closure, the latter can practically be neglected. When considering stress fields far from a crack (or external loads, bending moments, forces), this means that two sets of loads variable with time are the original set and the set obtained from the original one by eliminating the part of the load that leads to the onset of compression on the top of the crack, are practically equivalent in stress magnitude defining the crack growth.

The very approach to calculating the equivalents in two stages, in which the lower among two values is taken as goal one (see subsection 8.1), is due to the insufficient development of the issue. Therefore, in this paper, the task was posed: after investigating the compression half-cycle effect upon damaging (see subsection 8.4), clarify the existing recommendations for calculating the equivalents between cyclic loads at the stage of the fatigue crack growth.

The calculated values of the equivalents of the sign-variable and repeated-stress cycles considered in this paper, obtained according to the recommendations of stage I (see subsection 8.1), are given in Table 8.11. Since the compared sign-variable and repeated-stress cycles had the same levels of  $\sigma_{max}$ , calculated values of the equivalents for stage II for all loads in this case were 1.0. As a result, according to the recommendations of the paper, the lower value should be taken from the two obtained at the I and II stages, i.e. 1.0.

The experimental values of the equivalents are also given in Table 8.12.

Since the experimental values of the equivalents were variable along the crack length, then the table represents their maximum values, which occurred at small crack lengths ( $L_{crack} = 2$  mm), taking into account the nonlinear increase in the crack growth rate.

As follows from the table, the experimental values of the equivalents were 1.1-1.4 times higher than the calculated ones, i.e. the verified assumption that there is no effect of the negative part of cyclic loads on the damage at the stage of crack growth in the considered range of crack lengths is incorrect.

From the condition of coincidence of the experimental and theoretical values of equivalents using the calculation method described above, the values of the endurance curve exponent were determined. The calculation was carried out taking into account the compressive loads (see I stage, subsection 8.1). The obtained values of  $m_p$  are given in Table 8.12. These values varied in the range  $m_p = 0.5 \dots 0.7$ .

Considering the narrow variation range of the  $m_p$  values (see Table 8.11) with an average value of  $m_p = 0.6$ , as well as the nature of the change in the values of the equivalents along the crack length (see Figs 8.26 to 8.28, 8.33), as a technique for accounting for the effect of compressive loads under condition of the fatigue crack growth for aluminum alloys the following can be recommended:

- Calculation of equivalents is carried out in accordance with stage I recommendations (see subsection 8.1);
- Endurance curve exponent is taken equal to  $m = 0.6$  instead of  $m = 3$ .

Therefore, when calculating the equivalents for the fatigue damage value of two initial sets of cyclic loads containing the negative part of the load, each unit cycle, characterized by an amplitude of  $2\sigma_a$  and an average value of  $\sigma_m$  (or maximum  $\sigma_{max}$  and minimum  $\sigma_{min}$  values), was reduced to an equivalent repeated-stress cycle with the maximum cycle value  $\sigma_0$ , as well as according to the existing recommendations, by the formula

$$\sigma_0 = \begin{cases} \sqrt{2\sigma_a \cdot \sigma_{max}} & \text{for } \sigma_m \geq 0, \\ \sqrt{2(\sigma_a + 0.2\sigma_m)} & \text{for } \sigma_m \leq 0 \text{ and } \sigma_{max} \geq 0, \\ 0 & \text{for } \sigma_{max} < 0. \end{cases}$$

and with an equivalent transition with regard to occurrence of failure between repeated-stress cycles on the endurance curve of the form  $N\sigma_m = \text{const}$ , for aluminum alloy structures the exponent is taken equal to  $m = 0.6$  instead of  $m = 3$  according to the existing recommendations. Thus, it has been shown that the existing recommendations on the account of the effect of compressive loads at the stage of crack growth underestimate the effect of compressive loads upon damage. The technique has been proposed for taking into account the effect of the negative part of cyclic loads at the stage of a fatigue crack growth in the calculation of equivalents.

Table 8.12

## Parameters of Compared Cycles

Parameters of compared cycles			Design values of equivalents, $\varepsilon$		Test values of equivalents, $\varepsilon$ ( $L=2$ mm)		Design values of endurance curve index $m_p$ (compressive loads are accounted)
symmetrical-sign		repeated-stress	compressive loads are accounted, $m=3$ (I stage)	compressive loads are not accounted, $m=3$ (II stage)	B95 material	D16 material	
$\sigma_{max}$ , MPa	$\sigma_{min}$	$\sigma_{max}$ , MPa					
1	2	3	4	5	6	7	8
80	-40	80	1.84	1	1.13	1.14	0.6
	-60		2.32		1.18	1.20	0.59
	-80		2.83		1.26	1.24	0.67
	-100		3.77		1.28	1.25	0.61
	-120		4.89		1.34	1.32	0.64
	-140		6.22		1.37	1.40	0.62
100	-40	100	1.66	1	1.10		0.57
	-60		2.02		1.19		0.74
	-80		2.41		1.20		0.62
	-100		2.83		1.22		0.57
	-120		3.56		1.27		0.61
	-140		4.41		1.30		0.60
120	-40	120	1.54	1	1.08		0.54
	-60		1.84		1.12		0.56
	-80		2.15		1.17		0.61
	-100		2.48		1.17		0.52
	-120		2.83		-		-
	-140		3.43		1.23		0.54
140	-40	140	1.46	1	1.09		0.69
	-60		1.71		1.10		0.53
	-80		1.97		-		-
	-100		2.24		-		-
	-120		2.53		-		-
	-140		2.83		1.23		0.60

### Conclusions

1. To obtain reliable information about the fracture process in the tests on the persistence capability and residual strength of the airframe structure and structure specimens using the fractography method and reducing the complexity of fractographic studies, various ways of marking the program loading have been developed:

– by change in the number of cycles in flight in neighboring blocks by at least two cycles in programs of loading the wing such as "flight after flight";

- by inserting the program with changing "dynamics" from the insert to the insert for at least two cycles when loaded with reversed or repeated-stress cycles;

- by inserting of various combinations of blocks of small amplitude loads and periodic unloading when the wing is tested for residual strength;

The developed technique of marking the program loads allows to solve the following tasks:

- to determine the origination and growth kinetics of fatigue cracks, including those not available for visual observations, when testing the airframe structure and structural elements for persistence capability;

- to determine the sequence, kinetics of failure and critical size of fatigue damage when testing the wing for the residual strength;

- to reduce significantly (by an order of magnitude) complexity of fractographic studies of fatigue fractures.

The An-12, An-22, An 24, An-32, An-28, An-72, An-124 airplanes and their structural elements were tested for persistence capability with application of the developed method for marking the program loading.

2. The experimental study of preliminary single positive overload effect on the lifetime characteristics of specimens made of D16hT alloy with a hole under loading simulating a transport aircraft wing loading has been performed.

It has been shown that preliminary positive overload leads to an increase in fatigue life both at the stage prior to appearance of cracks and at the stage of their growth.

The effect of preliminary overloads was monotonous and increased with increasing their amounts:

- thus, application of the load  $K = 1.25$  had practically no effect on the fatigue characteristics both at the stage prior to appearance (up to  $L_{crack} = 0.2$  mm) and at the crack growth stage;

- with overload of  $K = 1.5$ , total durability increased by 1.07 times, while duration of crack growth increased by 1.12 times, the period before nucleation was 1.04 times;

- overload  $K = 2.0$  increased durability by approximately 1.7 times, the period before nucleation and duration of crack growth were increased by 1.6 and 1.9 times, respectively;

- increase in endurance at the stage of crack growth was mainly due to decrease in the rates in the concentrator zone (hole), which is evidently caused by the formation of a plasticity zone due to overload.

The obtained results of studies of positive preliminary single overload effect upon the fatigue life characteristics were used to justify the lifetime of the airframe load-bearing structure of the An-12, An-124 and An-124-100 aircraft.

3. The methodology for assessing the damaging effect of cyclic loads (USSR inventors certificate No. 1128768 dated 08.08.1984). It has been shown that the fractographic method makes it possible to determine the ratios of the damaging effect of cyclic loads at the stage of crack growth – so called equiva-

lents.

The developed methodology has the following advantages:

- comparison of the "instantaneous" values of crack growth rates corresponding to different loads was carried out in local zones, which practically excludes influence of the material structure heterogeneity;

- since the comparison of the groove pitch was carried out on the fracture surface of the same structural element, then influence of distribution of the given material properties, manufacturing technology, installation of the structural element in the test machine, test conditions was excluded;

- elimination of the factors listed above, which affect the scattering of the crack growth rates, leads to significant reduction in the volume of the target experiment;

- for determination of equivalents, fatigue fractures of various structural elements tested by loading programs can be used, for which it is possible to establish unambiguous compliance of loads and grooves, even if the fracture zones were not available for observation during testing;

- equivalents for several loads can be determined on one specimen.

4. The effect of the negative part of the cyclic loads at the stage of the fatigue crack growth in tested specimens made of aluminum alloys B95 and D16 was investigated using the method proposed in [63] (inventors certificate No. 1128768 dated 08.08.1984). The following has been established:

- application of the half-cycle compression increases the damaging effect of the load in comparison with the repeated-stress cycle of the same maximum level;

- with increasing compressive stresses, their damaging effect increases;

- with increasing tensile stresses at constant compressive stress, the relative effect of the compressive loads decreases;

- with increasing crack length, the damaging effect of compressive stresses decreases;

- under the investigated conditions of crack lengths ( $L_{crack} \leq 15$  mm) and the ratios of maximum and minimum stresses ( $\sigma_{max} = 140$  MPa,  $\sigma_{min} = -40 \dots -140$  MPa) the effect of compressive loads did not exceed 40% and was not less than 8%.

5. It has been shown that the existing recommendations to take into account the effect of compressive loads at the stage of crack growth underestimate the effect of compressive loads on occurrence of failure. The technique has been proposed for taking into account the effect of the negative part of the cyclic loads at the stage of crack growth when calculating the equivalents.

*Chapter 9***DEVELOPMENT OF METHOD  
TO DETERMINE FATIGUE CRACK CRITICAL LENGTH  
IN TESTING SINGLE STRUCTURAL SPECIMEN  
FOR RESIDUAL STRENGTH**

---

As shown in subsection 8.1, there was no method for determining the fatigue crack critical size in testing a single specimen of the structure. Therefore, in connection with the analysis of the survivability of a wing production break profile of a heavy transport aircraft, the task was to develop such a technique [30, 32].

The work was carried out in two stages:

1. Tests of specimens of various types, to some extent representing actual structure.

The purpose of these tests was to perform preliminary assessment of the crack critical sizes, as well as to develop a technique for testing the full-scale structure for residual strength.

2. Preparation and testing of full-scale wing structure in accordance with the developed technique for determining the critical dimensions of fatigue damage.

The results of previous fatigue tests of the wing tested for lifetime duration has shown that critical location defining the wing endurance is the cross-section of the production break profiles along the first row of bolts connecting the break profiles of to the skin and the internal load-bearing members (spar caps and docking stringers). Fatigue cracks appeared in the profiles at the edges of the loaded holes (angled cracks). Since there are a lot of holes in the section under investigation, it was also necessary to establish the sequence of the wing failure.

The wing break profiles are made of aluminum alloy B93T1. The part thickness in the critical section is approximately 28 mm. In this connection, the break profile failure occurs under conditions close to the plane-strain condition.

Structurally the break profile cross-section is located inside the package and is not available for visual monitoring or control by means of signaling devices.

For application of non-destructive testing methods (eddy current or X-ray control), it was necessary to perform laborious work to remove the detachable panels, loading devices, and also the first row bolts, which would lead to a long duration and laboriousness of the tests.

Therefore it was necessary to carry out the tests in such a way that, with the help of subsequent fractographic fracture studies, it would be possible to establish the kinetics of fracture and the critical size of the fatigue crack.

**9.1. DEVELOPMENT OF METHOD TO DETERMINE CRITICAL SIZE OF FATIGUE DAMAGE WHILE TESTING SPECIMENS FOR RESIDUAL STRENGTH**

Since the known methods for determining critical length of the fatigue crack



(see subsection 8.1) in this case are not applicable, then the wing test program was executed in several stages with the help of structural specimens (ref. drawing No. E-22-21-788), imitating the transverse wing joint (see subsection 8.1, Fig. 8.2).

At the first stage, the testing method was checked, consisting in successive growth of the crack at the load level corresponding to cycle 3-B-3 of a "standard flight" with the subsequent application of a given load. The idea was the following: to select such frequency of overload application to the specimens, that the specimen failure would occur after the last crack increment at a load close to the target, i.e. so that the crack increments between the overloads would be small.

Marked loading programs were used to determine the kinetics of failure. The principle of markup was that certain blocks of the program contained different number of dynamic cycles (see subsection 8.1).

Since the wing break lower profile was simulated and the problem of determining the crack growth rate was not set, the load program did not contain negative part of the load. The parameters of the load program are shown in Fig. 9.1.

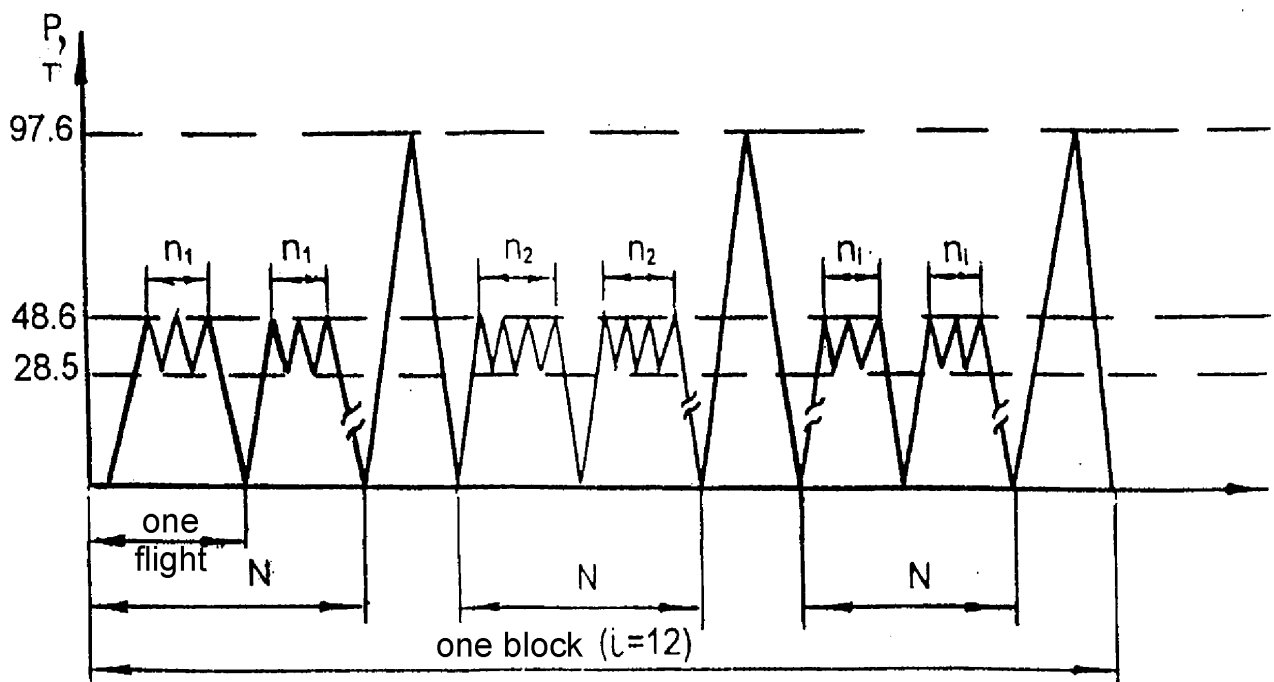


Fig.9.1. Type of Loading Program for Checking Technique of Determining Damage Critical Size at First Stage

Value of  $N$ :

1-st block –  $N = 100$  flights;

2-nd block –  $N = 200$  flights;

3-rd block –  $N = 300$  flights;

4-th block –  $N = 400$  flights;

5-th block –  $N = 500$  flights.

Values of  $n_i$  remain unchanged in all blocks:

$n1 = 0$ ;  $n2 = 4$ ;  $n3 = 7$ ;  $n4 = 1$ ;  $n5 = 9$ ;  $n6 = 3$ ;  $n7 = 6$ ;  $n8 = 2$ ;  $n9 = 10$ ;  $n10 = 5$ ;  $n11 = 8$ ;  $n12 = 11$ .

To initiate cracks at the hole edges in the break profiles the angled cuts (3×2) were made using an electroerosive method.

The first two specimens destructed under the first overload applied after 600 flights, in one case the specimen was destroyed at 69% of  $P^{op}$  of the case  $A'$ , and in the other case at  $P^{op}$ . The surface of the specimen fracture and the structure of the fracture surface are similar to those shown in Figs 8.2 and 8.3.

Fractographic studies have shown that origination of fatigue cracks from the cuts made by an electroerosive method occurred through 50 to 70 laboratory flights.

To determine the frequency of the overload application, it was necessary not to allow the first overload to lead to the failure of the specimen, so the operating time before the first overload was reduced to 400 laboratory flights.

Two specimens were tested. The failure of one specimen occurred under the first overload, and the destructive force was 89% of  $P^{op}$ .

The second specimen withstood the first overload, and its failure occurred only after 74,900 laboratory flights in section at the spar cap end from the crack, which originated from fretting corrosion. At the same time, 61 overloads were applied, and during testing, the amount of time between overloads was constantly increasing and at the end it was 5000 flights.

Since the failure of the specimen did not occur in the cross-section under consideration, the cross-section of the first row of bolts was opened and subjected to fractographic studies. Studies have shown that crack originated from the cut prior to the application of the first overload. After application of the overload, the pattern of striation could not be determined. The increment of the crack began to be observed only with an increase in the amount of time between overloads to 3000 laboratory flights. Thus, if the specimen did not collapse after application of the overload, a delay in the propagation of the fatigue crack occurs.

It became obvious that this type of loading is not suitable for testing the wing for residual strength, since the delay in the propagation of a crack after application of an overload can be so great that failure can occur elsewhere in the structure with larger operating times.

The second approach when choosing a loading program to determine the critical size of fatigue damage was application of repeated loads varying from zero to the maximum level of the given load (here  $P^{op}$ , case  $A'$ ).

It was assumed that during the test, the failure would occur at a load close to the predetermined value, and fracture analysis would determine the size of the damage.

Under this program, a simple specimen with a central unfilled hole made of material B-93 was tested. Stress  $\sigma_{gr}$  in the specimen reference section at the operational load was  $\sigma_{gr} = 300$  MPa. Failure of the sample occurred in the cross-section along the hole after 1200 cycles.

Fractographic studies have shown that under such a loading it is not possible to establish the boundary of the fatigue zone corresponding to the point of failure.

Therefore, this type of loading program can not be recommended for testing the full-scale wing structure.

During the third test stage the type of loading was tested, which consisted in the application of cycles of small amplitude at the operational load level. The idea of this loading is that during the test, failure of the structure will occur at a given load level (with an accuracy of one cycle).

Since loading will be carried out by cycles of small amplitude, the increment of the fatigue crack per cycle should be small, which leads to presence of clear boundaries of the fatigue zones corresponding to the failure moment.

Under such loading program, a structural specimen was tested (Ref. Dwg. E-22-21-912), simulating the transverse wing joint. This specimen was structurally similar to the specimen (Ref. Dwg. E-22-21-788), described in subsection 8.1 and shown in Fig. 8.2, with the difference that a cover plate and a spar cap of the side member were connected to two profiles and four rows of steel bolts, the first and second rows counted from the grippers having  $\varnothing 20 A_3$ , and bolts of the third and fourth rows –  $\varnothing 14 A_3$  and  $\varnothing 10 A_3$  respectively. Specimens simulated the same joint as the specimen given in Dwg. E-22-21-788 with a design version in a certain series of aircraft.

The loading program was similar to the program shown in Figure 8.9, with the exception of load relief to  $0.5P^{op}$  and number of cycles. As can be seen from the figure, the program used two amplitudes of the dynamic cycles, which were of 15% and 5% of the maximum operating load. When testing the specimen, the load was relieved to zero twice, related to the end of shifts. The alternation of loads with different amplitudes was performed after 1000 cycles.

Sample failure occurred after 79180 cycles done in section along the first row of bolts, where corner cuts were made.

Fractographic studies of the fracture surface showed that the boundaries of the fatigue zones are clearly visible at the fracture. The fatigue crack increment occurs mainly when loaded with cycles of greater amplitude, and blocks of loads with a reduced amplitude (5% of  $P^{op}$ ) practically do not give a crack increment and leave on the fracture surface concentric stripes that differ in color from concentric stripes – crack increments at larger amplitudes. Therefore, such load blocks can be used as markers for compiling marked loading program. Load relief to zero with subsequent increase to  $P^{op}$  led to a delay in the growth of cracks.

It became obvious that this loading technique allows one to determine the critical size of the damage when testing one specimen.

Under a similar load program, non-destructed joint sections of several specimens (Ref. Dwg. E-22-21-912) were tested, those tested under various loading programs and those tests were stopped after one joint section failed. At all the fractures, the dimensions of the damage at the failure moment were clearly revealed.

Application of the test procedure described above ensures failure of any type

of specimen at a given level of loading, and use of a loading program with markings makes it possible to perform a fractographic fracture analysis relatively simply, to observe crack growth and to determine its size before failure.

The technique disadvantage is that maximum level of cyclic loads and destructive load coincide. Due to this it becomes necessary to evaluate effect of these loading conditions on the crack critical dimensions and reliability of determining the actual fracture boundaries immediately before failure.

In order to verify validity of the results obtained by the developed method, a comparison was made between the results of tests of specimens (Ref. Dwgs E-22-21-788 and E-22-21-912 using Method I (see subsection 7.1) and developed technique.

According to Method I, the specimens were tested for static loading before failure after had been tested for endurance as described in subsection 8.1, tests were stopped after one joint section failed. Non-destroyed parts were combined (a specimen was assembled of two specimens), and the specimen was loaded to failure by a static load.

Test results (operating time up to the moment of loading by static load, magnitude of the breaking load and dimensions of cracks measured along the surface of the joint section by the criterion  $\Sigma L = L_1 + L_2 + d$ , where  $L_1$  and  $L_2$  are the lengths of cracks developing in opposite directions from holes,  $d$  is the hole diameter) are given in Table 9.1.

Table 9.1

Test Results

No.	Drawing and specimen number	Operating time till application of static load, cycles	Breaking load $P_{break, tf}$	Crack length $L_{crack} = L_1 + L_2 + d$ , mm
1	E22-21-788-1 No. 2	12000	144.5	14.5
2	E22-21-788-1 No. 13	80700	57.5	35.3
3	E22-21-788-1 No. 14	18500	140	18
4	E22-21-788-1 No. 17	42500	72.5	23.2
5	E22-21-788-1 No. 18	17000	104.5	22.4
6	E22-21-788-1 No. 1	20000	98	16.7
7	E22-21-788-1 No. 13	40000	63	43.9
8	E22-21-788-1 No. 16	17500	149.5	16
9	E22-21-788-1 No. 10	30200	69	42.9
10	E22-21-788-1 No. 15	56600	109	25.7
11	E22-21-788-1 No. 24	3861	75.1	31
12	E22-21-912-3 No. 3	400	87.1	25.5
13	E22-21-912-3 No. 4	200	73.6	24.2
14	E22-21-912-1 No. 16	600	67.4	29.2
15	E22-21-912-1 No. 15	600	97.6	27

Test results for specimens tested according to the developed method are given in Table 9.2.

Table 9.2

## Test Results for Specimens Tested According to Developed Method

No.	Drawing and specimen number	Operating time till application of static load, cycles	Breaking load $P_{break}$ , tf	Crack length $L_{crack} = L_1 + L_2 + d$ , mm
1	E22-21-912-3 No. 6	79182	97.6	40.1
2	E22-21-912-1 No. 6D	77241	97.6	27.7
3	E22-21-912-3 No. 6D	79200	97.6	32.9
4	E22-21-912-3 No. 5D	66161	97.6	26.8
5	E22-21-912-1 No. 15D	4942	97.6	28.3
6	E22-21-912-3 No. 3D	3900	97.6	31
7	E22-21-912-3 No. 4D	203	97.6	26

These results are plotted for comparison (Fig. 9.2).

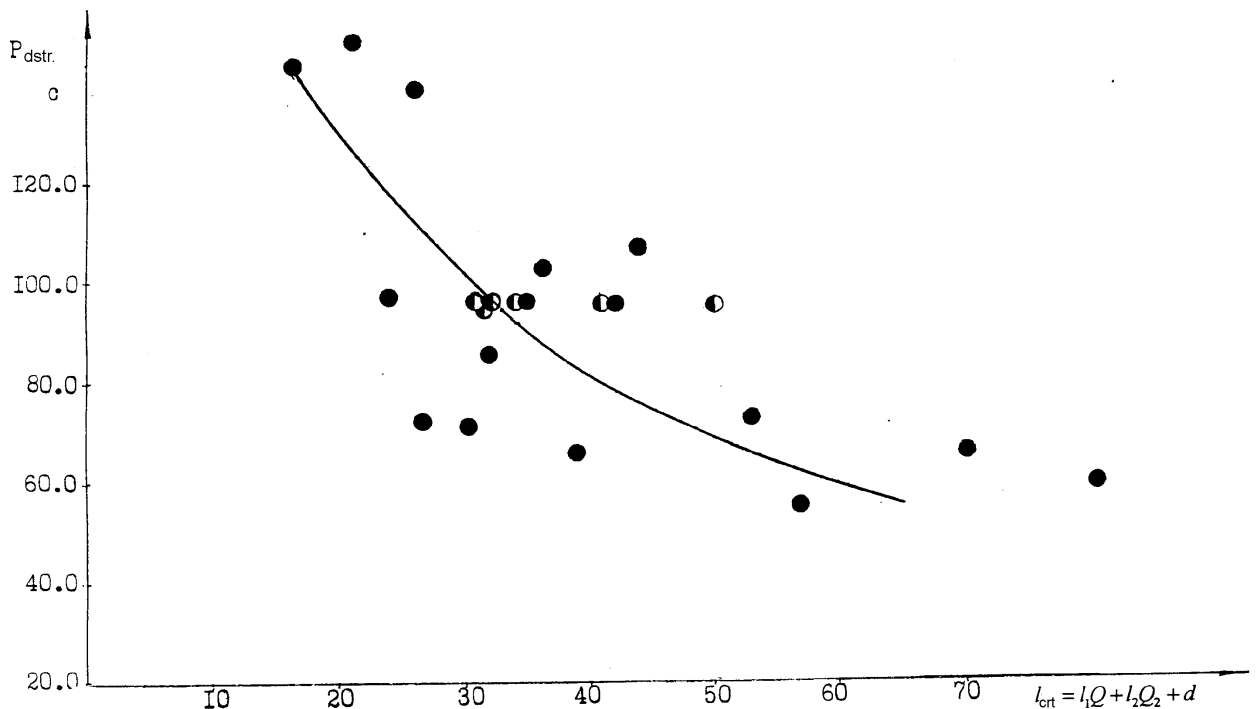


Fig. 9.2. Comparison of Damage critical size obtained by methods I and III when testing specimens for residual strength:

- – tests according to method I; ○ – tests according to method III.  $Q = f\left(\frac{a}{2l}\right)$

In this case, critical damage size  $L_{cr.fact.}$  was defined as the sum of the surface crack lengths propagated from one hole to the opposite sides, corrected by the coefficient  $\theta$ , which takes into account effect of the crack shape and the hole diameter [33].

As can be seen from Fig. 9.2, the results of testing the specimens according to method I and according to the developed method are well approximated by one curve, which confirms suitability of the developed procedure for testing

the full-scale construction.

Thus, on the basis of testing the structural specimens, the technique of loading the full-scale An-22 wing structure to determine critical length of the fatigue crack in the joint sections and preliminary estimation of its dimensions were carried out.

## 9.2. TEST OF FULL-SCALE WING STRUCTURE

The program for loading the An-22 aircraft wing with indication of the accepted stress values is shown in Fig. 9.3. The applied method of marking is described in subsection 8.1.

The wing tests were performed using a three-point loading scheme, which simplified the control of the loading system. In the process of preparing the wing for the tests the cuts were made in the joint section bolt holes of the first row. An electric spark method was used for cutting. The cuts were made in four sections, and several cuts were made in each section. The number and location of the cuts was determined on the basis of the endurance test results. At the same time, the aim was to take into account the multicentricity effect upon the crack critical size.

The complete destruction of the wing was preceded by a severe impact, after which the wing still maintained a cyclic load for some time. The moment when the impact was fixed is marked on the scheme of the loading program (Fig. 9.3).

Complete wing failure (Fig. 9.4) occurred immediately in two sections: one section with cuts and one without cuts.

The following data were obtained as a result of the fractographic study:

1. Primary failure occurred in a section with cuts. Failure in the section without cuts was a consequence of the dynamic load that arose at the moment of failure along the first section.

2. Centers of crack nucleation were defined, which in their development led to complete failure.

3. The dimensions of fatigue damage at which rapid propagation of cracks began were determined. Critical value subjected to the investigation of the cross section is the total crack length  $L = 30.0$  mm (hole diameter incl.), which took place before the reduction moment.

The dimensions of the critical fatigue damage from the results of the full-scale design tests are close to those obtained on the basis of estimates made as a result of testing the specimens using various methods.

4. It has been established that the first period of crack rapid propagation did not lead to complete failure, but ended with crack propagation stopped at the nearest bolt holes. The moment of the first crack "slippage" coincides with the moment of impact noted during the test.

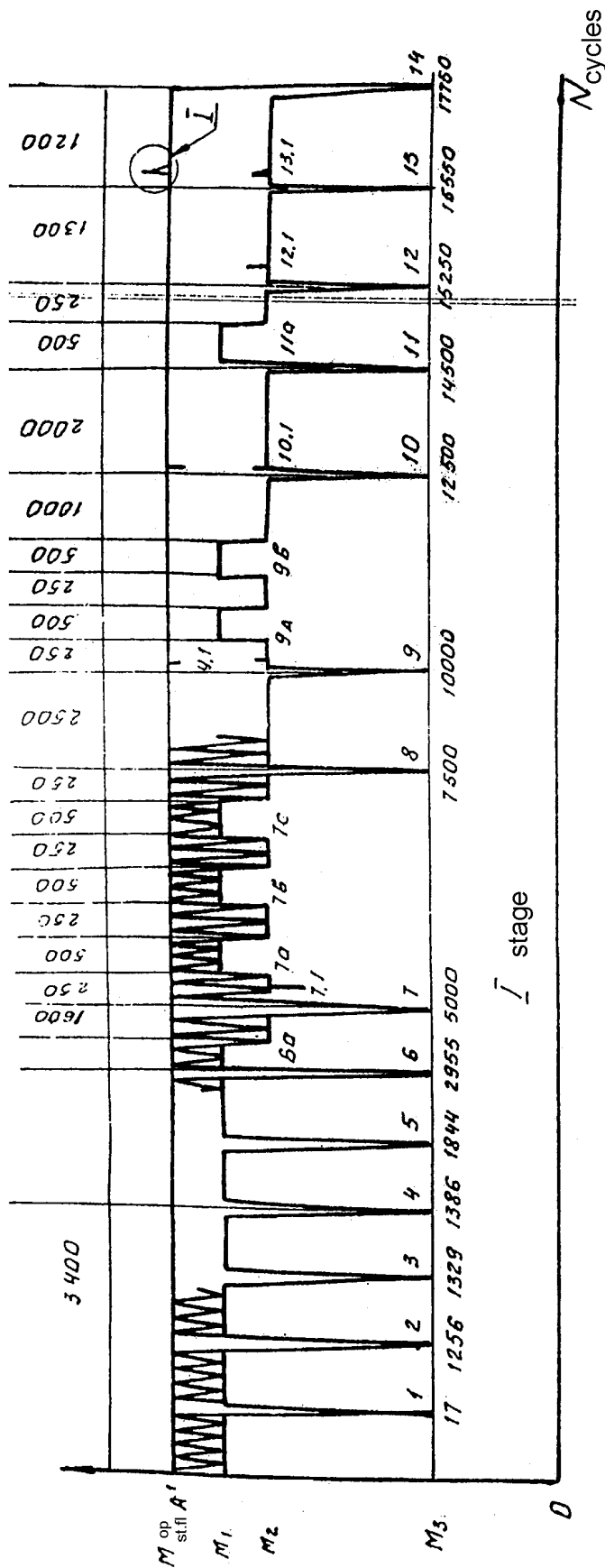


Fig. 9.3. Actual realization of loading program of An-22 No. 01-02 airplane wing for residual strength:

numbers from 1 to 39 are numbers of program unloading; a, b, c - marks;

I - example of designation for the excess of the operational level. Overload number 13.1 (13 - number of unloading, 1 - number of reloading in the interval between the 13th and 14th unloadings); II - example of designation for underloading. Underload number 21.2 (21 - number of underloads, 2 - number of underload in the interval between the 21st and 22nd unloadings); IV - example of a series of random unloadings; V is an example of a series of random underloads. All random deviations from program levels do not exceed 10% of  $M_{case A}^{op}$

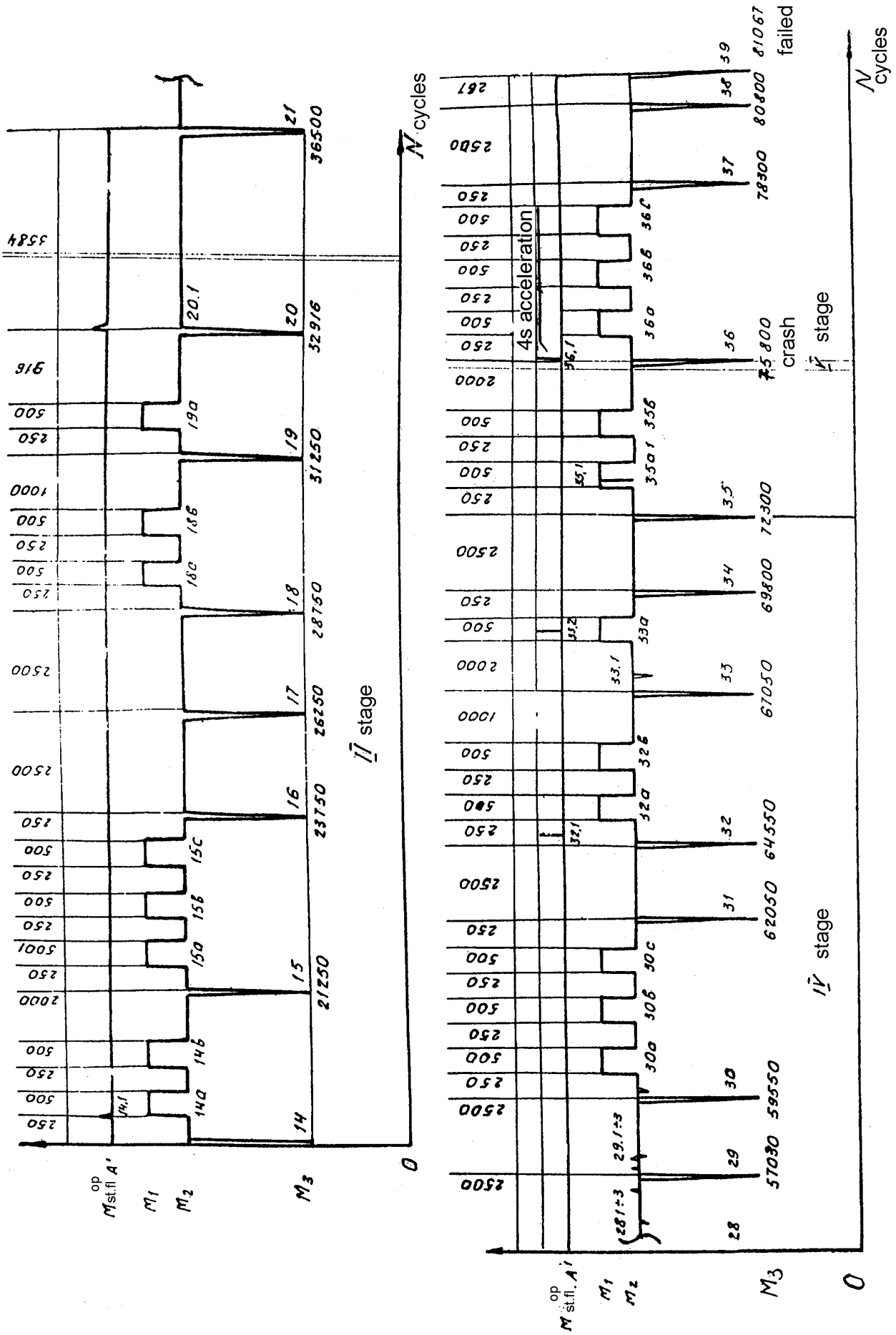


Fig. 9.3 — Actual realization of loading program of An-22 No. 01-02 airplane wing for residual strength (the end)



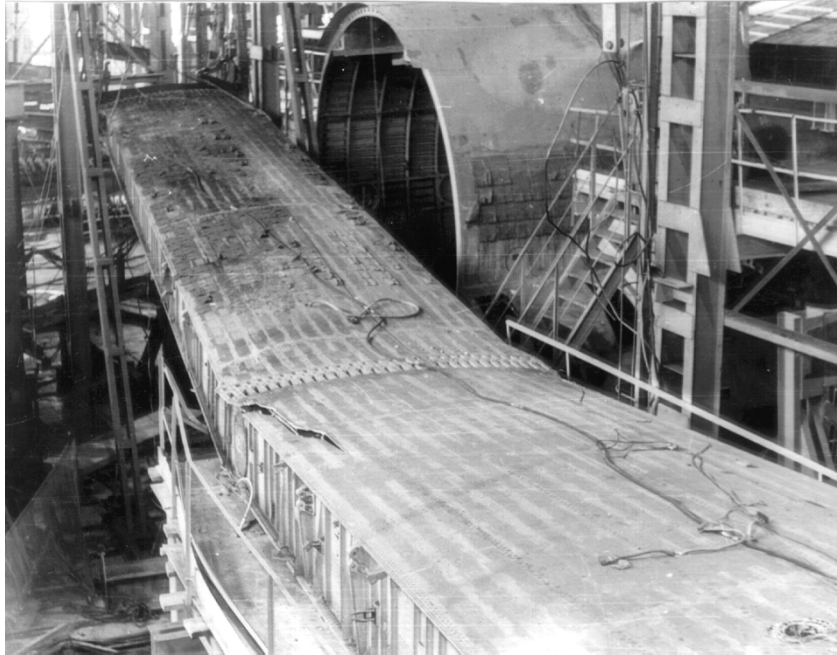


Fig. 9.4. Failure of An-22 Airplane No. 01-02 Wing While Testing for Residual Strength

5. It has been noted that the dynamic impulse, which occurred during the first fast increase in the crack length, caused the formation of "marks" in the fractures of other cracks present in the structure.

6. The period of the complete wing failure was preceded by a period of cyclic loading, which caused formation and development of fatigue zones at the bolted holes, where an intermediate stoppage of cracks occurred.

7. Rapid propagation of other cracks in the structure occurred only when the front of the main crack approached. In this connection, and also taking into account small critical sizes of cracks, it can be considered that there was no mutual influence of cracks.

### Conclusions

1. The technique for the experimental determination of the fatigue damage critical size when tested for the residual strength of a single structural specimen has been developed.

2. The developed technique is used to determine the fatigue crack critical length in the sections of the wing production breaks of the An-22 transport aircraft during the test for residual strength.

3. Adding of special marking loads in the loading program allowed to determine the crack critical size and to trace the entire process of structural failure.

4. The fatigue crack critical size in the lower section of the wing production break, made of material B93T1, was  $L_{cr} = 30$  mm (taking into account the hole diameter).

5. The results obtained refer to the massive elements of the construction of the alloy B93T1.

*Chapter 10*

**DEVELOPMENT OF TECHNIQUE FOR REALIZATION  
OF AVAILABLE LIFETIME CHARACTERISTICS IN OPERATION  
ACCOUNTING INDIVIDUAL LOADING**

---

10.1. DEVELOPMENT OF TECHNIQUE ACCOUNTING INDIVIDUAL WING LIFETIME DEPLETION

As shown in subsection 7.2, with the increase in the aircraft takeoff weight the operational range of flight parameters such as takeoff weight, weight of fuel placed in the wing, weight of payload, flight altitude and duration increase. Combination of these parameters determines change in the operating load, which makes for such aircraft a major share of the wing damage during flight. Damage to the heavy transport aircraft wing can significantly (several times) differ from flight to flight. Therefore, the value of the reliability coefficient  $\eta_3$ , taken when determining the aircraft assigned lifetime in accordance with the Airworthiness Requirements [20] equal to 1.5, may be insufficient or its actual value may be less than unity.

This means that determination of the airplane lifetime depletion by comparing the operating time in actual flights and hours with the lifetime established on the basis of standard flights may lead in some cases to the depletion of the lifetime of a specific aircraft prior the end of the assigned lifetime or to termination of the operation of aircraft capable of working in terms of endurance.

To solve this problem, a methodology was developed for estimating the depleted wing lifetime of the An-22 aircraft and work was done on the assessment for the aircraft fleet.

**Calculation of wing damage**

1. Determination of the wing loading that is the operating load (bending moment  $M_{bend}$ , stress  $\sigma$ ) spanwise at various stages of each flight (taxiing before takeoff, takeoff, climbing, cruising flight, descent, landing, taxiing after landing) without considering the impact of dynamic loads in the air and on the ground.

2. The statistics of recurrence of the accelerations in the aircraft center of gravity in flight is processed by the flight recorder records, either for each flight (if there is such information) or by the averaged processing data for a large number of flights of this type of aircraft.

3. According to the results of special flight experiment, the dependence of the recurrence of the wing dynamic loads in flight vs recurrence of accelerations in the center of gravity has been determined.

4. According to the results of special flight experiment, the dependence of the recurrence of the wing dynamic loads during ground operations has been determined, depending on the aerodrome pavement, aircraft take-off and landing weight, weight of fuel placed in the wing, duration and speed of taxiing, etc.

5. Based on the data given in items 2, 3, 4, maximum value of the dynamic load in flight and on the ground and the wing load ( $M_{bend}$ ,  $\sigma$ ) from the cycle

"Ground-Air-Ground" (G-A-G) for each flight or for a number of similar flights have been determined.

6. According to the existing methodology, overloads of each flight (G-A-G and the dynamic loads spectrum) are recalculated with regard to repeated-stress cycle corresponding to the "standard flight" damage, accepted in the conclusion about the lifetime.

Total depleted lifetime is determined in the same units, for the completed operation phase for each individual aircraft and compared with the established lifetime.

7. Calculation was carried out according to computer special program, the numerical data of which introduces the initial parameters of each flight of the aircraft in question, or according to a nomogram compiled for this type of aircraft.

The developed method received positive TsAGI review. It states that taking into account the individual loading of individual aircraft (or a group of aircraft) is, on the one hand, one of the important ways to use the possible reserves to increase lifetime, and on the other hand it is aimed at improving operational safety through the timely detection of increased aircraft loading.

At the same time, it has been noted that since the scattering of the load repeatability caused by atmospheric turbulence is not taken into account from the specimen to the specimen, no similar consideration is given for the scattering of the load repetition under ground operating conditions, then, in determining the assigned lifetime, the safety factor  $\eta_{safe}$  given in the Airworthiness Requirements should be partially kept equal  $\eta_{safe} = 1.2$ .

To develop a program for the individual depletion of the An-22 wing lifetime, the following works were performed:

1. Statistical processing of aircraft operation parameters in the number of 3693 flights.

2. Statistical processing of the An-22 airplane KZ-63 recorders records in the amount of 4505 hours.

3. Decoding of oscillographic records of bending moments in four sections of the wing for six different combinations of the aircraft mass and fuel mass in the wing when performing standard taxiing, take-off and landing runs at three base aerodromes during special flight experiment.

Individual depletion of the An-22 aircraft wing lifetime was introduced into the practice of aircraft operation.

The methodology of individual accounting of the wing lifetime depletion has been protected by the inventor's certificate [80].

The program for calculating the individual consumption of the An-22 aircraft wing lifetime was transferred to the Customer and with its help the An-22 fleet lifetime depletion has been estimated. This method also records the lifetime depletion of the An 12, An-124, An-124-100 aircraft. The results of calculations are used when establishing the assigned aircraft lifetime.

### **The calculation results of the wing damage in operation of the An-22, An-124, An-124-100 aircraft**

For the An-22 aircraft a flight performed from a concrete runway was selected as a standard flight with the following parameters:

airplane take-off weight	–	205 tf;
fuel take-off weight	–	60 tf;
payload	–	25 tf;
flight duration	–	5 h;
level altitude	–	7000 m;
taxiing duration	–	10 min.

Damage during this standard flight is taken as a measure of damage for the fatigue test programs. The lifetime is assigned in the same units, and the lifetime depletion was recorded in operation.

The results of calculating the individual depletion of the An 22 airplane wing lifetime over more than 30 years of operation has shown that, despite the fact that in certain flights and at certain operational stages the wing damage can differ significantly from the standard (up to three or more times), for a long period, the operating conditions are mixed and the average value becomes stable.

Damage to the accepted standard flight of the An-22 aircraft proved to be higher as compared to both the average flight for the fleet and the most loaded one.

In general, the ratio for the fleet was:

- for the lower wing surface, approximately 60% of the damage during standard flight;
- for the upper wing surface about 85% of the damage during standard flight.

For an aircraft with maximum intensity of lifetime depletion, damage to the wing lower surface being an average of one flight, is 73% of the damage during standard flight. For the An-124-100 aircraft, a combination of 13 flight profiles has already been adopted as a standard one.

For individual aircraft, the damage occurred in an average during operational flight was 22 ... 68% higher than the damage caused by a combination of standard flights taken as a unit for measuring damage.

For An-124-100 aircraft, which are a modification of the An-124 aircraft and used for commercial transportation in civil aviation, a combination of four standard flights was adopted as the unit of damage measurement. The results of calculations have shown that the most loaded airplanes among these aircraft are approaching damage to the standard flight, remaining slightly lower.

Damage to the same average flight in the operation of the An-124-100 aircraft is higher than the damage of such the An-124 flight as follows:

- on the wing bottom surface – by 1.7 times;
- on the upper surface of the wing – by 1.18 times.

Thus, for heavy transport aircraft, lifetime based on endurance conditions should be established in so-called standard flights, taken as a unit of measure-

ment of damage, and depletion of a lifetime is determined individually for each aircraft.

## 10.2. PECULIARITIES OF ESTABLISHING SPECIFIED LIFETIME TO AIRCRAFT PERIODICALLY USED FOR SPECIAL APPLICATIONS

If the medium-range aircraft operating conditions do not fundamentally change and it fulfills its basic functions, for example, as a transport aircraft, then the expected operating conditions can be determined quite accurately, taking into account that it would not be difficult to correct them later when extending the lifetime (see subsection 7.2). But if such a change occurs or can occur periodically and only for individual planes, then it is necessary to determine the possibility of damage during standard flight for the changed conditions and to define a procedure for recording the depletion of the specified lifetime established for the main operating conditions [81].

As examples of changes in operating conditions of individual aircraft, the following can be cited:

- increase in the aircraft maximum take-off weight upon the request of the operator;
- use of aircraft as special laboratory with special equipment and additional fuel tanks, for example, for patrolling, reconnaissance of fish and ice, flight of radio equipment of aerodromes, etc;
- aircraft-salons;
- planes of educational institutions, etc.

The operating conditions can change several times during the operation, depending on the need or change of the aircraft owner. For example, special use aircraft or flight schools are purchased by commercial companies that use them later for transport purposes and etc.

In this case, we will consider the issues of changes in the conditions of recording the lifetime depletion as exemplified by the An-26 airplane (and here there are differences depending on the type of equipment) used in the combined version – as a transport aircraft and fitted with equipment for flying over the radio engineering means of airdromes.

The aircraft operation in the latter case is characterized by three types of flights:

- flights for servicing the navigation systems of airdromes at low altitudes ( $H_{lvl} = 600$  m), with go-around operations of about 77 %; average flight duration  $T = 3$  h;
- flights for servicing of variable-profile navigation systems including low-level flights ( $H_{lvl} = 600$  m) with go-around operations and one-time exit to the altitude level ( $H_{lvl} = 4500$  m) – about 3 %;
- flights to the base aerodrome and to the airports for servicing navigation systems – about 20 %; these flights correspond to the standard operation of the An-26 aircraft.

All go-around operations during the flying over navigation systems are performed without extension of landing gear and flaps, an average of 15 go-around operations for the flight.

The results of the calculation have shown that possibility of damage to the An-26 aircraft wing during such a special flight is much higher than possibility of damage of the transport version wing. The equivalents were:

- for flights  $K = 4.1$ ;
- for flight hours  $K = 2.9$ .

It is recommended to count the depletion of the An-26 aircraft specified lifetime in flights and hours, not using actual operating time in flights and flight hours, but its equivalent, calculated by formula:

$$N_{equ} = N_{spec}K_{equ} + (N_{total} - N_{spec}),$$

where  $N_{equ}$  – the equivalent operating time in flights or hours;  $N_{spec}$  – the number of flights on the fly of navigation systems or the corresponding number of flying hours;  $N_{total}$  – total number of actual flights or flight hours from the moment of aircraft manufacturing;  $K_{equ}$  – the above values of equivalents.

Thus, it follows from the foregoing that for medium-class transport aircraft in case of their use in a mixed version (conventional and special applications), it is necessary to specify the order of depletion of the assigned lifetime, depending on the changed conditions of use. The principle of the phased establishment and prolongation of the lifetime, provided for by the Airworthiness Requirements makes it possible in this case also to take into account such changes in a timely manner.

### 10.3. PECULIARITIES OF OVERHAUL-PERIOD RENEWAL AND PROLONGATION OF LIFETIME TO AGING AIRCRAFT

Maintaining the airworthiness of aging aircraft, which began operating in the 1960s and 1970s, remains the most important task for Ukraine and CIS countries and similar aircraft abroad [82 – 84].

As noted in the paper [83], the main feature of ensuring safety of old aircraft is that they are operated beyond the design lifetimes in accordance with the requirements of modern standards on the principle of survivability, which was not incorporated into the construction at the design stage, that is it uses some "spontaneous" survivability, which each type of construction has in a varying degree. At the same time, as a rule, places with relatively low durability or those places for which the operation time in full-scale tests turned out to be insufficient, taking into account the reliability factors for a "safe" lifetime, as well as the places of construction, where corrosion damage is possible are operated by survivability.

In papers [83, 84] it is noted that in order to ensure the safety of operation of old aircraft, it is required to compile for them not only a basic conclusion for the operation of the fleet, but also an individual conclusion on every aircraft belonging to this fleet with the obligatory inspection of this aircraft prior to prolong

the lifetime in accordance with a specially developed program for it.

The need for such a conclusion in the transition period under modern conditions is caused by the following circumstances:

- presence of a large number of independent operators, whose standard flights differ significantly not only from each other, but also from the standard flight used in the base conclusion;
- difference between the airframe with the same operating hours on completed service bulletins, made improvements, number of repairs that can also affect the conditions of lifetime depletion;
- ability to collect and analyze data on the actual state of the aircraft fleet in the conditions of stopping their receipt in a centralized way;
- substantially different levels of maintenance, especially on the quality of control, in different airlines and aircraft bases;
- degradation of the properties of materials (crack resistance and durability) after long-term operation, etc.

The old ANTONOV aircraft designed in the 50-70's include An-8, An-12, An-22, An-24, An-26, An-30 planes. The design lifetime of the head groups of these aircraft currently has been exceeded twice or more times. In addition, taking into account the new economic conditions for many air companies being owners of only a few planes it is practically unrealistic to perform expensive capital repairs, the cost of which is comparable to the cost of the aircraft themselves, and also there is a need to prolong time between overhauls and lifetime. This prolongation is executed not only for older aircraft, but also for the next-generation aircraft An-32, An-72, An-74, An-28, An-124, An-124-100.

At Antonov State Company with the participation of the authors from the beginning of the 90s the following concept of providing the operation of old aircraft was adopted:

1. Substantiation and basic conclusion on the possibility and order of individual extension of lifetime and service life, periods between overhauls and aircraft service life under conditions of structural strength during long-term operation have been developed. So, for example, for the An-24 airplane, possibility to operate up to 42,000 flights, and 60,000 flying hours for 40 years has been substantiated.

For this aircraft, it was also justified to operate to the next repair within 6000 flights, 8000 flight hours, 10 years instead of the actual values: 5000 flights, 5000 flight hours and 5 years.

For An-12 aircraft, the relevant parameters are currently:

- Assigned lifetime and service life - 16,000 flights, 43,000 flying hours for 40 years,
- overhaul and service lives – 2500 flights, 8000 flight hours, 15 years instead of operating 2000 flights, 4000 flight hours, 6 years.

2. To extend the life or service life with regard to any of the parameters – assigned lifetime, assigned service life, or overhaul life or service life – a program is being developed to investigate the aircraft technical condition taking into

account also its individual characteristics:

- operating time in flights or hours and service life;
- completion of updates on service bulletins;
- availability of repair linings and their operating time;
- individual operating conditions, including usage as a special-purpose aircraft, and in wet tropical climates, etc.
- operating time after the last major overhaul, in which all closed cavities were inspected, for example, wing torsion boxes;
- information on rough landings or operating in areas of high turbulence, etc.

For An-12, An-22, An-124, An-124-100 aircraft, calculation of individual lifetime depletion has been performed, as described in subsection 9.1 of this work, taking into account flights from the "touch-and-go landing" (see subsection 9.4) and depending on the results of the calculation, the program of inspections should be updated.

For airplanes with a smaller take-off weight and, accordingly, with a smaller spread of operational parameters, for example, An-24, An-26, An-30, An-32, averages are compared for the last period of operation (after the last extension of lifetime or service life), such as the aircraft take-off weight, fuel take-off weight, payload mass, flight duration and level altitude, with the parameters of the standard flight taken as the unit of measurement of damage in the base conclusion.

Based on this comparison, the technical condition study program can also be adjusted.

3. The aircraft technical condition with participation of the specialists of the «ANTONOV» State Company, including non-destructive testing, with the drawing up of an act on the identified defects and malfunctions is being studied.

4. After elimination of defects, as evidenced by the act of the operating organization, an opinion is drawn up on a particular aircraft, indicating the conditions for depletion of the lifetime and service life.

According to this scheme of operation, the An-24 aircraft, for example, have now reached 40,000 flights (43,000 flights - Bulgarian aircraft), 57,000 flight hours and 35 years of service life at design values of 20,000 flights, 22,000 flight hours. This is an absolute record among the aircraft of the countries of the former USSR. This aircraft also has a record for the lifetime of landing gear (front and main legs) – 35,000 flights (not including An-2).

The values of time between overhauls and lifetimes achieved for the An-24 aircraft are 6,000 flights, 7,000 hours, 11 years.

For An-12 aircraft with a design lifetime of 15,000 flying hours, the following values are achieved: 15,000 flights, 40,500 flight hours and service life of 39 years. The reached values of time between overhauls and service life are 3,700 flights, 6700 hours, 14 years.

With the account of the aircraft lifetime characteristics the rate of their operation for An-24 aircraft, for example, the following values for the phased in-



crease in service life and lifetimes are accepted: 1,000 flights, 2,000 flight hours, from 1 to 2 years.

For An-12 aircraft of civil aviation, these values are: 500 flights, 500-1000 flying hours, 1 year.

To increase the economic efficiency of aircraft it is allowed for to operate them with increased take-off weight (up to 30% of flights). Thus, for the AN-24RV airplanes, instead of 21.5 tons according to the specifications, an increased take-off weight of 22.5 tons is permissible.

For An-26 aircraft, instead of 24 tons, take-off weight of 25 tons is allowed.

For An-12 aircraft, instead of 61 tons, take-off weight of 64 tons is allowed.

For An-32 aircraft, instead of 27 tons, a take-off weight of 28.5 tons is allowed.

Additional operating conditions, including aerodynamics, are determined by appropriate conclusions on the lifetime. For An-24, An-12 and other aircraft, which have specific operating conditions, for example, An-24 aircraft in version with ASLK complexes used for testing ground radio equipment for landing, or in the "fish-ice" variant for fish and ice reconnaissance, or An-12 in the jammer version, conditions for accounting of lifetime depletion for the aircraft as a whole and for its separate units, for example, flaps, landing gear, etc. are stipulated.

For the purpose of checking and confirming the aircraft lifetime characteristics fatigue tests of aircraft with operating hours were conducted. The tests were performed using marked loading programs (see Chapter 7), followed by disassembly, defect-analysis and fractographic studies.

Antonov State Company was testing the AN-12 airplane No. 11378, factory number 26-08 having total flying time of 12,376 flights, 31633 flying hours and service life of 27 years, and being at the stage of fractographic studies after disassembly and inspection for defects after completion of fatigue tests, An-24 aircraft No. 46445, factory number 44-07, produced in 1968, having total flying time 31,102 flights, 30,407 flight hours.

Total operating time in the laboratory of An-24 airplane No. 64445 was 55422 flights along with studying the survivability characteristics in critical locations. The tests were completed with checking for the residual strength in three stages with the consequent removal of repair pads from critical locations.

At the last stage, the wing was brought to destruction. After the fractographic studies of this aircraft has been completed, a justification was prepared, which proves possibility to prolong lifetime of the An-24 aircraft to the following values: 48,000 - 50,000 flights, 80,000 - 90,000 flight hours.

Antonov State Company conducts training of specialists of ATB and repair shops for methods of non-destructive control of critical locations for each type of aircraft and issues corresponding certificate for a period of 1 year. The need for such training is clearly demonstrated by the following example.

When performing the 7<sup>th</sup> overhaul on An-24 airplane No. 46635 (factory No. 89-01) (the operating time from the beginning of operation was 34639 flying hours, 23966 flights, after the last repair - 5251 flying hours, 3309 flights, previ-

ous repairs were carried out at the plant No. 412 GA, with operating time of 29388 flight hours, 20660 flights), a crack of the lower cap of the second wing spar was detected in the second rib of the center wing section along the radial transition of the tail hinged panel hinge lug. The crack completely cut the spar horizontal flange, and its length in the vertical flange was 75 mm. In addition, at the same location, a crack was found in the center wing section lower rear panel of 54-mm length.

As a result of the study, the following was stated:

1. Cracks that develop in the lower cap of the second spar and in the skin of the lower rear panel have fatigue nature. The origination of the crack occurred from the radius transition of the hinged panel attachment lug in the lower cap. In the skin, the crack originated from the hole edge of the first row of the skin fasteners to the cap horizontal flange.

2. The crack of 1 mm deep in the side member flange was detected after total flying time of 16740 flights. The crack growth time in the spar cap from the depth  $L = 1$  mm to the detection time was 7230 flights.

3. The crack originated from an industrial defect – deviation from the requirements of the drawing. On the airplane, the actual value of the transition radius of hinged panel attachment lug was 2.5 mm instead of the required radius of at least 10 mm.

It should be noted that in the airplane's log book there was a record of the implementation of the Service Bulletin No. 837-DK during the overhaul at the factory, with the operating time of 17032 flights, 24,391 flying hours starting from the beginning of operation. This bulletin is executed when 15,000 - 20,000 flights are operated.

According to the technology specified in the bulletin, the correspondence of the transition radius of the second spar lower cap lug to the drawing requirements with regard to the radius of the rounding to be not less than  $R = 10$  mm, finishing and absence of cuts. If deviation from the drawing requirements is detected, the transition radius to  $R$  not less than 10 mm is machined and required surface finish is reached. In addition, during each major overhaul after 15,000 flights, eddy current examination of this zone is required according to KNK 57.10.06 (requirement of Bulletin No. 115-P, which was put into effect in June 1985). In operation in accordance with paragraph 2.04.03.19 of the Maintenance Schedule issued in 1987 (item 4.04.65 of the Maintenance Schedule issued in 1991), an eddy current examination of the above-mentioned zone should be carried out, beginning from the operating time of 15,000 flights with interval of 900 flight hours, and beginning from 30000 flying hours with interval of 300 flight hours .

The development of a crack from length  $L = 3$  mm detectable by eddy current control to the final operating time occurred for  $N \cong 4500$  flights, i.e. this crack should have been detected in operation at least five times and once during major overhauls.

Operation and overhaul department had sent a telegram about the execu-

tion of a one-time control of the An-24 aircraft in the specified zone, according to paragraph 2.04.03.19 of technological card No. 90 of Maintenance Schedule issued in 1987 (paragraph 4.04.65 of the Maintenance Schedule issued in 1991) and the visual inspection of the lower rear panel nearby the second rib of the center wing section at a distance of 200 mm in each direction from the rib axis.

Based on the results of one-time inspection, any defect was not detected.

When performing maintenance of the An-24 airplane No. 47163, factory No. 17-05 (the operating time from the beginning of operation is 39791 flying hours, 35839 flights, after the last overhaul - 4822 flying hours, 3839 flights, the last 7th repair was carried out on 05/22/1989), a crack of the lower cap of the second spar of the right half-wing was detected in this zone. The length of the crack on the horizontal flange of the spar cap was of 44 mm, on the vertical flange – 40 mm.

When carrying out overhaul on the An-24 airplane No. 46492 (factory No. 82-05) (the operating time from the beginning of operation was 39622 flying hours, 28773 years, the previous overhaul was carried out in October 1990 with the operating time from the beginning of operation 34671 flying hour, 25919 flights), a crack of the lower cap of the second spar in this zone was detected. The length of the crack on the horizontal flange of the spar cap was of 24 mm, along the vertical flange – 19 mm.

When carrying out a one-time inspection on the An-24 airplane No. 46512 (plant No. 84-08) (the operating time from the beginning of operation was 38,648 flying hours, 32352 flights, the previous overhaul was performed in August 1990), a crack of the vertical flange of the lower cap of the second spar in the specified zone was revealed. The crack length was 14 mm.

As of 01.2001, only 6 cases of cracks in the lower cap of the second spar of the wing center section in this zone and 14 cases of cracks in a similar zone on the fourth rib were found.

The wing of the An-24 aircraft maintains the operational load with the destroyed cap of the rear spar in the said zone with the damaged skin along the cap width.

The service bulletin has been issued as specified the following works on refinement of places, where tabs fastening the tail portion at the lower cap of the second center wing section spar end in zones of ribs No. 2 and 4 and similar locations on the first spar in zones of ribs No. 2, 5 and 6 regardless of the condition of radius transitions during the next overhaul. The refinement involves shifting the radius transition and increasing the radius to 20 mm, followed by eddy current testing for cracks.

This example clearly demonstrates the need for a periodical training the specialists for NDT at ATB and factories performing overhauls by the developer specialists as for all critical areas of each aircraft and the personal involvement of the developer experts as the most qualified specialists in studies of technical condition of the aircraft whenever extending the lifetime and terms of service.

The greatest number of defects has been detected by the specialists of Antonov State Company when investigating the technical condition of aircraft during the extension of lifetime and service lives.

In addition to the training of the specialists the quality of work and safety of workers themselves are under influence of the following factors:

1. Equipping specialists with modern non-destructive testing tools (eddy current and ultrasonic, allowing to continuously monitor the relief when controlling, for example, torsion box panel thickness for corrosion on internal surfaces), flexible light guides, magnifiers with built-in illumination, convenient powerful flashlights in rubber shell, a set of convenient rotary mirrors, etc.

2. Dress code (summer and winter). It should be comfortable, there should also be shoes and hats.

3. Weather factors. In winter, work should only be carried out in heated rooms at the factory or ATB. This condition must be specified at the stage of signing a contract with the operating organization. It is impossible to carry out work qualitatively and safely to study the technical state at sub-zero temperatures.

These issues are also solved by Antonov State Company. Non-destructive testing devices of the new generation (ultrasonic and eddy current) have been ordered and received, the issue of equipping all specialists involved in the study of technical state with comfortable branded clothing, etc. was solved. Thus, application of the above-described concept of individual prolongation of lifetime and service life of the Antonov aircraft allows ensure their safe operation with the maximum use of life capabilities.

#### 10.4. DEVELOPMENT OF METHOD TO EXECUTE AIRCRAFT TRAINING TOUCH-AND-GO LANDINGS TO REDUCE DEPLETION OF AIRFRAME STRUCTURE LIFETIME

As noted in subsection 7.2, flight training programs for airplane crews include training flights to enhance piloting techniques for take-offs and landings. The percentage of such training flights is quite high. Reducing the airframe structural damage, of the wing in particular, as it basically determines the airframe strength, could be achieved if standard flights with a full cycle of stages are replaced by flights with successive takeoffs immediately after landing. Reducing the airframe damage will be achieved by eliminating intermediate taxiing, and for the wing in addition – due to a decrease in the G-A-G cycle range.

To test this technique to reduce the level of the wing load, as well as determine the specifics in the technique of piloting the flight tests were performed on specially equipped An-22 airplane No. 02-03. The tests were carried out by the flight testing department of the enterprise flight test and development bas (FTDB). In flight tests, the loads acting on the wing as bending moments in the root sections of the left and right wing were measured. The tests were conducted at Gostomel and Boryspil airfields. The results of the tests had shown that execution of the "touch-and-go landing" flight does not possess difficulty in pilot-

ing and can be recommended for flying crew training.

Loads were investigated when performing "touch-and-go" landings with symmetrical and asymmetrical engine thrusts, middle and front CG position, and also when landing according to the Flight Operations Manual (FOM) [85].

To study the wing loads while developing the methodology of training flights using the "touch-and-go landing" method on the An-22 No. 02-03 airplane, the following tasks were accomplished:

In order to assess flight safety when performing "touch-and-go landing" with failed engine, as well as to check the piloting technique during continued take-off, the following kinds of flight were performed: combined landings-take-offs with asymmetrical thrust of engines with power plant # 4 turned off; with power plant # 4 failed after change of the engine power prior to lift-off (continued "touch-and-go landing"); with power plant # 4 failed at the moment of touching the ground (interrupted "touch-and-go landing").

During these flights, the CG position  $X_{CG} = 27\%$ , airplane weight  $G_{a-pl} = 188$  tons, fuel weight  $G_{fuel} = 59$  tons.

1. Combined landings with CG position  $X_{CG} = 27\%$ , airplane weight  $G_{a-pl} = 189...185$  ton-force, fuel weight  $G_{fuel} = 60...56$  ton-force.

2. Combined landings-take-offs with CG position  $X_{CG} = 22\%$ , airplane weight  $G_{a-pl} = 180$  ton-force, fuel weight  $G_{fuel} = 42$  ton-force.

3. Landings according to Flight Operations Manual with CG position  $X_{CG} = 27\%$ , airplane weight  $G_{a-pl} = 177$  ton-force, fuel weight  $G_{fuel} = 48$  τ and  $X_m = 22\%$ , airplane weight  $G_{a-pl} = 172$  ton-force, fuel weight  $G_{fuel} = 34$  ton-force.

Piloting with combined landings-take-offs was carried out as follows:

- landing approach gliding with flaps extended at  $25^\circ$  over standard glide path with speed  $V_{app} = 280$  km/h;
- touching the runway surface with the wheels of the main landing gear supports at speed  $V_{ind} = 280$  km/h;
- Increase the engine power (TCL advance) to takeoff or nominal amount;
- separation of the main wheels from the runway surface at a speed not lower than  $V_{ind} = 240$  km/h;
- transition to climb.

When performing "touch-and-go landing" landings and take-offs with CG position of  $22\%$  the engine power was chaged at flight speeds  $V_{ind} = 200$  and  $220$  km/h, lift-off was carried out at the takeoff and rated power with the landing gear strut being extende and retracted, in contrast to the flights with CG position  $X_{CG} = 27\%$ , where the speed at TCL advance was  $V_{ind} = 230 ... 250$  km/h with the retracted nose strut.

Flights were executed from the unpaved runway of the Gostomel airfield and the concrete runway of the Boryspil airport. In total, 17 combined landings-take-offs and 4 landings according to FOM were performed. To assess the load characteristics of the product structure the following was recorded: load at the center of gravity, bending moment at the root section of the left and right wing

consoles. Strain gauges on the wing were located on the panels between the second and third spars on the sixth rib ( $Z = 3,695$  m). K20-21 oscilloscopes with the 8ANCH-7M and K-10 amplifiers were used as control and measuring equipment. Registration of overloads at the center of gravity of the product was carried out by the MP-95 sensor. On-ground calibration of the measuring channels of the wing was carried out by the loading method. During execution of "touch-and-go landings" and take-offs when recording loads on the wing, the equipment was switched on in the parking lot before take-off and switched off after the flaps had been retracted. Next switching on was carried out for 10-20 s during go-around flight in the levelled portion ( $H = 400$  m,  $n_y = 1.0$ ,  $\sigma_3 = 0$ ), and then before the flaps were extended for landing.

All records of loads on the wing during flight tests were accompanied by information on the flight weight of the fuel.

Patterns of oscillograms of the recordings of wing loads with combined landings-take-offs ("touch-and-go landing") and when landing according to FOM are shown in Figures 10.1 and 10.2. The processing of load records on the wing in "touch-and-go landing" flights was carried out for the following stages:

- at the moment of touching the runway with the wheels of the main landing gear;
- with increasing the operating power of the engines;
- at the moment of separation of the main wheels from the runway surface;
- on the horizontal part of the go-around flight and when performing landings according to FOM – only at the moment of touching the ground.

For the reference "zero" the loads were taken at the parking lot when the engines were running at ground idle.

Loads in the form of increments of bending moments  $\Delta M$  to the parking value were determined by the formula

$$\Delta M_i = (A_i - A_o)K,$$

where  $A_o$  is the ordinate of the recorded value in the parking lot, mm;  $A_i$  is the recorded ordinate in the check point of the mode in question, mm;  $K$  is the calibration factor, tm/mm.

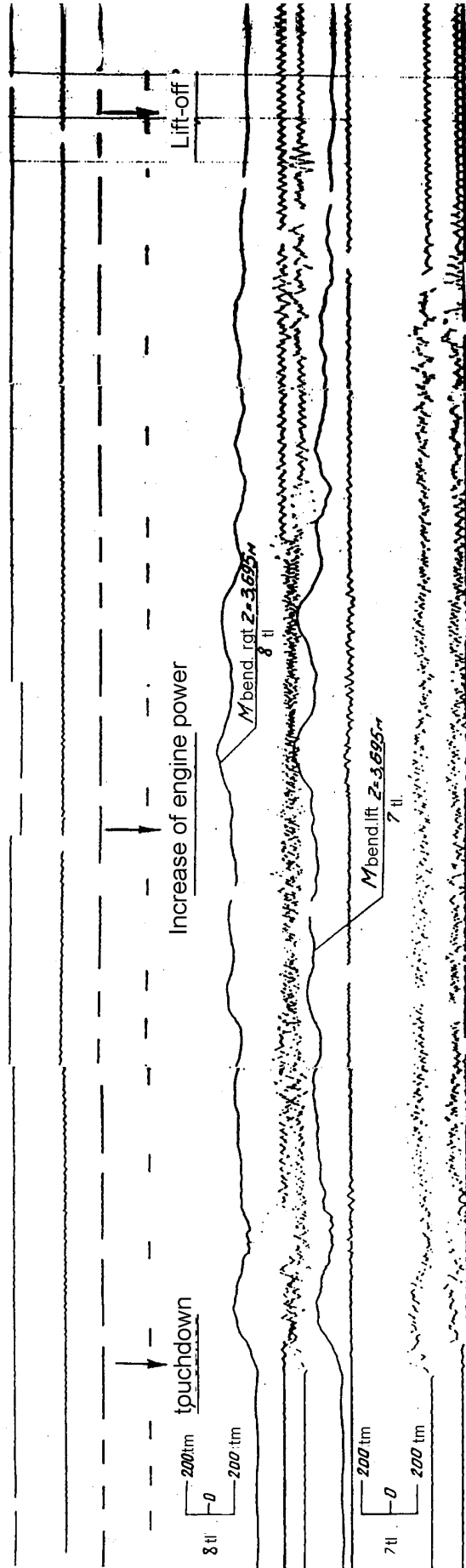


Fig. 10.1. Fragment of oscylogram of recording loads on wing of An-22 aircraft # 02-03.

Flight has been executed on 01/29/08 at Gostomel unpaved aerodrome.

Landing combined with take-off - "touch-and-go landing",  $G_{a-pl} = 177.8$  tons;  $G_{fuel} = 48.8$  tons;  $X_{CG} = 27\%$

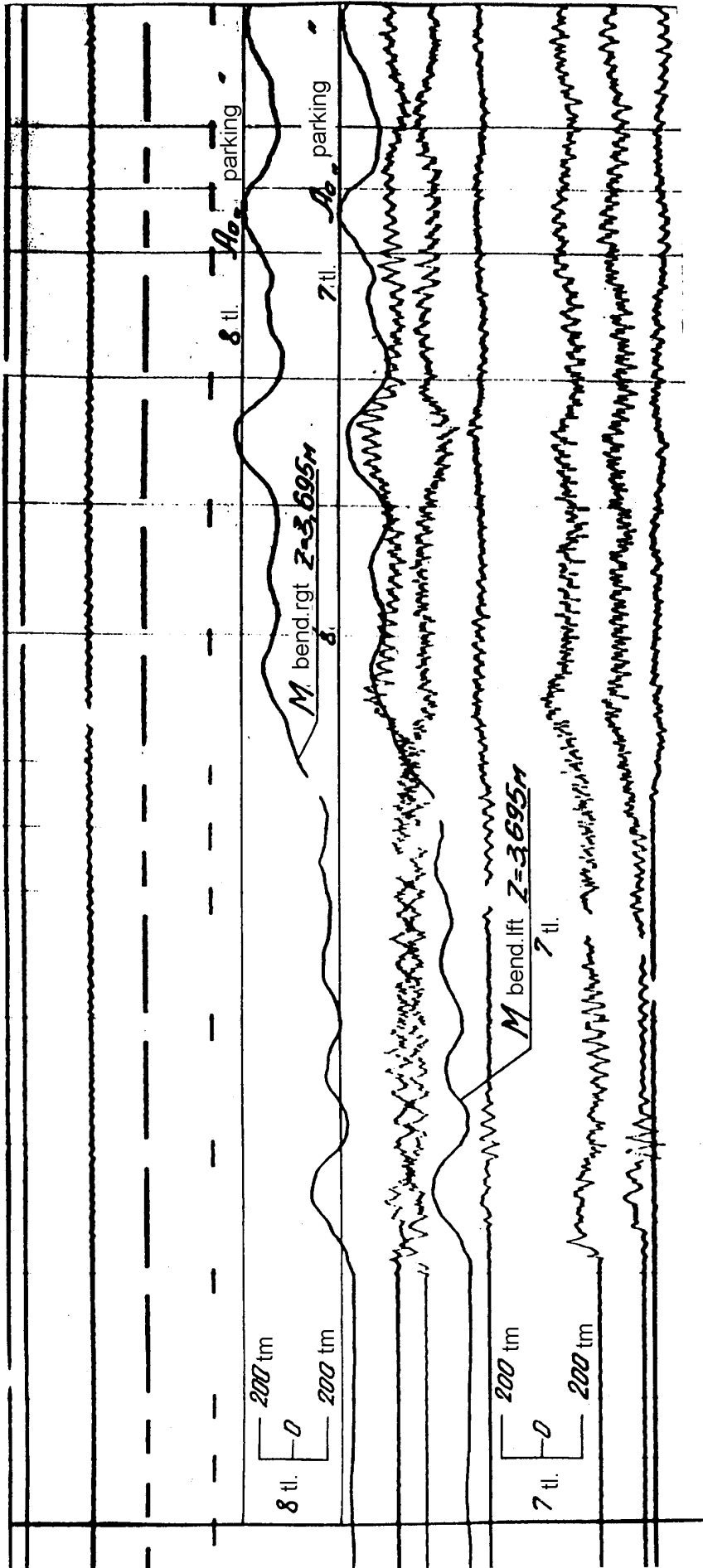


Fig. 10.2. Fragment of oscylogram of recording loads on wing of An-22 aircraft # 02-03.

Flight has been executed on 01/29/08 at Gostomel unpaved aerodrome.

Landing executed according to "Instruction for Crew",  $G_{a-pl} = 177.8$  tons;  $G_{fuel} = 48.8$  tons;  $X_{CG} = 27\%$



Values of bending moments during parking  $M_{park}^{t-off}$  were determined by calculation using the program for calculating the individual depletion of the wing lifetime (see subsection 10.1).

The conducted flight experiment on execution of combined landings-take-offs made it possible to determine the wing loads under dynamic loading when the main LG touched runway, at the moment of increasing the engine power and at the moment of lift-off.

The data obtained has shown that when flying as touch-and-go landing, the wing during the ground phase is in a position close to the balanced one, i.e. decreases the cycle G-A-G range. This is due to the fact that the aircraft speed of th during the "landing-take-off" regime is not lower than  $V = 200$  km/h.

To estimate the degree of reduction of cycle G-A-G during the "touch-and-go landing" flight the ratio of the wing bending moment maximum span at the points of lift-off and increasing the engine power to the maximum (cycle G-A-G) was determined during landing according to FOM with those same flight parameters.

The G-A-G cycle range during flight according to FOM was determined by the "Lifetime" program. For flights using the "touch-and-go landing" method the minimum bending moment was determined by the results of the flight experiment, and the maximum value was taken to be the same as of the flight according to FOM. The G-A-G cycle range in execution of the "touch-and-go landing" flights in the variant  $X_m = 27\%$ ,  $G_{a-pl} = 189 \dots 177$  tf,  $G_{fuel} = 60 \dots 47$  tf comprises 40 ... 78% of the full G-A-G cycle range during conventional landing.

In the "touch-and-go landing" version,  $X_m = 22\%$ ,  $G_{a-pl} = 180 \dots 172$  tons,  $G_{fuel} = 42 \dots 34$  tf comprises 32 ... 46% of the full G-A-G cycle range.

During "touch-and-go landing" flight with an asymmetric engine thrust  $X_m = 27\%$ ,  $G_{a-pl} = 188$  tf,  $G_{fuel} = 59 \dots 22$  tf that is 57% of the full G-A-G cycle range.

The bending moment span during execution of the "touch-and-go landing" along the entire test volume was in average about 45% of the full G-A-G cycle range during normal landing.

Figure 10.3 shows the range of the wing bending moment variation when performing "touch-and-go landing" landings-take-offs.

Vertical g-force at the aircraft center of gravity while performing "touch-and-go landing" landings-take-offs at the moment of touching the runway was  $n_y = (1,25 \dots 1,41)g$ , while landing according to FOM,  $n = (1,25 \dots 1,41) g$ , that is the g-forces almost coincided.

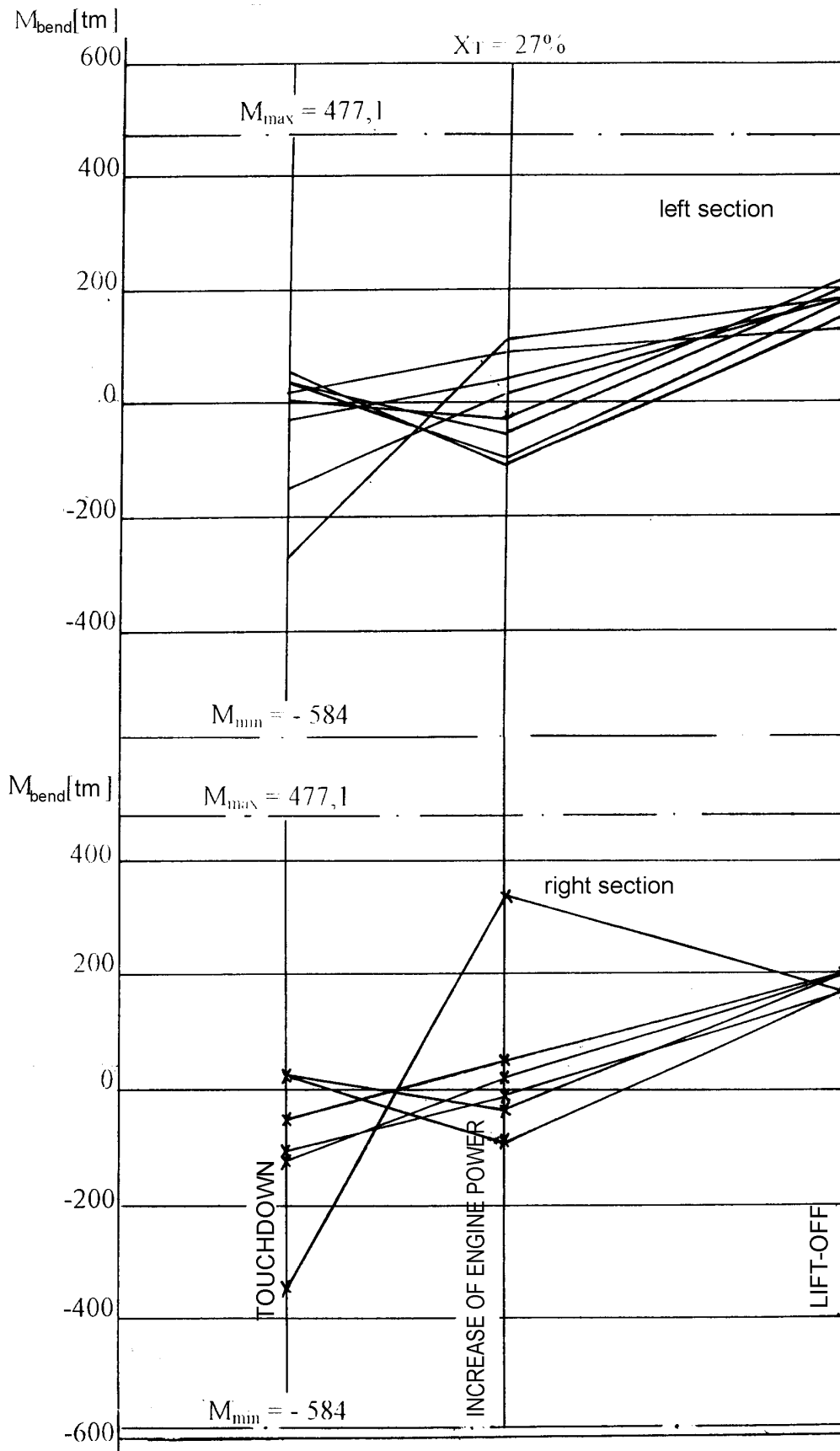


Fig. 10.3. Range of variation of  $M_{bend}$  in wing root sections  $Z = 3.695$  m while performing "touch-and-go landing" flights

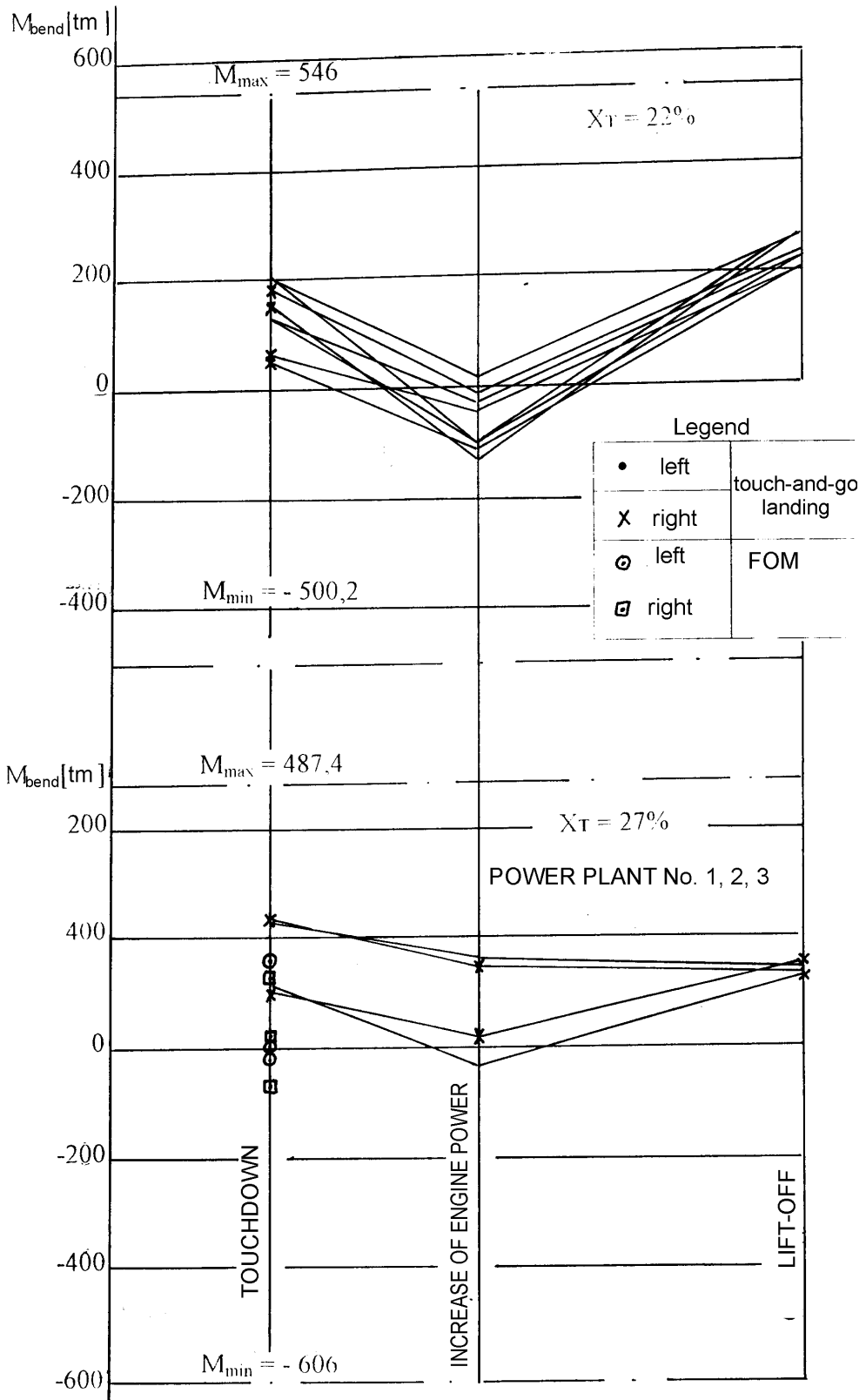


Fig. 10.3. Range of variation of  $M_{bend}$  in wing root sections  $Z = 3.695$  m

while performing “touch-and-go landing” flights (the end)  
Permissible operational g-force during rough landings  $n^{op} = 2.5$ .

### Comparison of occurrence of damage to the wing during “touch-and-go landing” flights and when piloting according to FOM.

As it has been shown in subsection 7.2, during “touch-and-go landing” flight the wing at the ground is not completely unloaded and is in condition close to the unloaded one. At the same time stresses in the wing do not change sign as in flight performed according to FOM, but decrease from the maximum values during flight (the lower surface is stretched, the upper surface is compressed) to zero.

Fig. 10.4 shows schematically variation of bending moments in the wing root section in flight according to the instructions and in touch-and-go landing.

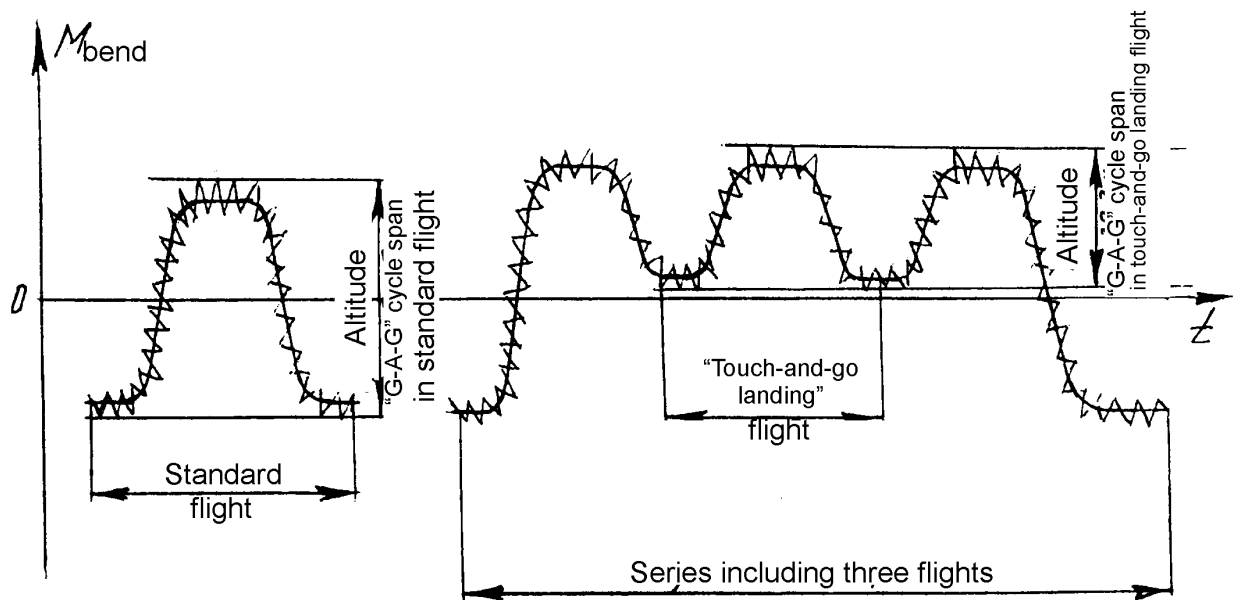


Fig. 10.4. Variation of Bending Moment in Wing Root Section in Standard and “Touch-and-go Landing” Flights

To calculate the wing damage in “touch-and-go landing” flights in this experiment, a program was used to calculate the individual lifetime depletion (see subsection 10.1). The initial data for calculating occurrence of damage of the specified program are the following parameters of flight performed according to FOM:  $G_{t-off}$  – aircraft take-off weight;  $G_{fuel}$  – fuel weight before take-off;  $H_{flt}$  – flight altitude;  $t_{flt}$  – flight duration.

When calculating occurrence of damage for all flights, the average CG position  $X_{CG} = 25\%$  has been accepted (due to its insignificant effect on occurrence of damage).

Damage to the wing in “touch-and-go landing” flight was determined as the sum of the damage caused by the turbulent atmosphere, which was assumed the same as in standard flight, and damage during the “G-A-G” cycle during

touch-and-go landing.

As a measure of the wing damage the occurrence of damage in a standard flight was taken. The results of the calculation have shown that damage to the wing bottom surface when performing one flight using the "touch-and-go landing" method averaged 27% of the damage to the wing in normal flight throughout the entire volume of the experiment. In case of touch-and-go landings with touching the runway surface by the nose landing gear wheel (two flights), the average damage to the wing lower surface in the touch-and-go landing was 38% of the damage to the wing in flight according to FOM. Since in a series of touch-and-go landings the first take-off and the last landing are carried out in the same way as in standard flight, depending on the number of touch-and-go landings in the series, the average damage rate per flight varies. The change in the damage to the wing lower surface on average, per flight, depending on the volume of the touch-and-go landings is shown in Table 10.1. In this case, the damage of one flight under FOM with the same parameters is taken as a unit.

Table 10.1

#### Change in Damage to Wing Lower Surface on Average per Flight

Number of flights in series	Occurrence of failures in flight according to FOM $\xi_{FOM}$	Occurrence of failures of wing bottom surface in series of "touch-and-go landing" flights $\xi_{std}$	$K = \xi_{std}/\xi_{FOM}$
1	1.0	-	-
2	2.0	1.271	0.64
3	3.0	1.542	0.51
4	4.0	1.813	0.45
5	5.0	2.084	0.42
6	6.0	2.355	0.39
7	7.0	2.626	0.38
8	8.0	2.897	0.36
9	9.0	3.168	0.35
10	10.0	3.439	0.34

Since during the "touch-and-go landing" flight the wing upper surface is almost always compressed, i. e. is not damaged, then its damage in a series of "touch-and-go landing" flights equals the damage of one standard flight.

As can be seen from Table 10.1, as the series of "touch-and-go landing" flights increases from two to ten, the average damage to the wing lower surface for the flight drops from 64 to 34% of the wing damage in standard flight. Thus, replacement of standard training flights with a full cycle of flight stages – taxiing – takeoff – flight – landing – taxiing, for "touch-and-go landing" flights, excluding intermediate taxiing, leads to significant lifetime savings.

Based on the results of the flight tests, the "Supplement" was issued to the "Instruction to the An-22 Aircraft Crew" [85] on the issue "Sequential "touch-

and-go landing" flights" and the use of this technique was started in the training of crews.

The conducted studies of the loading of the An-22 aircraft wing during the flight by the "touch-and-go landing" method have shown that due to unloading of the wing at the ground stage its damage is significantly reduced. Thus, with an increase in the number of the "touch-and-go landing" flights from two to ten, the average damage to the wing lower surface during the flight drops from 64 to 34% of the damage to the wing in standard flight (flight by FOM).

#### 10.5. DEVELOPMENT OF RECOMMENDATIONS FOR OPERATING DIVISIONS ON RATIONAL USE OF AN-22 AIRCRAFT LIFETIME

Based on the methodology for determining the aircraft wing lifetime depletion in service (see subsection 10.1) and the methodology for performing training flights with "touch-and-go landing" (see subsection 10.4), recommendations have been developed for operating organizations to rationally deplete the An-22 aircraft lifetime.

Recommendations on the rational use of the lifetime are coordinated with TsAGI. The reference manual on the rational use of the strength life during operation of the An-22 aircraft was approved by the Customers.

Influence of the taxiing speed. The analysis of the operating conditions of the An-22 aircraft has shown that when training flights are conducted, aircraft taxiing is carried out at speeds varying from 10 to 60 km/h in a wide range.

To determine the influence of the taxiing speed on the wings' damage, a special flight experiment was conducted to measure the wing dynamic loads during taxiing over concret taxiways with velocities  $V_{tax} = 15, 30, 45$  and 60 km/h. Based on the results of the experiment, comparative calculation of the damage to the wing upper surface (to which the major part of the damage occurs during the taxiing phase) was carried out using the program for calculating the individual lifetime depletion for two flight profiles:

Flight 1:  $G_{t-off} = 175$  tf;  $G_{fuel} = 50$  tf;  $H_{IVl} = 500$  m;  $T_{flt} = 20$  min

Flight 2:  $G_{t-off} = 205$  tf;  $G_{fuel} = 50$  tf;  $H_{IVl} = 7000$  m;  $T_{flt} = 3$  h

Calculation results are given in Table 10.2.

The curves of the dependence of the relative damage vs taxiing speed are shown in Figure 10.5.

Obtained results have shown that the speed of taxiing has a certain influence on the wing damage. Change in the taxiing speed within the range from 0 to 30 km/h has practically no effect on the wing damage. With further increase in the taxiing speed, occurrence of damage begins to increase substantially. Thus, with an increase in the taxiing speed to 45 km/h, the damage to the wing upper surface increases by approximately 20%, with an increase to 60 km/h –

by approximately 30%.

Table 10.2

Damage of Wing Upper Surface Relative to Different Taxiing Rates

Flight parameters	$V_{tax}$ , km/h	Relative Damage
Flight 1: $G_{t-off} = 175$ tf; $G_{fuel} = 50$ tf; $H_{IVL} = 500$ m; $T_{flt} = 20$ min	15	0.99
	30	1
	45	1.23
	60	1.33
Flight 2: $G_{t-off} = 205$ tf; $G_{fuel} = 50$ tf; $H_{IVL} = 7000$ m; $T_{flt} = 3$ h	15	0.99
	30	1
	45	1.19
	60	1.23

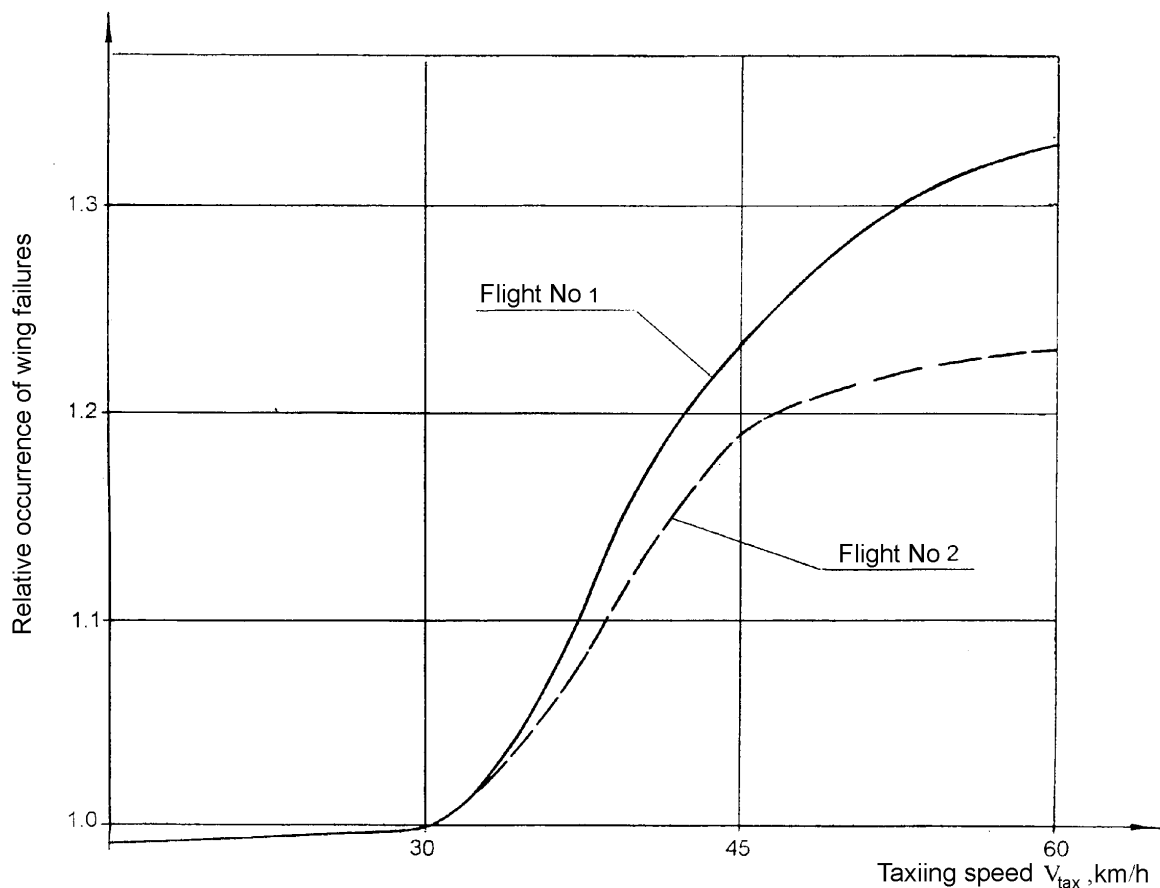


Fig. 10.5. Influence of Taxiing Speed upon Occurrence of Wing Failure

The most reasonable values of taxiing speed in training flights are 20 km/h to 30 km/h.

Influence of reducing flight speed during descend and circuit flight. Influence of reducing flight speed during descend and circuit flight upon occurrence of wing damage (bottom surface, which takes maximum damage share in flight) is analyzed on examples of flights at altitudes  $H = 7000$  m and  $H = 500$  m. Flight parameters are given in Table 10.3.

Table 10.3

## Speed of Circuit Flight

Flight Stage		Up to Third Turn	Third Turn
Flight Weight, tf		160	160
		180	180
		200	200
		220	220
Flight	optimal	380	350
		380	370
		380	380
		400	380
speed $V_{IAS}$ , km/h	minimum permissi- ble	315	315
		335	335
		355	355
		375	375

The flight speed was reduced as follows. For flights at altitude of  $H = 7000$  m, the rate of descent from the level altitude to altitude of 3000 m was reduced from  $V_{IAS} = 460$  km/h according to the instruction [85] to  $V_{IAS} = 420$  km/h. Circuit flight speeds before landing and flying at altitude of  $H = 500$  m were reduced to the minimum values allowed by the instruction [85] (see Table 10.3). While descending from 3000 m to altitude of circuit flight, the flight speed was steepless changed to the value corresponding to the approach speed.

When comparing occurrence of the wing damage in flights with the descent rates according to the instruction [85] and the flights with reduced speeds, the traveled path both during descent and at the circle altitude is assumed to be the same.

The obtained estimates of the damage occurrence of the considered flight profiles are given in Table 10.4.

“Touch-and-go landings”. Reduction in occurrence of wing damage can be achieved by replacing routine training circuit flights with flights with successive takeoffs immediately after landing (see subsection 10.2).

When the series of touch-and-go landings was increased from two to ten, the average damage to the wing lower surface during the flight drops to 64 ... 34% compared to the wing damage in standard flight (according to FOM), and occurrence of damage to the upper surface in the series of touch-and-go



landings was practically equal to the occurrence of damage in standard flight. Therefore you need to strive to reduce the flight duration at low altitudes.

Table 10.4

## Comparative Estimates of Occurrence of Wing Damage

No.	Flight Parameters	Occurrence of Damage, Std. Flight		Relative Occurrence of Damage $K^{(*)}$
		Flight speed acc. to Instruction $V_{desc}=460$ km/h $V_{cre}=380$ km/h	Reduced Flight Speeds $V_{desc}=420$ km/h $V_{cre}=315$ km/h	
1	$G_{t-off} = 175$ tf; $G_{fuel} = 50$ tf; $H_{lvl} = 500$ m; $T_{flgt} = 10$ min	0.307	0.259	0.84
2	$G_{t-off} = 175$ tf; $G_{fuel} = 50$ tf; $H_{lvl} = 500$ m; $T_{flgt} = 20$ min	0.381	0.300	0.80
3	$G_{t-off} = 175$ tf; $G_{fuel} = 50$ tf; $H_{lvl} = 500$ m; $T_{flgt} = 30$ min	0.438	0.336	0.77
4	$G_{t-off} = 205$ tf; $G_{fuel} = 50$ tf; $H_{lvl} = 7000$ m; $T_{flgt} = 1$ h	0.996	0.862	0.87
5	$G_{t-off} = 205$ tf; $G_{fuel} = 50$ tf; $H_{lvl} = 7000$ m; $T_{flgt} = 2$ h	1.155	1.010	0.875
6	$G_{t-off} = 205$ tf; $G_{fuel} = 50$ tf; $H_{lvl} = 7000$ m; $T_{flgt} = 3$ h	1.360	1.197	0.88

Note:  $K^{(*)}$  is the ratio of occurrence of wing damage in flight with reduced velocities to occurrence of wing damage during flight according to FOM [85].

As follows from Table 10.4, a decrease in the flight speed during the descent and circuit flying by about 40 ... 60 km/h as compared to the instruction [85], resulting in a 15 ... 25% reduction in the wing damage.

Influence of the flight elevation and duration. The effect of flight altitude on the damage to the wing (bottom surface) is most significant at low altitudes, less than 1500 meters. For example, damage in a half-hour flight at an altitude of 400 m is

60 ... 80% higher than damage in the similar flight at an altitude of 4000 meters.

Therefore, it is necessary to strive to reduce the flight duration at low altitudes.

Influence of the initial fueling. Large fueling leads to significant increase in the occurrence of the wing damage (upper surface). So, for example, an increase in the fuel charge from 30 to 80 tons leads to more than double increase in occurrence of damage.

Therefore, it is advisable to carry out flights, in particular training with small and medium fueling (30 ... 60 ton-force).

Influence of an aerodrome pavement. The type of an aerodrome pavement has significant effect on the wing damage (upper surface). Damage to the wing during take-off and landing, performed from a ground airfield, is 1.5 to 2 times greater than the damage to the wing during take-off and landing from a concrete aerodrome.

Complexion of exercises. Possibility of reducing the damages of the wing during the integration of exercises is considered for flight examples with the following parameters:  $G_{t-off} = 175$  тс;  $G_{fuel} = 50$  tons;  $H = 3000$  m;  $T_{fgt} = 30$  min.

For the safety margin it was assumed that combination of exercises performed in individual flights into one flight leads to an increase in the flight duration by  $n$  times, where  $n$  is the number of combined exercises.

Calculation results of the wing damage under complexion of two and three exercises in one flight (taking into account the assumptions made above) are given in Table 10.5. Based on the results obtained in Table 10.5, the following conclusion can be drawn. Compared with the damage in an uncomplex flight, the damage per one exercise in combining two and three exercises in one flight decreases and amounts to:

- on the lower surface of the wing – 57 and 42 % respectively;
- on the upper surface – 49 and 32 % respectively.

Thus, integration of exercises in one flight allows significantly reduce the intensity of the wing lifetime depletion. Combining exercises in training flights is one of the most effective ways to solve the issue of rational lifetime use in the aircraft operation.

Assessment of possible reduction of the wing damage. An assessment of the possible reduction in the wing damage by optimizing the modes and profiles of training flights was carried out on the basis of the following assumptions:

1. The share of training flights in the An-22 aircraft operation according to the results of processing the operation statistics is assumed equal to 70%.

2. In accordance with the aircraft crew training course the following distribution of training flights is accepted:

- 40% of all training flights are flights in a circle or  $0,7 \times 40 \% = 28$  % of the total number of flights in operation;
- 60% of the flights to the zone or  $0,7 \times 60 \% = 42$  % of the total number of flights in operation.

Table 10.5

Damage to Wing When Combining Two and Three Exercises in One Flight

No	Flight parameters	Number of exercises in one flight ( $n_i$ )	Lower Surface			Upper Surface		
			Damage $N_{eq}^{std}$ (standard flight)	Damage $N_{eq,i}^{std}$ (standard flight)	Damage $N_{eq,i}^{std}$ (standard flight)	Damage $N_{eq}^{std}$ (standard flight)	Damage $N_{eq,i}^{std}$ (standard flight)	Damage $N_{eq,i}^{std}$ (standard flight)
1	$G_{t-off} = 175$ tf; $G_{fuel} = 50$ tf; $H_{lvl} = 3000$ m; $T_{flgt} = 30$ min	1	0.4143	1.0	1.0	0.7628	1.0	1.0
2	$G_{t-off} = 175$ tf; $G_{fuel} = 50$ tf; $H_{lvl} = 3000$ m; $T_{flgt} = 1.0$ hour	2	0.4732	1.14	0.57	0.7500	0.98	0.49
3	$G_{t-off} = 175$ tf; $G_{fuel} = 50$ tf; $H_{lvl} = 3000$ m; $T_{flgt} = 1.5$ hour	3	0.5657	1.27	0.42	0.7359	0.96	0.32

3. It has been assumed that 80% of the circuit flights can be executed in a "touch-and-go landing" way – five in a series ( $0.28 \times 80\% = 22.4\%$  of the total number of operational flights) and 50% of flights to the zone due to a wider combination of exercises in one flight – three exercises in one flight ( $0.42 \times 50\% = 21\%$  of the total number of operational flights).

In addition, it is assumed that all training flights can be performed with reduced flight speeds during the descent and circuit phases.

Distribution of damage in scheduled and training flights based on the analysis of operation statistics and the corresponding theoretical calculations is given in Table 10.6.

Table 10.6

Damage in Scheduled and Training Flights

No.	Surface	Damage in Scheduled Flight [standard flight]	Damage in Training Flight	
			circuit flight	flight to zone
1	Bottom	1.0	0.3	0.5
2	Upper	1.0	0.8	0.8

Distribution of the wing failure in operation without optimization and with the optimization of modes and profiles of training flights in accordance with the assumptions made above is as follows:

1. Without optimization of modes and profiles of training flights.

Operation equivalent (otherwise - the average damage to one flight in operation)  $N_{eq,\Sigma}$  will be determined as the sum of the components of damage from scheduled flights ( $N_{eq}^{sched}$ ) and training circuit flights ( $N_{eq}^{tr.circ.}$ ) and flights to the zone ( $N_{eq}^{tr.zone}$ ):

$$N_{eq,\Sigma} = N_{eq}^{sched} + N_{eq}^{tr.circ.} + N_{eq}^{tr.zone}.$$

Value of this equivalent of damage in the damage units for standard flight will be equal:

– for bottom surface

$$N_{eq,\Sigma}^{bott} = 0.3 \times 1.0 + 0.28 \times 0.3 + 0.42 \times 0.5 = 0.3 + 0.084 + 0.21 = 0.594 \text{ (standard flight);}$$

– for upper surface

$$N_{eq,\Sigma}^{upp} = 0.31 \times 1.0 + 0.28 \times 0.8 + 0.42 \times 0.8 = 0.3 + 0.224 + 0.336 = 0.86 \text{ (standard flight).}$$

2. With optimization of modes and profiles of training flights.

Operation equivalent ( $N_{eq,\Sigma}^I$ ) is determined as a sum of damage components in scheduled flights ( $N_{eq}^{sched}$ ), training flights – standard circuit flights ac-

according to the instruction [85] ( $N_{eq}^{tr. circ}$ ), training flights with touch-and-go landings ( $N_{eq}^{t-and-go}$ ), flight to zone without combination of exercises in one flight ( $N_{eq}^{tr.zone}$ ) and flights to zone with combination of exercises in one flight ( $N_{eq}^{comb}$ ):

$$N_{eq\Sigma}^1 = N_{eq}^{sched} + N_{eq}^{tr. circ} + N_{eq}^{t-and-go} + N_{eq}^{tr.zone} + N_{eq}^{comb}.$$

Value of the operational equivalent for the considered case of optimizing the modes and profiles of training flights accounting reduction of the flight speed during descend and circuit flying will be:

– for lower surface

$$N_{eq\Sigma}^{bott} = 0.3 \times 1.0 + 0.056 \times 0.3 \times 0.8 + 0.224 \times 0.3 \times 0.42 \times 0.8 + 0.21 \times 0.5 \times 0.875 + 0.21 \times 0.5 \times 0.42 \times 0.875 = 0.3 + 0.013 + 0.023 + 0.092 + 0.039 = 0.467 \text{ (standard flight);}$$

– for upper surface

$$N_{eq\Sigma}^{upp} = 0.3 \times 1.0 + 0.056 \times 0.8 + 0.224 \times 0.8 \times 0.2 + 0.21 \times 0.8 + 0.21 \times 0.8 \times 0.32 = 0.3 + 0.045 + 0.036 + 0.168 + 0.054 = 0.603 \text{ (standard flight).}$$

Thus reduction in occurrence of the wing damage due to mentioned above optimization of the modes and profiles of training flights will be:

– over the wing lower surface

$$K_{L.s} = N_{eq\Sigma}^{L.s.} / N_{eq\Sigma}^{L.s.} = 0.467 / 0.594 = 0.79;$$

– over the wing upper surface

$$K_{u.s} = N_{eq\Sigma}^{u.s.} / N_{eq\Sigma}^{u.s.} = 0.603 / 0.86 = 0.7.$$

Based on the results obtained above, it can be concluded that optimizing the modes and profiles of training flights will significantly reduce the defectiveness of the wing and, consequently, prolong the aircraft operation in the fleet. In accordance with the received estimates, rational use will allow to prolong the aircraft operation by at least 20 ... 30% of the lifetime value without additional constructive measures.

Estimation of possible fuel economy. Below, an approximate estimate is made of the possible fuel economy of the aircraft fleet due to optimizing the modes and profiles of training flights. The estimation was carried out in accordance with the assumptions made above on the distribution of flights in operation. Data on fuel consumption in various flight regimes are taken from the "Instruction to the An-22 Aircraft Crew" [85].

In the circuit training flights, performed by the touch-and-go landing method intermediate taxiings are excluded. The share of circuit training flights executed as touch-and-go landing is equal to 22.4%. According to the instruction [85], the hourly fuel consumption of one engine on taxiing is 1615 kgf/h. Duration of a standard taxiing is 8 minutes. Fuel economy for four engines during the touch-and-go landing flight consisting of five flights in the case considered above, taking into account the share of flights of this type will be:

$$\Delta G_{fuel} = 0.224 \times 4 \times 8 / 60 \times 1615 \times 4 / 5 = 154.4 \text{ kgf.}$$

For training flights to the zone, in the case of a combination of three exercises in one flight, two intermediate taxiing phases, two intermediate climbing phases and two intermediate landing phases are excluded. Fuel economy for the above flight profile is determined based on the instruction [85]:

during climbing	– 1450 kgf;
during descending to circle altitude	– 180 kgf;
during circuit and landing	– 1350 kgf;
during taxiing	– $4.1615 \times 8/60 = 860$ kgf.

Taking into account the above share of training flights to the zone with the combination of exercises in one flight (21%), fuel economy in flight of the type considered

$$\Delta G_{fuel2} = 0.21(1540 + 180 + 1350 + 860)2/3 = 537.6 \text{ kgf/flight.}$$

Consequently, the total fuel economy per flight is as follows:

$$\Delta G_{fuel\Sigma} = \Delta G_{fuel1} + \Delta G_{fuel2} = 154.4 + 537.6 = 692 \text{ kgf/flight.}$$

If we take the average annual flight number of an An-22 aircraft to 150 flights, the average annual fuel savings for one aircraft will be as follows:

$$G_{fuel} = 150 \times 692 = 103.8 \text{ tf.}$$

Based on the above analysis of the possible reduction of the wing damage by optimizing the modes and profiles of training flights, the following conclusions can be drawn:

1. The most rational taxi speeds when performing training flights lie within the range 20...30 km/h.

Exceeding the taxiing speed of 30 km/h (maximum according to the “Instruction for the An-22 Crew” [85]) leads to a significant increase in the damage to the wing. Thus, when taxiing at a speed of 60 km/h, the wing failure increased by about 30% compared to the taxi damage at a speed of 30 km/h.

2. Reducing the flight speed during descending and circuit flight phases is significant in terms of reducing the damage to the wing. Thus, reduction in the speed of descent and flight in a circle to about 40 ... 60 km/h compared to the recommended values in the “Instruction for the An-22 crew” [85] gives a decrease in damage of 15 to 25%.

3. Replacement of standard training circuit flights with flights with successive take-offs immediately after landing (touch-and-go landing) allows to reduce significantly the wing failure.

When the series of touch-and-go landing flights increases from two to ten, the average damage to the wing during the flight drops to 64 ... 34% of the damage to the wing in standard flight (according to the instruction [85]), and the damage to the upper surface in the series of touch-and-go landing flights almost equal to the damage of one standard flight.

4. The effect of flight altitude on the damage to the wing (lower surface) is most significant at low altitudes, less than 1500 meters. For example, the damage in a half-hour flight at an altitude of 400 m is 60 ... 80% higher than that of the corresponding flight at an altitude of 4000 m. Therefore, it is necessary to strive to reduce the flight duration at low altitudes.

5. Large fueling leads to a significant increase in the damage to the wing (upper surface). So, for example, an increase in the fuel charge from 30 to 80 tons leads to more than a twofold increase in damage. Therefore, it is advisable to carry out flights, in particular training, with small and medium fuel charge (30

... 60 ton-force).

6. The type of the aerodrome pavement has a significant effect on the wing damage (upper surface). Damage to the wing during take-off and landing, performed from a soil airfield, is 1.5 to 2 times greater than damage to the wing during take-off and landing from a concrete aerodrome.

7. Combining exercises in training flights is one of the most effective ways to solve the problem of rational use of the wing lifetime. The effect of reducing the wing failure due to combination of exercises is very significant. So, for example, combination of three exercises in one flight leads to a decrease in the damage to the wing lower surface by about 60%, to the upper surface – about 70%.

8. Estimation of possible saving of wing lifetime depletion due to the described above optimization of modes and profiles of training flights (taking into account the real share of training flights in the operation of aircraft in the fleet) testifies to the possibility of extending the aircraft fleet operation within 20 ... 30% of the lifetime value without additional constructive measures.

9. Optimizing the modes and profiles of training flights also saves a significant amount of fuel. According to the assessment, the average annual fuel savings for one aircraft will be at least 100 tons.

### **Conclusions**

1. Conducted researches have shown that for heavy transport planes the lifetime on conditions of endurance needs to be established in the so-called standard flights used as the unit of measurement of damage occurrence, and depletion of the lifetime is determined individually for each airplane.

2. Methodology has been developed for determining the lifetime depletion of transport aircraft wing (Inventor's Certificate No. 308038, USSR, dated 04.07.1988), which allows to determine the lifetime depletion for each aircraft, depending on the specific conditions of its operation, timely make adjustments, and also to develop measures for the rational use of the lifetime by airplanes.

3. For medium-class transport aircraft in case of their use in a mixed version (conventional and special applications), it is necessary to specify the order of depletion of the assigned lifetime, depending on the changed conditions of operation. The principle of step-by-step establishment and prolongation of the lifetime until discarded allows for such changes to be taken into account in a timely manner.

4. Application of individual prolongation of lifetime and service life of the airplanes of the Antonov State Company allows to ensure their safe operation with the maximum use of the lifetime capabilities of the structure. The necessity of training specialists of the ATB and the repair shops by the specialists of the Design Bureau for Nondestructive Testing Methods with reference to each type of aircraft and to each critical location is shown, as well as the participation of the DB specialists in the studies of aircraft technical condition.

5. A method for executing successive take-offs and landings of an airplane

has been developed (inventor's certificate 1320993 USSR dated 01.03.1987). The conducted studies of the An-22 aircraft wing loading during implementation of this method have shown that, due to unloading wing when being on the ground level, occurrence of its failure is significantly reduced. Thus, with an increase in the series of touch-and-go landing flights from two to ten, the average damage to the wing lower surface for the flight drops from 64% to 34% compared to the wing damage in standard flight (flight by FOM). Since during the touch-and-go landing flight the wing upper surface is practically compressed all the time, i.e. is not damaged, then its total damage in a series of touch-and-go landing flights equals the damage in one standard flight.

Based on the results of the flight studies, "Supplement" was drawn up to the "Instruction for the An-22 Airplane Crew" [85], providing for the execution of training flights for mastering takeoffs using the touch-and-go landing method.

The touch-and-go landing flight procedure is recommended for the implementation of training flights for all types of transport aircraft and is used, in particular, for AN-32, AN-124 and AN-124-100 aircraft.

6. "Recommendations for Operation" and "Reference Manual on the Rational Use of the An-22 Airplane Lifetime" have been developed.

The influence of the following factors on the airframe failure during training flights has been considered:

- taxiing speed;
- reducing the flight speed during descent and go-around phases;
- touch-and-go landing flights;
- flight level and duration;
- initial refueling;
- type of aerodrome paving;
- integration of training exercises.

The following has been revealed:

A. The most rational taxi speeds while executing training flights lies within the range of 20 ... 30 km/h. Exceeding taxiing speed of 30 km/h (being the maximum according to the "Instruction to the An-22 Crew" [85]) leads to significant increase in the occurrence of the wing failures. Thus, when taxiing at a speed of 60 km/h, occurrence of the wing failures is increased by about 30% compared to the occurrence of failures in taxiing at a speed of 30 km/h.

B. Reducing the speed of flight during descent and go-around is significant from the point of view of reducing the occurrence of the wing failures. Thus, reduction in the speed of descent and go-around to 40 ... 60 km/h in comparison with the value recommended in the "Instruction to the An-22 Crew" [85] reduces occurrence of failure by 15 ... 25%.

C. The effect of flight altitude on the wing damage (bottom surface) is most significant at low altitudes, less than 1500 meters. For example, occurrence of damage during a half-hour flight at altitude of 400 m is 60 ... 80% higher than occurrence of damage during flight at altitude of 4000 meters. Therefore, it is necessary to strive to reduce the duration of flight at low altitudes.



D. Greater fueling results in a significant increase in the wing damage (upper surface). So, for example, an increase in the fuel charge from 30 to 80 tons leads to more than a twofold increase in damage. Therefore, it is advisable to carry out flights, in particular training, with small and medium fuel charge (30 ... 60 ton-force).

D. The type of aerodrome pavement has a significant effect on the wing failure (upper surface). Damage to the wing during take-off and landing, performed from a soil airfield, is 1.5 to 2 times greater than the damage to the wing during take-off and landing from a concrete aerodrome.

E. Combining exercises in training flights is one of the most effective ways to solve the problem of rational use of the wing lifetime. The effect of reducing the wing damage by combining exercises is very significant. So, for example, combination of three exercises in one flight leads to decrease in the damage to the wing lower surface by 60%, to the upper surface – about 70%.

G. Possible savings in the wing lifetime depletion by optimizing the modes and profiles of training flights (taking into account the real share of training flights in the operation of the considered airplane within the fleet) can be of 20-30% without additional constructive measures, and the average annual fuel saving for one aircraft is approximately 100 tons.

Z. Developed methods and the concept of individual determination of lifetime and service lives adopted by the "ANTONOV" State Enterprise make it possible to maximize the airframe structure lifetime capabilities while ensuring the required level of safety, as evidenced, for example, by the An-24 aircraft, 43,000 flights by Bulgarian airplanes), 57,000 flight hours and a service life of 35 years.

*Chapter 11*  
**IMPLEMENTATION OF DEVELOPED METHODS  
TO DETERMINE AND EMBED  
AVAILABLE SERVICE LIFE CHARACTERISTICS  
OF TRANSPORT AIRCRAFT**

---

The methods for determining and embedding the available lifetime characteristics of transport aircraft presented in this paper were developed by the «ANTONOV» State Company for more than 20 years and introduced into the practice of the «ANTONOV» STATE COMPANY as they were developed.

1. The developed methods for marking loading programs in laboratory tests, described in subsection 8.1, are applied at «ANTONOV» STATE COMPANY since 1979 when fatigue tests of the wings of An-12, An-22 airplanes (including testing the wing for residual strength in order to determine critical size of the fatigue crack in the joint profile), An-24, An-28, An-32, An-72, An-124 airplanes and design samples, which is confirmed by the act of implementation.

Application of the marked loading programs allowed, with the help of subsequent fractographic studies, to obtain reliable information on the kinetics of fatigue cracks in the critical structural elements of these aircraft and to use it when establishing the assigned lifetime.

The developed marking technique allowed to significantly (by an order of magnitude) reduce the complexity of fractographic studies.

The results obtained were used in establishing the assigned resource for the An-22 aircraft.

The developed technique for the experimental determination of the critical size of the fatigue crack makes it possible to determine this size when testing for the residual strength of one "specimen".

2. The developed technique for the experimental determination of the critical size of fatigue damage in the testing of a single specimen of a structure (see subsection 8.2) has made it possible to determine a fatigue crack critical size in the lower profile of the An-22 airplane wing joint made of V93T1 material, and determine the entire process of destruction. The critical length of the crack in the joint profile  $L_{cr} = 30$  mm (taking into account the hole diameter).

The results obtained were used in establishing the assigned lifetime for the An-22 aircraft.

The developed technique for the experimental determination of the fatigue crack critical size makes it possible to determine this size when testing one "specimen" for the residual strength.

3. The results obtained in investigation of the regularities of a single preliminary positive overload effect upon the characteristics of the fatigue life of specimens of D16chT alloy with a hole under loading simulating the loading of the An-124 transport airplane wing (see subsection 8.3.), were used to justify the

load-bearing structure lifetime of the An-124 and An-124-100 aircraft.

The problem of the preliminary positive overload effect upon the fatigue life characteristics in the subsequent endurance and survivability tests was especially relevant after the ANTONOV State Company adopted the concept of combining the fatigue and static tests of the AN-124 airplane on one specimen, which saved one aircraft.

The researches carried out allowed to determine the degree of preliminary positive overload effect upon lifetime characteristics at the stage preceding the appearance of a crack and the stage of its growth.

4. Development of a technique for assessing the damaging effect of cyclic loads at the crack growth stage (inventors certificate 1128768 dated 08.08.1984) made it possible to apply it in studying the regularities of the compressive loads effect at the stage of fatigue crack growth and clarify the existing method of taking into account influence of cyclic load negative part at the stage of crack growth when calculating equivalents [78].

5. The developed method for determining depletion of a transport aircraft wing lifetime (inventor's certificate 308038 dated 01.02.1990, see subsection 8.1) is used in establishing the assigned lifetime to the An-12, An-22, An-124, An-124-100 airplanes.

Application of this method makes it possible to determine depletion of a lifetime by each aircraft, depending on the specific conditions of its operation, to timely make adjustments to the operation, and also to develop measures for the rational use of the lifetime by airplanes.

The economic effect of using the method of individual accounting only the lifetime depletion of the An-22 aircraft wing amounted to ≈\$360 million.

Application of the above-described ANTONOV approach to individual prolongation of the service lives and lifetimes of the ANTONOV aircraft allows them to operate safely with the maximum use of the lifetime capabilities of the power structure of the airframe.

6. At the ANTONOV State Company since the beginning of the 1990s, the concept of an individual approach to the extension of the lifetimes and service lives of the Antonov airplanes described in subsection 9.3 was adopted.

The essence of the concept is that to ensure safety of ageing aircraft. It is required to draw up for them not only basic conclusions on the operation of the fleet, but individual conclusions for each airplane from this fleet, with obligatory inspection of this plane before the extension of the lifetime in accordance with specially developed program. Research of the technical condition of a particular aircraft should be performed by specialists certified by the ANTONOV State Company, with the participation of specialists from the ANTONOV StC. In the future, this approach is recommended by TsAGI for use by aircraft engineering firms [83, 84].

Application of the above-described ANTONOV approach to individual prolongation of the service lives and lifetimes of the ANTONOV aircraft allows them to operate safely with the maximum use of the life capabilities of the airframe

load-bearing structure.

7. The developed methodology for performing training flights of aircraft from the touch-and-go landing in order to reduce depletion of the wing's lifetime (inventor's certificate 1320993 dated 01.03.1987, see subsection 9.4) is applied when carrying out training flights on An-22, An-32, An-124 and An-124-100 airplanes. This technique is recommended for the training of crews in the implementation of training flights on all types of transport aircraft.

Application of this technique reduces depletion of the airframe structure lifetime and fuel consumption.

8. Recommendations (see subsection 9.5) have been developed for the operation with regard to rational depletion of the An-22 airplane lifetime. The analysis was made with the purpose to find possible reduction in wing damage and fuel economy by optimizing the modes and profiles of training flights of the An-22 airplane.

Thus, all the developed methods for determining and embedding available lifetime characteristics of transport aircraft, described in this paper, have been introduced into practice of establishing and prolonging assigned lifetime to the airplanes of the ANTONOV State Company.

## CONCLUSIONS

Based on the theoretical and experimental studies carried out, we can state the following:

1. Various ways to mark the loading program during testing for survivability and residual strength have been developed:

- changing the number of cycles of "dynamics" in neighboring blocks by at least two cycles in programs such as "flight after flight";
- insertions of a program with changing dynamics from insert to insert for at least with two cycles when loaded in symmetric or repeated stress-cycle;
- insertions of various combinations of blocks of small-amplitude loads and periodic load relieving while testing the structure for residual strength.

The developed marking technique makes it possible to determine the instants of nucleation and the kinetics of propagation of fatigue cracks, including in areas inaccessible to visual observation, the critical size of fatigue damage and significantly (by an order) reduce complexity of fractographic studies.

The developed methods for marking the loading program were used or are used in the tests on the survivability and residual strength of the An-24, An-28, An-12, An-22, An-32, An-72, An-124, -22, An-124, An-70 airplanes.

2. A technique has been developed for the experimental determination of the critical dimensions of fatigue damage in testing a single specimen of a structure for residual strength.

The technique was used to determine the critical size of the fatigue crack in the profiles of the An-22 airplane wing technological break when testing the full-scale specimen. The critical size of the fatigue crack in the lower profile of the wing technological break made of the V93T1 material was  $L_{wing} = 30$  mm (taking into account the diameter of the hole).

3. The experimental investigation of the preliminary single positive overload effect regularity on the fatigue life characteristics of the specimens with a hole made of D16chT alloy under loading simulating the loading of the wing of a transport airplane has been performed.

The following has been established:

A. It has been shown that preliminary positive overload leads to an increase in fatigue life both at the stage prior to nucleation of cracks and at stage of their propagation.

B. The effect of preliminary positive overloads is monotonic and increases with increasing value. Thus, application of overload with  $K = 1.25$  had practically no effect on the fatigue characteristics both at the pre-nucleation stage (up to  $L_{crack} = 0.2$  mm) and at the crack propagation stage. Under overload  $K = 1.5$ , total durability increased by 1.07 times. At the same time, duration of the crack propagation increased by 1.12 times, the period prior to nucleation - by 1.04 times. Overload  $K = 2.0$  increased durability by approximately 1.7 times, and the period before nucleation and duration of crack propagation were increased by 1.6 and 1.9 times, respectively.

C. The increase in durability at the stage of crack propagation was mainly achieved due to a decrease in the rates in the zone of the concentrator (hole), which is obviously due to the formation of a plasticity zone because of the overload.

D. With the distance from the concentrator under the same overload, the effect of preloading on the rate of crack propagation decreases and at  $L \geq 12$  mm in length it is practically absent even under the maximum overload  $K = 2.12$ .

The conducted studies of the effect of preliminary overloads on the characteristics of fatigue life allowed to take into account this effect on the results of combined (fatigue and static) tests of the An-124 aircraft and to divide this influence at the stages before nucleation of a crack and its propagation.

E. The obtained results of studies of the positive preliminary single load effect on the characteristics of fatigue life were used to justify the service life of the airframe load-bearing structure of the An-12, An 124 and An-124-100 airplanes.

4. A technique for assessing the cyclic load damaging effect (investor's certificate 1128768) has been developed. It has been shown that the fractographic method makes it possible to determine the ratios-equivalents of the cyclic load damaging effect at the stage of crack propagation.

The methodology developed has the following advantages:

- comparison of the "instantaneous" values of crack propagation rates corresponding to different loads is carried out in local zones, which practically excludes influence of the material structure heterogeneity;

- since comparison of the groove pitch had been carried out on the fracture surface of the same structural element, the property scattering effect of the given material, manufacturing technology, installation of the structural element

in the testing machine, test conditions were excluded;

- elimination of the factors listed above, which affect the scattering of the crack propagation rate, leads to a significant reduction in the volume of the target experiment;

- for determination of equivalents, fatigue fractures of various structural elements tested by loading programs can be used, for which it is possible to establish unambiguous conformity of loads and grooves, even if the fracture zones were not available for observation during testing;

- equivalents for several loads can be determined on one specimen.

5. The regularities of the compressive load effect at stage of crack growth in specimens of aluminum alloys V95 and D16 were carried out using this method (inventor's certificate 1128768). The following has been established:

- application of the half-cycle compression increases the load damaging effect in comparison with the repeated stress-cycle of the same maximum level;

- with increasing compressive stresses, their damaging effect increases;

- with increasing tensile stresses at a constant compressive stress, the relative effect of the compressive loads decreases;

- with increasing crack length, damaging effect of the compressive stresses decreases;

- under the investigated conditions of crack lengths ( $L_{crack} \leq 15$  mm) and the ratios of maximum and minimum stresses ( $\sigma_{max} = 140$  MPa,  $\sigma_{min} = -40 \dots -140$  MPa) for materials D16 and V95, effect of the compressive loads did not exceed 40% and was not less than 8%.

6. It has been revealed that the existing recommendations for taking into account the compressive load effect when calculating the equivalents at the stage of crack growth underestimate the effect of compressive loads. The technique has been proposed for taking into account the effect of compressive loads when calculating the equivalents at the stage of crack growth.

7. It has been established that for heavy transport aircraft, the service life by endurance conditions should be assigned in so-called "standard flights", taken as a unit for measuring the occurrence of failure, and serving out the service life should be determined individually for each airplane.

8. The methodology has been developed for determining depletion of a transport aircraft wing service life (inventor's certificate 308038), which allows to determine depletion of lifetime by each aircraft depending on the specific conditions of its operation, make adjustments in time, and also develop measures for the rational use of the lifetime by airplanes .

The methodology for the individual depletion of the wing lifetime has been used when establishing the assigned lifetime to the An-12, An-22, An-124, An-124-100 airplanes.

The economic effect of using the method of individual depletion of a lifetime for the An-22 airplanes alone amounted to about \$ 360 million.

9. It has been shown that for medium-class transport aircraft in case of their use in a mixed version (conventional and special application), it is necessary to

specify the order of service life depletion depending on the changed conditions of use. The principle of the phased establishment and prolongation of the service life till retirement provided in the Airworthiness Requirements allows for the timely consideration of such changes.

10. The technique has been developed for performing successive flights of the aircraft "touch-and-go landing" (i.c. 1320993) to perform training flights for the crews. The conducted studies of the An-22 aircraft wing loading in flight using this method had shown that, due to load relief at the wing unloading when it is on the ground, occurrence of its failure is significantly reduced. Thus, with an increase in the number of "touch-and-go landing" flights from two to ten, the average occurrence of failure of the wing lower surface in flight drops from 64% to 34% compared to the wing damage in normal flight (flight according to Flight Manual).

Since during the "touch-and-go landing" flight the wing upper surface is almost always compressed, i.e. is not damaged, then its total damageability in a series of "touch-and-go landing" flights equals the occurrence of failure in one normal flight. The method of executing successive take-offs and landings of an airplane ("touch-and-go landing" flight) is used to train the crews on the An-32, An-22, An-124, An-124-100 aircraft.

11. "Recommendations for Operation" and "Reference Manual for Rational Use of An-22 Airplane Service Life" have been compiled and approved or agreed with TsAGI.

Influence of the following factors on the airframe damage while performing training flights has been considered:

- taxiing speed;
- reducing the flight speed during the descent phase and the circling flight;
- touch-and-go landing flights;
- flight level and duration;
- initial refueling;
- type of aerodrome paving;
- integration of training exercises.

The possible saving of the wing service life due to optimization of modes and profiles of training flights (taking into account the real share of training flights in the operation of aircraft in the fleet) can be of 20 ... 30% without additional constructive measures, and the average annual fuel saving for one aircraft is about 100 tons.

12. The developed procedures and methods for identifying and implementing the available service life characteristics and the concept of individual determination of service life adopted by «ANTONOV» STATE COMPANY make it possible to identify maximally the service life capabilities of the airframe designs while ensuring the required level of safety, for example, the An-24 airplanes, which have been reached 40,000 flights that is the record time among the CIS members (43,000 flights by Bulgarian aircraft), 57,000 flight hours and a service life of 35 years.

**BIBLIOGRAPHY**

---

1. Проектирование самолетов [Текст]: учеб. для вузов / С. М. Егер, В. Ф. Мишин, Н. К. Лисейцев и др.; под ред. С. М. Егера. – 3-е изд., перераб. и доп. – М.: Машиностроение, 1983. – 616 с.
2. Авиационные правила. Ч. 25. Нормы летной годности самолетов транспортной категории. – МАК, 2004.
3. Разработка аванпроекта самолета [Текст]: учеб. пособие / А.К. Мяслица, Л.А. Малашенко, А.Г. Гребеников и др. – Х.: Нац. аэрокосм. ун-т «Харьк. авиац. ин-т», 2010. – 233 с.
4. Уголок неба – большая авиационная энциклопедия [Электронный ресурс] / Режим доступа: или URb: <http://www.airwar.ru/lanow.html>. – 24. 04. 2014 г.
5. Основы общего проектирования самолетов с газотурбинными двигателями [Текст]: учеб. пособие: в 2 ч. / П.В. Балабуев, С.А. Бычков, А.Г. Гребеников и др. – Х.: Нац. аэрокосм. ун-т «ХАИ», 2003. – Ч. 1. – 454 с.; – Ч. 2. – 390 с.
6. Шейнин, В. М. Весовое проектирование и эффективность пассажирских самолетов [Текст]: учеб. пособие. – Т. 1 / В. М. Шейнин, В. И. Козловский. – М.: Машиностроение, 1977. – 344 с.
7. NX для конструктора-машиностроителя [Текст] / П.С. Гончаров и др. – М.: ДМК Пресс, 2010. – 504 с.
8. Гребеников, А.Г. Методология интегрированного проектирования и моделирования сборных самолетных конструкций [Текст]: моногр. / А.Г. Гребеников. – Х.: Нац. аэрокосм. ун-т «ХАИ», 2006. – 532 с.
9. Grebenikov, A. Methodology of integrated designing and modelling of aircraft assembly structures: training guide / A. G. Grebenikov. – Kharkov: National Aerospace University «Kharkov Aviation Institute», 2010. – 427 p.
10. Гребеніков, О. Г. Методологія інтегрованого проектування збірних літакових конструкцій регламентованої довговічності [Електронний ресурс]: навч. посіб. / О.Г. Гребеніков. – Х.: Нац. аерокосм. ун-т ім. М. Є. Жуковського «Харк. авіац. ін-т», 2015. – 538 с. / Режим



доступу:

[http://library.khai.edu/library/fulltexts/metod/Grebenikov\\_Metodologija.pdf](http://library.khai.edu/library/fulltexts/metod/Grebenikov_Metodologija.pdf).

11. Principles of designing of airplanes with gas turbine engines: study guide / P.V. Balabuyev, S.A. Bichkov, A.G. Grebenikov and etc. – Kharkiv: National Aerospace University «Kharkiv Aviation Institute», 2013. – 731 p.
12. Конструктивно-технологические методы повышения усталостной долговечности элементов конструкции планера самолета в зоне функциональных отверстий [Текст] / Д.С. Кива, Г.А. Кривов, А.Г. Гребеников и др. – Киев: КВИЦ, 2015. – 188 с.
13. Гребеников, В.А. Обеспечение усталостной долговечности элементов конструкции планера самолета в зоне разъемных болтовых соединений [Текст]: моногр. / В.А. Гребеников. – Х.: Нац. аэрокосм. ун-т им. Н.Е. Жуковского «Харьк. авиац. ин-т», 2010. – 188.
14. Интегрированное проектирование и моделирование высокоресурсных растянутых панелей крыла транспортного самолета [Текст]: монография / А.Г. Гребеников, Е.Т. Василевский, В.А. Матвиенко и др. – Х.: Нац. аэрокосм. ун-т им. Н.Е. Жуковского «Харьк. авиац. ин-т», 2011. – 192 с.
15. Конструкционные материалы в самолетостроении / А. Г. Моляр, А. А. Коцюба, А. С. Бычков, О. Ю Нечипоренко. – К. : КВИЦ, 2015. – 396 с.
16. Наукові основи та методи проектування високоресурсної авіаційної техніки за допомогою комп'ютерних інтегрованих систем [Текст] / О.А. Коцюба, О.Г. Гребеніков, Є.Т. Василевський, А.М. Гуменний // Проблеми створення та забезпечення життєвого циклу авіаційної техніки: міжнар. наук.-техн. конф.: тези доп., 20-21 квіт. 2017 р. / М-во освіти і науки України, Нац. аерокосм. ун-т ім. М. Є. Жуковського «ХАІ». – Х., 2017. – С. 35 – 36.
17. Кива, Д. С. Научные основы интегрированного проектирования самолетов транспортной категории [Текст]: моногр. / Д. С. Кива, А. Г. Гребеников. – Х.: Нац. аэрокосм. ун-т им. Н.Е. Жуковского «Харьк. авиац. ин-т», 2014. – Ч. 1. – 439 с.; – Ч. 2. – 326 с.; – Ч. 3. – 376 с.

18. Интегрированное проектирование винтокрылых летательных аппаратов транспортной категории [Текст]: учебник: в 3 ч. / А. Г. Гребеников, Н. И. Москаленко, В. А. Урбанович и др.; под ред. В. А. Богуслаева. – Х. : Нац. аэрокосм. ун-т им. Н. Е. Жуковского «Харьк. авиац. ин-т». – Запорожье: изд. АО «МОТОР СИЧ», 2016. – Ч. 1. – 411 с.; – Ч. 2. – 454 с.; – Ч. 3. – 419 с..
19. Единые Нормы летной годности гражданских транспортных самолетов стран-членов СЭВ (ЕНЛГ - С). – 1985 .
20. Методы определения соответствия к АП 25.571 «Обеспечение безопасности конструкции по условиям прочности при длительной эксплуатации». 30.12.1996.
21. Нормы летной годности гражданских самолетов СССР (НЛГС-2): 2-е изд. - 1974.
22. D. M. Anderson and W. M. Mc Jee. Development and Application of Marker Loads for Fatigue Crack Growth Study on a Full-Seal Test Article. AIAA/ASME/SAE 17 th Structures Structural Dynamics and Materials Conference, 1976, pp. 126 - 132.
23. J. Schijve. The significance of fractography for investigations of fatigue crack growth under variable-amplitude loading. Fatigue and Fracture of Engineering Materials and Structures, v. 22, Number 2, 1999. – p. 87 - 99.
24. Екименков, Л. Н. Разработка циклограмм маркерного нагружения крыла транспортного самолета применительно к условиям квазислучайного нагружения полетными блоками различных типов [Текст] /Л. Н. Екименков, Ю. М. Стойда // Прочность авиационных конструкций. Тр. ЦАГИ. – М., 1998. – С. 189 - 195.
25. Шахатуни, Е. А. Ускорение фрактографического анализа усталостных изломов [Текст] / Е. А. Шахатуни, Л. М. Бурченкова, А. П. Еретин // Авиационная промышленность. –1979. – №7.
26. Применение «меченых» программ нагружения при усталостных испытаниях конструкций из алюминиевых сплавов [Текст] / Е. А. Шахатуни, С. И. Емельянов, Л. М. Бурченкова, А. П. Еретин // Тез. докл. VI науч.-техн. конф. по выносливости и ресурсу авиационных конструкций. – М., ЦАГИ, 6-8 июня 1979.

27. Шахатуни, Е. А. Практика маркирования усталостных программ нагружения [Текст] / Е. А. Шахатуни, Л. М. Бурченкова, А. П. Еретин // Тез. докл. VIII науч.-техн. конф. по ресурсу авиаконструкций. – Жуковский, 1986.
28. Применение «меченых» программ нагружения при усталостных испытаниях образцов и натуральных конструкций [Текст]/ Е. А. Шахатуни, С. И. Емельянов, Л. М. Бурченкова, А. П. Еретин. // Тез. докл. III науч.-техн. конф. - Новосибирск, 1981.
29. Экспериментальное определение критической длины трещины в натурной конструкции при заданном уровне остаточной прочности / С. И. Емельянов, Л. М. Бурченкова, А. П. Еретин, В. Д. Иньков // Тез. докл. VI науч.-техн. конф. по выносливости и ресурсу авиационных конструкций - М., ЦАГИ, 6-8 июня 1979.
30. Способ определения критической длины усталостной трещины: А.с. 693143 / Ю. Б. Дробот, А. М. Лазарев. - Кл: G01 №3/32, 1978.
31. Еретин, А. П. Определение критического размера усталостного повреждения при испытании одного «образца» [Текст] / А. П. Еретин // Открытые информационные и компьютерные интегрированные технологии. – Харьков: ГАКУ, 2001. - Вып. 9. – С. 70 - 81.
32. L. R. Holl, R. C. Shah, W. L. ENGSTROM. Fracture and Fatigue Crack Growth Behaviour of Surface Flaws and Flaws Originating at Fastener Holes. Technical Report AFFDL-TR-74-47, Volume I, May 1974.
33. Влияние предварительных перегрузок на характеристики усталостной долговечности / Е. А. Шахатуни, А. П. Еретин, В. Ф. Опанасенко, Л. М. Бурченкова // Авиационная промышленность. – 1990. – №12. – С. 9 – 10. ДСП.
34. SURESH S. Micromechanisms of Fatigue Crack Growth Retardation Following Overloads. Engineering Fracture Mechanics. – 1983.V. 18. – p. 577 – 593.
35. E. P. Probst, B. M. Hillberry. Fatigue Crack Delay and Arrest Due to Single Peak Tensile Overloads. A JAA JOURNAL 1974, V. 12 №3, pp. 330 - 335.
36. C. Bathias, M. Vancon Mechanisms of Overload Effect an Fatigue Crack

- Propagation in Aluminium Alloys. Engineering Fracture Mechanics, 1978, №2. – p. 409-423.
37. J .D. Bertel, A. Clerivet, C. Bathias. R Ratio Influence and Overload Effects on Fatigue Crack Mechanisms. «Advanced Fracture Reseach» Conference Proccedings, Cannes, 1986. – p. 943 - 951.
  38. J. Schijve. Accumulation of Fatigue Damage in Aircraft Materials and Structures AGARD - CP - 118, 1974.
  39. M. Lang and Marci. The influence of single and multiple overloads on fatigue crack propagation. Fatigue and Fracture of Engineering Materials and Structures, v. 22, Number 4, April 1999. – p. 251 - 271.
  40. M. M. I. Hammouda, S. S. Ahmad, M. H. Seleem and H. E. M. Sallam. Fatigue crack growth due to two successive single overloads. Fatigue and Fracture of Engineering Materials and Structures, v. 21, Number 12, December 1998. – p. 1537 - 1547.
  41. V. W. Trebules Jr. R. Roberts and R. W. Hertzberg (1973). Effect of multiple overloads on fatigue crack propagation in 2024-T3 aluminum alloy. In: ASTM STP 536. – p. 115 - 146.
  42. C. Amzallag, J. A. Le Duff, C. Ribin and G. Motter (1994). Crack closure measurements and analysis of fatigue crack propagation under variable amplitude loading. In: ASTM STP 1231. – p. 311 - 333.
  43. P.J. Bernard, T.C. Lindley and C.E. Richards (1976). Mechanisms of overload retardation during fatigue crack propagation. In: ASTM STP 595. – p. 78 - 97.
  44. R. D. Brown and J. Weertmann (1978). Effects of tensile overloads on crack closure and crack propagation rates in 7050 aluminum. Engng Fracture Mech.10. – p. 867 - 878.
  45. D. Damri and J. F. Knott (1976). Fatigue crack growth retardation affer single peak and block overloads in a structural steel. In: Proc. of the 4th Int. Conference on Fatigue and Fatigue Thresholds, 15-20 July. – p. 1505 - 1510.
  46. G .Marci (1979). Effects of the active plastic zone on fatigue crack growth rates. In: ASTM STP 677. – p. 168 - 186.
  47. H. Doker and V. Bachmann (1988). Determination of crack opening load

- by use of threshold behavior. In: ASTM STP 1982. – p. 247 - 259.
48. W. T. Matthews, F. I. Baratta and G. W. Driscoll (1971). Experimental observation of a stress intensity history effect upon fatigue crack growth rate.
  49. G. Marci (1980). The effects of the plastic wake zone on the conditions for fatigue crack propagation. *Int. J. Fracture Mech.* 16. – p. 133 - 153.
  50. Y. Park, D. de Vadder and D. Francoir (1992). In situ mid-width and near-surface measurements of the retardation of the propagation of a crack on overload. *Proceedings of the 9th European Conference on Fracture.* – p. 357 - 364.
  51. M. Darvish and S. Johansson (1995). Fatigue crack growth studies under combination of single overload and cyclic condensation environment. *Engng Fracture Mech.* 52. – p. 295 - 319.
  52. E. Welsch, D. Eifeer, B. Scholtes and E. Macherauch (1986). Residual stress distribution caused by overloading in the neighborhood of crack tips and their influence on the propagation of fatigue cracks. In: *Residual Stresses in Science and Technology* (E. Macherauch and Hauk, eds). DGM, Oberursel. – p. 785 - 792.
  53. H. Homma, H. Koksaka and H. Nakazawa (1984). Numerical analysis of fatigue striations after a single overload. In: *Fatigue 84, Proceedings International Conference on Fatigue Thresholds.* EMAS. – p. 927 - 936.
  54. M. M. I. Hommouda, S. S. E. Ahmad, M. H. Seleem and H. E. M. Sallam. Fatigue crack growth due to two successive single overloads. *Fatigue and Fracture of Engineering Materials and Structures.* – 1998. – V. 21. – p. 1537 - 1547.
  55. D. M. Shuter and Geary (1996). Some aspects of fatigue crack growth retardation behaviour following tensile overloads in a structural steel. *Fatigue Fract. Engng Mater. Struct.* 19(2/3) . – p. 185 - 199.
  56. Y. K. Tur and O. Vardar (1996). Periodic tensile overloads in 2024-T3 Al-alloy. *Engng Fracture Mech.* 53(1). – p. 69 - 77.
  57. N. A. Fleck (1985). Fatigue crack growth due to periodic underloads and overloads. *Acta Metall.* 33. – p. 1339 - 1354.
  58. Y. Lu and K. Li (1993). A new model for fatigue crack growth after a single

- overload. Enging Fracture Mech 46. – p. 849 - 859.
59. M. M. I. Hommonda, S. S. E. Ahmad, A. S. Sberbini and H. E. M. Sallam Deformation behaviour at the tip of a physically short fatigue crack to a single overload. Fatigue and Fracture of Engineering Materrials and Structures. V. 22, Number 2, 1999.
  60. Шахатуни, Е. А. Определение соотношения повреждающего действия нагрузок методом фрактографии [Текст] / Е. А. Шахатуни, Л. М. Бурченкова, А. П. Еретин // Тез. докл. VII науч.-техн. конф. по ресурсу самолетов. – М., ЦАГИ, 15 - 18 марта 1983.
  61. Mc Millan J. C., Pelloux R. M. «Fatigue Crack Propagation Under Program and Rondon Loads», ASTM STP 415, 1967.
  62. Способ оценки повреждающего действия циклических нагрузок: А. с. 1128768 / Е. А. Шахатуни, Л. М. Бурченкова, А. П. Еретин. - №3630861; Приоритет изобретения 29. 07. 1983.
  63. TM Hsu and L. M. Lassiter. Effects of Compressive Overloads on Fatigue Crack Growth. Journal of Aircraft, v. 12, Number 2, 1975. – p. 100 - 104.
  64. J. D. Bertel, A. Clerivet, C. Bathias. R.Ratio Influence and Overload Effects on Fatigue Crack Mechanisms. «Advanced Fracture Reseach». Conference Proccedings, Cannes, 1981. – p. 943 - 951.
  65. Takeshi Kanazawa, Susumu Mahida, Kougu Stoga. On the Effect of Cyclic Stress Ratio on the Fatigue Crack Propagation. Engeneering Fracture Mechanics. – 1975. Vol. 7. – p. 445 - 455.
  66. Albertin L., Hudak S. Effect of Compressive Loading on Fatigue Crack Growth Rate and Striation Spacing in Type 2219 - T851 Aluminum Alloy. Fractography and Materials Science, ASTM STP 733 1981. – p. 187 – 201.
  67. Marissen R. The Influence of Compression Loads and of  $dk/da$  on the Crack Propagation under Variable Amplitude Loading. Engineering Fracture Mechanics. – 1984. V. 5, №5. – p. 863 –879.
  68. M. Land (1998). The influence of compressive loads on fatigee crack propagation in metals. Fatigue Fract. Engng Mater. Struct. 21. – p. 65-84.
  69. M. Land and Huang. The influence of compressive loads on fatigue crack propagation in metals. Fatigue Fract. Engng Mater. Struct. V. 21, Number

- 1, 1988.
70. R. Pippan (1987). The growth of short cracks under cyclic compressions. *Fatigue Fract. Engng Mater. Struct* 1. – p. 267 - 270.
71. H. D. Dill and C. R. Saff (1977). Analysis of crack growth following compressive high loads based on crack surface displacements and contact analysis. *ASTM STR 673*. – p. 141 - 152.
72. E. Zaikren and R. O. Ritchie (1985). On the role of compression overloads in influencing crack closure and the threshold condition for fatigue crack growth in 7150 aluminum alloy. *Engng Fract. Mech.* 22. – p. 35 - 48.
73. R. L. Corlson and G. A. Kardometeas (1993). Effects of compressive load excursions on fatigue crack growth. *Int. J. Fatigue* 16. – p. 141 - 146.
74. R. I. Stephens, G. W. Mc Burney and L. J. Oliphant (1974). Fatigue crack growth with negative R-ratio following tensile overloads. *Int. J. Fract* 10. – p. 587 - 589.
75. W. X. Alzos, A. C. Skat and B. M. Hillberry (1976). Effect of single overloads/underload cycles on fatigue crack propagation. *ASTM STP 959*. – p. 41 - 60.
76. R. Marissu, K. H. Trautmann and H. Nowack (1984). The influence of compression loads and of  $dk/da$  on the crack propagation under variable amplitude loading. *Engng Fract. Mech.* 21, 453 - 463.
77. Еретин, А. П. Методика учета отрицательной части циклических нагрузок при определении эквивалентов на стадии роста усталостной трещины [Текст] / А. П. Еретин // Открытые информационные и компьютерные интегрированные технологии. сб. науч. тр. Нац. аэрокосм. ун-та им. Н. Е. Жуковского «ХАИ». – Вып. 8.–Х.–2000.– С. 102 – 117.
78. Учет индивидуального расходования ресурса крыла / Е. А. Шахатуни, В. М. Никитин, А. П. Еретин, С. И. Мельников // Тез. докл. VI науч.-техн. конф. по выносливости и ресурсу авиационных конструкций. – М., ЦАГИ, 6 - 8 июня 1979.
79. Способ определения расхода ресурса конструкции транспортного самолета: А. с. 308038. / А. И. Фролков, В. Л. Райхер, Е. А. Шахатуни, А. П. Еретин и др. №3206153/40-23; Заявлено

- 4.07.88; Опубл. 01.02.1990.
80. Еретин, А. П. Учет индивидуальной нагруженности планера самолета в эксплуатации при установлении назначенных ресурсов // Открытые информационные и компьютерные интегрированные технологии. сб. науч. тр. Нац. аэрокосм. ун-та им. Н. Е. Жуковского «ХАИ». – Вып. 9.– Х.–2001 – С. 50 – 57.
  81. Методология и опыт обеспечения безопасности конструкции стареющих самолетов / А. Ф. Селихов, В. Г. Лейбов, Г. И. Нестеренко, В. Л. Райхер // Прочность авиационных конструкций. Тр. ЦАГИ. – М., 1998. – С. 21 – 29.
  82. Поддержание летной годности конструкций аттестованных самолетов по условиям ресурса / В. С. Дубинский, Г. И. Нестеренко, В. Л. Райхер, Ю. А. Стучалкин // Прочность авиационных конструкций. Тр. ЦАГИ. – М., 1998. – С. 73 – 75.
  83. Нестеренко, Г. И. Усталость и живучесть конструкций стареющих самолетов [Текст] / Г. И. Нестеренко // Прочность авиационных конструкций. Тр. ЦАГИ. – М., 1998. – С. 67 – 72.
  84. Инструкция экипажу самолета Ан-22 .– Изд. 2-е. Ч. II, 1975.
  85. Анализ напряженно-деформированного состояния авиационных конструкций в системе ANSYS [Текст]: учеб. пособие / В. Н. Анпилов, А. Г. Гребеников, Ю. Н. Геремес и др. – Х. : Нац. аэрокосм. ун-т им. Н. Е. Жуковского «Харьк. авиац. ин-т», АНТО «КНК», ANSYS Inc., 2008. – 410 с.
  86. Механіка руйнування і міцність матеріалів: довід. пос. / Під заг. ред. В.В.Панасюка. Т.15: Осташ О.П. Структура матеріалів і втомна довговічність елементів конструкцій. – Львів: СПОЛОМ, 2015. – 312 с.
  87. Механіка руйнування і міцність матеріалів: довід. пос. / Під заг. Ред. В.В.Панасюка. Т.9: Міцність і довговічність авіаційних матеріалів та елементів конструкцій / О.П. Осташ, В.М. Федірко, В.М. Учанін, С.А. Бичков, О.Г. Моляр, О.І. Семенець, В.С. Кравець, В.Я. Дереча. Під ред. О.П. Осташ, В.М. Федірка. – Львів: СПОЛОМ, 2007. – 1068 с.



**В. О. Богуслаєв, О. Г. Гребеніков, М. І. Москаленко та ін.**

**SCIENTIFIC GROUNDS OF STRUCTURAL AND PRODUCTION  
CONCEPTS TO PROVIDE AIRCRAFT LIFE TIME  
Study Guide**

**Translated by E. N. Chmovzh, M. V. Kyrylenko,  
S. N. Shapovalov  
Editors: E. N. Chmovzh, M. V. Kyrylenko, S. N. Shapovalov  
Technical editor: M. V. Kyrylenko  
Computer Make-up: E. N. Chmovzh, M. V. Kyrylenko,  
O. M. Stoliarchuk**

**Cons. Plan, 2019**

**Signed for print 30.09.2019**

**Format 60×84<sup>1</sup>/<sub>8</sub>. Offset paper No 2. Offset print**

**Printer's sheets . Ed.-publ. sh. .**

**Order 394. Number of copies: 50. Free price**

---

**National Aerospace University by N.E. Zhukovsky  
«Kharkiv Aviation Institute»  
17 Chkalov Str., Kharkiv-70, 61070  
<http://www.khai.edu>  
«KhAI» Publishing Center  
17, Chkalov Str., Kharkiv-70, 61070  
[izdat@khai.edu](mailto:izdat@khai.edu)**